Regulation of synaptic function and plasticity by cyclin-dependent kinase 5

by

Susan C. Su

B.S. Biology
Duke University, 2004

Submitted to the Department of Brain and Cognitive Sciences
in Partial Fulfillment of the Requirements for the Degree of

Doctor of Philosophy in Neuroscience
at the
Massachusetts Institute of Technology

February 2013

Signature of Author _____
Department of Brain and Cognitive Sciences
September 21, 2012

Certified by _____
Li-Huei Tsai, PhD
Picower Professor of Neuroscience
Thesis Supervisor

Accepted by _____
Matthew A. Wilson, PhD
Sherman Fairchild Professor of Neuroscience
Director of Graduate Education for Brain and Cognitive Science

Regulation of synaptic function and plasticity by cyclin-dependent kinase 5

by

Susan C. Su

Submitted to the Department of Brain and Cognitive Sciences on September 21, 2012, in partial fulfillment of the requirements for the degree of Doctor of Philosophy in Neuroscience

Abstract

The neuronal serine/threonine kinase cyclin-dependent kinase 5 (Cdk5) is activated by its regulatory subunit, p35, to post-translationally modify substrates through phosphorylation. In this thesis, I provide several lines of evidence that Cdk5 plays a critical role in synaptic function and plasticity. First, we characterized the function of Cdk5 in learning and memory by region-specific Cdk5 ablation. From multiple Cdk5 conditional knockout mouse models, we determined that Cdk5 is essential for memory formation and synaptic plasticity. Loss of Cdk5 in the hippocampus disrupts the cAMP pathway due to increased phosphodiesterase proteins. This dysregulation of cAMP signaling can be attenuated by a phosphodiesterase inhibitor to restore levels of protein phosphorylation, synaptic plasticity, and memory. Moreover, forebrain-specific deletion of Cdk5 affected multiple aspects of behavior that can partially be rescued by lithium treatment. We next identified the N-type calcium channels as a presynaptic substrate of Cdk5. We described how Cdk5-mediated phosphorylation of the N-type calcium channel increased calcium influx and channel open probability. This in turn enhanced the association of the N-type calcium channel with the active zone protein RIM1, which impacted vesicle docking and neurotransmission. Finally, we identified the postsynaptic density protein Shank3 as a Cdk5 substrate and observed that Cdk5-mediated phosphorylation of Shank3 plays a critical role in maintaining dendritic spine morphology and synaptic plasticity. Our collective results demonstrate a central role for Cdk5 in regulating both presynaptic and postsynaptic functions and provide better insight into how specific targets of Cdk5 can impact a general mechanism underlying synaptic transmission, synaptic plasticity, and cognitive function.

Thesis Supervisor: Li-Huei Tsai, PhD
Title: Picower Professor of Neuroscience

Acknowledgements

My thesis advisor: Li-Huei Tsai, for her mentorship in pursuing interesting and important scientific questions, passion for science, strength in running a lab, encouragement to strive to do one's best every day, wit and humor, kindness and generosity, friendship and company, together with Lon and Jessica. It has been a tremendous learning experience which has only been made possible with Li-Huei's guidance and support.

All Tsai lab members – past and present – for their mentorship and collaboration, continual feedback and support, expertise in a variety of subjects in and outside of lab, camaraderie and friendships, energy and spirit, and an appetite for good food and drink.
Former members: Scott Adams, Biafra Ahononu, Joshua Buchman, Froylan Calderon de Anda, Marie Carlén, Kai-Siang Chen, Kelly Dennehy, Andrew Devlin, Laurel Drane, Christopher Frank, Jun Gao, Xuecai Ge, Paola Giusti-Rodríguez, Ji-Song Guan, Martin Kahn, Eumie Kang, Dohoon Kim, Cillian King, Ester Kwon, Yingwei Mao, Gloria Mak, Konstantinos Meletis, Kristie Ota, Ana Lucia Rosario, Charlotta Rühlmann, Benjamin Samuels, Megumi Sasaki, Katie Schlieper, Karun Singh, Takahiro Soda, Chen-Wei Tsai, Rachel Tsunemoto, Neal White, Zhigang Xie, Takao Yoshimizu
Current members: Adam Bero, Rebecca Canter, Sukhee Cho, Matthew Dobbin, Omer Durak, Zachary Flood, Elizabeth Gjoneska, Johannes Gräff, Shawn Hennessey, Ji Hu, Nadine Joseph, Yea Jin Kaeser-Woo, Tak Ko, Yuan-Da Lin, Ram Madhabhushi, Alison Mungenast, Alexi Nott, Ling Pan, Christine Park, Trongha Phan, Ping-Chieh Pao, Emma Quinn, Damien Rei, Andrii Rudenko, Alireza Samiei, Jinsoo Seo, Sandra Siegert, Mali Taylor, Wenyuan Wang, Ying Zhou

Collaborators: Steven Carr, Karl Clauser, Maria Ericsson, Rachael Neve**,** Jen Pan, David Yue

Summer undergraduate students: Dalton Hughes and Khaing Win, for infusing new energy into projects and to the lab and for their assistance in various experiments.

BCS 2006 classmates & friends: for the enduring friendships that have been formed and those that have endured. Our adventures have been memorable and fun.

Former lab mentors and their lab members: Mary Foster, whose enthusiasm and passion for research was an inspiration to her lab, Pate Skene, whose lab first stimulated my interest in neuroscience, and friendships with Howard Bomze, Athy Robinson, and Sherilynn Black.

Committee members: Troy Littleton**,** Mriganka Sur and Weifeng Xu for their feedback and scientific mentorship.
The BCS administration: Brandy Baker, denise heintze, and Susan Lanza for managing the impossible in keeping track of all of us students and providing support.

My parents and sister: Philip, Judy, and Sandy Su, for their unconditional love, support and encouragement. My extended family who are overseas in Taiwan who have been updated on my progress through my parents and could not make it to the US. John and Cathy Strunk, who have been kind and patient. Nathan Strunk, for his constant support and encouragement, a true partnership throughout the entire graduate school process.

Table of Contents

Chapter 1

Introduction[1]

Summary

Cyclin-dependent kinase 5 (Cdk5) is a multifaceted serine/threonine kinase protein with important roles in the nervous system. Two related proteins, p35 and p39, activate Cdk5 upon direct binding. Over the past decade, Cdk5 activity has been demonstrated to regulate many events during brain development, including neuronal migration as well as axon and dendrite development. Recent evidence also suggests a pivotal role for Cdk5 in synaptic plasticity, behavior, and cognition. Dysfunction of Cdk5 has been implicated in a number of neurological disorders and neurodegenerative diseases including Alzheimer's disease, amyotrophic lateral sclerosis, Neimann-Pick type C disease, and ischemia. Hyperactivation of Cdk5 due to the conversion of p35 to p25 by the calcium-dependent protease calpain during neurotoxicity also contributes to the pathological state. This introduction surveys recent literature surrounding Cdk5 in synaptic plasticity and homeostasis, with particular emphasis on Cdk5 kinase activity under neurodegenerative conditions.

[1] This chapter was previously published as: Su, SC and Tsai, LH. (2011). Cyclin-dependent kinases in brain development and disease. Annual Review of Cell and Developmental Biology 27:465-491.

As neurological disorders such as Alzheimer's disease (AD) progressively impact an aging population, there is a heightened urgency to determine the cellular and molecular events underlying these devastating illnesses. Cyclin-dependent kinase 5 (Cdk5) has received substantial attention as a result of its unique properties in the central nervous system (Dhavan & Tsai 2001, Smith et al. 2001). This chapter highlights recent discoveries regarding Cdk5 in neural development, synaptic plasticity, and synaptic homeostasis with particular emphasis on how Cdk5 dysregulation contributes to neurodegeneration.

Discovery and characterization of cyclin-dependent kinase 5

Cdk5 was initially discovered and cloned on the basis of its sequence homology to other cyclin-dependent kinases such as cdc2, cdk2, and cdk3 (Lew et al. 1992, Meyerson et al. 1992). Formally known as PSSALRE, Cdk5 shares 60% homology with cdc2. Unlike the other cyclin-dependent kinases, however, Cdk5 is not directly involved in the cell cycle. Using histone H1 as a substrate, the preferred sequence of the proline-directed serine/threonine kinase Cdk5 is X(S/T)PX(H/K/R), where S/T represents serine/threonine, X is any amino acid, P is the required proline residue, and H/K/R are basic residues (Beaudette et al. 1993). Cdk5 is highly expressed in the brain and requires binding to a regulatory subunit protein, p35, for activation (Tsai et al. 1994). Notably, p35 messenger RNA is expressed in postmitotic cells of the mouse embryo and overlaps with Cdk5 expression in the central nervous system (Tsai et al. 1993, 1994). The discovery and cloning of p25, a truncated form of p35, hinted at the possibility of Cdk5 as the kinase responsible for phosphorylating neurofilament (NF) proteins (Lew et al. 1994). **Figure 1** highlights several currently known Cdk5-mediated functions, while **Table 1** provides a more comprehensive list of identified Cdk5 substrates.

Early discoveries in neural cytoarchitecture

Cdk5 knockout (KO) mice produced using gene-targeting techniques display perinatal lethality owing to neuronal migration deficits and impaired axonal transport of NFs (Ohshima et al. 1996). In p35 KO mice, a dramatic inversion of cortical layering is evident in which the newly generated postmitotic neurons fail to migrate past older neurons on radial glia (Chae et al. 1997). The animals suffer adult seizures and lethality, and they exhibit alterations in cell orientation as well as dendrite and axon trajectories (Chae et al. 1997, Wenzel et al. 2001). A p35

homolog termed p39 was isolated (Tang et al. 1995) and found to localize to the synapse (Humbert et al. 2000b). The p35 and p39 double-null deletion mouse model exhibits a phenotype most similar to the Cdk5 KOs including severe disruption of various central nervous system components, an absence of Cdk5 kinase activity, lamination defects, and perinatal lethality (Ko et al. 2001). Therefore, p35 and p39 are the sole activators of Cdk5. The collective studies highlight Cdk5 and p35 as necessary components for establishing proper neocortical lamination.

Cyclin-Dependent Kinase 5 and p35 in Neurite Development and Neuronal Migration

During embryonic development, Cdk5 is highly expressed in the cell body and axons of neurons. Furthermore, Cdk5/p35 colocalize to axonal growth cones (Nikolic et al. 1996, Tsai et al. 1993). If dominant negative Cdk5 (Cdk5-DN) constructs interfering with endogenous p35 binding or the ATP binding pocket are expressed (D144N or K33T), or if p35 expression is reduced, neurite outgrowth is inhibited. Conversely, Cdk5 and p35 overexpression leads to longer neurites.

Cdk5/p35 mediates neurite outgrowth through Pak 1 kinase (Nikolic et al. 1998) and interaction between phosphorylated Y15 Cdk5, tyrosine kinase c-Abl, and Cables (Zukerberg et al. 2000). Other studies link Cdk5 phosphorylation of receptor tyrosine kinases TrkB in brain-derived neurotrophic factor-stimulated dendrite outgrowth (Cheung et al. 2007), phosphorylation of the collapsin-response-mediated protein for semaphorin 3A-induced growth-cone collapse (Brown et al. 2004, Harada et al. 2001), phosphorylation of ephexin and WAVE1 in dendritic spine development (Fu & Ip 2007). Moreover Cdk5/p35 activity downstream of the Erk signaling pathway has been implicated in nerve growth factor-dependent neurite outgrowth (Harada et al. 2001), and Cdk5/p35 also interacts with ubiquitin ligase mind bomb 1 (Mib1) during neurite morphogenesis (Choe et al. 2007). Recent work has uncovered a role for s-nitrosylation, a post-translational modification, on Cdk5 activity in regulation of neurite growth and branching (Zhang et al. 2010). Thus, Cdk5/p35 is essential for neurite development and maintenance of proper cytoskeletal architecture.

Cytoskeletal substrates of Cdk5 include NF proteins and the microtubule (MT)-associated protein tau (Baumann et al. 1993, Lew et al. 1994, Paudel et al. 1993), which is heavily phosphorylated by multiple proline-directed kinases including Cdk5, glycogen synthase kinase 3 β (GSK-3β), and MT-associated protein (MAP) (Mandelkow & Mandelkow 1998, Paglini et al.

1998). Tau phosphorylation is thought to allow it to regulate MT polymerization, a particularly important function discussed below in terms of Cdk5 and AD (De Vos et al. 2008).

Cdk5 phosphorylates multiple proteins to mediate neuronal migration, including NUDEL, a Lis-1-interacting protein that cooperates with dynein, an MT-interacting motor protein (Niethammer et al. 2000, Sasaki et al. 2000); the tyrosine kinase FAK, which is phosphorylated to allow regulation of an MT fork to direct proper neuronal migration through nuclear translocation (Xie et al. 2003); doublecortin (Dcx), which allows for increased cytoskeletal dynamics during neuronal migration (Tanaka et al. 2004); Dix-domain containing 1 (Dixdc1), which interacts with psychiatric illness risk gene Disrupted in Schizophrenia-1 (DISC1) and NUDEL during migration (Singh et al. 2010); and DISC1 which mediates neural progenitor migration (Ishizuka et al. 2011).

Cdk5 is a critical regulation of synaptic transmission

Presynaptic substrates and neurotransmission

At presynaptic terminals of chemical synapses, vesicles containing neurotransmitters undergo docking and fusion, or exocytosis, at the active zone to allow neurotransmitter release across the synaptic cleft (Murthy and De Camilli 2003, Sudhof 2004). Presynaptic calcium influx triggers vesicle fusion and exocytosis by the SNARE (soluble *N*-ethylmaleimide-sensitive fusion attachment receptor) complex proteins, consisting of v-SNARES (synaptobrevin or VAMP) and t-SNARES (SNAP-25, syntaxin). Recycling of synaptic vesicle proteins occurs through clathrin-mediated synaptic vesicle endocytosis (SVE). Components of SVE machinery include the accessory protein AP-2, dynamin and amphiphysin proteins to pinch off the vesicle from the active zone using GTP hydrolysis, synaptojanin I to assist in synaptic vesicle uncoating, and other dephosphin proteins. The phosphatase calcineurin removes the phosphate groups from the dephosphins in response to calcium influx and allows for synaptic vesicle exocytosis, and rephosphorylation by protein kinases, including Cdk5, are critical for continued SVE (Nguyen & Bibb 2003).

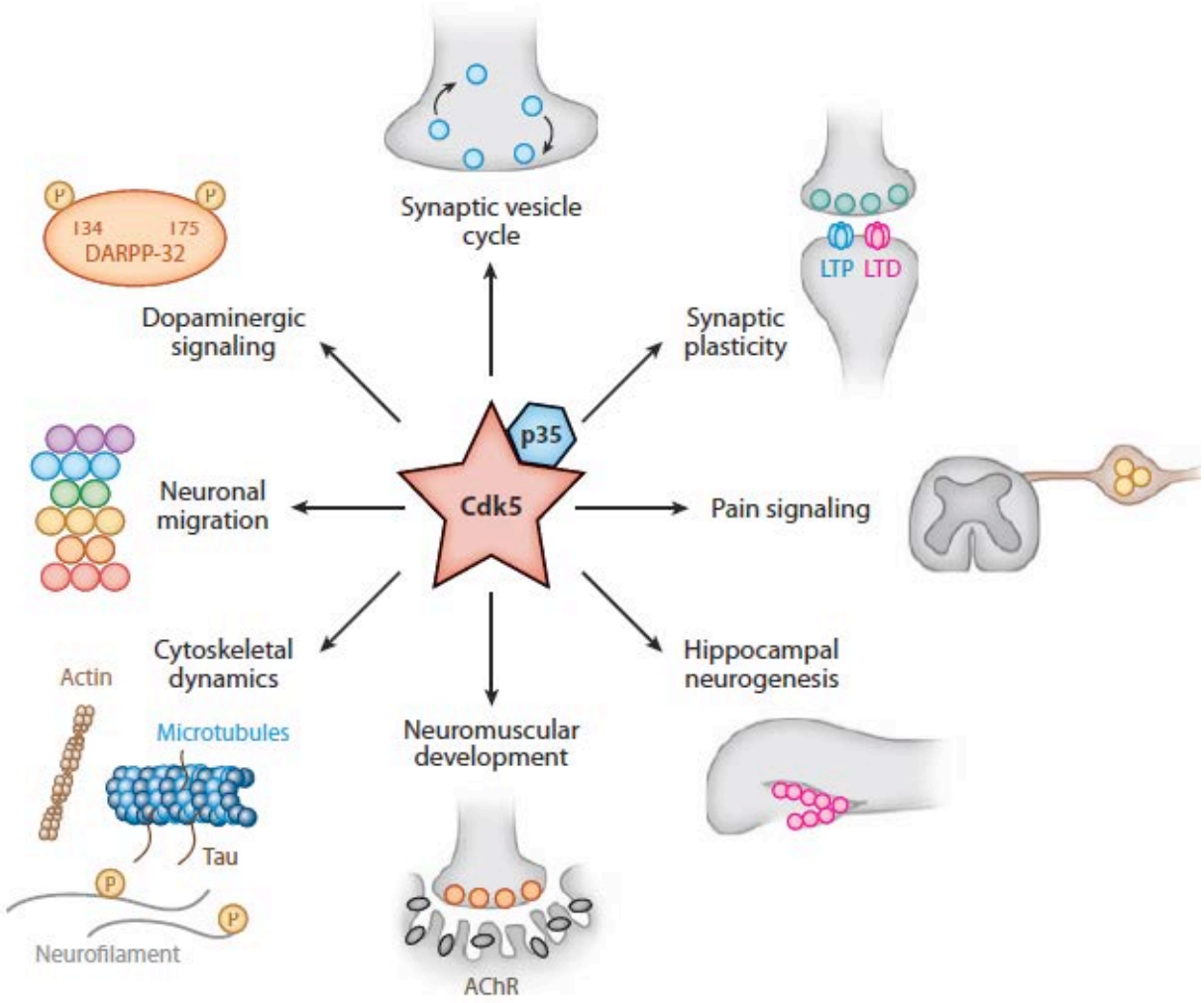

Figure 1 Cyclin-dependent kinase 5 (Cdk5) impacts various cellular processes and is vital for proper neuronal function. Cdk5 requires p35 binding for activation and regulates many events including neuronal migration, cytoskeletal dynamics, and neurite outgrowth. Cdk5 plays a critical role in dopaminergic neuron signaling and regulates components of the synaptic vesicle cycle. Recent evidence suggests a pivotal role for Cdk5 in synaptic plasticity, behavior, and cognition. Additionally, Cdk5 has been implicated in a number of molecular pathways such pain signaling, adult neurogenesis, and neuromuscular development. Abbreviations: AChR, acetylcholine receptor; Cdk5, cyclin-dependent kinase 5; DARPP, dopamine cyclic-AMP regulated phosphoprotein; LTD, long-term depression; LTP, long-term potentiation.

Table 1. List of major identified Cdk5 substrates and their functional categories

Category	Functional outcome	P-sites	References
Neuronal migration			
β-Catenin	N-cadherin-mediated cell adhesion, binding	Multiple	Kwon et al. 2000, Kesavapany et al. 2001
Disabled 1	Control of neuronal positioning, reelin interaction	S491	Keshvara et al. 2002
Dixdc1	Allowing interaction between DISC1 and NUDEL	S250	Singh et al. 2010
DISC1	Switch between progenitor proliferation and migration	S710	Ishizuka et al. 2011
Doublecortin	Lowered affinity to microtubules, reduced effect on polymerization	S297	Tanaka et al. 2004
FAK	Nuclear translocation through microtubule fork	S732	Xie et al. 2003
NUDEL	Regulation of dynein and axonal transport	S198, T219, S231	Niethammer et al. 2000, Sasaki et al. 2000
p27(kip1)	Actin organization, cortical neuronal migration	S10, T187	Kawauchi et al. 2006
Neurite outgrowth			
Cables	Dissociation of Cdk5/Cables/c-Abl complex, neurite outgrowth	Multiple	Zukerberg et al. 2000
CRMP2	Semaphorin 3A–induced growth cone collapse	S522	Brown et al. 2004
c-Src	Neural development, neurite outgrowth, function	S75	Kato & Maeda 1999
MAP1B	Regulation of axonal formation and elongation	Multiple	Pigino et al. 1997, Paglini et al. 1998
p39	Regulation of actin cytoskeletal dynamics	Multiple	Humbert et al. 2000a
PAK1	Actin polymerization, cytoskeletal reorganization	T212	Nikolic et al. 1998
RasGRF2	Altered RasGRF2, microtubule protein accumulation	S737	Kesavapany et al. 2004
TrkB	BDNF-stimulated dendritic outgrowth	S478	Cheung et al. 2007
Synaptic vesicle cycle			
Amphiphysin 1	Regulation of synaptic vesicle endocytosis	S262, S272, S276, S285, T310	Floyd et al. 2001, Liang et al. 2007
Dynamin 1	Clathrin-mediated synaptic vesicle endocytosis	S774, S778	Tomizawa et al. 2003, Tan et al. 2003
Munc18	Modulation of synaptic vesicle exocytosis	T574	Shuang et al. 1998, Fletcher et al 1999
Pctaire1	Synaptic vesicle exocytosis via NSF interaction	S95	Cheng et al. 2002
Septin 5	Reduction of sept5 binding to syntaxin	S17	Taniguchi et al. 2007
Synapsin 1	Impact on cytoskeletal components, actin bundling	S551, S553	Matsubara et al. 1996
Synaptojanin 1	Interaction with other endocytosis components	S1144	Lee et al. 2004
Synaptic transmission and plasticity			
CASK	Promotion of synaptogenesis, presynaptic proteins	S51, S395	Samuels et al. 2007
$Ca_V1.2$	Decreased calcium influx upon glucose stimulation	S783	Wei et al. 2005a
$Ca_V2.1$	Synaptic plasticity and neurotransmitter release	aa724–981	Tomizawa et al. 2002
DARPP-32	Signal transduction modulation in striatal neurons	T75	Bibb et al. 1999
δ-Catenin	Dendritic morphogenesis, synaptic activity	S300, S357	Poore et al. 2010

Table 1 (*Continued*)

Category	Functional outcome	P-sites	References
Kalirin-7	Formation, regulation of dendritic spine protrusion	T1590	Xin et al. 2008
NR2A	NMDA current, LTP, ischemia-mediated cell death	S1232	Li et al. 2001, Wang et al. 2003
PP-1	Signaling pathways involving PKA, calcineurin	S6, S67	Nguyen et al. 2007
PP-1 inhibitor	Multiple cellular functions and signaling pathways	T72	Agarwal-Mawal & Paudel 2001
PSD-95	Clustering size of K^+ channels at dendritic spines	T19, S25	Morabito et al. 2004
SPAR	Plk2-mediated degradation during synaptic scaling	S1328	Seeburg et al. 2008
TH	Presynaptic component in dopamine synthesis	S31	Moy & Tsai 2004, Kansy et al. 2004
Neurodegenerative disease			
APP	Potential localization of the β-amyloid protein	T668	Iijima et al. 2000
Huntingtin	Reduction in huntingtin aggregation and formation	S434, S1181, S1201	Luo et al. 2005, Anne et al. 2007
MEF2D	Inhibition of transcriptional factors and cell death	S444	Smith et al. 2006
NF	Regulation of axonal transport of NF	Multiple	Lew et al. 1994, Ackerley et al. 2003, Gong et al. 2003
Parkin	Modulation of synphilin-1/α-synuclein inclusions	S131	Avraham et al. 2007
Prx2	Tuning sensitivity of neuron to oxidative stress	T89	Qu et al. 2007, Rashidian et al. 2009
Tau	Accumulation and disruption of axonal transport	Multiple	Baumann et al. 1993, Kobayashi et al. 1993
Other			
Ape1	Involvement in regulation of DNA damage, cell death	T232	Huang et al. 2010
ATM	DNA damage, ATM activation, neuronal death	S794	Tian et al. 2009
β-2 syntrophin	Regulatory mechanism of insulin secretion	S75	Schubert et al. 2010
Bcl-2	Neuroprotective effect, neuronal survival	S70	Cheung et al. 2008
Cdh1	Mediates cyclin B1 accumulation in excitotoxicity	S40, T121, S163	Maestre et al. 2008
ErbB3	Nrg-induced AChR expression at the NMJ	T871, S1204	Fu et al. 2001
GR	Regulate glucocorticoid receptor transcriptional activity	S203, S211, S232, S246 and others	Kino et al. 2007, Adzic et al. 2009
JNK3	Inhibition of JNK activity and reduced apoptosis	T131	Li et al. 2002
MEK1	Down-regulation of MAPK signaling pathway	T286	Sharma et al. 2002
mSds3	HDAC transcriptional co-repressor complex	S228	Li et al. 2004
p35	Promotion of ubiquitin-mediated proteolysis	S8, T138, S170, T197	Tsai et al. 1994, Patrick et al. 1998
p53	Increased cell cycle arrest or cell death genes	S33, S315	Zhang et al. 2002
Paxillin	Involvement in oligodendrocyte differentiation	S244	Miyamoto et al. 2007
PIPKIγ	Blocked PI(4,5)P2 synthesis at synapses and at focal adhesions	S650	Lee et al. 2005
PPARγ	Obesity-linked phosphorylation in fat cells	S273	Choi et al. 2010

Table 1 (*Continued*)

Category	Functional outcome	P-sites	References
Rb	Cellular growth, differentiation, apoptosis	Multiple	Lee et al. 1997, Hamdane et al. 2005
S6K1	Regulation of S6K1 catalytic activity	S411	Hou et al. 2007
STAT3	Transcription of target genes c-fos and junB	S727	Fu et al. 2004
Talin	Regulation of Smurf1-mediated talin ubiquitination	S425	Huang et al. 2009
TRPV-1	Modulation of nociceptive signaling in DRG	T407	Pareek et al. 2007

Abbreviations: AChR, acetylcholine receptor; Ape1, apurinic /apyrimidinic endonuclease 1; APP, amyloid precursor protein; ATM, Ataxia telangiectasia mutated; Bcl-2, B-cell CLL/lymphoma 2; BDNF, brain-derived neurotrophic factor; Cables, Cdk5 and Abl enzyme substrate; CASK, calcium/calmodulin-dependent serine *protein* kinase; $Ca_V1.2$, L-type voltage-gated calcium channel; $Ca_V2.1$, P/Q-type voltage-gated calcium channel; Cdh1, cadherin-1; CRMP2, Collapsin response mediator protein 2; c-Src, non-receptor tyrosine kinase; DARPP-32, Dopamine- and cAMP-regulated phosphoprotein, Mr 32 kDa; DISC1, Disrupted in schizophrenia1; DRG, dorsal root ganglion; Dixdc1, Dix-domain containing 1; ErbB3, receptor tyrosine-protein kinase erbB3; FAK, focal adhesion kinase; GR, glucocorticoid receptor; HDAC, histone deacetylase; JNK3, c-Jun N-terminal kinase 3; LTP, long-term potentiation; MAP1B, microtubule-associated protein 1B; MEK1, MAP kinase kinase-1; MEF2D, myocyte enhancer factor 2D; Munc18, mammalian uncoordinated 18; NF, neurofilament; NMJ, neuromuscular junction; NR2A, N-methyl D-aspartate receptor subunit 2A; NR2B, N-methyl D-aspartate receptor subunit 2B; Nrg, neuregulin; NSF, N-ethylmaleimide sensitive factor; p27(kip1), cyclin-dependent kinase inhibitor; p35, regulatory activator of cyclin-dependent kinase 5 Mr 35 kDa; p39, regulatory activator of cyclin-dependent kinase 5; p53, tumor protein 53; PAK1, p21-Activated Kinase; paxillin, focal adhesion-associated adaptor protein; pctaire1, cyclin-dependent kinase 16 (cdk16); PIPKI, phosphatidylinositol(4) phosphate 5 kinase type I gamma; PPARγ, Peroxisome proliferator-activated receptor gamma; Plk2, polo-like kinase 2; PP-1, protein phosphatase-1; Prx2, peroxiredoxin 2; PSD-95, Postsynaptic density protein 95; RasGRF, ras guanine nucleotide releasing factor 2; Rb, retinoblastoma protein; S6K1, S6 kinase 1; SPAR, spine-associated Rap guanosine triphosphatase activating protein; STAT3, signal transducer and activator of transcription 3; TH, tyrosine hydroxylase; TRPV-1, Transient Receptor Potential Vanilloid-1.

Role in synaptic vesicle exocytosis and endocytosis

The synaptic vesicle cycle requires Cdk5 phosphorylation of presynaptic proteins implicated in both endocytosis and exocytosis. Munc18, a protein that interacts with syntaxin1A and is thought to be an essential complex in vesicle fusion, is phosphorylated by Cdk5/p35 (Fletcher et al. 1999, Shuang et al. 1998). In vitro, Cdk5/p35 forms a complex with Munc18 and syntaxin1A that is dissociated upon the addition of ATP, which suggests that Cdk5 phosphorylation of Munc18 may allow for syntaxin1A to form a SNARE complex and promote neurotransmitter release. The interaction between another protein implicated in exocytosis, Sept5, and syntaxin1 is also regulated by Cdk5/p35 (Taniguchi et al. 2007).

Cdk5 also phosphorylates the presynaptic protein CASK to facilitate synapse development (Samuels et al. 2007) and the P/Q-type voltage-gated calcium channel ($Ca_V2.1$) to inhibit its interaction between SNAP-25 and synaptotagmin in vitro (Tomizawa et al. 2002). Application of roscovitine, a cyclin-dependent kinase inhibitor, increases the field excitatory postsynaptic potential (fEPSP) slope in acute hippocampal slice preparations and upregulates glutamate release from synaptosomes, suggesting that blocking the action of Cdk5 results in a long-term potentiation (LTP) of synaptic strength. However, in addition to its role in the cytoplasm, roscovitine acts on the extracellular domain of $Ca_V2.1$ to slow channel deactivation kinetics and allow calcium influx (Yan et al. 2002). Therefore, exactly how Cdk5/p35 regulates synaptic transmission remains unclear.

Several components of the SVE are Cdk5 targets; these include synapsin I (Matsubara et al. 1996), amphiphysin (Floyd et al. 2001), synaptojanin I (Lee et al. 2004), and dynamin I (Tan et al. 2003, Tomizawa et al. 2003). However, one report indicates that Cdk5 phosphorylation disrupts SVE (Tomizawa et al. 2003), while another supports the notion that Cdk5 is essential for SVE (Tan et al. 2003). To add further complexity, Cdk5 is involved in activating Pctaire1, a key component in the phosphorylation and regulation of *N*-ethylmaleimide sensitive fusion protein, which is necessary for disassembling the SNARE complex (Cheng et al. 2002). It has been suggested that Cdk5 is necessary for the activity-dependent slow component of SVE (Evans and Cousin 2007). Continued work will better elucidate the intricate dynamics between Cdk5 and calcineurin in mediating exocytosis and the multiple stages of SVE.

Cyclin-dependent kinase 5 and modulation of transmission

Dopaminergic signaling in striatum

A prominent area of Cdk5 research centers on dopaminergic signaling pathways (Chergui et al. 2004). Cdk5 directly phosphorylates the N-terminal regulatory domain of tyrosine hydroxylase, the dopamine-synthesis catalytic enzyme in presynaptic terminals (Moy & Tsai 2004). Postsynaptically, Cdk5 phosphorylation of DARPP-32 (dopamine cyclic-AMP regulated phosphoprotein) on the T75 residue allows DARPP-32 to become a protein kinase A (PKA) inhibitor and therefore a protein phosphatase 1 activator, thus allowing phosphatase activity (Bibb et al. 1999). Conversely, if DARPP-32 is phosphorylated solely at T34 by PKA through the dopamine D1 receptor signaling pathway, it inhibits protein phosphatase 1 and promotes net phosphorylation activity as a kinase.

Following chronic cocaine exposure, as well as in ΔFosB mice, mRNA and protein levels of Cdk5/p35 are upregulated in medium spiny striatal neurons (Bibb et al. 2001). During acute cocaine exposure, PKA is activated to downregulate T75 phosphorylation. However, following chronic cocaine exposure, Cdk5 is activated to dampen the locomotor response as a part of a novel homeostatic mechanism, and subsequent phosphorylation of T75 will decrease D1/PKA signaling. Additional work examining the homeostatic regulation by Cdk5 in dopaminergic neurons will be critical for a more complete understanding of the cellular and molecular mechanisms underlying drug abuse and addiction.

Glutamatergic transmission in the hippocampus

The postsynaptic density (PSD) found on dendritic spines of excitatory synapses of the mammalian central nervous system is comprised of a vast and complex network of proteins that provide a dynamic, compartmentalized framework for receiving inputs from hundreds of presynaptic axonal contacts (Sheng & Hoogenraad 2007). Systematic biochemical and animal model studies have established how each PSD protein interacts with the others to establish the neural circuitry for proper synaptic transmission. Despite considerable advances, there is still an incomplete understanding of the PSD; therefore, identifying novel Cdk5 substrates will provide a more comprehensive outlook on how the PSD network is formed and maintained.

The PSD has a large abundance of PSD-95 and PSD-95 family-related proteins, which outnumber most of the other proteins at the electron-microscope level. PSD-95, along with PSD-

93, SAP-102, and SAP-97, belong to the MAGUK (membrane-associated guanylyl kinase) family of proteins. At the postsynaptic terminal of an excitatory glutamatergic synapse in the mouse hippocampus, Cdk5 phosphorylates the N-terminal domain of PSD-95 to regulate the synaptic recruitment and clustering of ion channels, particularly the potassium K^+ channels, and the NMDA (N-methyl D-aspartate) receptors (Morabito et al. 2004).

The NMDA receptors bind PSD-95 and are critical for the induction of synaptic transmission. Upon glutamate release and spillover into the synaptic cleft, the magnesium block is removed from the NMDA receptor pore to allow calcium influx. In one study, Cdk5 phosphorylation of the NMDA receptor NR2A subunit facilitates receptor activity and LTP in area CA1 of the mouse hippocampus (Li et al. 2001). Cdk5 also phosphorylates NR2A during neurotoxic conditions such as ischemia, which enhances NMDA receptor-mediated currents during hippocampal CA1 cell death (Wang et al. 2003). The Cdk5-dependent phosphorylation of NR2B, another major subunit of the NMDA receptor, retains its cell-surface expression via reduced activity-dependent endocyosis (Zhang et al. 2008).

CaMKII is another highly abundant PSD molecule that forms a holoenzyme upon calcium-dependent activity and whose activation is well known to play a role in LTP (Lisman et al. 2002). Thus, CaMKII may form a core PSD complex critical for the induction of synaptic transmission. The N-terminal regions of both p35 and p39 interact with α-actinin protein, a protein implicated in the anchoring of receptors to the actin cytoskeleton, and their C-termini bind the α isoform of CaMKII (CaMKIIα) (Dhavan et al. 2002). Biochemical and immunohistochemical data reveal a ternary structure consisting of p35, p39, α-actinin, and CaMKIIα that is dependent on calcium influx primarily through the NMDA receptor, which leads to activation of CaMKIIα via autophosphorylation at T286.

Cdk5 interacts with another important signaling complex in the PSD known as the ephrins and ephrin receptors in ephrin-A1-mediated regulation of spine density (Fu et al. 2007). Cdk5 was recently demonstrated to phosphorylate the PSD protein kalirin-7 at T1590 (Xin et al. 2008). Kalirin-7 mediates spine formation as well as synaptic plasticity and behavior, and kalirin-7 KOs display reduced hippocampal spine density, deficient LTP, and behavior abnormalities (Ma et al. 2008). The absence of kalirin-7 results in decreased Cdk5 levels at the PSD, suggesting that Cdk5 phosphorylation of kalirin-7 is a critical aspect for proper synaptic formation and function of the PSD. Cdk5 can also regulate dendritic spine formation by

phosphorylating WAVE1 to modulate its interaction with the Arp2/3 actin polymerization complex (Kim et al. 2006). The collecive findings indicate that Cdk5-mediated phosphorylation of PSD proteins does not occur as separate, static events but rather in a dynamic, activity-dependent manner that has implications on the downstream signaling pathways and feedback loops.

Cdk5, p35, and p25 in synaptic plasticity

Owing to the embryonic lethality of Cdk5-null animals, various mouse models have been developed to either diminish Cdk5 postnatally or hyperactivate Cdk5. Loss of Cdk5 activity can be achieved through p35 KO animals (Chae et al. 1997) or conditional knockout (cKO) of Cdk5 (Hawasli et al. 2007, Hirasawa et al. 2004, Takahashi et al. 2010). However, a striking and unexpected finding that p25, a truncated form of p35, deregulates Cdk5 activity has opened a new field of study (Patrick et al. 1999). This Cdk5/p25 complex can be studied by generating a p25 transgenic mouse model in which p25 is expressed under a neural promoter (Ahlijanian et al. 2000, Bian et al. 2002, Cruz et al. 2006).

Early studies involving Cdk5 and synaptic plasticity utilize pharmacological methods such as roscovitine or olomoucine to reduce Cdk5 activity. Protocols eliciting LTP and long-term depression (LTD) can vary widely, but the end result is the long-lasting enhancement or depression of fEPSPs compared with baseline, prestimulation levels, in synaptic transmission of the examined area (Bliss and Collingridge 1993). The first hint that loss of Cdk5 activity directly affects plasticity came from p35 KO mice in which LTP as induced by tetanic stimulation (100 Hz) appears to be normal in area CA1 of the hippocampus, but low-frequency stimulation used to induce LTD (1 Hz, 15 min) reveals a marked deficit in LTD (Ohshima et al. 2005). Whereas LTP is thought to correlate with memory formation, LTD may play a role in weakening synapses and perhaps blocking memory formation (Malenka and Bear 2004). Intriguingly, LTP can be reversed or depotentiated in the p35 KO slices.

Cdk5 cKO animals were subsequently created using the Cre-loxP system, which crossed the mouse NF heavy-chain Cre promoter mouse line to Cdk5-floxed mice (Hirasawa et al. 2004). Despite the perinatal ablation of Cdk5, the mice exhibit neuronal migration defects, and synaptic plasticity was not examined here. Another Cdk5 cKO line was derived under a prion promoter and regulated temporally by the estrogen-receptor transgene (Hawasli et al. 2007). In this line,

Cdk5 cKO mice display an enhancement of hippocampal-dependent spatial memory as assayed by the Morris water-maze task and contextual fear memory, and LTP is greater compared with that of control mice. The evoked excitatory postsynaptic current showed that the NMDA, but not the AMPA (α-amino-3-hydroxy-5-methyl-4-isoxazolepropionic acid), receptor-mediated current is enhanced in the mutant mice, which is attributed to greater surface NR2B levels and a reduction in NMDAR degradation.

Conversely, p25, a truncated form of p35, binds and hyperactivates Cdk5. Therefore, to study how aberrant Cdk5 signaling may play a role in modulating synaptic plasticity, a p25 transgenic mouse model was employed using an inducible system whereby spatial specificity is achieved through the αCaMKII promoter, which is highly expressed in excitatory neurons of the forebrain (Mayford et al. 1996), and temporal specificity is regulated using the tetracycline-controlled transactivator system (Cruz et al. 2003).

Strikingly, short-term, two-week p25 expression in αCaMKII p25 Tg adult mice (CK-p25 Tg) dramatically enhances learning and memory in contextual fear conditioning and the Morris water-maze task (Fischer et al. 2005). This behavioral effect corresponds with a facilitation of hippocampal area CA1 LTP and an increase in dendritic spine formation. Importantly, the mice do not display overt deficits in motor responses or neurodegeneration. Electrophysiology experiments reveal no significant differences in synaptic transmission or presynaptic alterations but instead hint at the possibility of enhanced NMDAR function. However, long-term, six-week induction of p25 results in severe neuronal loss, memory impairments, and LTP deficits. It has been proposed that elevated p25 levels is an early, perhaps compensatory, step in neurodegeneration. Together, results from various Cdk5/p35 KO and p25 transgenic mouse models propose a mechanism of NMDAR-dependent LTP mediated by Cdk5 that exerts influence on cognitive function.

Cdk5 and synaptic homeostasis

An intriguing theme emerging from the study of synaptic plasticity using mouse models of Cdk5, p35, and p25 is the notion that specific molecules may dynamically shape compensatory mechanisms in the brain and, furthermore, maintain a steady-state level of signaling known as synaptic homeostasis. Recent work implicates Cdk5 in synaptic homeostasis, which raises the fundamental question of how Cdk5 functions in normal and disease states.

The phenomenon of synaptic scaling has been studied in cultured hippocampal neurons where cells regulate their postsynaptic AMPA receptor-mediated response to activity (Rutherford et al. 1998, Turrigiano et al. 1998). This synaptic scaling, or homeostasis, can be important for network stabilization during periods of development, plasticity, and disease. Under conditions where neural activity is silenced using tetrodotoxin, which blocks action potentials, several molecules including brain-derived neurotrophic factor (Rutherford et al. 1998), Arc (Shepherd et al. 2006), and adenylyl cyclase 1 (Gong et al. 2007) are involved in the homeostatic response. Less is known about the molecular pathways underlying sustained, heightened activity. Cdk5 has recently been identified as a novel molecule involved in synaptic homeostasis.

During periods of elevated activity, Cdk5 phosphorylates SPAR, a postsynaptic RapGap scaffolding molecule, prior to phosphorylation and subsequent degradation of SPAR by polo-like kinase 2 (Plk2) (Seeburg et al. 2008). Plk2 is necessary to downregulate the synaptic response during chronically elevated activity, but it can bind SPAR only when SPAR is phosphorylated by Cdk5. Blocking Cdk5 will also inhibit synaptic weakening in response to heightened activity. Thus, Cdk5 is a key player in the regulation of downstream signaling cascades involved in synaptic homeostasis.

Another study directly establishes Cdk5 as an integral player in controlling synaptic transmission (Kim & Ryan 2010). Acutely silencing Cdk5 using roscovitine or short-hairpin RNA increases presynaptic neurotransmitter release. Furthermore, the interaction between Cdk5 and calcineurin maintains the recycling vesicle pool to provide fine-tuning of synaptic vesicle release at the nerve terminal. Chronic silencing of neuronal activity using tetrodotoxin downregulates Cdk5 levels by a yet-undetermined mechanism. A comprehensive analysis investigating how activity regulates Cdk5 localization and function will further reveal its importance in modulation of synaptic homeostasis at pre- and postsynaptic terminals.

Activity-dependent regulation of Cdk5

One long-standing question has been how Cdk5 is regulated, either by its upstream signaling pathways or by controlling kinase activity. Previous hints suggest that Cdk5 is phosphorylated on Y15 to increase its kinase activity (Zukerberg et al. 2000), yet phosphorylation at a neighboring site T14 on Cdk5 inactivates other Cdks in addition to Cdk5 (Matsuura & Wang 1996). It has also been established that phosphorylation at T160, but not

S159, is required for activation (Poon et al. 1997, Qi et al. 1995). The X-ray crystal structure of the Cdk5/p25 complex provided further support of an unusual kinase-substrate binding relationship, the unphosphorylated S159 at the T loop of Cdk5 is necessary for formation of the Cdk5/p25 complex (Tarricone et al. 2001). In addition, p35 undergoes activity-dependent degradation via the ubiquitin-proteosome pathway (Patrick et al. 1998, Wei et al. 2005b).

Notably, the activation of calpain, a calcium-dependent protease, cleaves p35 to produce p25 during neurotoxicity (Lee et al. 2000, Patrick et al. 1999). Elevated activity leading to neurotoxic conditions in synapses of cultured neurons can be induced through several pathways, including amyloid β (Aβ) treatment, excitotoxicity from excessive intracellular calcium levels due to ischemia or excessive glutamate spillover across the synaptic cleft, or chemical compounds, such as hydrogen peroxide or ionomycin. Neurotoxic treatments activate calpain, which in turn cleaves the N-terminal fragment of p35 to liberate the p25 fragment. This Cdk5/p25 complex accumulates predominantly in the cytoplasm and nucleus due to loss of a myristolation tag and exhibits a longer half-life compared with that of Cdk5/p35 which is localized mainly in the cell periphery (Patrick et al. 1999).

The significance of Cdk5/p25 in disease is further supported by observations of p25 accumulation in AD brains (Patrick et al. 1999, Tseng et al. 2002). Also present in the same neurons of AD brains are neurofibrillary tangles (NFTs). Interestingly, p25, but not p35, is found in neurons containing NFTs as demonstrated by AT8 antibody staining. Tau hyperphosphorylation is observed using another antibody, PHF-1 (paired helical fragment 1). Cdk5/p25 is responsible for the phosphorylation event (Hashiguchi et al. 2002), which renders tau less likely to associate with MTs. Furthermore, overexpressing Cdk5/p25 in primary neurons causes cytoskeleton disruptions and ultimately apoptotic cell death as shown by fragmented nuclei. These studies highlight the first associations between p25 and neurodegenerative diseases such as AD and suggest that the unique properties associated with Cdk5/p25 hyperactivation may play a critical role in the pathogenesis of NFTs and neuronal death.

Alzheimer's Disease

Theories of Alzheimer's Disease

AD is a devastating neurodegenerative disease primarily affecting the elderly, although in rare cases there are inherited, familial AD (FAD). The pathological hallmarks of AD include

neuronal and synaptic loss, NFTs, and the presence of Aβ (amyloid beta) plaques in the postmortem brain. While the exact cause of sporadic AD is unknown, several hypotheses have garnered attention as contributing factors (Hardy & Selkoe 2002, Small & Duff 2008). The amyloid hypothesis posits that Aβ peptides, derived from the proteolytic processing of the transmembrane β-amyloid precursor protein (APP), accumulate and cause impairments in AD patients. FAD patients possess mutations in the APP gene, leading to an extensive area of APP studies using multiple animal models. Yet other FAD patients have presenilin 1 and 2 (PS1, PS2) mutations, genes which encode the proteolytic enzyme γ-secretase involved in the cleavage of APP to generate Aβ. Two other key enzymes in Aβ generation are α-secretase and β-secretase. After initial cleavage of the extracellular region of APP by either α- or β-secretase, γ-secretase cleavage occurs in the transmembrane domain to release either the non-pathogenic form of Aβ (p3) mediated by α-secretase or the pathogenic (Aβ42) peptide mediated by β-secretase. Another hypothesis suggests that tau hyperphosphorylation, in which tau filaments aggregate into insoluble NFTs, dampen cellular activity and lead to cognitive impairment. NFTs are also found in patients with frontotemporal dementia.

p25-mediated neurodegeneration

To examine how dysregulation of Cdk5 by p25 may play a role in synaptic plasticity, a p25 transgenic (p25-Tg) mouse model was created using a neuron-specific enolase promoter expressing human p25 cDNA (Ahlijanian et al. 2000). The mice exhibit increased locomoter activity and appear less anxious as tested by the elevated-plus maze. Moreover, dramatic axonal swelling and hyperphosphorylation of tau and NFs were detected. In a second p25 transgenic mouse model, p25 overexpression driven by the CaMKII promoter triggered neurodegeneration and activated microglia but not tau phosphorylation or Aβ formation (Mullyaert et al. 2008).

To examine further how Cdk5 may play a role in tau aggregation and tangle formation, a mouse model overexpressing human mutant tau (P301L) was crossed to the p25-Tg mice (Noble et al. 2003). Enhanced Cdk5 activity, axonopathy, and greater tau phosphorylation at known Cdk5 sites are observed in P301L/p25 double-transgenic mice. Furthermore, insoluble, aggregated tau and NFT are markedly increased in the brainstem. Around the same time, two other p25-Tg mouse models were generated using the CMV (cytomegalovirus) or the PGDF (platelet growth-derived factor) promoter, but neither produced noticeable increases in tau

phosphorylation or neuronal apoptosis (programmed cell death due to extrinsic or intrinsic pathways) (Bian et al. 2002, Takashima et al. 2001). Crossing Cdk5, p35, and tau in a triple transgenic mouse model did not generate NFTs (Van den Haute et al. 2001), suggesting tau phosphorylation may be due to elevated, potent Cdk5/p25 activity.

Although other p25 mouse models do not exhibit signs of neurodegeneration, in CK-p25 Tg mice (Cruz et al. 2003) long-term overexpression of p25 produces characteristic hallmarks of frontotemporal dementia and AD: progressive neuronal loss resulting in a dramatic reduction in brain weight, astrogliosis, enhanced NF phosphorylation as assayed by SMI34, tau hyperphosphorylation using AT-8 and PHF-1 antibodies, a higher abundance of sarkosyl-insoluble tau, and late-stage NFT-like pathology from Bodian silver staining and Thioflavin-S staining (Cruz et al. 2003). The pathological events in the CK-p25 Tg mice occur in the cortex and hippocampus, areas primarily affected in neurodegenerative diseases. Furthermore, p25 induction markedly enhances Aβ production and accumulation preceding neuron death, providing evidence that p25 overexpression can generate Aβ pathology in vivo (Cruz et al. 2006). The presence of increased β-secretase enzyme activity may act together with γ-secretase to generate the toxic Aβ42 fragment from APP. The phenotypes may be dose dependent, as a lower-expressing mouse model of p25 can partially ameliorate watermaze learning deficits and fear conditioning due to a proposed compensatory mechanism (Angelo et al. 2003).

APP is phosphorylated by Cdk5, which may affect its localization (Iijima et al. 2000, Lee et al. 2003) and Aβ induces Cdk5 hyperactivity, presumably due to Cdk5/p25, to phosphorylate tau in another AD model, Tg2576 (Otth et al. 2002). Intriguingly, double PS1/PS2 KO animals exhibit memory impairment, reduction in NMDARs and CREB-mediated gene expression, and accelerated, progressive neurodegeneration accompanied by an increase in p25 levels and hyperphosphorylated tau (Saura et al. 2004). A recent study utilized viral-mediated knockdown of Cdk5 to reduce NFTs in a 3X-Tg AD model, providing support for modulating p25 levels or overall Cdk5 activity as potential strategies in therapeutically targeting AD (Piedrahita et al. 2010). Aberrant Cdk5/p25 activity is also found in other neurodegenerative diseases (discussed below, also refer to **Figure 2**). Yet another potential therapeutic strategy is to reduce Aβ pathology by targeting β-secretase enzyme to diminish the neurodegeneration observed in various AD mouse models, including the CK-p25 Tg mice.

Epigenetic regulation in learning and memory

Epigenetics refers to long-lasting changes based on the modification of DNA or protein structures, such as chromatin, without altering the DNA sequence itself (Borrelli et al. 2008). Modifications include phosphorylation, DNA methylation, chromatin acetylation by histone acetylases (HATs) on histone complexes, and chromatin deacetylation by histone deacetylases (HDACs). HATs are generally viewed as relaxing the chromatin to permit gene transcription, whereas HDACs are seen as mainly functional for transcriptional repression. Recent publications have addressed the contribution of epigenetics, particularly individual HDACs, to other forms of neurological diseases in animal models (Fischer et al. 2010).

In work uncovering a link between Cdk5 in epigenetics, CK-p25 Tg mice (Cruz et al. 2003) exhibiting signs of neurodegeneration were placed into an enriched environment. Despite massive neuronal loss, CK-p25 Tg mice in an enriched environment have enhanced learning ability as a result of new synapse formation in the surviving neurons and can remarkably recover their older memories (Fischer et al. 2007). Chromatin remodeling results in altered acetylation levels of various residues on histones H3 (lysine 14 or K14) and H4 (K5). The CK-p25 Tg mice treated with the broad HDAC inhibitor (HDACi) sodium butyrate show increased acetylation levels of H3 and H4, improved learning, and, most dramatically, restored access to long-lost memories in a similar manner to that seen in an enriched environment. Thus, altered epigenetic regulation in disease states may potentially be abrogated by drugs that target particular chromatin-remodeling enzymes.

Molecular alterations occur in the neuronal landscape prior to neurodegeneration in CK-p25 Tg mice. After two weeks of p25 induction, Cdk5/p25 inhibits HDAC1 and upregulates a number of genes involved in neuronal cell death, cell-cycle reactivation, and DNA double-strand breaks as measured by γH2AX staining and increased transcription of cyclins A, B, E, E2F1, Ki-67, and PCNA genes (Kim et al. 2008). Restoring HDAC1 can prevent neurons from undergoing double-strand breaks and cell death in a rodent model of ischemia. Cdk5 also phosphorylates nuclear ATM, a key molecule in mediating DNA damage responses and cell death (Tian et al. 2009), Ape1, a protein involved in DNA repair (Huang et al. 2010), and mSds3, a component of the HDAC transcriptional corepressor complex (Li et al. 2004). The results highlight the importance of epigenetic regulation in disease. Indeed, Cdk5/p25 appears to be involved in parallel processes ranging from DNA damage, epigenetic modifications, to neurodegeneration.

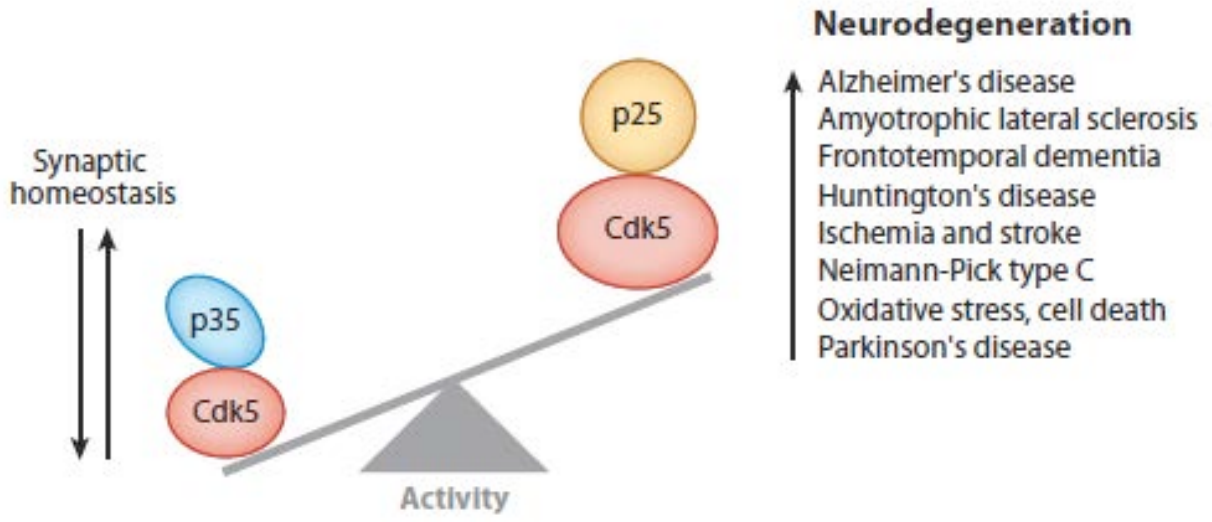

Figure 2 Cdk5, p35, and p25 are critical components in maintaining synaptic homeostasis with implications on neurodegenerative diseases. An emerging hypothesis predicts that Cdk5 mediates a neuronal intrinsic property in regulating synaptic homeostasis. Maintaining appropriate levels of Cdk5 signaling provides a compensatory mechanism by which the cell normally responds to environmental stressors until severe disruptions lead to irreversible damage. Aberrant, mistargeted Cdk5 activity due to neurotoxicity and calpain-mediated cleavage of p35 to p25 will cause an imbalance in synaptic excitability and the generation of the Cdk5/p25 complex. Elevated and sustained Cdk5/p25 activity consequently modulates downstream events leading to DNA damage, epigenetic changes, and neurodegeneration.

Cdk5 and neurodegenerative diseases

The etiology of many diseases such as AD, Parkinson's, and amyotrophic lateral sclerosis (ALS) is unknown, and these sporadic (idiopathic) cases comprise the majority of neurodegenerative diseases. Signature pathological hallmarks characterize each disease with different brain regions initially, and preferentially, affected. Nonetheless, as each disease progresses, neuronal death is severe and cognitive impairments are profound. Cdk5/p35 may serve as the common mechanism of neurodegeneration given its early function in response to neurotoxic agents that give rise to Cdk5/p25 activation in a particular cellular compartment. As Cdk5/p25 has been implicated in many neurodegenerative diseases, it merits closer examination.

Amyotrophic Lateral Sclerosis

ALS is a rapid, progressive disease in which spinal motor neurons degenerate, leading to muscle atrophy, loss of movement, and eventually death. The copper/zinc superoxide dismutase 1 (SOD1) was identified in ALS patients as a gene that contained point mutations (Bowling et al. 1993). SOD1 normally eliminates free radicals in the body, and although the exact role of SOD1 in ALS remains unknown, it is thought that mutant SOD1 aggregate to provoke multiple intrinsic toxicities including mitochondrial dysfunction, neurite and axonal abnormalities, and axonal transport impairments.

In a mouse model of ALS (SOD1G37R), the p25/p35 ratio was enhanced (Nguyen et al. 2001). The NF heavy chain, a Cdk5 substrate, was hyperphosphorylated in the spinal cord as examined by AT-8 and PHF-1, which causes an abnormal distribution that colocalizes with Cdk5/p25. It is suggested that the NF heavy chain in the perikarya (cell body) may serve as a phosphorylation sink for Cdk5/p25, which would confer a protective effect on the neuron by sequestering the complex and preventing further toxicity.

The relationship between p25, neurodegenerative diseases, and epigenetics was further examined in the CK-p25 Tg mouse model (Kim et al. 2007). In CK-p25 Tg as well as SOD1G37R mice, there is an increase in histone deacetylase sirtuin 1 (SIRT1) levels throughout neurodegeneration. SIRT1 confers a neuroprotective effect on multiple organisms, and it is activated by the compound resveratrol. In vivo, application of resveratrol, a SIRT1 activator, or SIRT1 injections into the mouse brain protect against neurodegeneration and cognitive decline in

the CK-p25 Tg mice. There is an increase in the tumor suppressor p53 in CK-p25 Tg mice, but activation of SIRT1 by resveratrol reduces acetylation and total p53 levels.

Recently, mutations were identified in FUS/TLS, a DNA/RNA binding protein, of familial ALS patients in which FUS/TLS accumulated abnormally in the cytoplasm (Kwiatkowski et al. 2009, Vance et al. 2009). Mutations in TAR DNA binding protein (TDP-43), a gene with a structure similar to FUS/TLS, is also implicated in ALS (Sreedharan et al. 2008). One study found that TDP-43 is phosphorylated at serine residues and ubiquitinated in both ALS and frontotemporal dementia (Neumann et al. 2006). It would be interesting to speculate whether Cdk5/p25 interacts with components of the DNA/RNA processing pathways in ALS and if Cdk5/p25 colocalizes to cytoplasmic aggregates of FUS/TLS and TDP-43.

Niemann-Pick Type C

Niemann-Pick type C (NPC) is caused by mutations on the NPC gene and is an autosomal-recessive neurodegenerative disorder that occurs without the presence of Aβ, causing distorted lipid storage in neurons, dendritic and axonal abnormalities, demyelination, and neuronal death (Elleder et al. 1985). NFTs, comprised of PHFs and phosphorylated tau, are present in those with NPC disease (Auer et al. 1995).

Although one study did not find greater Cdk5/p25 activity as measured by tau phosphorylation using NPC KO mouse models (Sawamura et al. 2001), another group found an increase in hyperphosphorylated tau (Bu et al. 2002). Additionally, kinase assays reveal an increase in Cdk5 activity in the NPC KO mice corresponding to an increase in p25 levels in human and mouse NPC models, in which Cdk5/p25 colocalizes with hyperphosphorylated tau in brain tissue. Inhibitors of Cdk5 attenuate the effects of tau hyperphosphorylation and motor defects (Zhang et al. 2004).

The issue of whether Cdk5/p25 is required for the pathogenesis in ALS and NPC, or even AD, remains unresolved and is complicated by the lack of a reduction in tau pathology onset and progression using p35 KO mice in animal models of ALS and NPC (Hallows et al. 2006, Takahashi & Kulkarni 2004). However, it cannot be ruled out that another Cdk5 coactivator, p39 may compensate for loss of p35 function in these diseases or whether deletion of p35 throughout development serves as a representative animal model for neurodegeneration.

Ischemia and Stroke

The use of a cerebral focal ischemia paradigm in rodent models can increase Cdk5 activity (Green et al. 1997, Hayashi et al. 1999). Moreover, ischemia induces hippocampal CA1 pyramidal cell death primarily by Cdk5 phosphorylation of NR2A receptors (Wang et al. 2003). In hippocampal CA1 neurons, p25 is induced following ischemia, and inhibiting Cdk5 using Cdk5-DN protects them from cell death. It is proposed that ischemia, a form of excitotoxicity, induces calpain activity to generate p25, which then allows Cdk5/p25 phosphorylation of the NR2A receptors. This, in turn, results in an increased channel conductance and potentiates its function, which ultimately causes cell death. The activation of NR2A receptors may require calcium influx through the AMPA receptors as well, which can account for multiple sources of calcium during excitotoxicity that stimulate calpain. Interestingly, Cdk5/p25 has been implicated in promotion of cell apoptosis in neurons that have been subjected to endoplasmic reticulum-mediated stress, suggesting an interplay between ischemia and other cellular compartments in which Cdk5/p25 is activated (Saito et al. 2007).

Consistent with the known events underlying p25 generation, Cdk5 also appears to mediate the excitotoxic component of cell death by an NMDA receptor-dependent pathway (Rashidian et al. 2005), whereas inhibition of the cell-cycle regulator Cdk4 may be involved in the delayed component of cell death. This suggests that Cdk5/p25 may be present during the early phase of neurotoxicity and acts in concert with chromatin remodeling enzymes, such as HDAC1, in regulating the transcription of cell-cycle genes. The link between Cdk5, p25, and cell-cycle gene regulation provides a converging avenue for further research, especially regarding DNA damage and its relationship to neuronal loss.

Recent work utilizes in vivo models of ischemia to examine Cdk5 in neuronal death. Under ischemic conditions, Cdk5 activity mediates excitotoxic cell death by phosphorylating cytoplasmic peroxiredoxin 2 (Prx 2) (Qu et al. 2007, Rashidian et al. 2009). In contrast, under focal ischemia by endothelin-1 application in the striatum, Cdk5 activity is present in the nucleus and facilitates neuronal death by phosphorylating myocyte enhancer factor 2D (MEF2D) (Smith et al. 2006). MEF2D was previously identified as a Cdk5 substrate in which it is degraded following phosphorylation in neurotoxiciy-induced apoptosis (Gong et al. 2003). The regional and substrate specificities in different ischemia models point to different components of neuronal death that share a common pathway involving Cdk5/p25. Cdk5/p25 hyperactivity is linked to

NFTs after transient ischemia (Wen et al. 2007), perhaps sharing similar mechanisms with AD or frontotemporal dementia.

Parkinson's Disease

Parkinson's disease (PD) is a neurodegenerative disorder characterized by α-synuclein-containing Lewy body inclusions, loss of dopaminergic neurons in the substantia nigra pars compacta, and impaired motor skills and cognition (Olanow & Tatton 1999). Symptoms include tremors, muscle rigidity, and postural instability. Current treatments for PD include dopamine agonists or deep-brain stimulation. In animal models, application of the chemical compound 1-methyl-4-phenyl-1,2,3,6-tetrahydropyridine (MPTP) is sufficient to induce the pathological consequences of PD.

Cdk5/p35 is elevated in the Lewy bodies of postmortem PD brains (Brion & Couck 1995, Nakamura et al. 1997, Takahashi et al. 2000) but not in others (Muntane et al. 2008). In MPTP-administered mice, greater Cdk5/p25 levels and robust kinase activity were observed in dopaminergic neurons (Smith et al. 2003). MPTP treatment does not affect other Cdks including Cdk2 or Cdk4, and treatment with either a Cdk5 inhibitor or Cdk5-DN virus attenuates neuronal death in dopaminergic neurons. The findings parallel Cdk5 signaling in the striatum because MPTP treatment also increases levels of ΔFosB, a transcriptional regulator of Cdk5 that is upregulated during drug addiction. However, in this mouse model of PD, Cdk2 and Cdk4 do not appear to play a critical role in MPTP-induced neuron death, in contrast to ischemia models.

A recent study identified parkin, a gene most frequently implicated in familial PD, as a Cdk5 interaction partner and substrate (Avraham et al. 2007). Parkin may confer a neuroprotective effect by its function as a ubiquitin ligase enzyme with substrates including α-synuclein, synphilin-1, and p38. Cdk5/p35 phosphorylation of parkin can diminish the auto-ubiquitination activity of parkin, which then modulates synphilin-1/α-synuclein inclusion formation.

Further work on the modulation of dopaminergic signaling by Cdk5/p35 revealed that Cdk5/p35 interacts with and phosphorylates Prx2 to downregulate its activity (Qu et al. 2007). Prx2 is thought to play a neuroprotective role, and diminishing Prx2 in neurons mediates neuronal death through reactive oxygen species both in vitro and in a MPTP mouse model of PD specifically in dopaminergic neurons of the substantia nigra pars compacta. Interestingly, MPTP

mediates calpain cleavage to generate Cdk5/p25, consistent with Prx2 phosphorylation during ischemia, and deregulates phosphorylation of the transcription factor MEF2D (Smith et al. 2006). Moreover, in human PD postmortem brain samples, an increase in phospho-Prx2 can be detected. These findings complement recent observations of Cdk5/p35 signaling in the nucleus in which the phosphorylated apurinic/apyrimidinic endonuclease 1 (Ape1) substrate exhibits decreased endonuclease activity, resulting accumulated DNA damage and MPTP-mediated neuronal death (Huang et al. 2010). Increased phospho-Ape1 is also observed in human PD and AD brains. An emerging notion suggests that Cdk5/p35 is active in different cellular compartments of dopaminergic neurons and that it can potentially trigger various factors in a cascade that is detrimental to neuronal integrity.

Huntington's Disease

Huntington's disease (HD) is an autosomal-dominant disorder caused by an expansion in the number of CAG-repeats in the Huntington gene, leading to abnormally large polyglutamine (poly-Q) repeats in the huntington (htt) protein (Cattaneo et al. 2001). HD patients exhibit involuntary tremors called chorea, physical impairments, and irreversible cognitive decline. Cdk5 phosphorylates htt in cytoplasmic fractions, which results in reduced caspase cleavage of htt and, in turn, lessens its aggregate formation and toxicity (Luo et al. 2005). There is a reduction of Cdk5 in late-stage HD patients, and the stabilization of Cdk5/p35 interaction is impaired by mutant htt. Reduction of Cdk5 activity is in contrast to previous observations in PD patients or mouse models of ALS and ischemia, and it could reflect a late-stage compensatory mode.

A separate study identified additional htt Cdk5 phosphorylation sites that confer a neuroprotective effect (Anne et al. 2007). Generation of phosphomutants mimic toxic htt and is mediated in part by p53. Moreover, γH2AX staining shows Cdk5/p35 phosphorylation of htt during DNA damage, which is consistent with Cdk5/p25 and DNA damage in CK-p25 Tg mice (Kim et al. 2008). Phosphorylation of htt precedes neuronal death, providing yet another line of evidence in a different disease system that Cdk5/p35 is upstream of a complex signaling cascade involving cell-cycle genes and DNA damage in postmitotic neurons, all of which are early events preceding neuronal death.

There was no examination of p25 levels in the previous mouse studies; nonetheless, Cdk5/p25 activity or p25/p35 ratio are predicted to be elevated during disease states. Whereas Cdk5 and p35 levels are decreased in postmortem HD brain samples, Cdk5 phosphorylation and p25 levels mediated by calpain activity are increased in dopaminergic neurons (Paoletti et al. 2008). Because the striatum is affected in HD and mutant htt is present in dopaminergic neurons, Cdk5/p25 can be regulated by intracellular calcium levels and phosphorylation downstream of the dopamine D1 receptor as well as the NMDA receptor. Therefore, Cdk5/p25 may initially function in an activity-dependent manner similar to other diseases such as PD but diverge in the final outcomes through currently unknown mechanisms.

Potential therapeutic approaches

In addition to its role in neurodegenerative disease, Cdk5 is involved in neurogenesis by regulating the progression of newly born granule cells in the adult hippocampus of mouse brain (Jessberger et al. 2008, Lagace et al. 2008). Recent studies have also focused on the non-neuronal functions of Cdk5 (also see Table 1). Cdk5 is present in adipose tissue, as Cdk5/p25 hyperphosphorylation of the diabetes target gene PPARγ inhibits the transcription of antiobesity genes (Choi et al. 2010). Other studies implicate Cdk5/p35 in neuregulin-induced acetylcholine receptor formation at the neuromuscular junction (Fu et al. 2001, 2005), pain signaling in the dorsal root ganglion (Pareek et al. 2006, 2007), cellular senescence (Mao and Hinds 2010), and pancreatic cancer cell signaling (Feldman et al. 2010). Furthermore, the importance of Cdk5 activity has been demonstrated in other model organisms, including *Drosophila* for proper axon formation and guidance (Connell-Crowley et al. 2000, Connell-Crowley et al. 2007), and *Caenorhabditis elegans* for proper targeting of presynaptic components to axons (Ou et al. 2010), synaptic vesicle organization in facilitating synapse formation of DD motoneurons (Park et al. 2011) or regulating glutamate receptor abundancy to their ventral nerve cords (Juo et al. 2007). Thus, Cdk5 presents an attractive target for therapeutic intervention during both developmental and aging processes.

Given the ever-increasing discoveries expanding the functions of Cdk5, it would be beneficial to examine and develop novel Cdk5 inhibitors for the treatment of various disorders. Cdk5 inhibitors such as roscovitine, olomoucine, or butyrolactone-1 are widely used, but the main disadvantage is their inhibition of other Cdks (Glab et al. 1994, Glicksman et al. 2007,

Meijer et al. 1997). Taken together, developing therapies for neurodegeneration and other non-neuronal disorders may include a combinatorial approach designed in order to activate HDAC1 to maintain DNA integrity, target p35 to block p25 generation, and reduce Cdk5 activity with novel Cdk5-specific inhibitors.

Conclusions

Research over the past two decades on Cdk5 has provided informative data on its diverse cellular functions. Not only is Cdk5 essential for proper neural development and migration, but Cdk5/p35 is also critically involved in neurite and axonal outgrowth, synaptic plasticity, cognition, and behavior. Work on Cdk5/p25 has yielded considerable insight into the pathogenesis of various neurological disorders. Nevertheless, it remains unresolved how Cdk5 regulates synaptic plasticity during initial events of neurotoxicity and how excessive Cdk5/p25 activity affects pathological events leading to neurodegeneration. Collectively, examining Cdk5 in the greater context of homeostatic regulation may be beneficial in elucidating neurological disorders affecting cognition.

References

Ackerley S, Thornhill P, Grierson AJ, Brownlees J, Anderton BH, et al. (2003). Neurofilament heavy chain side arm phosphorylation regulates axonal transport of neurofilaments. J. Cell Biol. 161:489-95.

Adzic M, Djordjevic J, Djordjevic A, Niciforovic A, Demonacos C, et al. (2009). Acute or chronic stress induce cell compartment-specific phosphorylation of glucocorticoid receptor and alter its transcriptional activity in Wistar rat brain. J Endocrinol. 202:87-97.

Agarwal-Mawal A, Paudel HK. (2001). Neuronal Cdc2-like protein kinase (Cdk5/p25) is associated with protein phosphatase 1 and phosphorylates inhibitor-2. J. Biol. Chem. 276:23712-18.

Ahlijanian MK, Barrezueta NX, Williams RD, Jakowski A, Kowsz KP, et al. (2000). Hyperphosphorylated tau and neurofilament and cytoskeletal disruptions in mice overexpressing human p25, an activator of cdk5. Proc. Natl. Acad. Sci. USA 97:2910-15.

Angelo M, Plattner F, Irvine EE, Giese KP. (2003). Improved reversal learning and altered fear conditioning in transgenic mice with regionally restricted p25 expression. Eur. J. Neurosci. 18:423-31.

Anne SL, Saudou F, Humbert S. (2007). Phosphorylation of huntingtin by cyclin-dependent kinase 5 is induced by DNA damage and regulates wild-type and mutant huntingtin toxicity in neurons. J. Neurosci. 27:7318-28.

Auer IA, Schmidt ML, Lee VM, Curry B, Suzuki K, et al. (1995). Paired helical filament tau (PHFtau) in Niemann-Pick type C disease is similar to PHFtau in Alzheimer's disease. Acta Neuropathol. 90:547-51.

Avraham E, Rott R, Liani E, Szargel R, Engelender S. (2007). Phosphorylation of Parkin by the cyclin-dependent kinase 5 at the linker region modulates its ubiquitin-ligase activity and aggregation. J. Biol. Chem. 282:12842-50.

Baumann K, Mandelkow EM, Biernat J, Piwnica-Worms H, Mandelkow E. (1993). Abnormal Alzheimer-like phosphorylation of tau-protein by cyclin-dependent kinases cdk2 and cdk5. FEBS Lett. 336:417-24.

Beaudette KN, Lew J, Wang JH. (1993). Substrate specificity characterization of a cdc2-like protein kinase purified from bovine brain. J. Biol. Chem. 268:20825-30.

Bian F, Nath R, Sobocinski G, Booher RN, Lipinski WJ, et al. (2002). Axonopathy, tau abnormalities, and dyskinesia, but no neurofibrillary tangles in p25-transgenic mice. J. Comp. Neurol. 446:257-66.

Bibb JA, Chen J, Taylor JR, Svenningsson P, Nishi A, et al. (2001). Effects of chronic exposure to cocaine are regulated by the neuronal protein Cdk5. Nature 410:376-80.

Bibb JA, Snyder GL, Nishi A, Yan Z, Meijer L, et al. (1999). Phosphorylation of DARPP-32 by Cdk5 modulates dopamine signalling in neurons. Nature 402:669-71.

Bliss TVP, Collingridge GL. (1993). A synaptic model of memory: long-term potentiation in the hippocampus. Nature 361:31-9.

Borrelli E, Nestler EJ, Allis CD, Sassone-Corsi P. (2008). Decoding the epigenetic language of neuronal plasticity. Neuron 60:961-74.

Bowling AC, Schulz JB, Brown RH Jr, Beal MF. (1993). Superoxide dismutase activity, oxidative damage, and mitochondrial energy metabolism in familial and sporadic amyotrophic lateral sclerosis. J. Neurochem. 61:2322-25.

Brion JP, Couck AM. (1995). Cortical and brainstem-type Lewy bodies are immunoreactive for the cyclin-dependent kinase 5. Am. J. Pathol. 147:1465-76.

Brown M, Jacobs T, Eickholt B, Ferrari G, Teo M, et al. (2004). α2-Chimaerin, cyclin-dependent kinase 5/p35, and its target collapsin response mediator protein-2 are essential components in semaphorin 3A-induced growth-cone collapse. J. Neurosci. 24:8994-9004.

Bu B, Li J, Davies P, Vincent I. (2002). Deregulation of cdk5, hyperphosphorylation, and cytoskeletal pathology in the Niemann-Pick type C murine model. J. Neurosci. 22:6515-25.

Cattaneo E, Rigamonti D, Goffredo D, Zuccato C, Squitieri F, Sipione S. (2001). Loss of normal huntingtin function: new developments in Huntington's disease research. Trends Neurosci. 24:182-88.

Chae T, Kwon YT, Bronson R, Dikkes P, Li E, Tsai LH. (1997). Mice lacking p35, a neuronal specific activator of Cdk5, display cortical lamination defects, seizures, and adult lethality. Neuron 18:29-42.

Cheng K, Li Z, Fu WY, Wang JH, Fu AK, Ip NY. (2002). Pctaire1 interacts with p35 and is a novel substrate for Cdk5/p35. J. Biol. Chem. 277:31988-93.

Chergui K, Svenningsson P, Greengard P. (2004). Cyclin-dependent kinase 5 regulates dopaminergic and glutamatergic transmission in the striatum. Proc. Natl. Acad. Sci. USA 101:2191-96.

Cheung ZH, Chin WH, Chen Y, Ng YP, Ip NY. (2007). Cdk5 is involved in BDNF-stimulated dendritic growth in hippocampal neurons. PLoS Biol. 5:e63.

Choe EA, Liao L, Zhou JY, Cheng D, Duong DM, et al. 2007. Neuronal morphogenesis is regulated by the interplay between cyclin-dependent kinase 5 and the ubiquitin ligase mind bomb 1. J. Neurosci. 27:9503-12.

Choi JH, Banks AS, Estall JL, Kajimura S, Bostrom P, et al. (2010). Anti-diabetic drugs inhibit obesity-linked phosphorylation of PPARγ by Cdk5. Nature 466:451-56.

Connell-Crowley L, Le Gall M, Vo DJ, Giniger E. (2000). The cyclin-dependent kinase 5 Cdk5 controls multiple aspects of axon patterning in vivo. Curr Biol. 10:599-602.

Connell-Crowley L, Vo D, Luke L, Giniger E. (2007). Drosophila lacking the Cdk5 activator, p35, display defective axon guidance, age-dependent behavioral deficits and reduced lifespan. Mech. Dev. 124:341-9.

Cruz JC, Kim D, Moy LY, Dobbin MM, Sun X, et al. (2006). p25/cyclin-dependent kinase 5 induces production and intraneuronal accumulation of amyloid β in vivo. J. Neurosci. 26:10536-41.

Cruz JC, Tseng HC, Goldman JA, Shih H, Tsai LH. (2003). Aberrant Cdk5 activation by p25 triggers pathological events leading to neurodegeneration and neurofibrillary tangles. Neuron 40:471-83.

De Vos KJ, Grierson AJ, Ackerley S, Miller CC. (2008). Role of axonal transport in neurodegenerative diseases. Annu. Rev. Neurosci. 31:151-73.

Dhavan R, Greer PL, Morabito MA, Orlando LR, Tsai LH. (2002). The cyclin-dependent kinase 5 activators p35 and p39 interact with the α-subunit of Ca^{2+}/calmodulin-dependent protein kinase II and α-actinin-1 in a calcium-dependent manner. J. Neurosci. 22:7879-91.

Dhavan R, Tsai LH. (2001). A decade of CDK5. Nat. Rev. Mol. Cell Biol. 2:749-59.

Elleder M, Jirasek A, Smid F, Ledvinova J, Besley GT. (1985). Niemann-Pick disease type C. Study on the nature of the cerebral storage process. Acta Neuropathol. 66:325-36.

Evans GJ, Cousin MA. (2007). Activity-dependent control of slow synaptic vesicle endocytosis by cyclin-dependent kinase 5. J. Neurosci. 27:401-11.

Feldmann G, Mishra A, Hong SM, Bisht S, Strock CJ, et al. (2010). Inhibiting the cyclin-dependent kinase CDK5 blocks pancreatic cancer formation and progression through the suppression of Ras-Ral signaling. Cancer Res. 70: 4460-9.

Fischer A, Sananbenesi F, Mungenast A, Tsai LH. (2010). Targeting the correct HDAC(s) to treat cognitive disorders. Trends Pharmacol. Sci. 31:605-17.

Fischer A, Sananbenesi F, Pang PT, Lu B, Tsai LH. (2005). Opposing roles of transient and prolonged expression of p25 in synaptic plasticity and hippocampus-dependent memory. Neuron 48:825-38.

Fischer A, Sananbenesi F, Wang X, Dobbin M, Tsai LH. (2007). Recovery of learning and memory is associated with chromatin remodelling. Nature 447:178-82.

Fletcher AI, Shuang R, Giovannucci DR, Zhang L, Bittner MA, Stuenkel EL. (1999). Regulation of exocytosis by cyclin-dependent kinase 5 via phosphorylation of Munc18. J. Biol. Chem. 274:4027-35.

Floyd SR, Porro EB, Slepnev VI, Ochoa GC, Tsai LH, De Camilli P. (2001). Amphiphysin 1 binds the cyclin-dependent kinase (cdk) 5 regulatory subunit p35 and is phosphorylated by cdk5 and cdc2. J. Biol. Chem. 276:8104-10.

Fu AK, Fu WY, Cheung J, Tsim KW, Ip FC, et al. (2001). Cdk5 is involved in neuregulin-induced AChR expression at the neuromuscular junction. Nat. Neurosci. 4:374-81.

Fu AK, Fu WY, Ng AK, Chien WW, Ng YP, et al. (2004). Cyclin-dependent kinase 5 phosphorylates signal transducer and activator of transcription 3 and regulates its transcriptional activity. Proc. Natl. Acad. Sci. USA 101:6728-33.

Fu AK, Ip FC, Fu WY, Cheung J, Wang JH, et al. (2005). Aberrant motor axon projection, acetylcholine receptor clustering, and neurotransmission in cyclin-dependent kinase 5 null mice. Proc. Natl. Acad. Sci. USA 102:15224-29.

Fu AK, Ip NY. (2007). Cyclin-dependent kinase 5 links extracellular cues to actin cytoskeleton during dendritic spine development. Cell Adh. Migr. 1:110-12.

Fu WY, Chen Y, Sahin M, Zhao XS, Shi L, et al. (2007). Cdk5 regulates EphA4-mediated dendritic spine retraction through an ephexin1-dependent mechanism. Nat. Neurosci. 10:67-76.

Glab N, Labidi B, Qin LX, Trehin C, Bergounioux C, Meijer L. (1994). Olomoucine, an inhibitor of the cdc2/cdk2 kinases activity, blocks plant cells at the G1 to S and G2 to M cell cycle transitions. FEBS Lett. 353:207-11.

Glicksman MA, Cuny GD, Liu M, Dobson B, Auerbach K, et al. (2007). New approaches to the discovery of cdk5 inhibitors. Curr. Alzheimer Res. 4:547-49.

Gong B, Wang H, Gu S, Heximer SP, Zhuo M. (2007). Genetic evidence for the requirement of adenylyl cyclase 1 in synaptic scaling of forebrain cortical neurons. Eur. J. Neurosci. 26:275-88.

Gong X, Tang X, Wiedmann M, Wang X, Peng J, et al. (2003). Cdk5-mediated inhibition of the protective effects of transcription factor MEF2 in neurotoxicity-induced apoptosis. Neuron 38:33-46.

Green SL, Kulp KS, Vulliet R. (1997). Cyclin-dependent protein kinase 5 activity increases in rat brain following ischemia. Neurochem. Int. 31:617-23.

Hallows JL, Iosif RE, Biasell RD, Vincent I. (2006). p35/p25 is not essential for tau and cytoskeletal pathology or neuronal loss in Niemann-Pick type C disease. J. Neurosci. 26:2738-44.

Hamdane M, Bretteville A, Sambo AV, Schindowski K, Begard S, et al. (2005). p25/Cdk5-mediated retinoblastoma phosphorylation is an early event in neuronal cell death. J. Cell Sci. 118:1291-98.

Harada T, Morooka T, Ogawa S, Nishida E. (2001). ERK induces p35, a neuron-specific activator of Cdk5, through induction of Egr1. Nat. Cell Biol. 3:453-59.

Hardy J, Selkoe DJ. (2002). The amyloid hypothesis of Alzheimer's disease: progress and problems on the road to therapeutics. Science 297:353-56.

Hashiguchi M, Saito T, Hisanaga S, Hashiguchi T. (2002). Truncation of CDK5 activator p35 induces intensive phosphorylation of Ser202/Thr205 of human tau. J. Biol. Chem. 277:44525-30.

Hawasli AH, Benavides DR, Nguyen C, Kansy JW, Hayashi K, et al. (2007). Cyclin-dependent kinase 5 governs learning and synaptic plasticity via control of NMDAR degradation. Nat. Neurosci. 10:880-86.

Hayashi T, Warita H, Abe K, Itoyama Y. (1999). Expression of cyclin-dependent kinase 5 and its activator p35 in rat brain after middle cerebral artery occlusion. Neurosci. Lett. 265:37-40.

Hirasawa M, Ohshima T, Takahashi S, Longenecker G, Honjo Y, et al. (2004). Perinatal abrogation of Cdk5 expression in brain results in neuronal migration defects. Proc. Natl. Acad. Sci. USA 101:6249-54.

Hou Z, He L, Qi RZ. (2007). Regulation of s6 kinase 1 activation by phosphorylation at ser-411. J. Biol. Chem. 282:6922-28.

Humbert S, Dhavan R, Tsai LH. (2000a). p39 activates cdk5 in neurons, and is associated with the actin cytoskeleton. J Cell Sci 113:975-83.

Humbert S, Lanier LM, Tsai LH. (2000b). Synaptic localization of p39, a neuronal activator of cdk5. Neuroreport 11:2213-16.

Huang C, Rajfur Z, Yousefi N, Chen Z, Jacobson K, Ginsberg MH. (2009). Talin phosphorylation by Cdk5 regulates Smurf1-mediated talin head ubiquitylation and cell migration. Nat Cell Biol. 11:624-30.

Huang E, Qu D, Zhang Y, Venderova K, Haque ME, et al. (2010). The role of Cdk5-mediated apurinic/apyrimidinic endonuclease 1 phosphorylation in neuronal death. Nat. Cell Biol. 12:563-71.

Iijima K, Ando K, Takeda S, Satoh Y, Seki T, et al. (2000). Neuron-specific phosphorylation of Alzheimer's β-amyloid precursor protein by cyclin-dependent kinase 5. J. Neurochem. 75:1085-91.

Ishizuka K, Kamiya A, Oh EC, Kanki H, Seshadri S, et al. (2011). DISC1-dependent switch from progenitor proliferation to migration in the developing cortex. Nature 473:92-6.

Jessberger S, Aigner S, Clemenson GD Jr, Toni N, Lie DC, et al. (2008). Cdk5 regulates accurate maturation of newborn granule cells in the adult hippocampus. PLoS Biol. 6:e272.

Juo P, Harbaugh T, Garriga G, Kaplan JM. (2007). CDK-5 regulates the abundance of GLR-1 glutamate receptors in the ventral cord of Caenorhabditis elegans. Mol Biol Cell. 18:3883-93.

Kansy JW, Daubner SC, Nishi A, Sotogaku N, Lloyd MD, et al. (2004). Identification of tyrosine hydroxylase as a physiological substrate for Cdk5. J. Neurochem. 91:374-84.

Kato G, Maeda S. (1999). Neuron-specific Cdk5 kinase is responsible for mitosis-independent phosphorylation of c-Src at Ser75 in human Y79 retinoblastoma cells. J. Biochem. 126:957-61.

Kawauchi T, Chihama K, Nabeshima Y, Hoshino M. (2006). Cdk5 phosphorylates and stabilizes p27kip1 contributing to actin organization and cortical neuronal migration. Nat. Cell Biol. 8:17-26.

Kesavapany S, Amin N, Zheng YL, Nijhara R, Jaffe H, et al. (2004). p35/cyclin-dependent kinase 5 phosphorylation of ras guanine nucleotide releasing factor 2 (RasGRF2) mediates Rac-dependent extracellular signal-regulated kinase 1/2 activity, altering RasGRF2 and microtubule-associated protein 1b distribution in neurons. J. Neurosci. 24:4421-31.

Kesavapany S, Lau KF, McLoughlin DM, Brownlees J, Ackerley S, et al. (2001). p35/cdk5 binds and phosphorylates β-catenin and regulates β-catenin/presenilin-1 interaction. Eur. J. Neurosci. 13:241-47.

Keshvara L, Magdaleno S, Benhayon D, Curran T. (2002). Cyclin-dependent kinase 5 phosphorylates disabled 1 independently of Reelin signaling. J. Neurosci. 22:4869-77.

Kim D, Frank CL, Dobbin MM, Tsunemoto RK, Tu W, et al. (2008). Deregulation of HDAC1 by p25/Cdk5 in neurotoxicity. Neuron 60:803-17.

Kim D, Nguyen MD, Dobbin MM, Fischer A, Sananbenesi F, et al. (2007). SIRT1 deacetylase protects against neurodegeneration in models for Alzheimer's disease and amyotrophic lateral sclerosis. EMBO J. 26:3169-79.

Kim SH, Ryan TA. (2010). CDK5 serves as a major control point in neurotransmitter release. Neuron 67:797-809.

Kim Y, Sung JY, Ceglia I, Lee KW, Ahn JH, et al. (2006). Phosphorylation of WAVE1 regulates actin polymerization and dendritic spine morphology. Nature 442:814-17.

Kino T, Ichijo T, Amin ND, Kesavapany S, Wang Y, et al. (2007). Cyclin-dependent kinase 5 differentially regulates the transcriptional activity of the glucocorticoid receptor through phosphorylation: clinical implications for the nervous system response to glucocorticoids and stress. Mol Endocrinol. 21:1552-68.

Ko J, Humbert S, Bronson RT, Takahashi S, Kulkarni AB, et al. (2001). p35 and p39 are essential for cyclin-dependent kinase 5 function during neurodevelopment. J. Neurosci. 21:6758-71.

Kobayashi S, Ishiguro K, Omori A, Takamatsu M, Arioka M, et al. (1993). A cdc2-related kinase PSSALRE/cdk5 is homologous with the 30 kDa subunit of tau protein kinase II, a proline-directed protein kinase associated with microtubule. FEBS Lett. 335:171-75.

Kwiatkowski TJ Jr, Bosco DA, Leclerc AL, Tamrazian E, Vanderburg CR, et al. (2009). Mutations in the FUS/TLS gene on chromosome 16 cause familial amyotrophic lateral sclerosis. Science 323:1205-8.

Kwon YT, Gupta A, Zhou Y, Nikolic M, Tsai LH. (2000). Regulation of N-cadherin-mediated adhesion by the p35-Cdk5 kinase. Curr. Biol. 10:363-72.

Lagace DC, Benavides DR, Kansy JW, Mapelli M, Greengard P, et al. (2008). Cdk5 is essential for adult hippocampal neurogenesis. Proc. Natl. Acad. Sci. USA 105:18567-71.

Lee JH, Kim HS, Lee SJ, Kim KT. (2007). Stabilization and activation of p53 induced by Cdk5 contributes to neuronal cell death. J. Cell Sci 120:2259-71.

Lee KY, Helbing CC, Choi KS, Johnston RN, Wang JH. (1997). Neuronal Cdc2-like kinase (Nclk) binds and phosphorylates the retinoblastoma protein. J Biol Chem 272: 5622-26.

Lee MS, Kao SC, Lemere CA, Xia W, Tseng HC et al. (2003). APP processing is regulated by cytoplasmid phosphorylation. J. Cell Biol. 163:83-95.
Lee MS, Kwon YT, Li M, Peng J, Friedlander RM, Tsai LH. (2000). Neurotoxicity induces cleavage of p35 to p25 by calpain. Nature 405:360-64.
Lee SY, Wenk MR, Kim Y, Nairn AC, De Camilli P. (2004). Regulation of synaptojanin 1 by cyclin-dependent kinase 5 at synapses. Proc. Natl. Acad. Sci. USA 101:546-51.
Lee SY, Voronov S, Letinic K, Nairn AC, Di Paolo G, De Camilli P. (2005). Regulation of the interaction between PIPKI gamma and talin by proline-directed protein kinases. J Cell Biol. 168:789-99.
Lew J, Beaudette K, Litwin CM, Wang JH. (1992). Purification and characterization of a novel proline-directed protein kinase from bovine brain. J. Biol. Chem. 267:13383-90.
Lew J, Huang QQ, Qi Z, Winkfein RJ, Aebersold R, et al. (1994). A brain-specific activator of cyclin-dependent kinase 5. Nature 371:423-26.
Li BS, Sun MK, Zhang L, Takahashi S, Ma W, et al. (2001). Regulation of NMDA receptors by cyclin-dependent kinase-5. Proc. Natl. Acad. Sci. USA 98:12742-47.
Li BS, Zhang L, Takahashi S, Ma W, Jaffe H, et al. (2002). Cyclin-dependent kinase 5 prevents neuronal apoptosis by negative regulation of c-Jun N-terminal kinase 3. EMBO J. 21:324-33.
Li Z, David G, Hung KW, DePinho RA, Fu AK, Ip NY. (2004). Cdk5/p35 phosphorylates mSds3 and regulates mSds3-mediated repression of transcription. J. Biol. Chem. 279:54438-44.
Liang S, Wei FY, Wu YM, Tanabe K, Abe T, et al. (2007). Major Cdk5-dependent phosphorylation sites of amphiphysin 1 are implicated in the regulation of the membrane binding and endocytosis. J. Neurochem. 102:1466-76.
Lisman J, Schulman H, Cline H. (2002). The molecular basis of CaMKII function in synaptic and behavioural memory. Nat. Rev. Neurosci. 3:175-90.
Luo S, Vacher C, Davies JE, Rubinsztein DC. (2005). Cdk5 phosphorylation of huntingtin reduces its cleavage by caspases: implications for mutant huntingtin toxicity. J. Cell Biol. 169:647-56.
Ma XM, Kiraly DD, Gaier ED, Wang Y, Kim EJ, et al. (2008). Kalirin-7 is required for synaptic structure and function. J. Neurosci. 28:12368-82.
Maestre C, Delgado-Esteban M, Gomez-Sanchez JC, Bolanos JP, Almeida A. (2008). Cdk5 phosphorylates Cdh1 and modulates cyclin B1 stability in excitotoxicity. EMBO J. 27:2736-45.
Malenka RC, Bear MF. (2004). LTP and LTD: an embarrassment of riches. Neuron 44:5-21.
Mandelkow EM, Mandelkow E. (1998). Tau in Alzheimer's disease. Trends Cell Biol. 8:425-27.
Mao D, Hinds PW. (2010.) p35 is required for CDK5 activation in cellular senescence. J. Biol. Chem. 285:4671-80.
Matsubara M, Kusubata M, Ishiguro K, Uchida T, Titani K, Taniguchi H. (1996). Site-specific phosphorylation of synapsin I by mitogen-activated protein kinase and Cdk5 and its effects on physiological functions. J. Biol. Chem. 271:21108-13.
Matsuura I, Wang JH. (1996). Demonstration of cyclin-dependent kinase inhibitory serine/threonine kinase in bovine thymus. J. Biol. Chem. 271:5443-50.
Mayford M, Bach ME, Huang YY, Wang L, Hawkins RD, Kandel ER. (1996). Control of memory formation through regulated expression of a CaMKII transgene. Science 274:1678-83.

Meijer L, Borgne A, Mulner O, Chong JP, Blow JJ, et al. (1997). Biochemical and cellular effects of roscovitine, a potent and selective inhibitor of the cyclin-dependent kinases Cdc2, Cdk2 and Cdk5. Eur. J. Biochem. 243:527-36.

Meyerson M, Enders GH, Wu CL, Su LK, Gorka C, et al. (1992). A family of human Cdc2-related protein kinases. EMBO J. 11:2909-17.

Miyamoto Y, Yamauchi J, Chan JR, Okada A, Tomooka Y, Hisanaga S, Tanoue A. (2007). Cdk5 regulates differentiation of oligodendrocyte precursor cells through the direction phosphorylation of paxillin. J. Cell Sci. 140:4355-66.

Morabito MA, Sheng M, Tsai LH. (2004). Cyclin-dependent kinase 5 phosphorylates the N-terminal domain of the postsynaptic density protein PSD-95 in neurons. J. Neurosci. 24:865-76.

Moy LY, Tsai LH. (2004). Cyclin-dependent kinase 5 phosphorylates serine 31 of tyrosine hydroxylase and regulates its stability. J. Biol. Chem. 279:54487-93.

Muntane G, Dalfo E, Martinez A, Ferrer I. (2008). Phosphorylation of tau and α-synuclein in synaptic-enriched fractions of the frontal cortex in Alzheimer's disease, and in Parkinson's disease and related α-synucleinopathies. Neuroscience 152:913-23.

Murthy VN, De Camilli P. (2003). Cell biology of the presynaptic terminal. Ann Rev Neurosci 26: 701-28.

Muyllaert D, Terwe D, Kremer A, Snnvik K, Borghgraef P, et al. (2008). Neurodegeneration and neuroinflammation in Cdk5/p25-inducible mice: a model for hippocampal sclerosis and neocortical degeneration. Am. J. Pathol. 172:470-85.

Nakamura S, Kawamoto Y, Nakano S, Akiguchi I, Kimura J. (1997). p35nck5a and cyclin-dependent kinase 5 colocalize in Lewy bodies of brains with Parkinson's disease. Acta Neuropathol. 94:153-57.

Neumann M, Sampathu DM, Kwong LK, Truax AC, Micsenyi MC, et al. (2006). Ubiquitinated TDP-43 in frontotemporal lobar degeneration and amyotrophic lateral sclerosis. Science 314:130-33.

Nguyen C, Bibb JA. (2003). Cdk5 and the mystery of synaptic vesicle endocytosis. J. Cell Biol. 163:697-99.

Nguyen C, Nishi A, Kansy JW, Fernandez J, Hayashi K, et al. (2007). Regulation of protein phosphatase inhibitor-1 by cyclin-dependent kinase 5. J. Biol. Chem. 282:16511-20.

Nguyen MD, Lariviere RC, Julien JP. (2001). Deregulation of Cdk5 in a mouse model of ALS: toxicity alleviated by perikaryal neurofilament inclusions. Neuron 30:135-47.

Niethammer M, Smith DS, Ayala R, Peng J, Ko J, et al. (2000). NUDEL is a novel Cdk5 substrate that associates with LIS1 and cytoplasmic dynein. Neuron 28:697-711.

Nikolic M, Chou MM, Lu W, Mayer BJ, Tsai LH. (1998). The p35/Cdk5 kinase is a neuron-specific Rac effector that inhibits Pak1 activity. Nature 395:194-98.

Nikolic M, Dudek H, Kwon YT, Ramos YF, Tsai LH. (1996). The Cdk5/p35 kinase is essential for neurite outgrowth during neuronal differentiation. Genes Dev. 10:816-25.

Noble W, Olm V, Takata K, Casey E, Mary O, et al. (2003). Cdk5 is a key factor in tau aggregation and tangle formation in vivo. Neuron 38:555-65.

Ohshima T, Ogura H, Tomizawa K, Hayashi K, Suzuki H, et al. (2005). Impairment of hippocampal long-term depression and defective spatial learning and memory in p35 mice. J. Neurochem. 94:917-25.

Ohshima T, Ward JM, Huh CG, Longenecker G, Veeranna, et al. (1996). Targeted disruption of the cyclin-dependent kinase 5 gene results in abnormal corticogenesis, neuronal pathology and perinatal death. Proc. Natl. Acad. Sci. USA 93:11173-78.

Olanow CW, Tatton WG. (1999). Etiology and pathogenesis of Parkinson's disease. Annu. Rev. Neurosci. 22:123-44.

Otth C, Concha II, Arendt T, Stieler J, Schliebs R, et al. (2002). AβPP induces Cdk5-dependent tau hyperphosphorylation in transgenic mice Tg2576. J. Alzheimers Dis. 4:417-30.

Ou CY, Poon VY, Maeder CI, Watanabe S, Lehrman EK, et al. (2010). Two cyclin-dependent kinase pathways are essential for polarized trafficking of presynaptic components. Cell 141(5):846-858.

Paglini G, Pigino G, Kunda P, Morfini G, Maccioni R, et al. (1998). Evidence for the participation of the neuron-specific CDK5 activator P35 during laminin-enhanced axonal growth. J. Neurosci. 18:9858-69.

Paoletti P, Vila I, Rife M, Lizcano JM, Alberch J, Gines S. (2008). Dopaminergic and glutamatergic signaling crosstalk in Huntington's disease neurodegeneration: the role of p25/cyclin-dependent kinase 5. J. Neurosci. 28:10090-101.

Pareek TK, Keller J, Kesavapany S, Agarwal N, Kuner R, et al. (2007). Cyclin-dependent kinase 5 modulates nociceptive signaling through direct phosphorylation of transient receptor potential vanilloid 1. Proc. Natl. Acad. Sci. USA 104:660-65.

Pareek TK, Keller J, Kesavapany S, Pant HC, Iadarola MJ, et al. (2006). Cyclin-dependent kinase 5 activity regulates pain signaling. Proc. Natl. Acad. Sci. USA 103:791-96.

Park M, Watanabe S, Poon VYN, Ou CY, Jorgensen EM, Sheng K. (2011). CYY-1/Cyclin Y and CDK-5 differentially regulate synapse elimination and formation for rewiring neural circuits. Neuron 70:742-57.

Patrick GN, Zhou P, Kwon YT, Howley PM, Tsai LH. (1998). p35, the neuronal-specific activator of cyclin-dependent kinase 5 (Cdk5) is degraded by the ubiquitin-proteasome pathway. J. Biol. Chem. 273:24057-64.

Patrick GN, Zukerberg L, Nikolic M, de la Monte S, Dikkes P, Tsai LH. (1999). Conversion of p35 to p25 deregulates Cdk5 activity and promotes neurodegeneration. Nature 402:615-22.

Paudel HK, Lew J, Ali Z, Wang JH. (1993). Brain proline-directed protein kinase phosphorylates tau on sites that are abnormally phosphorylated in tau associated with Alzheimer's paired helical filaments. J. Biol. Chem. 268:23512-18.

Piedrahita D, Hernandez I, Lopez-Tobon A, Fedorov D, Obara B, et al. (2010). Silencing of CDK5 reduces neurofibrillary tangles in transgenic Alzheimer's mice. J. Neurosci. 30:13966-76

Pigino G, Paglini G, Ulloa L, Avila J, Caceres A. (1997). Analysis of the expression, distribution and function of cyclin dependent kinase 5 (Cdk5) in developing cerebellar macroneurons. J. Cell Sci. 110(Pt. 2):257-70.

Poon RY, Lew J, Hunter T. (1997). Identification of functional domains in the neuronal Cdk5 activator protein. J. Biol. Chem. 272:5703-8.

Poore CP, Sundaram JR, Pareek TK, Fu A, Amin N, et al. (2010). Cdk5-mediated phosphorylation of δ-catenin regulates its localization and GluR2-mediated synaptic activity. J. Neurosci. 30:8457-67.

Qi Z, Huang QQ, Lee KY, Lew J, Wang JH. (1995). Reconstitution of neuronal Cdc2-like kinase from bacteria-expressed Cdk5 and an active fragment of the brain-specific activator. Kinase activation in the absence of Cdk5 phosphorylation. J. Biol. Chem. 270:10847-54.

Qu D, Rashidian J, Mount MP, Aleyasin H, Parsanejad M, et al. (2007). Role of Cdk5-mediated phosphorylation of Prx2 in MPTP toxicity and Parkinson's disease. Neuron 55:37-52.

Rashidian J, Iyirhiaro G, Aleyasin H, Rios M, Vincent I, et al. (2005). Multiple cyclin-dependent kinases signals are critical mediators of ischemia/hypoxic neuronal death in vitro and in vivo. Proc. Natl. Acad. Sci. USA 102:14080-85.

Rashidian J, Rousseaux MW, Venderova K, Qu D, Callaghan SM, et al. (2009). Essential role of cytoplasmic Cdk5 and Prx2 in multiple ischemic injury models, in vivo. J. Neurosci. 29:12497-505.

Rutherford LC, Nelson SB, Turrigiano GG. (1998). BDNF has opposite effects on the quantal amplitude of pyramidal neuron and interneuron excitatory synapses. Neuron 21:521-30.

Samuels BA, Hsueh YP, Shu T, Liang H, Tseng HC, et al. (2007). Cdk5 promotes synaptogenesis by regulating the subcellular distribution of the MAGUK family member CASK. Neuron 56:823-37.

Sasaki S, Shionoya A, Ishida M, Gambello MJ, Yingling J, et al. (2000). A LIS1/NUDEL/cytoplasmic dynein heavy chain complex in the developing and adult nervous system. Neuron 28:681-96.

Saito T, Konno T, Hosokawa T, Asada A, Ishiguro K, Hisanaga S. (2007). p25/cyclin-dependent kinase 5 promotes the progression of cell death in nucleus of endoplasmic reticulum-stressed neurons. J. Neurochem. 102:133-40.

Saura CA, Choi, SY, Beglopoulos V, Malkani S, Zhang D, et al. (2004). Loss of presenilin function causes impairments of memory and synaptic plasticity followed by age-dependent neurodegeneration. Neuron 42:23-36.

Sawamura N, Gong JS, Garver WS, Heidenreich RA, Ninomiya H, et al. (2001). Site-specific phosphorylation of tau accompanied by activation of mitogen-activated protein kinase (MAPK) in brains of Niemann-Pick type C mice. J. Biol. Chem. 276:10314-19.

Schubert S, Knoch KP, Ouwendijk J, Mohammed S, Bodrov Y, et al. (2010). β2-Syntrophin is a Cdk5 substrate that restrains the motility of insulin secretory granules. PLoS ONE 5:e12929.

Seeburg DP, Feliu-Mojer M, Gaiottino J, Pak DT, Sheng M. (2008). Critical role of CDK5 and Polo-like kinase 2 in homeostatic synaptic plasticity during elevated activity. Neuron 58:571-83.

Sharma P, Veeranna, Sharma M, Amin ND, Sihag RK, et al. (2002). Phosphorylation of MEK1 by cdk5/p35 down-regulates the mitogen-activated protein kinase pathway. J Biol Chem. 277:528-34.

Sheng M, Hoogenraad CC. (2007). The postsynaptic architecture of excitatory synapses: a more quantitative view. Annu. Rev. Biochem. 76:823-47.

Shepherd JD, Rumbaugh G, Wu J, Chowdhury S, Plath N, et al. (2006). Arc/Arg3.1 mediates homeostatic synaptic scaling of AMPA receptors. Neuron 52:475-84.

Shuang R, Zhang L, Fletcher A, Groblewski GE, Pevsner J, Stuenkel EL. (1998). Regulation of Munc-18/syntaxin 1A interaction by cyclin-dependent kinase 5 in nerve endings. J. Biol. Chem. 273:4957-66.

Singh KK, Ge X, Mao Y, Drane L, Meletis K, et al. (2010). Dixdc1 is a critical regulator of DISC1 and embryonic cortical development. Neuron 67:33-48.

Small SA, Duff K. (2008). Linking Aβ and tau in late-onset Alzheimer's disease: a dual pathway hypothesis. Neuron 60:534-42.

Smith DS, Greer PL, Tsai LH. (2001). Cdk5 on the brain. Cell Growth Differ 12:277-83.

Smith PD, Crocker SJ, Jackson-Lewis V, Jordan-Sciutto KL, Hayley S, et al. (2003). Cyclin-dependent kinase 5 is a mediator of dopaminergic neuron loss in a mouse model of Parkinson's disease. Proc. Natl. Acad. Sci. USA 100:13650-55.

Smith PD, Mount MP, Shree R, Callaghan S, Slack RS, et al. (2006). Calpain-regulated p35/Cdk5 plays a central role in dopaminergic neuron death through modulation of the transcription factor myocyte enhancer factor 2. J. Neurosci. 26:440-47.

Sreedharan J, Blair IP, Tripathi VB, Hu X, Vance C, et al. (2008). TDP-43 mutations in familial and sporadic amyotrophic lateral sclerosis. Science 319:1668-72.

Sudhof TC. (2004). The synaptic vesicle cycle. Annu. Rev. Neurosci. 27:509-47.

Takahashi M, Iseki E, Kosaka K. (2000). Cyclin-dependent kinase 5 (Cdk5) associated with Lewy bodies in diffuse Lewy body disease. Brain Res. 862:253-56.

Takahashi S, Kulkarni AB. (2004). Mutant superoxide dismutase 1 causes motor neuron degeneration independent of cyclin-dependent kinase 5 activation by p35 or p25. J. Neurochem. 88:1295-304.

Takahashi S, Ohshima T, Hirasawa M, Pareek TK, Bugge TH, et al. (2010). Conditional deletion of neuronal cyclin-dependent kinase 5 in developing forebrain results in microglial activation and neurodegeneration. Am. J. Pathol. 176:320-29.

Takashima A, Murayama M, Yasutake K, Takahashi H, Yokoyama M, Ishiguro K. (2001). Involvement of cyclin dependent kinase5 activator p25 on tau phosphorylation in mouse brain. Neurosci. Lett. 306:37-40.

Tan TC, Valova VA, Malladi CS, Graham ME, Berven LA, et al. (2003). Cdk5 is essential for synaptic vesicle endocytosis. Nat. Cell Biol. 5:701-10.

Tanaka T, Serneo FF, Tseng HC, Kulkarni AB, Tsai LH, Gleeson JG. (2004). Cdk5 phosphorylation of doublecortin ser297 regulates its effect on neuronal migration. Neuron 41:215-27.

Tang D, Yeung J, Lee KY, Matsushita M, Matsui H, et al. (1995). An isoform of the neuronal cyclin-dependent kinase 5 (Cdk5) activator. J. Biol. Chem. 270:26897-903

Tarricone C, Dhavan R, Peng J, Areces LB, Tsai LH, Musacchio A. (2001). Structure and regulation of the Cdk5-p25(nck5a) complex. Mol. Cell 8:657-69.

Tian B, Yang Q, Mao Z. (2009). Phosphorylation of ATM by Cdk5 mediates DNA damage signalling and regulates neuronal death. Nat. Cell Biol. 11:211-18.

Tomizawa K, Ohta J, Matsushita M, Moriwaki A, Li ST, et al. (2002). Cdk5/p35 regulates neurotransmitter release through phosphorylation and downregulation of P/Q-type voltage-dependent calcium channel activity. J. Neurosci. 22:2590-97.

Tomizawa K, Sunada S, Lu YF, Oda Y, Kinuta M, et al. (2003). Cophosphorylation of amphiphysin I and dynamin I by Cdk5 regulates clathrin-mediated endocytosis of synaptic vesicles. J. Cell Biol. 163:813-24.

Tsai LH, Delalle I, Caviness VS Jr, Chae T, Harlow E. (1994). p35 is a neural-specific regulatory subunit of cyclin-dependent kinase 5. Nature 371:419-23.

Tsai LH, Takahashi T, Caviness VS Jr, Harlow E. (1993). Activity and expression pattern of cyclin-dependent kinase 5 in the embryonic mouse nervous system. Development 119:1029-40.

Tseng HC, Zhou Y, Shen Y, Tsai LH. (2002). A survey of Cdk5 activator p35 and p25 levels in Alzheimer's disease brains. FEBS Lett. 523:58-62.

Turrigiano GG, Leslie KR, Desai NS, Rutherford LC, Nelson SB. (1998). Activity-dependent scaling of quantal amplitude in neocortical neurons. Nature 391:892-96.

Van Den Haute C, Spittaels K, Van Dorpe J, Lasrado R, Vandezande K, et al. (2001). Coexpression of human cdk5 and its activator p35 with human protein tau in neurons in brain of triple transgenic mice. Neurobiol. Dis. 8:32-44.

Vance C, Rogelj B, Hortobagyi T, De Vos KJ, Nishimura AL, et al. (2009). Mutations in FUS, an RNA processing protein, cause familial amyotrophic lateral sclerosis type 6. Science 323:1208-11.

Wang J, Liu S, Fu Y, Wang JH, Lu Y. (2003). Cdk5 activation induces hippocampal CA1 cell death by directly phosphorylating NMDA receptors. Nat. Neurosci. 6:1039-47.

Wei FY, Nagashima K, Ohshima T, Saheki Y, Lu YF, et al. (2005a). Cdk5-dependent regulation of glucose-stimulated insulin secretion. Nat. Med. 11:1104-8.

Wei FY, Tomizawa K, Ohshima T, Asada A, Saito T, et al. (2005b). Control of cyclin-dependent kinase 5 (Cdk5) activity by glutamatergic regulation of p35 stability. J. Neurochem. 93:502-12.

Wen Y, Yang SH, Liu R, Perez EJ, Brun-Zinkernagel AM, et al. (2007). Cdk5 is involved in NFT-like tauopathy induced by transient cerebral ischemia in female rats. Biochim. Biophys. Acta 1772:473-83.

Wenzel HJ, Robbins CA, Tsai LH, Schwartzkroin PA. (2001). Abnormal morphological and functional organization of the hippocampus in a p35 mutant model of cortical dysplasia associated with spontaneous seizures. J. Neurosci. 21:983-98.

Xie Z, Sanada K, Samuels BA, Shih H, Tsai LH. (2003). Serine 732 phosphorylation of FAK by Cdk5 is important for microtubule organization, nuclear movement, and neuronal migration. Cell 114:469-82.

Xin X, Wang Y, Ma XM, Rompolas P, Keutmann HT, et al. (2008). Regulation of Kalirin by Cdk5. J. Cell Sci. 121:2601-11.

Yan Z, Chi P, Bibb JA, Ryan TA, Greengard P. (2002). Roscovitine: a novel regulator of P/Q-type calcium channels and transmitter release in central neurons. J. Physiol. 540:761-70

Zhang J, Krishnamurthy PK, Johnson GV. (2002). Cdk5 phosphorylates p53 and regulates its activity. J. Neurochem. 81:307-13.

Zhang M, Li J, Chakrabarty P, Bu B, Vincent I. (2004). Cyclin-dependent kinase inhibitors attenuate protein hyperphosphorylation, cytoskeletal lesion formation, and motor defects in Niemann-Pick type C mice. Am. J. Pathol. 165:843-53.

Zhang S, Edelmann L, Liu J, Crandall JE, Morabito MA. (2008). Cdk5 regulates the phosphorylation of tyrosine 1472 NR2B and the surface expression of NMDA receptors. J. Neurosci. 28:415-24.

Zhang P, Yu PC, Tsang AHK, Chen Y, Fu AKY, et al. (2010). S-nitrosylation of cyclin-dependent kinase 5 (Cdk5) regulates its kinase activity and dendrite growth during neuronal development. J. Neurosci. 30:14366-70.

Zukerberg LR, Patrick GN, Nikolic M, Humbert S, Wu CL, et al. (2000). Cables links Cdk5 and c-Abl and facilitates Cdk5 tyrosine phosphorylation, kinase upregulation, and neurite outgrowth. Neuron 26:633-46.

Chapter 2

Cdk5 is required for memory function and hippocampal plasticity via the cAMP signaling pathway[2]

Summary

Memory formation is modulated by pre- and post-synaptic signaling events in neurons. The neuronal protein kinase Cyclin-Dependent Kinase 5 (Cdk5) phosphorylates a variety of synaptic substrates and is implicated in memory formation. It has also been shown to play a role in homeostatic regulation of synaptic plasticity in cultured neurons. Surprisingly, we found that Cdk5 loss of function in hippocampal circuits results in severe impairments in memory formation and retrieval. Moreover, Cdk5 loss of function in the hippocampus disrupts cAMP signaling due to an aberrant increase in phosphodiesterase (PDE) proteins. Dysregulation of cAMP is associated with defective CREB phosphorylation and disrupted composition of synaptic proteins in Cdk5-deficient mice. Rolipram, a PDE4 inhibitor that prevents cAMP depletion, restores synaptic plasticity and memory formation in Cdk5-deficient mice. Collectively, our results demonstrate a critical role for Cdk5 in the regulation of cAMP-mediated hippocampal functions essential for synaptic plasticity and memory formation.

---

[2] The findings presented in this chapter were previously published as: *Guan JS, *Su SC, Jun G, Joseph N, Xie Z, Zhou Y, Durak O, Zhang L, Zhu JJ, Clauser KR, Carr SA, Tsai LH. (2011). Cdk5 is required for memory function and hippocampal plasticity via the cAMP signaling pathway. PloS One 6(9):e25735.

I generated the Cdk5f/f and Cdk5f/f/CW2 mouse lines, prepared the synaptosomal enrichment of Cdk5f/f and Cdk5f/f/CW2 samples for the total and phosphoproteomic screen, conducted biochemical analysis on Cdk5f/f/CW2 and Cdk5f/f/T29 with rolipram treatment, and conducted control behavioral experiments.

Introduction

The hippocampus is considered to be a key region for long-term memory formation in humans and rodents (Morris et al., 1982; Squire, 1987), yet the molecular mechanisms underlying memory formation are still not fully understood. Transgenic mouse studies using hippocampal region-specific knockout of the NMDA receptor NR1 subunit strongly support the hypothesis that synaptic plasticity, especially NMDAR-mediated synaptic plasticity, is crucial for normal learning and memory (McHugh et al., 2007; Nakazawa et al., 2002). Numerous genetic and molecular studies have revealed that NMDAR activation, and its downstream cascade of events, are critical for synaptic plasticity. These events include calcium entry, autophosphorylation of CaMKII, activation of protein phosphatases, and the relocation and modification of AMPA receptors (Barria et al., 1997; Giese et al., 1998; Lee et al., 2000). Perturbations in the molecular cascade downstream of the NMDAR pathway result in defects in both long-term potentiation (LTP) and memory formation. Blocking the NMDAR pathway, in addition, impacts long-term depression (LTD). Interestingly, the PKC gamma mutant mouse, which displays normal LTD and impaired LTP, exhibits a relatively mild behavioral deficit (Abeliovich et al., 1993). Thus, both forms of synaptic plasticity (LTD and LTP) are required for memory formation.

The cyclic AMP (cAMP) pathway is also critically involved in synaptic plasticity and learning and memory. The second messenger cAMP, as well as the cAMP-dependent protein kinase A (PKA), have been implicated in short- and long-lasting synaptic plasticity and intrinsic neuronal excitability in *Aplysia* by activating cAMP-responsive element binding protein (CREB)-dependent transcription (Mozzachiodi et al., 2008). Accumulating data regarding the molecular events underlying CREB-dependent learning and memory in *Drosophila*, mice, and rats all indicate that CREB activation by phosphorylation at the Serine 133 residue is required for the maintenance of LTP and formation of long-term memory (Silva et al., 1998). The maintenance of LTP and long-term memory are also both dependent on PKA activity and CREB-mediated transcription (Frey et al., 1993). Cyclic nucleotide phophodiesterases (PDEs) catalyze the conversion of cAMP and cGMP into AMP and GMP, respectively, and are important for the homeostatic regulation of cyclic nucleotide-mediated signaling events. The PDEs are grouped into several families, two of which, PDEs 4 and 7, exclusively target cAMP. Rolipram, a PDE4-specific small molecule inhibitor, has antidepressant effects (Wachtel, 1983) and was recently

found to facilitate memory formation and synaptic plasticity in rodents (Vitolo et al., 2002). Rolipram was also shown to reverse synaptic plasticity and memory deficits in $CBP^{+/-}$ mice, a mouse model of Rubinstein-Taybi syndrome (Alarcon et al., 2004; Bourtchouladze et al., 2003).

Cyclin-dependent kinase 5 (Cdk5) was initially classified as a cyclin-dependent kinase based on sequence homology to other Cdks that operate in the cell cycle (Meyerson et al., 1992). Cdk5 has been implicated in almost every aspect of brain development and neural function including neuronal migration, neurite extension, synaptic transmission, and synaptic plasticity (Fischer et al., 2005; Niethammer et al., 2000; Ou et al., 2010; Tanaka et al., 2004; Zukerberg et al., 2000). Intriguingly, Cdk5 gain-of-function mutations result in an increased number of synapses *in vivo* and the facilitation of LTP in slices (Fischer et al., 2005), whereas the loss of Cdk5 activity in p35 knockout mice results in impaired hippocampal LTD (Ohshima et al., 2005). In contrast, an inducible Cdk5 conditional knockout mouse model exhibited facilitated LTP and enhanced memory formation via reduced degradation of the NR2B subunit of the NMDA receptor (Hawasli et al., 2007). Despite a greater understanding of how Cdk5 is critically important for synapse formation, the *in vivo* role for Cdk5 as a part of a signaling pathway crucial to hippocampal learning and memory remains unclear.

In the current report, we found that Cdk5 loss of function in distinct hippocampal circuits resulted in impairments in various memory functions and synaptic plasticity, observations distinct from previously reported findings using a different Cdk5 mouse model (Hawasli et al., 2007). In addition, multiple PDE isoforms were markedly upregulated, which led to the dysregulation of cAMP pathway and impaired CREB phosphorylation. Remarkably, the observed deficiencies in Cdk5 conditional knockout mice can be rescued by rolipram treatment. Taken together, these results indicate a key function for Cdk5 in regulating cAMP signaling via modulation of PDE expression to facilitate synaptic plasticity and hippocampal-dependent memory formation.

Methods

Animals

Animals were derived from the C57BL/6J strain obtained from Jackson Labs (Bar Harbor, ME) due to their common use in genetic crossing and maintaining genetically modified mouse lines. The mice were group housed in the small animal facility at the Department of Brain and Cognitive Sciences of Massachusetts Institute of Technology (Cambridge, MA) with a 12-hr light dark cycle and ad libitum feeding. All experiments were conducted in compliance with the humane animal care standards outlined in the NIH Guide for the Care and Use of Experimental Animals and were reviewed and approved by the MIT Committee on Animal Care (CAC).

Generation of region-specific Cdk5 mutant mice

We constructed a targeting vector in which two loxP sequences were inserted into the Cdk5 gene. The first loxP sequence was placed before exon 1 and the second loxP sequence was placed between exons 5 and 6 so that they flanked exons 1-5 of the twelve total exons in the Cdk5 genomic sequence. The mice homozygous for the loxP-Cdk5-loxP sequence (henceforth named "floxed Cdk5" or simply 'Cdk5f/f') were generated through standard homologous recombination procedures (**Figure 1**). The Cdk5-loxP construct was linearized by Pme1 digestion and electroporated into embryonic stem cells. The homologous recombinant clones were identified by Southern blot (see next section). The chimeric mice were crossed to Flp transgenic mice (Susan Dymecki) to remove the neomycin cassette. Floxed mice were genotyped using the PCR primer sequences: (forward) cagtttctagcacccaactgatgta and (reverse) gctgtcctggaactccatctataga cagtttctagcacccaactgatgta and reverse: gctgtcctggaactccatctataga. Floxed Cdk5 mice were maintained on a C57BL/6 background.

For region-specific ablation of Cdk5, we used mouse lines predominantly expressing Cre in excitatory neurons of hippocampal areas CA1 or CA3 and forebrain. We crossed Cdk5f/f mice with Cre transgenic mice, T29-2, which mediate Cre/loxP recombination predominantly in CA1 pyramidal cells (Tsien et al., 1996a; Tsien et al., 1996b) to generate Cdk5f/f/T29 mice ($Cre^{T29\text{-}2}$;fCdk5/fCdk5). Cdk5f/f/CW2 mice were generated by crossing the CW-2 Cre mice to the Cdk5f/f mice (Zeng et al., 2001) in order to ablate Cdk5 in excitatory neurons of the forebrain. To create Cdk5f/f/KA1 mice, we crossed Cdk5f/f mice with Cre transgenic mice, G32-4, which express Cre predominantly in CA3 pyramidal cells (Nakazawa et al., 2002). We

confirmed CA1, forebrain, and CA3 Cre expression pattern by crossing the Cre lines to the ROSA26-EYFP line (Srinivas et al., 2001). For the following experiments, we used Cdk5 homozygous floxed littermates (Cdk5f/f) as controls. Cdk5f/f/T29, Cdk5f/f/CW2, and Cdk5f/f/KA1 mice are viable and do not exhibit any obvious developmental defects, in contrast to the embryonic lethality of Cdk5 KO mice produced by conventional gene knockout strategies (Ohshima et al., 1996). We confirmed the ablation of Cdk5 in areas CA1 or CA3 by immunohistochemistry. Cdk5 is expressed in most areas of the mouse brain. In the hippocampus, we found that Cdk5 expression level in area CA1 was decreased in Cdk5f/f/T29 mice compared to controls. Importantly, there were no differences in Cdk5 expression levels between the Cdk5f/f/T29 and control mice in area CA3 and dentate gyrus (DG). Cdk5 immunoreactivity in CA3 was reduced in the Cdk5f/f/KA1 mice compared to controls. Cdk5 was absent in the cell bodies of pyramidal cells in area CA1 of the Cdk5f/f/T29 mice and in area CA3 of Cdk5f/f/KA1 mice. Morphological and histochemical examinations did not reveal obvious abnormalities in brains from Cdk5f/f/T29, Cdk5f/f/CW2, or Cdk5f/f/KA1 mice. Tissues collected from micro-dissected area CA1 of the Cdk5f/f/T29 versus control mice (Cdk5f/f) revealed that Cdk5 protein levels are largely reduced in the CA1 region of these mice.

Southern blotting

The following modified protocol was used: tail lysis overnight, followed by DNA extraction. Ten μg of genomic DNA was digested with BamHI and EcoRI overnight, followed by electrophoresis on a 0.8% agarose gel. The gel was then incubated in 2 gel volumes of 0.25 M HCl for 20 min at room temperature, briefly rinsed with ddH_2O, then incubated in 2 gel volumes of denaturation buffer (0.5 M NaOH, 1.5 M NaCl) two times, 15 min each. The gel was briefly rinsed with ddH_2O and subsequently incubated in 2 gel volumes of renaturation buffer two times, 30 min each. The transfer was set up overnight on a sandwich consisting of 3 cm high paper towel stack, the agarose gel, a nitrocellulose membrane (Micron Separation, Inc.), and filter paper with a bridge. The membrane was then rinsed and baked in a 80 °C oven under a vacuum for 2 hr, rinsed 2 times in 2X SSC buffer (for 1 L 20X SSC: 3 M NaCl, 0.3 M Sodium Citrate, pH 7.0), and prehybridized in ULTRAHTb (Ambion) for 1 hr at 42 °C in the hybridization chamber. The probe was made using a DECAprime II kit (Ambion, Cat #1455). The reaction was incubated at 37 °C for 7 min, terminated by 1 μl 0.5M EDTA, and unincorporated

nucleotides were removed using spin columns (NuAway, Ambion). Radiolabel incorporation was measured using a scintillation counter. 10^7 cpm per ml of probe was transferred to the prehybridized blot and incubated overnight at 42 °C. The membrane was then washed sequentially: 2X SSC, 0.1% SDS for 20 min at 65 °C, 0.1X SSC, 0.1% SDS for 20 min three times at 65 °C. The blot was then dried and developed with film.

Behavior

Adult (2.5-3.5 month old) mice were used for all behavior, biochemical, and immunohistochemistry studies. We observed that the Cre expression in the T29-2 line is no longer restricted to the CA1 region in 4-month-old mice. Interestingly, the spreading of Cre expression in these mice, and thus Cdk5 knockdown, occurs at a time when the Cdk5f/f/T29 mice begin to suffer seizures, and these mice begin to die around 6-8 months of age. Cdk5f/f/KA1 mice appear to be normal even after 1 year of age.

Contextual fear conditioning

Training consisted of a 3 min exposure of mice to the conditioning box (context) followed by a foot shock (2 sec, 0.5/0.8/1.0 mA, constant current). The memory test was performed 24 hr later by re-exposing the mice to the conditioning context for 3 min. Freezing, defined as a lack of movement except for heartbeat and respiration associated with a crouching posture, was recorded every 10 sec by two trained observers (one was blind to the experimental conditions) during the 3 min trial for a total of 18 sampling intervals. The mean number of observations indicating freezing from both observers was expressed as a percentage of the total number of observations.

Cued fear conditioning

Training consisted of a 3 min exposure of mice to the conditioning box, followed by a tone (30 sec, 20 kHz, 75 dB sound pressure level (SPL) and a foot shock (2 sec, 0.8 mA, constant current) (Radulovic et al., 1999). The memory test was performed 24 hr later by exposing the mice for 3 min to a novel context followed by an additional 3 min exposure to a tone (20 kHz, 75 dB SPL). Freezing was recorded every 10 sec by two trained observers as described above.

Morris water maze

The water maze with hidden platform paradigm (Morris et al., 1982) was performed in a circular tank (diameter 1.8 m) filled with opaque water. A platform (11 × 11 cm) was submerged below the water's surface in the center of the target quadrant. The swimming path of the mice was recorded by a video camera and analyzed by the Videomot 2 software (TSE). For each training trial, the mice were placed into the maze consecutively from one of four random points of the tank. Mice were allowed to search for the platform for 60 s. If the mice did not find the platform within 60 s, they were gently guided to it. Mice were allowed to remain on the platform for 15 s. Two consecutive training trials were given every day; the latency for each trial was recorded for analysis. During the memory test (probe test), the platform was removed from the tank, and the mice were allowed to swim in the maze for 60 s.

Immunohistochemistry and immunoblotting

Immunohistochemistry was performed as described previously (Guan et al., 2009). Briefly, brains were fixed in 4% paraformaldehyde and stained with antibodies against Cdk5 and pCREB. Five random fields from each experiment were obtained and quantified with the observer blind to genotype. The antibodies and dilutions used were as follows. For immunohistochemistry: Cdk5 (MBS240590**,** MyBioSource, 1:800); pCREB(S133) (Millipore 06-519, 1:200). Immunoblotting was performed on mouse forebrains or microdissected hippocampi. Brain lysates were obtained by dounce homogenization of tissue in radioimmunoprecipitation (RIPA) buffer. The RIPA buffer composition is as follows: 50 mM Tris pH 8, 150 mM NaCl, 1% NP-40, 0.5% sodium deoxycholate, 0.1% SDS with protease and phosphatase inhibitor tablets (Roche). Lysates were incubated on ice and cleared with a 13,000 rpm spin and protein content was quantified (BCA protein assay, Bio-Rad Technologies). Ten micrograms of protein was diluted with 2X sample buffer consisting of the following: 100 mM Tris pH 6.8, 4% SDS (w/v), 0.2% bromophenol blue (w/v), 20% glycerol (v/v), 200 mM DTT. Samples were boiled at 95 °C for 5 minutes and resolved on a 10% SDS-polyacrylamide gel with 8% stacking gels using Laemmli buffer. Proteins were transferred by electrophoresis using tris-glycine wet transfer onto PVDF membranes (Millipore) for 1 hr on ice. After blocking with blocking buffer (5% non-fat dry milk/0.1% Tween-20/TBS) for 1 hr, membranes were probed with various antibodies overnight at 4 °C. Membranes were washed three times using 0.1%

Tween-20/TBS, incubated with secondary antibodies (enhanced chemiluminescence mouse or rabbit IgG, HRP-Linked F(ab')2 fragment from sheep, GE Healthcare, diluted at 1:15,000) for 1 hr at room temperature. Membranes were washed again and developed using Western Lightning ECL substrate (Perkin Elmer). All antibodies were diluted in blocking buffer. Membrane stripping (before reprobing) was performed with stripping buffer: (2%SDS, 62.5 mM Tris-HCL pH 6.8, 100 mM 2-mecaptoethanol) and incubation for 30 minutes at 50 °C (with rocking), followed by two washing steps with excess TBST, and blocking as usual. Immunoblots were quantified using ImageJ (NIH). Statistical analysis was performed using Prism software. Antibodies used for immunoblots: Cdk5 (DC-17, Tsai laboratory, 1:500); pCaMKII(T286) (Cell Signaling Technology #3361, 1:2000); pCREB(S133) (Millipore 06-519, 1:2000); pGluR1(S845) (Chemicon Ab5849); pGluR1(S831) (Chemicon, Ab5847); GluR1 (Abcam); pPP1 (Cell Signal 2581); pp1a (Abcam); DARRP-32 T75 (Cell Signal #2301); DARRP-32 T34 (Cell Signal #2304); actin (Sigma #5316).

Phosphatase assay

Whole hippocampi were dissected and homogenized in 3.75 mM Tris-HCl, pH7.4, 15 mM KCl, 3.75 mM NaCl, 250 μM EDTA, 50 μM EGTA, 30% (w/v) sucrose, 30% (v/v) glycerol, protease inhibitor cocktail (Sigma), 100 μM PMSF using a Dounce homogenizer, then centrifuged (1000 g, 10 min). For each sample, the supernatant (cytoplasmic fraction) and pellet (nuclear fraction) were separated. Each fraction was resuspended in the same buffer without sucrose, but including 15 mM PMSF, using a Dounce homogenizer then triturated with a 26 G syringe before purification on PiResin (Innova Biosciences). Phosphatase activity was determined by incubating 2 μL sample with 0.15 mM RII substrate (BIOMOL) and 5 nM tautomycin (to inhibit PP1) or 5 nM tautomycin + OA (to inhibit PP1 and PP2A activity) in 50 mM Tris-HCl, pH 7.0, 100 μM Na2EDTA, 5 mM DTT, 0.01% Brij35 at 30 °C for 10 min. The reaction was terminated by adding TCA followed by centrifugation (13,000 g, 5 min). The amount of free phosphates released in the reaction was measured with BIOMOL Green reagent (BIOMOL) at 620 nm and background-subtracted. For total phosphatase activity, tautomycin and OA were removed from the reaction. PP1 and PP2A activity was calculated using the ratio of phosphatase activity with inhibitors and total phosphatase activity.

Electrophysiology

Three to four month old Cdk5f/f/T29 mice or their Cdk5f/f control littermates were sacrificed by cervical dislocation, and hippocampi were rapidly dissected in ice-cold oxygenated artificial CSF (ACSF). Transverse hippocampal slices (400 μm thick) were placed in a chamber and continuously perfused with oxygenated ACSF consisting of (in mM): 119 NaCl, 2.5 KCl, 2.5 $CaCl_2$, 1.3 $MgSO_4$, 1 NaH_2PO_4, 26.2 $NaHCO_3$, 11 D-glucose, pH 7.4. A bipolar stimulating electrode (0.002 in diameter nichrome wire; A-M Systems) placed in the stratum radiatum was used to elicit action potentials in CA3 Schaffer collateral axons. An ACSF-filled glass microelectrode with a resistance between 0.5 and 3 MΩ was placed in the stratum radiatum region of area CA1 and was used to record the field excitatory post-synaptic potentials (fEPSP). Data were acquired using HEKA EPC10 and analyzed by Patchmaster. Peak fEPSP amplitudes from stimulators were required to be at least 2 mV, and stimulus intensity was set to produce 40% of the maximal response. Baseline responses were recorded for 20 min. fEPSPs were evoked at area CA1 synapses by stimulating Schaffer collaterals at a low frequency (2 per min) to establish a stable baseline. Immediately following LTP induction with 2 trains of high-frequency stimulation (HFS, 100 Hz, 1s), with an interval of 20 s, slices from Cdk5f/f/T29 and control Cdk5f/f mice showed an increase in fEPSP slope and amplitude, suggesting that short-term potentiation (STP) occurs in all groups.

PSD preparation

Forebrains from Cdk5f/f and Cdk5f/f/CW2 mice were homogenized and postsynaptic densities (PSD) isolated in ice-cold buffers with protease and phosphatase inhibitor cocktails (Roche) as previously described with minor modifications (Peng et al., 2004). Briefly, mouse forebrains were isolated and homogenized in ice-cold Buffer A (0.32 M Sucrose, 6 mM Tris (pH 8), 1 mM $MgCl_2$, 0.5 mM $CaCl_2$) with a Teflon homogenizer (15 strokes). Homogenized brain extracts were spun at 1400 × g for 10 min. The supernatant (S1) was saved and the subsequent pellet (P1) was homogenized again (5 strokes). After centrifugation at 700 × g, the supernatant (S1') was saved and pooled with S1. Pooled S1 and S1' was centrifuged at 13,800 × g for 10 min to collect the pellet (P2). P2 was resuspended in Buffer B (0.32 M Sucrose, 6 mM Tris pH 8; 5 strokes). The P2 suspension was loaded onto a discontinuous sucrose gradient (0.85 M/1 M/1.15 M sucrose solution in 6 mM Tris, pH 8.0), followed by centrifugation for 2 h at 82,500 × g in a

SW-41 rotor. The synaptosome fraction between 1 M and 1.15 M sucrose was collected with a syringe needle and adjusted to 4 ml with Buffer B. Equal volumes of Buffer C (12 mM Tris pH 8; 1% Triton X-100) was added and mixed for 15 min and then spun at 32,800 × g in a Ti70.1 rotor for 20 min. The PSD-enriched pellet was resuspended in 40 mM Tris (pH 8) and protein concentration was measured using a BCA assay. To prepare samples for mass spectrometry, solubilized PSD proteins were reduced with 10 mM DTT for 30 min at 60 °C. After cooling to room temperature, the sample was then alkylated with 25 mM iodoacetamide for 30 min at room temperature. After adding 2X sample buffer (100 mM Tris pH 6.8, 200 mM DTT, 4% SDS, 0.2% Bromophenol blue, 20% glycerol), the PSD samples were then boiled at 95°C for 5 min and 30 µg of each sample was loaded for separation on an 4-12% SDS-PAGE gradient gel (Invitrogen).

In-gel Digestion and Mass Spectrometry

Lanes from the gel were excised, cut into 13 fields as shown in Figure S4B and digested overnight at 37 °C with an excess of sequencing grade trypsin. Peptides were extracted from the gel with 50% acetonitrile/0.1% trifluoroacetic acid and concentrated in a Speed-Vac. Tryptic digests were analyzed with an automated nano LC-MS/MS system, consisting of an Agilent 1100 nano-LC system (Agilent Technologies, Wilmington, DE) coupled to an LTQ-Orbitrap Fourier transform mass spectrometer (Thermo Fisher Scientific, San Jose, CA) equipped with a nanoflow ionization source (James A. Hill Instrument Services, Arlington, MA). Peptides were eluted from a 10 cm column (Picofrit 75 µm ID, New Objectives) packed in-house with ReproSil-Pur C18-AQ 3 µm reversed phase resin (Dr. Maisch , Ammerbuch Germany) using a 90 min acetonitrile/0.1% formic acid gradient at a flow rate of 200 nl/min to yield ~15 s peak widths. The elution portion of LC gradient was 3-7% solvent B in 2 min, 7-37% in 58 min, 37-90% in 3 min, and held at 90% solvent B for 5 min. Data-dependent LC-MS/MS spectra were acquired in ~3 s cycles; each cycle was of the following form: one full Orbitrap MS scan at 60,000 resolution followed by 8 MS/MS scans in the ion trap on the most abundant precursor ions using an isolation width of 3 m/z. Dynamic exclusion was enabled with a mass width of ± 25 ppm, a repeat count of 1, and an exclusion duration of 12 sec. Charge state screening was enabled along with monoisotopic precursor selection to prevent triggering of MS/MS on precursor ions with

unassigned charge or a charge state of 1. Normalized collision energy was set to 30 with an activation Q of 0.25 and activation time of 30 ms.

Protein identification, quantification, and phosphosite determination

All MS data was interpreted using the using the Spectrum Mill software package v4.0 beta (Agilent Technologies, Santa Clara, CA). Similar MS/MS spectra acquired on the same precursor m/z within ± 60 sec were merged, and poor quality MS/MS spectra which failed the quality filter of having a sequence tag length > 0 (i.e., minimum of two masses separated by the in-chain mass of an amino acid) were excluded from searching. MS/MS spectra were searched against the International Protein Index (IPI) mouse database version 3.48. Initial search parameters included: ESI linear ion trap scoring parameters, trypsin enzyme specificity with a maximum of two missed cleavages, 30% minimum matched peak intensity, ± 20 ppm precursor mass tolerance, ± 0.7 Da product mass tolerance, and carbamidomethylation of cysteines as a fixed modification. Allowed variable modifications were oxidized methionines, deamidation of asparagine, and pyro-glutamic acid modification at N-terminal glutamines with a precursor MH+ shift range of -18 to 65 Da. Identities interpreted for individual spectra were automatically designated as valid by applying the scoring threshold criteria provided below to all spectra in a two-step process. First, protein mode was used, which requires two or more matched peptides per protein while allowing a range of medium to excellent scores for each peptide. Second, peptide mode was applied to the remaining spectra, allowing for excellent scoring peptides that are detected as the sole evidence for particular proteins. Protein mode thresholds: protein score >20, peptide (score, Scored Percent Intensity, delta rank1 - rank2) peptide charge +2: (>8, >65%, > 2) peptide charge +3: (>9, >65%, > 2) peptide charge +4: (>9, >70%, > 2) peptide charge +2: (>6, >90%, > 1). Peptide mode thresholds: peptide charge +2 and +3 (>13, >70, > 2) peptide charge +4 (>15, >70, > 2) respectively. The above criteria yielded a false discovery rate of < 1% as estimated by target-decoy based searches using reversed sequences. MS/MS spectra of phosphopeptides were interpreted in a second round of searches against only the subset of proteins confidently identified from the unphosphorylated peptides observed during the initial round of searches. The allowed variable modifications were expanded to include phosphorylated serine, threonine, and tyrosine, with a precursor MH+ shift range of -18 to 177 Da (no more than 2 phosphosites/peptide). The spectrum of each phosphopeptide was manually inspected by an

expert. For ~10% of phosphosites observed the MS/MS spectra lack sufficient information to assign the site of phosphorylation to a particular Ser, Thr, or Tyr residue.

The relative abundances of proteins were determined using extracted ion chromatograms (XICs) for each peptide precursor ion in the intervening high resolution FT-MS scans of the LC-MS/MS runs. An individual protein's abundance was calculated as the sum of the ion current measured for all quantifiable peptide precursor ions with MS/MS spectra confidently assigned to that protein. Peptides were considered not quantifiable if they were shared across multiple subgroups of a protein or the precursor ions had a poorly defined isotope cluster (i.e. the "subgroup specific" and "exclude poor isotope quality precursor" XIC filters in Spectrum Mill were enabled). Proteins were considered not quantifiable if there were fewer than two distinct peptides observed in either the control or cKO samples. Since equivalent amounts of total protein were loaded in each lane of the gel, and both samples were subsequently treated equivalently, no further normalization was done when calculating protein abundance ratios between the two samples. The peak area for the XIC of each precursor ion subjected to MS/MS was calculated automatically by the Spectrum Mill software in the intervening high-resolution MS1 scans of the LC-MS/MS runs using narrow windows around each individual member of the isotope cluster. Peak widths in both the time and *m*/*z* domains were dynamically determined based on MS scan resolution, precursor charge, and *m*/*z* subject to quality metrics on the relative distribution of the peaks in the isotope cluster *vs.* theoretical.

Quantitative RT-PCR primers

AC1: cagcaggaaccaaggctaag; tggccacattgactgtgttt; AC3: tgaggagagcatcaacaacg; tggtgtgactcctgaagctg; AC8: ggactgtccccagagaaaca; cttactcccgtgctgtccat; pde1A: catgattgggttccatgttg; cagccaactctttccacctc; pde1b: tgcccttctctccactctgt; tgggctgacttttaggcttg; PDE2A: gaccgatggagatgatggac; acttgtgggacaccttggtc; PDE4D1: tatgaaggagcagccctcatg; ccaggacatcttcctgctctg; PDE4D4: tggccagtttctggtaggcctc; gagctacccgtggtcgctac; PDE4D6: ccaggacatcttcctgctctg; cacattttagaacttgctgtcac; PDE4D7: tggccagtttctggtaggcctc; actactcaaaaccgcaccatgg; PDE4B: ggaaaaatcccaggttggtt; cagtccctgctcctctcatc

Results

Associative and spatial memories are impaired in Cdk5f/f/T29 mice

To evaluate the consequences of Cdk5 ablation in hippocampal neurons, Cdk5f/f/T29 mice were generated using the Cre line T29-2 (Tsien et al., 1996a; Tsien et al., 1996b), in which Cre is highly expressed in CA1 pyramidal neurons of the hippocampus (**Table 1, Figure 1A-D, Figure 2A, 2B**), and subjected to various behavior tasks.

Mouse strain	Cre promoter	Cdk5 knockout region
Cdk5f/f/T29	CaMKIIα (T29-1)	Restricted mainly to hippocampal area CA1
Cdk5f/f/KA1	Kainate receptor-1	Restricted mainly to hippocampal area CA3
Cdk5f/f/CW2	CaMKIIα (CW2)	Restricted to forebrain excitatory neurons

Table 1. Cdk5 mutant mouse strains generated for analysis. The mouse strains used for analysis include three genotypes: Cdk5f/f/T29, Cdk5f/f/KA1, and Cdk5 f/f/CW2. Three different Cre promoter lines were used to generate these genotypes by breeding the Cre line to the Cdk5 floxed lines to obtain the CA1, CA3, and forebrain-specific knockdown of Cdk5. In all experiments, 2.5-3.5 month old mice were used, and age-matched littermate Cdk5f/f mice were used as controls.

The ablation of Cdk5 using T29-Cre does not lead to significant changes in overall brain architecture or cell survival (**Figure 1F**). We noted in the T29-Cre line that Cre-mediated Cdk5 knockout is relatively specific to area CA1 in young mice (2.5-3.5 months old), with the deletion of Cdk5 spreading to cortical and other brain regions in older (4 month-old) mice. Beginning at 5 months of age, Cdk5f/f/T29 mice suffered mild to severe seizures and died by 8 months, which might be due to the spreading of T29-Cre expression (Fukaya et al., 2003; Rampon et al., 2000). Therefore, we used 2.5 to 3.5 month-old mice to perform all behavior tests. Cdk5f/f/T29 mice were trained using Pavlovian fear conditioning paradigm 24 hours prior to a memory test. Cdk5f/f/T29 mice exhibited significantly reduced freezing behavior compared to control littermates (Cdk5f/f) in the context-dependent memory test (**Figure 2C**). Consistent with the notion that the hippocampus is not required for cued fear conditioning, Cdk5f/f/T29 mice did not exhibit significantly different freezing behavior compared to controls in the tone-dependent memory test (**Figure 2C**). Moreover, the reduced freezing behavior in Cdk5f/f/T29 mice was not due to motor defects or impaired pain sensation, as their locomotor activity and response to electrical foot shock were similar to control mice (**Figure 2D, 2E**). No significant differences in anxiety levels were detected using the open field test (**Figure 1G**). Notably, after repeated fear conditioning training, control Cdk5f/f mice exhibited increased freezing behavior after three days of training, while Cdk5f/f/T29 mice demonstrated no increase in freezing behavior (**Figure 2F**). These results suggest that memory consolidation is impaired in the Cdk5f/f/T29 mice.

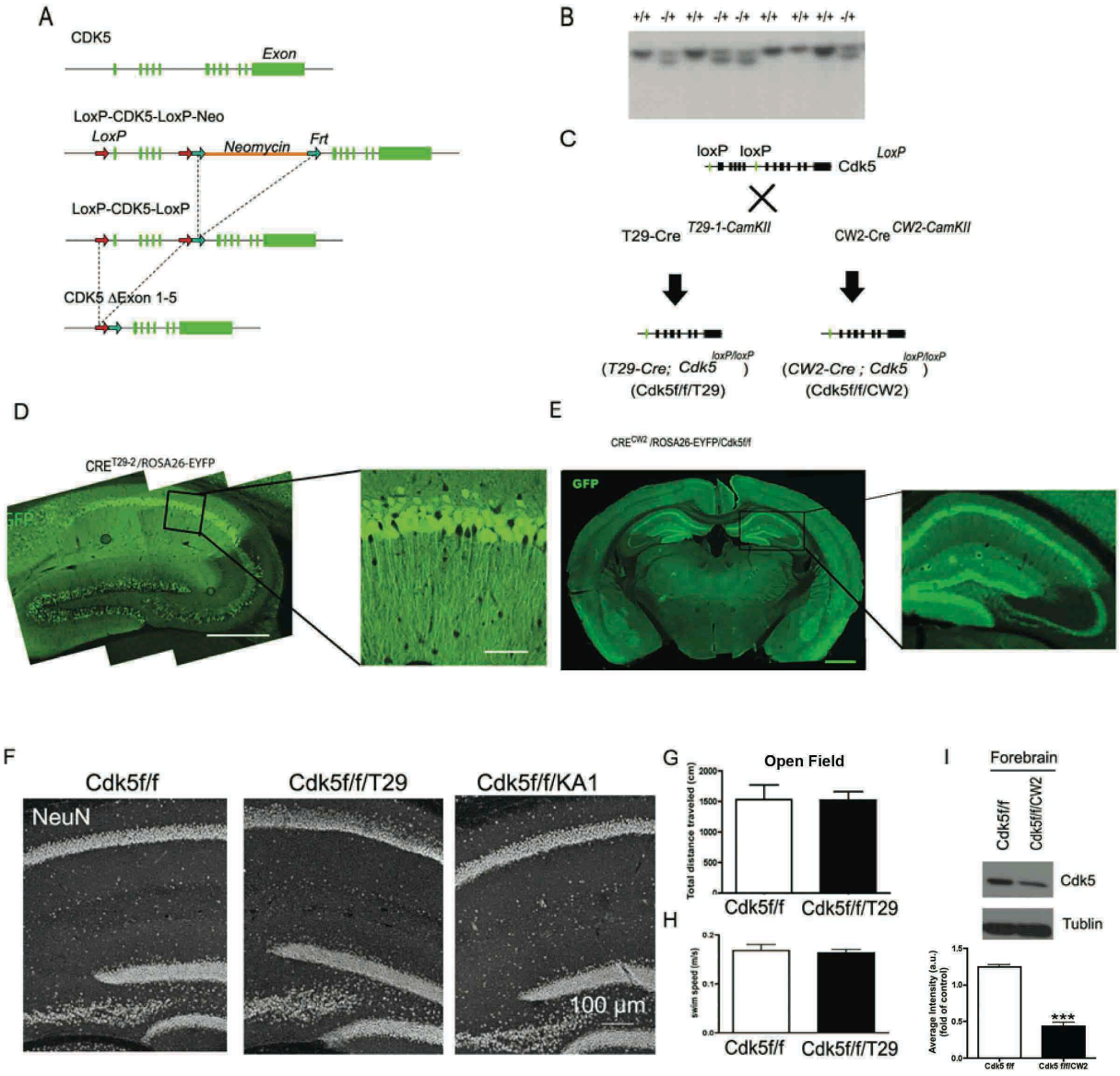

Figure 1. Generation of mouse models with Cdk5 ablation in hippocampal areas CA1 and CA3.
A. Cre/loxP recombination system design Cdk5 conditional knockouts. Exons 1-5 of CDK5 are flanked with loxP sites. **B**. Southern blot indicating the correct insertion of loxP sites. **C**. The Cre/loxP strategy designed for cell-type-restricted Cdk5 knockout in area CA1 (Cdk5f/f/T29) or forebrain (Cdk5f/f/CW2). The Cre expression is driven by the αCaMKII promoter which is found in excitatory neurons **D**. Immunostaining for GFP in the hippocampus of reporter CRE^{T29-2} / R26Sor mice. The T29-2 Cre line (area CA1-specific CRE line) was crossed to the reporter line R26Sor. Scale bar = 1 mm. **E**. Immunostaining for GFP in the hippocampus of reporter CRE^{CW2} / R26Sor. The CW2 Cre line (forebrain-specific CRE line) was crossed to the reporter line R26Sor. **F.** Representative pictures showing NeuN labeling in the hippocampus of Cdk5f/f, Cdk5f/f/T29 and Cdk5f/f/KA1 mice (3 month old). No obvious neuronal loss was seen in the different groups. **G.** Open field test for Cdk5f/f and Cdk5f/f/T29 mice. No differences were observed during the first 5 min of activity in the open field. **H**. Swimming speeds for Cdk5f/f and Cdk5f/f/T29 mice during the Morris water maze task. No significant difference was observed**. I.** Western immunoblot showing the reduction of Cdk5 in the forebrain of Cdk5f/f/CW2 mice and quantification (n=3 mice per group).

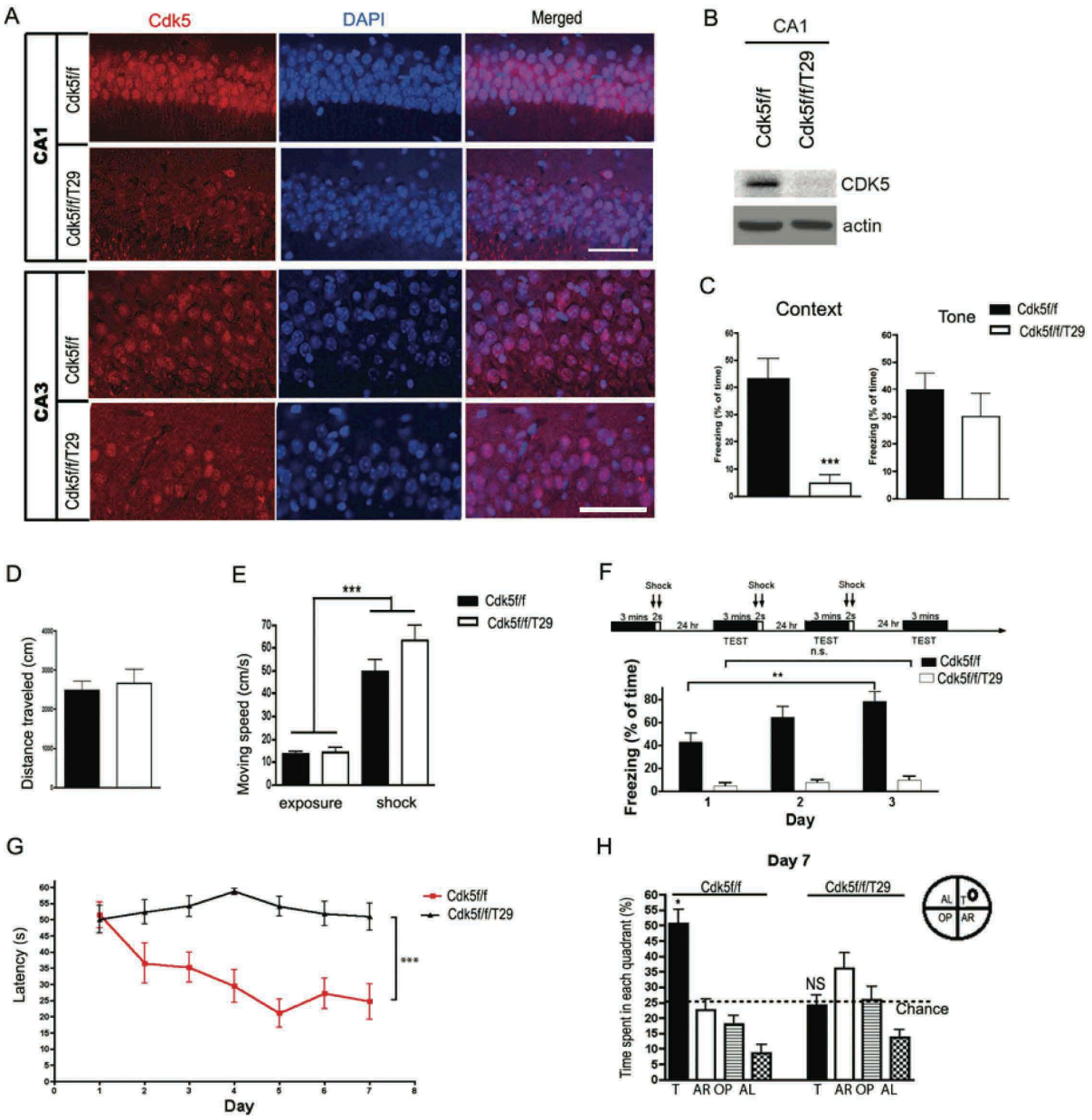

Figure 2. Associative and spatial learning are impaired in Cdk5f/f/T29 mice.
A. Immunostaining for Cdk5 in hippocampal areas CA1 and CA3 in Cdk5f/f, Cdk5f/f/T29 mice. Scale bars, 100 μm. **B**. Western blot showing the reduction of Cdk5 in micro-dissected area CA1 of Cdk5f/f/T29 mice. **C**. Context- and tone-dependent (cued) fear conditioning tests for Cdk5f/f/T29 and Cdk5f/f (control) mice. Cdk5f/f, n=16; Cdk5f/f/T29, n=16 for context; Cdk5f/f, n=8; Cdk5f/f/T29 n=8 for tone-dependent task. **D**. Distance traveled during the initial 3 min exposure to the training box. **E**. The velocity during the 3 min of training and electrical foot shock. **F**. In context-dependent fear conditioning test, Cdk5f/f and Cdk5f/f/T29 mice were trained for 3 continuous days. Cdk5f/f, n=8; Cdk5f/f/T29, n=8. **G**. Morris water maze test. Escape latencies of Cdk5f/f mice improved significantly faster than Cdk5f/f/T29 mice. N=8 for each group. **H**. On day 7, a probe trial was conducted in which the swimming time in each quadrant was quantified. T, target quadrant; L, left quadrant; O, opposite quadrant; R, right quadrant. *p<0.05; **p<0.005; ***p<0.001.

We next utilized the Morris water maze hidden-platform paradigm to evaluate hippocampal-dependent spatial learning in the Cdk5f/f/T29 mice. Over the course of the training period, Cdk5f/f mice displayed a significant decrease in the latency to find the hidden platform (51.5± 4.1 s, day 1; 24.7±5.5 s, day 7). However, the Cdk5f/f/T29 mice consistently showed longer escape latencies during the training period that did not improve over time (50.1±4.3s, day 1; 51.0 ±4.2 s, day 7; control *vs.* KO group, $p<0.0001$, one way ANOVA; **Figure 2G**). During the probe trial on day 7, when the platform was removed from the swimming pool, Cdk5f/f/T29 mice spent a comparable duration in the four quadrants, while the Cdk5f/f mice spent significantly more time in the target quadrant (T), where the platform had previously been placed (**Figure 2H**). The decreased time spent by the Cdk5f/f/T29 mice in the target quadrant compared to Cdk5f/f was not due to motor defects, as the swimming speed of Cdk5f/f/T29 mice was similar to Cdk5f/f mice (**Figure 1H)**. Thus, the ablation of Cdk5 in CA1 pyramidal neurons significantly impairs spatial learning.

To confirm these results in another mouse model, we used the forebrain-targeted Cre line (Zeng et al., 2001) (CW2 line; CaMKII promoter transgenic mice, **Figure 1C, 1E**) to generate forebrain-targeted Cdk5 deletion in excitatory neurons (**Figure 1I**). Consistent with the Cdk5f/f/T29 mice, the Cdk5f/f/CW2 mice displayed impaired spatial learning in the Morris water maze task and contextual fear conditioning (**Chapter 5**). Our data strongly suggest that ablation of Cdk5 in excitatory neurons impairs memory formation without apparent neuronal death (**Figure 3A, 3B**).

Pattern completion-based memory retrieval is impaired in Cdk5f/f/KA1 mice

To evaluate Cdk5 function in other neuronal populations, we utilized a kainate receptor subunit KA1 promoter Cre line (G32-4) (Nakazawa et al., 2003), which expresses Cre mainly in CA3 pyramidal neurons, to generate conditional Cdk5 KO mice (Cdk5f/f/KA1) (**Figure 4A-C, Figure 5A**). In contrast with Cdk5f/f/T29 mice, no seizure activity was observed in these Cdk5f/f/KA1 mice (data not shown). Therefore, 2.5-3.5 month-old Cdk5f/f/KA1 mice were subsequently used for behavior tests. The Cdk5f/f/KA1 mice did not show significant differences in freezing behavior 24 hr after contextual fear conditioning training compared to littermate (Cdk5f/f) controls (52.2±3.9% in Cdk5f/fs *vs.* 39.2±6.9% in Cdk5f/f/KA1; **Figure 5B**).

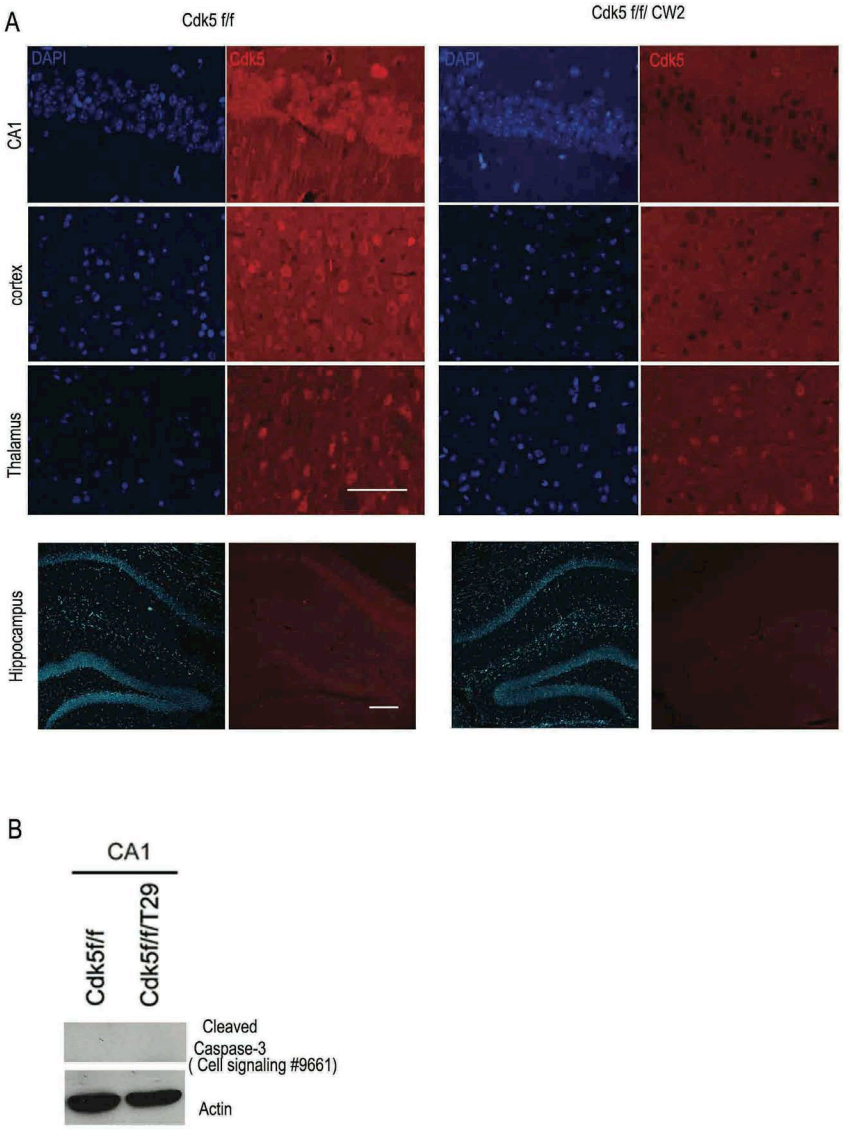

Figure 3. Examination of neuronal morphology and cell death in Cdk5 mutant mice.
A. Cdk5f/f (control) and Cdk5f/f/CW2 mice were stained with DAPI and imaged in area CA1 of the hippocampus, the cortex, and thalamus. No overall differences in neuronal morphology or cell death were observed. Scale bars, 100 μm.
B. Immunoblots from Cdk5f/f and Cdk5f/f/T29 micro-dissections of area CA1 of the hippocampus do not reveal any activated cell death markers as assayed by cleaved caspase-3.

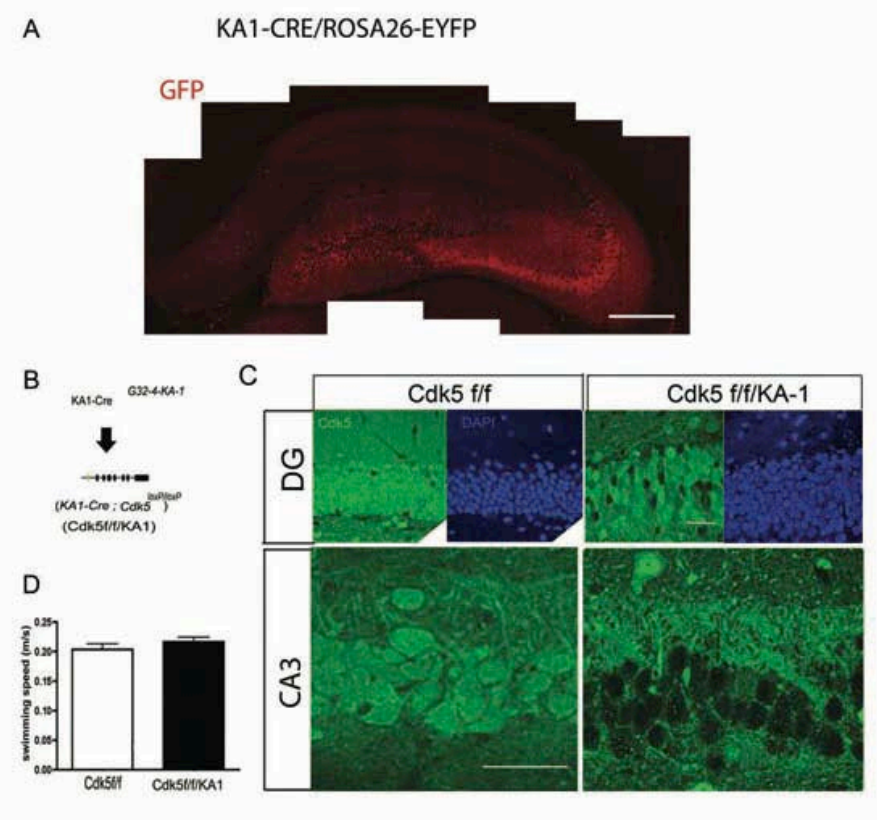

Figure 4. Region-specific recombination in the hippocampus.
A. Immunostaining for GFP in the hippocampus of reporter CRE$^{G32\text{-}4}$/ R26Sor. G32-4 Cre mice (CA3-specific CRE line, denoted as Cdk5f/f/KA1) were crossed to the reporter line R26Sor. Scale bar = 1 mm. **B.** the generation of Cdk5f/f/KA1 mice in which Cdk5 is depleted in hippocampal area CA3. **C.** Immunostaining for Cdk5 in areas CA3 and DG of control mice Cdk5f/f and Cdk5f/f/KA1. Scale bar = 100 μm. **D**. Swimming speeds for Cdk5f/f and Cdk5f/f/KA1 mice. No significant differences were observed.

However, upon being tested in the training chamber one month after the training, Cdk5f/f/KA1 mice exhibited dramatically reduced freezing behavior compared to the Cdk5f/f mice (55.9±5.8% in Cdk5f/fs *vs.* 20.5±6.1% in Cdk5f/f/KA1). This result suggests that either long-term memory consolidation or long-term memory retrieval is impaired in the Cdk5f/f/KA1 mice. This observation cannot be attributed to the loss of the ability to express freezing behavior, because further training of these mice in the contextual fear conditioning chamber led to equal freezing behavior of Cdk5f/f/KA1 and Cdk5f/f mice when tested 24 hr after an additional training (1 month re-train group, **Figure 5B**). The behavioral phenotype is not due to alterations in moving ability (**Figure 5C**).

The Cdk5f/f/KA1 mice were then tested with the Morris water maze hidden-platform task. During training, the Cdk5f/f/KA1 mice exhibited similar spatial learning behavior to the Cdk5f/f littermates (**Figure 5D**). The average escape latencies did not differ between the two groups (Cdk5f/f/KA1, 58.3±1.1s (day 1) to 34.5±4.8s (day 15); Cdk5f/f 58.3±1.3s (day 1) to 38.6±4.4s (day 15)). The probe trial revealed that the Cdk5f/f/KA1 mice display similar searching patterns as the control littermates, spending more time in the target quadrant when presented with full spatial cues (**Figure 5E**). However, when presented with partial spatial cues during the probe trial (day 16), the Cdk5f/f/KA1 mice did not spend significantly more time in the target quadrant (**Figure 5F**). When presented with partial cues in the hidden platform test, the Cdk5f/f/KA1 mice displayed significantly increased escape latencies (45.7±5.9s) compared to the control mice (25.7±5.2s) in reaching the target position (**Figure 5G**). The frequency of the Cdk5f/f/KA1 mice crossing the platform was also significantly lower than controls (**Figure 5H**). No differences in swimming speeds were observed between Cdk5f/f/KA1 and Cdk5f/f mice (**Figure 4D**). These results suggest that Cdk5 is essential for pattern completion-based memory formation, a form of memory previously described as involving hippocampal CA3 circuits (Nakazawa et al., 2003).

Collectively, ablation of Cdk5 in hippocampal area CA1 impairs memory formation while the loss of Cdk5 function in hippocampal area CA3 affects pattern completion, consistent with previously established memory functions in these particular hippocampal circuits (Nakazawa et al., 2003; Tsien et al., 1996b). No neuronal degeneration or dramatic morphological changes were observed in these mice (**Figure 1F, 3**). These results provide compelling evidence for an integral role of Cdk5 in regulating hippocampus-dependent memory

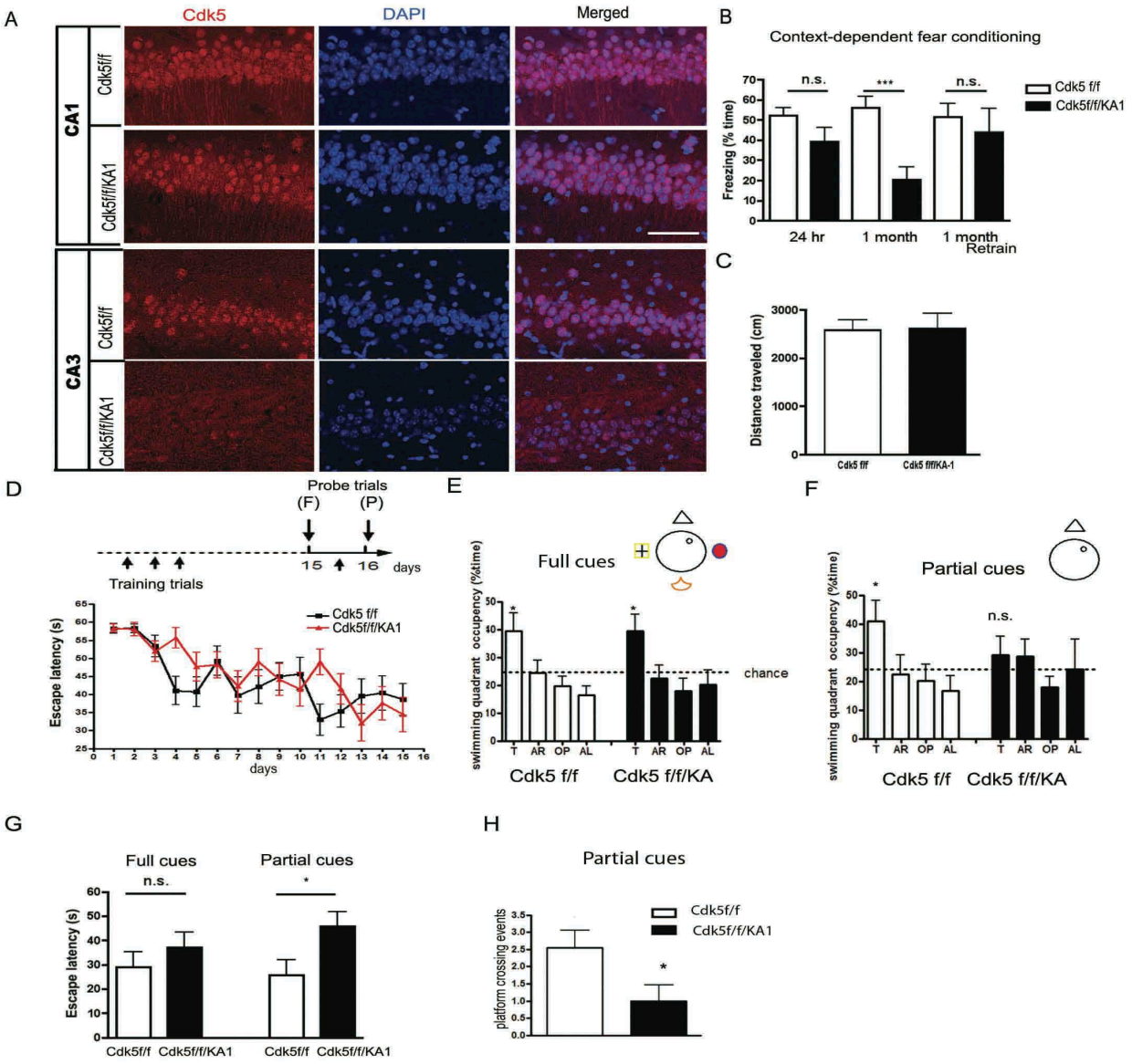

Figure 5. Memory retrieval is impaired in Cdk5f/f/KA1 mice.
A. Immunostaining for Cdk5 in hippocampal areas CA1 and CA3 in Cdk5f/f and Cdk5f/f/KA1 mice. Scale bar, 100 μm. **B**. Contextual-dependent fear conditioning test for Cdk5f/f/KA1 mice. Cdk5f/f, n=10; Cdk5f/f/KA1, n=8. **C**. Distance traveled during the initial 3 min exposure to the training box. **D**. Morris water maze training paradigm (top). Mice were trained for 16 days. On day 15, they were tested in a probe trial with full visual cues around the tank, followed by an additional training trial. On day 16, mice were tested in another probe trial with most of the visual cues removed around the tank. (Bottom) Latencies for the mice to reach the platform during training did not show significant differences between Cdk5f/f/KA1 (n=10) and Cdk5f/f mice (n=10). (P), partial cues, (F), full cues. **E**. Cdk5f/f/KA1 mice showed similar preferences toward the target quadrant as the Cdk5f/f group in a full cue trial on day 15. **F**. Cdk5f/f/KA1 mice did not show preferences toward the target quadrant in the partial-cue-trial on day 16. **G**. Cdk5f/f/KA1 mice take more time to reach the hidden platform position than Cdk5f/f mice in the partial cue, but not the full cue, trial. **H**. In the probe trial with partial cues, the average number of crossings over the platform position is much lower for the Cdk5f/f/KA1 group than that for the Cdk5f/f group. *p<0.05; **p<0.005.

functions. As synaptic plasticity and the signaling molecules involved in hippocampus-dependent memory events are best understood in area CA1, we utilized three-month-old Cdk5f/f/T29 mice for subsequent studies to dissect the downstream molecular pathway by which Cdk5 regulates learning and memory in the hippocampus.

Impaired synaptic plasticity in Cdk5 mutant mice

As synaptic plasticity has been implicated in memory formation, we therefore evaluated synaptic plasticity in the hippocampus of Cdk5f/f/T29 mice by examining long-term potentiation (LTP) in CA1 neurons. Acute transverse slices (400 μm) were obtained from Cdk5f/f/T29 or Cdk5f/f mice, and field excitatory postsynaptic potentials (fEPSPs) were evoked by placing an electrode on the Schaffer collateral pathway. After 15 min of baseline recording, LTP was induced using two trains of high-frequency stimulation (HFS; 100 Hz, 1 s). Forty-five minutes after HFS, field excitatory postsynaptic potentials (fEPSPs) remained elevated in the Cdk5f/f slices (121.88 ± 7.04%; **Figure 6A**). In contrast, fEPSPs decayed to baseline in the Cdk5f/f/T29 slices (109.13 ± 6.79%; **Figure 6A**, *p<0.01 Cdk5f/f *vs.* Cdk5f/f/T29). Presynaptic transmission was unimpaired, as measured by the paired-pulse facilitation (PPF) ratio, which measures the probability of presynaptic neurotransmitter release (**Figure 6B**). The input-output curves generated by plotting the fEPSP slopes against the slopes of the fiber volley were also indistinguishable, suggesting normal basal synaptic transmission (**Figure 6C**). However, Cdk5f/f/T29 slices exhibited defects in post-tetanic potentiation (PTP; **Figure 6D**). Although PTP is thought to be mainly affected by presynaptic mechanisms, postsynaptic injection of Ca^{2+} chelators, which affects postsynaptic cAMP activation, have also been found to block PTP (Bao et al., 1997). Thus, neuronal Cdk5 ablation is associated with both LTP and PTP deficits in hippocampal CA1 neurons. We then proceeded to evaluate long-term depression (LTD). Low-frequency stimulation (LFS; 1Hz, 900 pulses, 15 min) of the Schaffer collateral pathway induced a long-lasting synaptic depression in the Cdk5f/f animals. In contrast, LTD could not be induced in Cdk5f/f/T29 mice (**Figure 6E**). These data indicate that both LTP and LTD measures of synaptic plasticity are largely impaired in the Cdk5 mutant mice, which is consistent with their memory deficits.

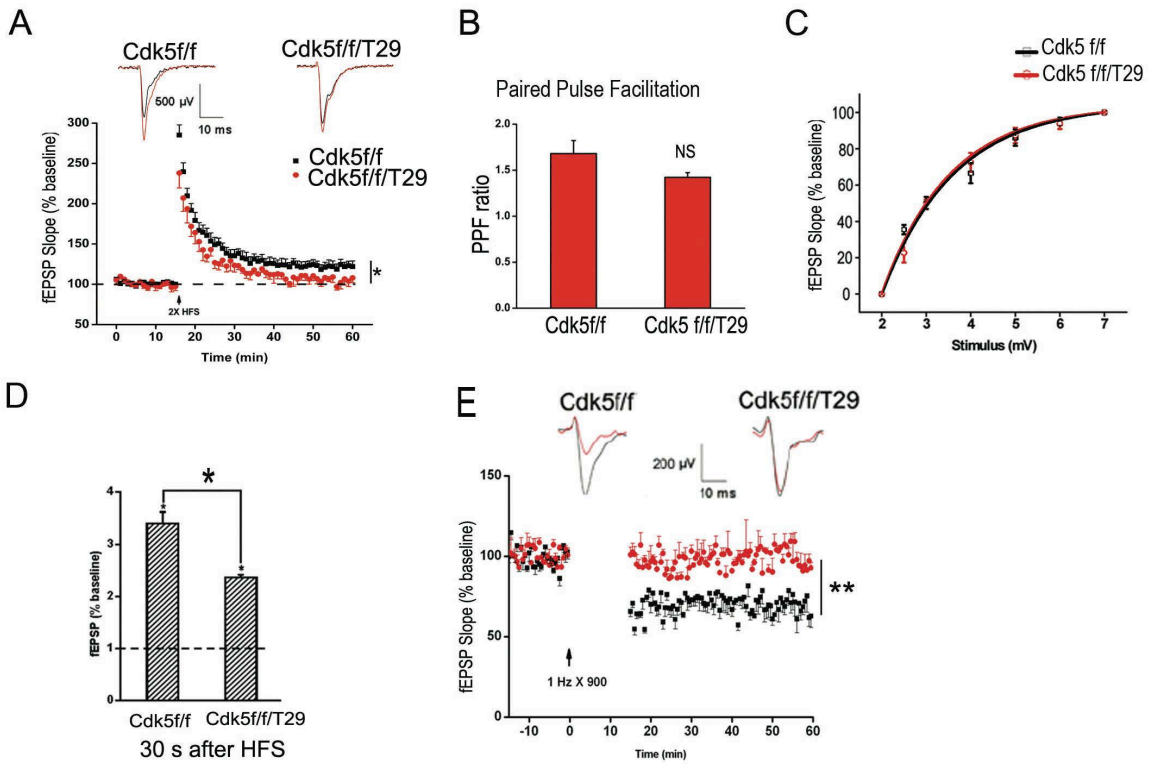

Figure 6. Synaptic plasticity is largely impaired in Cdk5f/f/T29 mice.
A. Acute hippocampal slices obtained from 2-month-old Cdk5f/f/T29 and Cdk5f/f mice were stimulated with two trains of HFS (100 Hz, 1 s) in area CA1. Field EPSPs (fEPSPs) were measured from area CA1 in Cdk5f/f and Cdk5f/f/T29 mice (n=8 for each group). **B**. Paired-pulse facilitation (PPF) in Cdk5f/f mice and Cdk5f/f/T29 and (n=9 for each group). **C**. The input-output curve indicates normal basal synaptic transmission in the Cdk5f/f/T29 mice. **D.** Post-tetanic potentiation (PTP) from Cdk5f/f/T29 mice was lower than in Cdk5f/f mice 30s after two trains of HFS (100 Hz, 1 s). **E**. LTD was measured in area CA1 of acute hippocampal slices from Cdk5f/f and Cdk5f/f/T29 after low frequency stimulation (1 Hz, 900 pulse; n=6 for each group).

Disruption of CREB activity in Cdk5f/f/T29 mice

To dissect the molecular pathways involved in Cdk5-mediated synaptic plasticity and memory formation, we evaluated well-established signaling molecules involved in memory formation in the Cdk5f/f/T29 mice. CREB is an important transcription factor essential for expression of genes important for synaptic plasticity. A decrease in phosphorylated CREB on Serine 133 pCREB(S133), a modification required for CREB-mediated transcriptional activity during memory formation (Deisseroth et al., 1998), was detected in Cdk5f/f/T29 mice using an anti-pCREB(S133) antibody. The reduction of pCREB(S133) was specific to area CA1 neurons (**Figure 7A, 7B**), as no reduction of pCREB(S133) was detected in either cortical or CA3 neurons, where Cdk5 expression was unaffected. In hippocampal area CA1 lysates, pCREB(133) was markedly decreased in the Cdk5f/f/T29 compared to the Cdk5f/f mice (**Figure 7C**).

NMDA receptors are major mediators of synaptic plasticity, and in a different Cdk5 conditional knockout mouse model, it was demonstrated that NR2B degradation is impaired, resulting in increased surface expression of NR2B and enhanced synaptic plasticity (Hawasli et al., 2007). The degradation of NR2B was reported to be regulated by phosphorylation of Tyrosine 1472 (Y1472) on NR2B via Cdk5 (Zhang et al., 2008). We found no differences in NR2A and NR2B protein levels in area CA1 between Cdk5f/f/T29 and Cdk5f/f mice (**Figure 7C**). Moreover, pNR2B (Y1472) was not altered in CA1 hippocampal lysates from Cdk5f/f/T29 mice compared to control littermates. Thus, the synaptic plasticity and learning behavior deficits observed in the Cdk5f/f/T29 mouse are associated with impaired CREB phosphorylation, but not with alterations in total NR2A/NR2B protein levels, or NR2B Y1472 phosphorylation.

The insertion of GluR1-containing AMPA receptors into the synapse constitutes a major mechanism underlying the plasticity produced by the activation of CaMKII and LTP induction (Hayashi et al., 2000). We found that the GluR1 phosphorylation on S831, a site phosphorylated by CaMKII (Roche et al., 1996), was increased in Cdk5f/f/T29 samples compared to controls at basal levels (**Figure 7D**). In addition, GluR1 phosphorylation on S845, a PKA site (Roche et al., 1996), was also upregulated (**Figure 7D**). Conversely, the activity of protein phosphatases 1 and 2 (PP1 and PP2) was reduced in the Cdk5f/f/T29 mice (**Figure 7E**). Thus, decreased phosphatase activity may contribute to increased GluR1 phosphorylation. These results indicate that perturbations in intracellular signaling pathways related to synaptic plasticity occur in the absence of Cdk5.

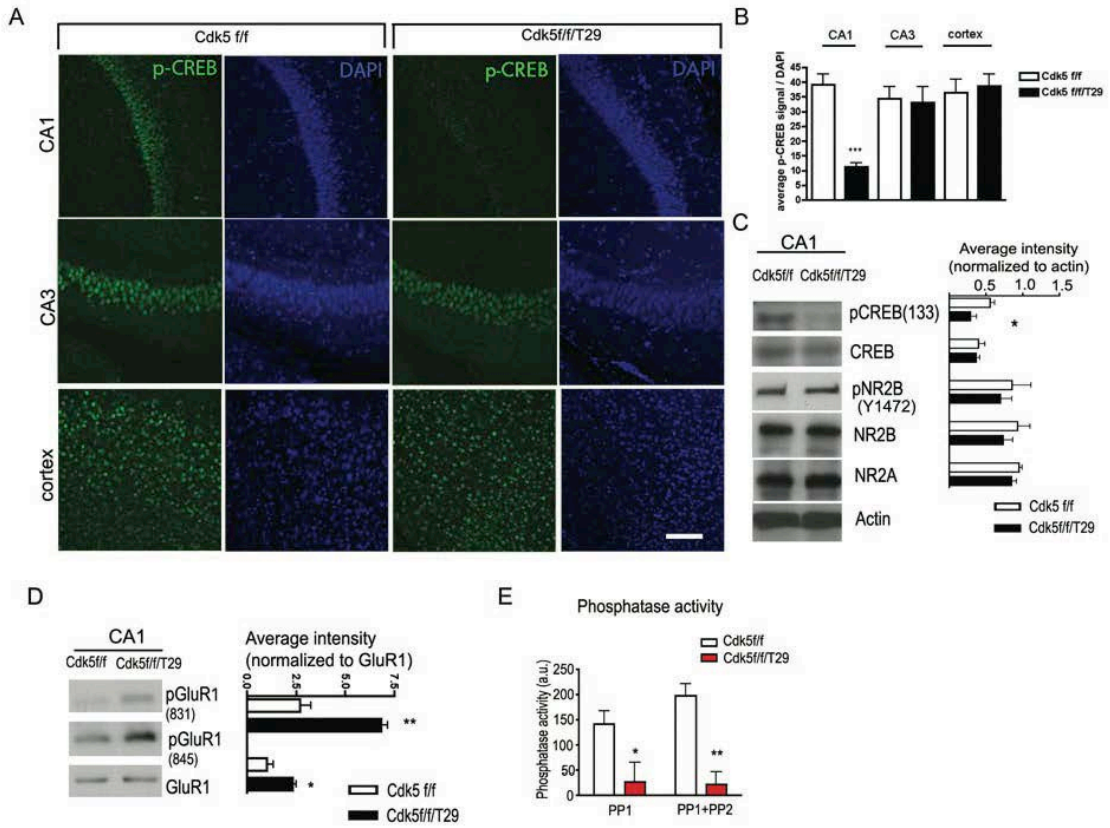

Figure 7. Impaired CREB phosphorylation and hyper-phorsphorylation of GluR1 in Cdk5f/f/T29 mice.

Immunostaining (**A**) and quantification (**B**) of pCREB in hippocampal CA1 and cortex. Scale bar = 100 μm. **C**. Western blots of micro-dissected CA1 tissue show reduced pCREB levels. **D**. Western blots of micro-dissected CA1 tissue reveals hyper-phosphorylation of GluR1. **E.** Area CA1 phosphatase activity in Cdk5f/f and Cdk5f/f/T29 mice (n=3, each group). *p<0.05, **p<0.005, ***p<0.001.

Proteomic analysis reveals protein composition changes in Cdk5 mutant mice

To further decipher the mechanism by which Cdk5 influences synaptic plasticity, we applied a total, unbiased, proteomic approach to analyze changes in protein composition and phosphorylation in synaptosomal preparations of control and mutant mice. To this end, brains from control and Cdk5f/f/CW2 mice were homogenized and subjected to standard synaptosomal, postsynaptic density (PSD) isolation. Solubilized PSD proteins were run on an SDS-PAGE gel that was sliced into thirteen fields, and sequenced by LC/MS/MS (**Figure 8A, 8B, Figure 9A**). Approximately 1595 distinct, differentially expressed peptide groups were detected from control (Cdk5f/f) and Cdk5f/f/CW2 PSD preparations; of these, 700 peptides, implicated in dendritic spine/synapse formation, synaptic vesicle exocytosis, small GTPase signaling pathways, and ion channel functions, contain consensus Cdk5 phosphorylation sites. Among these potential Cdk5 substrates, the abundance of 296 proteins was increased, and the abundance of 51 proteins was decreased, in the Cdk5f/f/CW2 mice compared with controls (**Figure 9B**). These proteins comprised multiple different categories, including motor proteins and protein involved in membrane trafficking and kinase/phosphatase activity. Interestingly, consistent with the western immunoblotting results, NMDA receptor subunits did not show significant changes (<1.5 fold) in the PSD fractions (**Figure 9C**; Grin2a, 2b). In contrast, multiple GluRs showed dramatic increase in the PSD fractions (**Figure 9C**; Gria1-4), suggesting increased synaptic AMPA receptors protein levels in the mutant mice. Overall, the drastic changes of protein composition in the PSD of Cdk5f/f/CW2 *vs*. controls suggest a key role of Cdk5 in regulating synaptic protein expression and abundance.

To further probe the mechanism underlying the phenotype of the Cdk5 conditional knock-out mice, we used our proteomic data to examine potential Cdk5 targets that could affect CREB activation. Among the known regulators of cAMP signaling pathway, cyclic nucleotide phosphodiesterase (PDE) proteins, enzymes that catalyze the conversion of cAMP and AMP into cGMP and GMP, respectively, were markedly increased in the Cdk5f/f/CW2 mice (**Figure 9C**). Conversely the adenylyl cyclase (AC) family proteins, which catalyze ATP to cAMP (Levin et al., 1992), were not detected in our proteomic data set, suggesting a low abundance of those proteins in the PSD preparation.

To further confirm the proteomic analysis, mRNA levels of AC family members were measured in control and mutant mice. Group 1 ACs are represented by AC1, AC3, and AC8, and

are stimulated by calmodulin in a Ca^{2+}-dependent manner (Wong et al., 1999). We examined the mRNA levels of AC1, 3, and 8, but did not observe differences in the Cdk5f/f/T29 mice compared to controls (**Figure 9D**). However, we detected increased mRNA expression of PDE family proteins in the Cdk5 mutant mice using quantitative PCR with hippocampal RNA extracts. After signal normalization, mRNAs for PDE1a, PDE4D1, PDE4D4, PDE2a, and PDE4b were significantly increased in the Cdk5f/f/T29 mouse hippocampus compared to Cdk5f/f (**Figure 9E**). PDE4 proteins exclusively target cAMP and is a specific target for rolipram, while PDE1 and 2 also target cGMP. While cAMP has been shown to regulate LTP (Blitzer et al., 1995; Frey et al., 1993), cGMP is involved in regulating LTD (Calabresi et al., 1999), The increase in the PDE1 and 2 isoforms, which deplete cGMP, in Cdk5f/f/T29 mice might be a contributing factor to the loss of LTD. Thus, increased PDE expression in the Cdk5f/f/T29 mice may impair LTP and LTD induction via depletion of cAMP and cGMP.

Cdk5 loss of function blocks activation of the cAMP activation pathway, which can be restored by rolipram

To further test the hypothesis that the dysregulated cAMP signaling, by virtue of increased PDE expression, underlies the observed plasticity and behavioral phenotypes exhibited by the Cdk5 mutant mice, we evaluated the consequences of the pharmacological inhibition of these enzymes in the Cdk5f/f/T29 mice. Rolipram, a PDE4-specific small molecule inhibitor, was recently reported to facilitate memory formation and synaptic plasticity in rodents (Vitolo et al., 2002). In Cdk5f/f mice, rolipram treatment resulted in the increased phosphorylation of GluR1 at S845, consistent with a role for cAMP signaling and PKA phosphorylation of S845 (**Figure 10A**). At basal levels, phosphorylation of GluR1 at both S831 and S845 in Cdk5f/f/T29 mice is significantly higher compared to Cdk5f/f controls. However, rolipram treatment in Cdk5f/f/T29 mice selectively reduces phosphorylation of GluR1 at S831, indicating that the inhibition of PDE4 may affect GluR1 phosphorylation preferentially at the CaMKII phosphorylation site. To further examine if PDE inhibition, and therefore persistent cAMP signaling, has influences on other biochemical changes in Cdk5f/f/T29 mice, we evaluated PP1 activity. As PDEs are upregulated in the Cdk5 mutant mice, we explored the consequences of PDE inhibition by rolipram. Interestingly, blocking PDE4 activity by rolipram (0.1mg/kg, i.p.) in Cdk5f/f/T29 mice restores PP1 activity (**Figure 10B**).

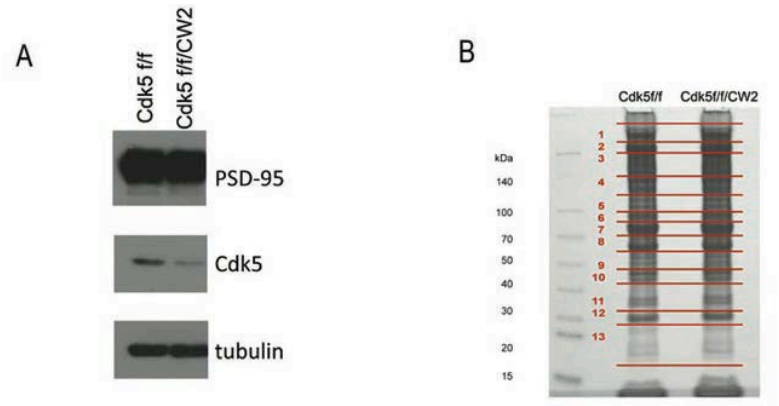

Figure 8. Mass-spectrometry preparation of PSD samples.
A. Western immunoblotting of PSD proteins after preparation. Cdk5 is significantly reduced in forebrain PSD preparations of Cdk5f/f/CW2 mice. **B.** Coomassie blue staining of PSD proteins on an SDS-PAGE gel. Thirteen gel slices were obtained from each lane in preparation for LC/MS/MS.

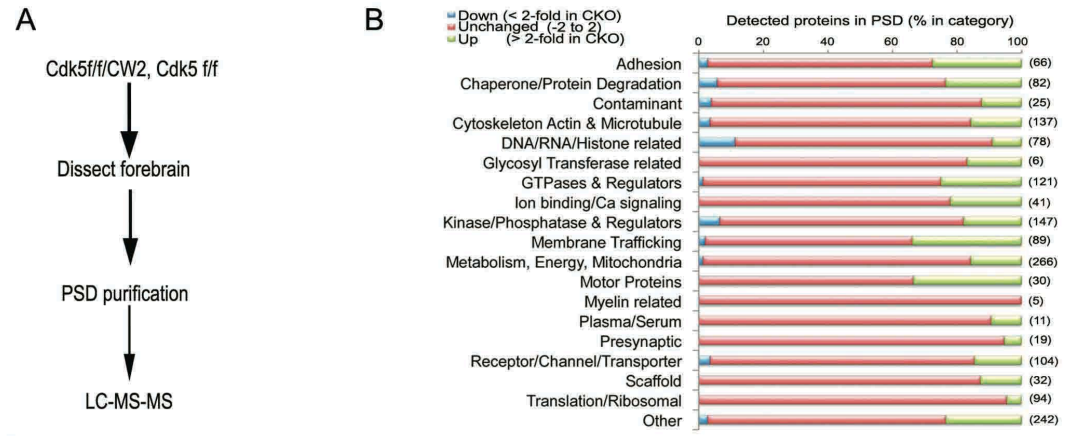

C

Channels

Gene	accession number	Ratio (cKO/control)	total intensity control	cKO
Grin2b	IPI00321320	1.4	1.88E+09	2.65E+09
Grin2a	IPI00118380|IPI00848800	1.1	8.01E+08	7.02E+08
Gria2	IPI00608015|IPI00845711|IPI00466699|IPI00136967|IPI00751228	1.3	2.24E+09	2.92E+09
Gria1	IPI00407939|IPI00850565	1.6	1.79E+07	2.81E+07
Gria3	IPI00131472	1.4	9.45E+07	1.30E+08
Gria4	IPI00881877	3.6	3.69E+07	1.33E+08
Slc25a12	IPI00308162|IPI00135651	1.6	1.58E+09	2.57E+09
Cacnb4	IPI00626660|IPI00131720|IPI00473235|IPI00228423|IPI00420995|IPI00420994|IPI00420996	1.0	4.51E+08	4.71E+08
Cacnb3	IPI00788326|IPI00788347|IPI00133518	1.1	3.37E+08	3.07E+08
Cacnb1	IPI00321850|IPI00421276|IPI00421277|IPI00828389|IPI00421278|IPI00648787	1.6	3.35E+07	5.41E+07

Structure/Scaffold

Gene	accession number	Ratio (cKO/control)	total intensity control	cKO
Spnb2	IPI00319830|IPI00121892|IPI00831369|IPI00281849|IPI00556909	1.3	2.73E+10	3.52E+10
Actg1	)|IPI00874780|IPI00648161|IPI00885570|IPI00856609|IPI00857335|IPI00229224|IPI00754167	1.3	2.40E+10	3.12E+10
Bsn	IPI00134093|IPI00461199	1.0	2.11E+10	2.01E+10
Syngap1	IPI00663736|IPI00890338	1.6	1.50E+10	2.33E+10
PSD-95	IPI00122094|IPI00622720|IPI00626797|IPI00460450|IPI00648595	1.3	9.74E+09	1.25E+10
Pclo	IPI00225140|IPI00468100|IPI00752192|IPI00754054|IPI00876448|IPI00473889|IPI00889854	1.0	6.80E+09	7.08E+09

PDEs

Gene	accession number	Ratio (cKO/control)	total intensity control	cKO
Pde1a	IPI00121336|IPI00874497|IPI00223497|IPI00553355|IPI00551326|IPI00750963|IPI00460850	1.4	3.06E+07	2.15E+07
Pde1b	IPI00118900|IPI00225618|IPI00133376|IPI00466650	1.6	1.65E+07	2.57E+07
Pde4b	3|IPI00465959|IPI00316902|IPI00466648|IPI00894911|IPI00894848|IPI00895234|IPI00649977	3.6	6.88E+06	2.47E+07
Pde2a	IPI00762623|IPI00623742|IPI00380799|IPI00652772	1.9	1.61E+08	3.03E+08

PLC pathway

Gene	accession number	Ratio (cKO/control)	total intensity control	cKO
Grm5 (mGluR5)	IPI00659932|IPI00553387|IPI00867815	1.3	4.93E+07	3.26E+07
Plcb1	IPI00468121|IPI00130045|IPI00323250|IPI00752907	1.0	2.43E+07	2.47E+07
Inpp5a	IPI00223274|IPI00856931|IPI00653599	1.6	1.54E+07	2.46E+07
Itpr2	PI00263233|IPI00856392|IPI00137400|IPI00222043|IPI00896035	1.3	1.52E+07	2.03E+07

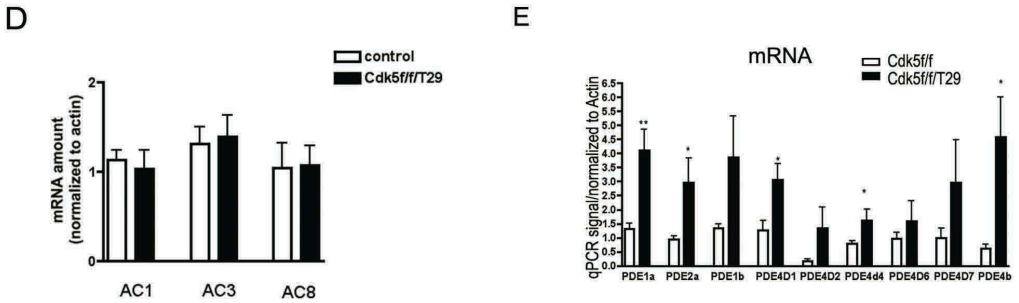

Figure 9. Proteomic analysis of post-synaptic densities reveals changes in PDE proteins in CDK5 mutant mice.

A. Procedure sequence for mass-spectrometry analysis with PSDs from control (Cdk5f/f) and Cdk5f/f/CW2 (cKO) mice. **B**. Summary of detected protein abundance differences categorized by various protein functions. **C.** Representative molecules changes detected in Cdk5 cKO mice. Red number indicates reduction folds; black number indicates increase folds. **D**. RT-qPCR results of ACs in hippocampal CA1 in Cdk5f/f and Cdk5f/f/T29. qPCR signals were normalized to actin in each sample (n=3). **E.** RT-qPCR results of PDEs from hippocampal area CA1 in Cdk5f/f and Cdk5f/f/T29.

We next evaluated the effect of rolipram pretreatment on the activity-induced phosphorylation of CREB(S133) in the Cdk5f/f/T29 mouse. Rolipram (0.1 mg/kg) was administered into Cdk5f/f or Cdk5f/f/T29 mice 20 min before contextual fear conditioning training. Animals were sacrificed 20 min after training and hippocampal area CA1 was dissected for biochemical processing. Training increased pCREB(S133) in area CA1 of Cdk5f/f mice (**Figure 10C**), whereas the saline-injected Cdk5f/f/T29 group did not show any increase in pCREB(S133) levels after training (**Figure 10D**). However, in rolipram-treated Cdk5f/f/T29 mice, contextual fear training induced a significant increase in pCREB in hippocampal area CA1, suggesting that rolipram treatment rescued the training-induced activation of pCREB (**Figure 10D**). Thus, Cdk5 enabled the activation of pCREB via the regulation of cAMP levels.

Rolipram treatment partially restores synaptic plasticity in Cdk5f/f/T29 mice

To determine if rolipram treatment influences synaptic plasticity, Cdk5f/f and Cdk5f/f/T29 mice were injected with rolipram (0.1 mg/kg) 20 min before the preparation of acute hippocampal slices for LTP and LTD recordings. Rolipram (0.7 μM) was present in the bath solution throughout the entire experiment. Cdk5f/f slices treated with rolipram alone did not demonstrate enhanced LTP induction compared to Cdk5f/f treated with saline (**Figure 10E)**. Consistent with our previous observations, Cdk5f/f/T29 mice treated with saline exhibited deficits in LTP. Remarkably, following HFS stimulation, fEPSPs remained potentiated (123.2±5.7%) in the hippocampal slices prepared from the rolipram-treated Cdk5f/f/T29 slices, comparable to the level of LTP induced in Cdk5f/f slices. Thus, inhibition of PDE4 by rolipram rescues LTP in the Cdk5f/f/T29 mice. In contrast, although fEPSPs were initially depressed in the rolipram-treated Cdk5f/f/T29 mice after LFS stimulation for LTD induction, synaptic depression was transient and rapidly decayed to baseline levels (**Figure 10F**). Thus, rolipram treatment is sufficient to restore LTP, but not LTD, in the Cdk5f/f/T29 mice. This is also consistent with a reduced phosphorylation of GluR1 on the CaMKII (S831) site, but not the PKA (S845) site (Lee et al., 2000), in the untrained mice.

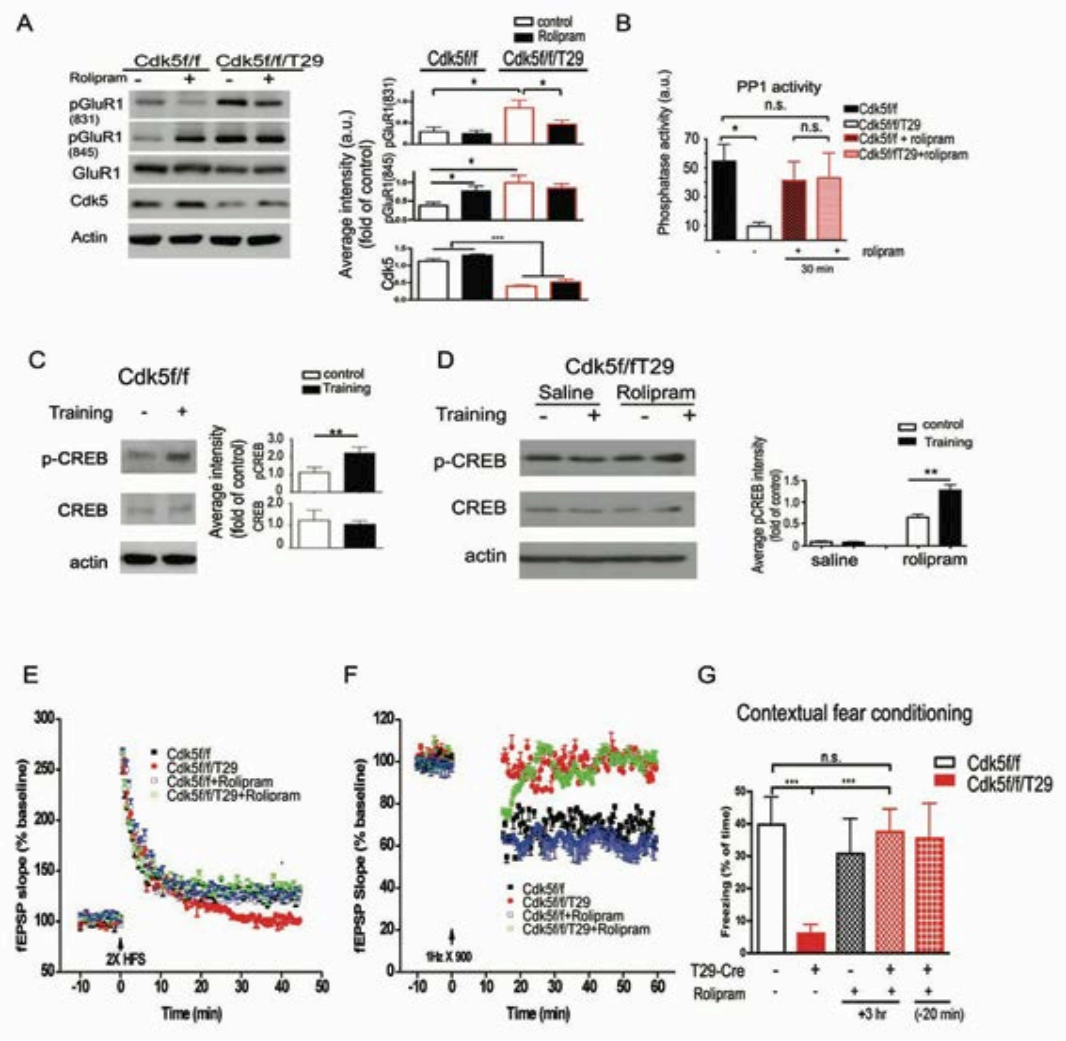

Figure 10. Inhibition of PDE4 by rolipram can restore LTP deficits and rescue memory impairments in Cdk5f/f/T29 mice.

A. Western blot from CA1 lysates after rolipram treatment. Samples were collected 20 min after rolipram or saline (control) injection. **B**. PP1 activity in area CA1 tissue was measured after rolipram treatment (0.1 mg/kg, i.p.). **C**. Western blots (left) for CA1 tissues from Cdk5f/f mice, with quantification (right). Mice were trained in a contextual fear conditioning paradigm followed by tissue harvest 20 min after training. n=5 for each group. **D**. Western blots (left) from micro-dissected CA1 tissues from Cdk5f/f/T29 mice with quantification (right). Rolipram (0.1 mg/kg, i.p.) was injected 20 min before contextual fear conditioning training. Samples were collected 20 min after training (n=3 for each group). **E**. Rolipram restored LTP deficits in the Cdk5f/f/T29 slices. Mice were injected with rolipram or vehicle (Veh) 20 min before sacrifice and slice preparation. Rolipram was also present in the bath solution at 0.7 μM. Slices were stimulated with two trains of HFS (100 Hz, 1 s; n=6 for each group; *p<0.05, between vehicle- and rolipram-treated groups in Cdk5f/f/T29 mice). **F**. Rolipram did not rescue the LTD impairment in Cdk5f/f/T29 slices (n=5 for each group). **G.** In a contextual fear conditioning task, the percent of time spent freezing in Cdk5f/f/T29 mice (n=16) is significantly lower than that of control Cdk5f/f mice (n=8). The percent freezing time for the Cdk5f/f/T29 mice injected with rolipram (0.1 mg/kg, i.p.) 20 min before training (n=8) or 3 hr after training (n=7) is similar to that of the control Cdk5 f/f mice.

Rolipram treatment rescues associative memory in Cdk5f/f/T29 mice

We next investigated whether rolipram could extend its ameliorative effects to the memory impairment caused by Cdk5 loss of function in hippocampal area CA1. Using the contextual fear conditioning paradigm, we found that rolipram administration (0.1 mg/kg) either 20 min before, or 3 hr after, training rescued the memory impairments in the Cdk5f/f/T29 mice (**Figure 10G**). When tested 24 hr after training, the average freezing time of Cdk5f/f/T29 mice was 5.9±2.6%. However, the average freezing time of Cdk5f/f/T29 mice receiving rolipram increased to 35.4±10.8% (the group treated 20 min before training) and 37.3±7.1% (the group treated 3 hr after training) respectively, which were comparable to the average freezing time of control mice (39.6±8.6%; **Figure 10G**). Rolipram treatment in control animals did not alter freezing behavior (30.6±11.0% *vs.* 39.6±8.6%) in the contextual fear conditioning tasks (**Figure 10G**). The rescue of contextual fear memory consolidation with rolipram treatment is especially remarkable considering the severity of the Cdk5f/f/T29 behavioral phenotype, in which untreated mice fail to express contextual fear memory even after three consecutive days of training (**Figure 2F**).

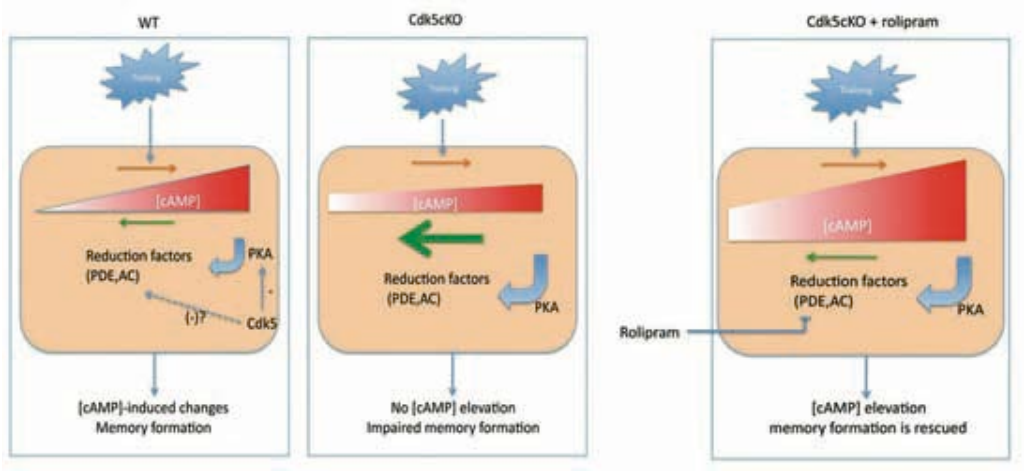

Figure 11. Cdk5 regulates homeostasis of the cAMP pathway.
Model figure demonstrating the proposed role of Cdk5/p35 in regulating the cAMP pathway and synaptic plasticity. Under normal conditions, activity stimulates cAMP and PKA activity, leading to altered cAMP-dependent changes in gene transcription and memory formation. Loss of Cdk5 severely attenuates cAMP signaling and impairs memory formation due to increased PDE activity. Rolipram, a PDE4 inhibitor, prevents the breakdown of cAMP and restores the signaling pathway mediating synaptic plasticity and memory formation.

Discussion

Cdk5 is essential for hippocampal-dependent learning and memory

Cdk5 is thought to be involved in the morphogenesis of synaptic connections, as well as in the regulation of synaptic transmission, through interactions at both presynaptic terminals and postsynaptic spines with proteins that include PSD-95 (Morabito et al., 2004), ErbB (Fu et al., 2001), Stat3 (Fu et al., 2004), DARPP-32 (Bibb et al., 1999), CASK (Samuels et al., 2007), and Eph4/ephexin1 (Fu et al., 2007). In contrast to an earlier study by Hawasli et al in which enhanced hippocampal synaptic plasticity and spatial learning behaviors were observed due to upregulated NMDA receptor subunit NR2B levels (Hawasli et al., 2007), we find that the neuron-specific Cdk5 loss of function has a detrimental effect on hippocampal-dependent associative and spatial memory, and impairs synaptic plasticity, but leads to unaltered NR2B levels. The differences between the previously reported findings and our current observations can be attributed to the methods used to generate the different Cdk5 knockout mouse models. In the previous Cdk5 conditional knockout study (Hawasli et al., 2007), the use of the prion promoter extends Cdk5 knockdown to general regions of the brain including the forebrain, striatum, cerebellum, and hippocampus (Borchelt et al., 1996; Boy et al., 2006; Weber et al., 2001). The prion promoter also drives expression in various neural cell types, including glial cells in which Cdk5 is also expressed (Boy et al., 2006; Lee et al., 2002). Thus, the regional loss of Cdk5 in different cell types may account for previous behavioral observations. Another distinction between these studies consists of acute versus chronic deletion of Cdk5, given the findings that chronic loss of Cdk5 in the inducible mouse model (8 weeks after ablation of Cdk5) resulted in significantly different behavior compared to the acute loss of Cdk5 function (2-4 weeks) (Hawasli et al., 2009). Therefore, while data from the prion promoter mouse model suggest that the widespread acute loss of Cdk5 in both neurons and glia is beneficial for cognition, chronic ablation of Cdk5 in hippocampal circuits led to learning impairments in our Cdk5 models prior to the spread of the Cre promoter expression. This suggests that the targeted deletion of Cdk5 in excitatory neurons of hippocampal areas CA1 and CA3 or forebrain is associated with impaired cAMP signaling, synaptic plasticity, and memory formation. We noticed a slight reduction of Cdk5 in the dentate gyrus of Cdk5f/f/KA1 mice (**Figure 4C**). Therefore, it is possible that Cdk5 may play a role in the DG that affects the observed behavioral phenotypes. In future experiments, it would be of interest to examine how loss of Cdk5 in other

brain regions (such as the DG), or in specific cell-types, including dopaminergic neurons, cholinergic neurons, or a subset of interneurons, impacts the various neural circuits and signaling pathways by which Cdk5 regulates memory formation.

The same strategy used to generate Cdk5 conditional knockout mice in the current work was previously used in studies targeting the NR1 gene to study synaptic plasticity and evaluate the role of the NMDA receptor in areas CA1 and CA3 of the hippocampus (Nakazawa et al., 2003; Tsien et al., 1996b). The similarities between our findings and those using CA1- and CA3-targeted NR1 knockout mice support the notion that Cdk5 is involved in the CA1 spatial memory formation circuit, and in the CA3 pattern completion-based memory recall circuit. However, the memory deficit in the Cdk5f/f/T29 mice appears to be more severe than in mice lacking the NR1 receptor subunit in the CA1 region, as reflected by their poor performance on contextual fear conditioning tasks, even following repeated training. During the Morris water maze hidden platform training, the Cdk5f/f/T29 mice did not exhibit any decrease in average escape latencies despite repeated trainings. Our findings indicate that the more severe phenotype evident in Cdk5f/f/T29 may result from the involvement of Cdk5 in the regulation of cAMP pathways and synaptic transmission via the regulation of phosphatases and PDEs. Thus, Cdk5-mediated regulation of the cAMP pathway is required and essential for memory formation.

Cdk5 modulates PDE signaling pathways essential for synaptic plasticity

Mechanistically, the memory deficits caused by the ablation of Cdk5 are not due to developmental influences, as the postnatal nature of Cre expression with the T29-Cre line has been well-characterized (Tsien, 1998; Tsien et al., 1996a), and hippocampal morphology is not severely altered in any of our Cdk5 mutant mice. The learning phenotype also cannot be attributed to neurodegeneration, as there are no significant differences in the number of pyramidal neurons between the Cdk5-deficient mice and controls (**Figure 1F**). Instead, we identified an abnormal increase in the expression of several PDEs in the brain, suggesting that the cAMP pathway is impacted in the Cdk5 mutant mice. Furthermore, PDE inhibition by acute rolipram treatment restored LTP and CREB phosphorylation in Cdk5f/f/T29 mice. Importantly, rolipram treatment ameliorated the memory deficits observed in the Cdk5f/f/T29 mice. These data strongly support a novel role for Cdk5 in regulating memory via the cAMP pathway.

Earlier mouse genetic studies have elegantly demonstrated that increases in CREB phosphorylation, and subsequent CREB-mediated gene transcription, occur following contextual fear conditioning. Conversely, disrupting CREB leads to deficiencies in transcription-dependent long-term memory in mice (Bourtchuladze et al., 1994; Impey et al., 1998). The impaired cAMP signaling observed in Cdk5-deficient mice in our study is accompanied by a reduction in pCREB(S133) in the hippocampus in both basal and post-training conditions. Interestingly, the Cdk5f/f/T29 mutant mice demonstrated an early LTP impairment, a phenomenon independent of CREB-mediated transcription modifications (Barco et al., 2002). It should be noted that CREB is not the only target and effecter of cAMP, and earlier studies have shown that postsynaptic cAMP pathways directly regulate early LTP in the hippocampal CA1 area (Blitzer et al., 1995). Our results support the essential role of the cAMP pathway in modulating synaptic functions as well as in learning and memory.

We propose that the alteration of the cAMP pathway, resulting from increased PDE expression, is a major factor in the aberrant signaling pathways and behavior deficits observed in Cdk5-deficient mice (**Figure 11**). However, the detailed mechanism by which Cdk5 regulates PDEs remains unclear. Cdk5 might act upon multiple targets to regulate the levels of intracellular cAMP. We found that both the mRNA and protein levels of PDE4 are increased in Cdk5 mutant mice, which could result from a lack of inhibition by Cdk5 on targeted transcription factors such as MEF2 (Gong et al., 2003). In the Cdk5 mutant mice, we also detected a lack of pDARRP-32(T75) (data not shown), which would inhibit PKA signaling (Bibb et al., 1999; Chergui et al., 2004) and could indirectly affect cAMP levels via feedback regulation through the AC-cAMP-PKA axis (Bauman et al., 2006). Other possibilities include a direct regulation on the activity of AC by Cdk5, which cannot be excluded as an alternative interpretation based on our experimental evidence.

Other potential synaptic mechanisms regulated by Cdk5

Interestingly, in our PSD proteomic screen, many PSD molecules in pathways other than the cAMP pathway are altered in the absence of Cdk5, including receptor, channel, and trafficking molecules. For example, GluR4 and the L-type calcium channel, alpha 2, myo5a, Kif2a are increased, while ACCN1, GABA receptor type 2, and dynll2 are decreased, in the PSD of Cdk5 mutant mice (**Figure 9C**). The alterations in PSD protein composition resulting from the

loss of Cdk5 suggest that Cdk5 is an active participant at the synapse whose critical role in synaptic plasticity may be mediated via more than one distinct pathway.

Here we also identified altered AMPAR-dependent regulation, as measured by changes in GluR1 phosphorylation. In Cdk5f/f/T29 mice, we observed increased GluR1 phosphorylation at both S831 and S845 (**Figure 7D**). Partially increasing GluR1 phosphorylation at S831 might facilitate LTP (Barria et al., 1997; Lee et al., 2000), while the occlusion of GluR1 phosphorylation by the long-term deletion of Cdk5 is predicted to lead to a failure in LTP induction. The mouse models used in this study may therefore represent a chronic loss of Cdk5 in adult mice in which LTP occlusion is derived from persistent GluR1 phosphorylation. Intriguingly, rolipram treatment in the Cdk5f/f/T29 mice decreased the S831, but not S845, GluR1 phosphorylation and restored LTP, but not LTD, signaling. As PP1 phosphatase activity is also restored to control levels with rolipram application, one could speculate that PP1 regulates the bidirectional GluR1 signaling and LTP by the dephosphorylation of S831. However, as LTD is not restored in Cdk5f/f/T29 mice treated with rolipram, Cdk5 may act through a PDE4-independent pathway, such as the PDE1 and PDE2 pathways that deplete cGMP, in regulating LTD maintenance. Alternatively, Cdk5 may play a role in generating LTD that is separate from PDE function altogether.

Directions for future research

In the current work, we have elucidated a novel role for Cdk5 in the modulation of the cAMP pathway. We cannot exclude the possibility that other targets of Cdk5 may also be involved in the regulation of cAMP, such as the direct phosphorylation of PDE4 or AC by Cdk5. Future experiments include addressing the relationships between Cdk5 activity and intracellular signaling molecules such as cAMP or PP1 as key regulators of activity-dependent mechanisms of memory formation, along with work examining how GluR1 phosphorylation is regulated by Cdk5 and how this contributes to pathways by which Cdk5 maintains downstream signaling at the glutamatergic synapse. Recent evidence has highlighted Cdk5 as a critical molecule implicated in the downregulation of synaptic activity in hippocampal neurons (Seeburg et al., 2008) and in the regulation of synaptic transmission (Kim and Ryan, 2010). Further work on the molecular targets of Cdk5, including cAMP, will reveal the mechanisms by which Cdk5 maintains synaptic homeostasis.

The modulation of the PDEs and cAMP pathways has already been utilized to treat mouse models of cognitive decline, as rolipram was previously shown to be able to rescue the memory deficits in mouse models of Rubinstein-Taybi Syndrome (Alarcon et al., 2004), ischemia (Imanishi et al., 1997), and Alzheimer's disease (Gong et al., 2004; Vitolo et al., 2002). Our findings that rolipram ameliorates the memory deficits caused by ablation of Cdk5 in hippocampal CA1 neurons provides a compelling direction for future research in targeting PDEs and other cAMP pathway activators to restore memory deficits, particularly those associated with neurodegeneration and cognitive decline.

References

Abeliovich, A., Paylor, R., Chen, C., Kim, J.J., Wehner, J.M., and Tonegawa, S. (1993). PKC gamma mutant mice exhibit mild deficits in spatial and contextual learning. Cell *75*, 1263-1271.

Alarcon, J.M., Malleret, G., Touzani, K., Vronskaya, S., Ishii, S., Kandel, E.R., and Barco, A. (2004). Chromatin acetylation, memory, and LTP are impaired in CBP+/- mice: a model for the cognitive deficit in Rubinstein-Taybi syndrome and its amelioration. Neuron *42*, 947-959.

Bao, J.X., Kandel, E.R., and Hawkins, R.D. (1997). Involvement of pre- and postsynaptic mechanisms in posttetanic potentiation at Aplysia synapses. Science *275*, 969-973.

Barco, A., Alarcon, J.M., and Kandel, E.R. (2002). Expression of constitutively active CREB protein facilitates the late phase of long-term potentiation by enhancing synaptic capture. Cell *108*, 689-703.

Barria, A., Muller, D., Derkach, V., Griffith, L.C., and Soderling, T.R. (1997). Regulatory phosphorylation of AMPA-type glutamate receptors by CaM-KII during long-term potentiation. Science *276*, 2042-2045.

Bauman, A.L., Soughayer, J., Nguyen, B.T., Willoughby, D., Carnegie, G.K., Wong, W., Hoshi, N., Langeberg, L.K., Cooper, D.M., Dessauer, C.W*., et al.* (2006). Dynamic regulation of cAMP synthesis through anchored PKA-adenylyl cyclase V/VI complexes. Mol Cell *23*, 925-931.

Bibb, J.A., Snyder, G.L., Nishi, A., Yan, Z., Meijer, L., Fienberg, A.A., Tsai, L.H., Kwon, Y.T., Girault, J.A., Czernik, A.J*., et al.* (1999). Phosphorylation of DARPP-32 by Cdk5 modulates dopamine signalling in neurons. Nature *402*, 669-671.

Blitzer, R.D., Wong, T., Nouranifar, R., Iyengar, R., and Landau, E.M. (1995). Postsynaptic cAMP pathway gates early LTP in hippocampal CA1 region. Neuron *15*, 1403-1414.

Borchelt, D.R., Davis, J., Fischer, M., Lee, M.K., Slunt, H.H., Ratovitsky, T., Regard, J., Copeland, N.G., Jenkins, N.A., Sisodia, S.S*., et al.* (1996). A vector for expressing foreign genes in the brains and hearts of transgenic mice. Genet Anal *13*, 159-163.

Bourtchouladze, R., Lidge, R., Catapano, R., Stanley, J., Gossweiler, S., Romashko, D., Scott, R., and Tully, T. (2003). A mouse model of Rubinstein-Taybi syndrome: defective long-term memory is ameliorated by inhibitors of phosphodiesterase 4. Proc Natl Acad Sci U S A *100*, 10518-10522.

Bourtchuladze, R., Frenguelli, B., Blendy, J., Cioffi, D., Schutz, G., and Silva, A.J. (1994). Deficient long-term memory in mice with a targeted mutation of the cAMP-responsive element-binding protein. Cell *79*, 59-68.

Boy, J., Leergaard, T.B., Schmidt, T., Odeh, F., Bichelmeier, U., Nuber, S., Holzmann, C., Wree, A., Prusiner, S.B., Bujard, H*., et al.* (2006). Expression mapping of tetracycline-responsive prion protein promoter: Digital atlasing for generating cell-specific disease models. Neuroimage *33*, 449-462.

Calabresi, P., Gubellini, P., Centonze, D., Sancesario, G., Morello, M., Giorgi, M., Pisani, A., and Bernardi, G. (1999). A critical role of the nitric oxide/cGMP pathway in corticostriatal long-term depression. J Neurosci *19*, 2489-2499.

Chergui, K., Svenningsson, P., and Greengard, P. (2004). Cyclin-dependent kinase 5 regulates dopaminergic and glutamatergic transmission in the striatum. Proc Natl Acad Sci U S A *101*, 2191-2196.

Deisseroth, K., Heist, E.K., and Tsien, R.W. (1998). Translocation of calmodulin to the nucleus supports CREB phosphorylation in hippocampal neurons. Nature *392*, 198-202.

Fischer, A., Sananbenesi, F., Pang, P.T., Lu, B., and Tsai, L.H. (2005). Opposing roles of transient and prolonged expression of p25 in synaptic plasticity and hippocampus-dependent memory. Neuron *48*, 825-838.

Frey, U., Huang, Y.Y., and Kandel, E.R. (1993). Effects of cAMP simulate a late stage of LTP in hippocampal CA1 neurons. Science *260*, 1661-1664.

Fu, A.K., Fu, W.Y., Cheung, J., Tsim, K.W., Ip, F.C., Wang, J.H., and Ip, N.Y. (2001). Cdk5 is involved in neuregulin-induced AChR expression at the neuromuscular junction. Nat Neurosci *4*, 374-381.

Fu, A.K., Fu, W.Y., Ng, A.K., Chien, W.W., Ng, Y.P., Wang, J.H., and Ip, N.Y. (2004). Cyclin-dependent kinase 5 phosphorylates signal transducer and activator of transcription 3 and regulates its transcriptional activity. Proc Natl Acad Sci U S A *101*, 6728-6733.

Fu, W.Y., Chen, Y., Sahin, M., Zhao, X.S., Shi, L., Bikoff, J.B., Lai, K.O., Yung, W.H., Fu, A.K., Greenberg, M.E.*, et al.* (2007). Cdk5 regulates EphA4-mediated dendritic spine retraction through an ephexin1-dependent mechanism. Nat Neurosci *10*, 67-76.

Fukaya, M., Kato, A., Lovett, C., Tonegawa, S., and Watanabe, M. (2003). Retention of NMDA receptor NR2 subunits in the lumen of endoplasmic reticulum in targeted NR1 knockout mice. Proc Natl Acad Sci U S A *100*, 4855-4860.

Giese, K.P., Fedorov, N.B., Filipkowski, R.K., and Silva, A.J. (1998). Autophosphorylation at Thr286 of the alpha calcium-calmodulin kinase II in LTP and learning. Science *279*, 870-873.

Gong, B., Vitolo, O.V., Trinchese, F., Liu, S., Shelanski, M., and Arancio, O. (2004). Persistent improvement in synaptic and cognitive functions in an Alzheimer mouse model after rolipram treatment. J Clin Invest *114*, 1624-1634.

Gong, X., Tang, X., Wiedmann, M., Wang, X., Peng, J., Zheng, D., Blair, L.A., Marshall, J., and Mao, Z. (2003). Cdk5-mediated inhibition of the protective effects of transcription factor MEF2 in neurotoxicity-induced apoptosis. Neuron *38*, 33-46.

Guan, J.S., Haggarty, S.J., Giacometti, E., Dannenberg, J.H., Joseph, N., Gao, J., Nieland, T.J., Zhou, Y., Wang, X., Mazitschek, R.*, et al.* (2009). HDAC2 negatively regulates memory formation and synaptic plasticity. Nature *459*, 55-60.

Hawasli, A.H., Benavides, D.R., Nguyen, C., Kansy, J.W., Hayashi, K., Chambon, P., Greengard, P., Powell, C.M., Cooper, D.C., and Bibb, J.A. (2007). Cyclin-dependent kinase 5 governs learning and synaptic plasticity via control of NMDAR degradation. Nat Neurosci *10*, 880-886.

Hawasli, A.H., Koovakkattu, D., Hayashi, K., Anderson, A.E., Powell, C.M., Sinton, C.M., Bibb, J.A., and Cooper, D.C. (2009). Regulation of hippocampal and behavioral excitability by cyclin-dependent kinase 5. PLoS One *4*, e5808.

Hayashi, Y., Shi, S.H., Esteban, J.A., Piccini, A., Poncer, J.C., and Malinow, R. (2000). Driving AMPA receptors into synapses by LTP and CaMKII: requirement for GluR1 and PDZ domain interaction. Science *287*, 2262-2267.

Imanishi, T., Sawa, A., Ichimaru, Y., Miyashiro, M., Kato, S., Yamamoto, T., and Ueki, S. (1997). Ameliorating effects of rolipram on experimentally induced impairments of learning and memory in rodents. Eur J Pharmacol *321*, 273-278.

Impey, S., Smith, D.M., Obrietan, K., Donahue, R., Wade, C., and Storm, D.R. (1998). Stimulation of cAMP response element (CRE)-mediated transcription during contextual learning. Nat Neurosci *1*, 595-601.

Kim, S.H., and Ryan, T.A. (2010). CDK5 serves as a major control point in neurotransmitter release. Neuron *67*, 797-809.

Lee, H.K., Barbarosie, M., Kameyama, K., Bear, M.F., and Huganir, R.L. (2000). Regulation of distinct AMPA receptor phosphorylation sites during bidirectional synaptic plasticity. Nature *405*, 955-959.

Lee, M.K., Stirling, W., Xu, Y., Xu, X., Qui, D., Mandir, A.S., Dawson, T.M., Copeland, N.G., Jenkins, N.A., and Price, D.L. (2002). Human Œ±-synuclein-harboring familial Parkinson's disease-linked Ala-53 ‚Üí Thr mutation causes neurodegenerative disease with Œ±-synuclein aggregation in transgenic mice. Proceedings of the National Academy of Sciences of the United States of America *99*, 8968-8973.

Levin, L.R., Han, P.L., Hwang, P.M., Feinstein, P.G., Davis, R.L., and Reed, R.R. (1992). The Drosophila learning and memory gene rutabaga encodes a Ca2+/Calmodulin-responsive adenylyl cyclase. Cell *68*, 479-489.

McHugh, T.J., Jones, M.W., Quinn, J.J., Balthasar, N., Coppari, R., Elmquist, J.K., Lowell, B.B., Fanselow, M.S., Wilson, M.A., and Tonegawa, S. (2007). Dentate gyrus NMDA receptors mediate rapid pattern separation in the hippocampal network. Science *317*, 94-99.

Meyerson, M., Enders, G.H., Wu, C.L., Su, L.K., Gorka, C., Nelson, C., Harlow, E., and Tsai, L.H. (1992). A family of human cdc2-related protein kinases. EMBO J *11*, 2909-2917.

Morabito, M.A., Sheng, M., and Tsai, L.H. (2004). Cyclin-dependent kinase 5 phosphorylates the N-terminal domain of the postsynaptic density protein PSD-95 in neurons. J Neurosci *24*, 865-876.

Morris, R.G., Garrud, P., Rawlins, J.N., and O'Keefe, J. (1982). Place navigation impaired in rats with hippocampal lesions. Nature *297*, 681-683.

Mozzachiodi, R., Lorenzetti, F.D., Baxter, D.A., and Byrne, J.H. (2008). Changes in neuronal excitability serve as a mechanism of long-term memory for operant conditioning. Nat Neurosci *11*, 1146-1148.

Nakazawa, K., Quirk, M.C., Chitwood, R.A., Watanabe, M., Yeckel, M.F., Sun, L.D., Kato, A., Carr, C.A., Johnston, D., Wilson, M.A*., et al.* (2002). Requirement for hippocampal CA3 NMDA receptors in associative memory recall. Science *297*, 211-218.

Nakazawa, K., Sun, L.D., Quirk, M.C., Rondi-Reig, L., Wilson, M.A., and Tonegawa, S. (2003). Hippocampal CA3 NMDA receptors are crucial for memory acquisition of one-time experience. Neuron *38*, 305-315.

Niethammer, M., Smith, D.S., Ayala, R., Peng, J., Ko, J., Lee, M.S., Morabito, M., and Tsai, L.H. (2000). NUDEL is a novel Cdk5 substrate that associates with LIS1 and cytoplasmic dynein. Neuron *28*, 697-711.

Ohshima, T., Ogura, H., Tomizawa, K., Hayashi, K., Suzuki, H., Saito, T., Kamei, H., Nishi, A., Bibb, J.A., Hisanaga, S*., et al.* (2005). Impairment of hippocampal long-term depression and defective spatial learning and memory in p35 mice. J Neurochem *94*, 917-925.

Ohshima, T., Ward, J.M., Huh, C.G., Longenecker, G., Veeranna, Pant, H.C., Brady, R.O., Martin, L.J., and Kulkarni, A.B. (1996). Targeted disruption of the cyclin-dependent kinase 5 gene results in abnormal corticogenesis, neuronal pathology and perinatal death. Proc Natl Acad Sci U S A *93*, 11173-11178.

Ou, C.Y., Poon, V.Y., Maeder, C.I., Watanabe, S., Lehrman, E.K., Fu, A.K., Park, M., Fu, W.Y., Jorgensen, E.M., Ip, N.Y., *et al.* (2010). Two Cyclin-Dependent Kinase Pathways Are Essential for Polarized Trafficking of Presynaptic Components. Cell *141*, 846-858.

Peng, J., Kim, M.J., Cheng, D., Duong, D.M., Gygi, S.P., and Sheng, M. (2004). Semiquantitative proteomic analysis of rat forebrain postsynaptic density fractions by mass spectrometry. J Biol Chem *279*, 21003-21011.

Radulovic, J., Ruhmann, A., Liepold, T., and Spiess, J. (1999). Modulation of learning and anxiety by corticotropin-releasing factor (CRF) and stress: differential roles of CRF receptors 1 and 2. J Neurosci *19*, 5016-5025.

Rampon, C., Tang, Y.P., Goodhouse, J., Shimizu, E., Kyin, M., and Tsien, J.Z. (2000). Enrichment induces structural changes and recovery from nonspatial memory deficits in CA1 NMDAR1-knockout mice. Nat Neurosci *3*, 238-244.

Roche, K.W., O'Brien, R.J., Mammen, A.L., Bernhardt, J., and Huganir, R.L. (1996). Characterization of multiple phosphorylation sites on the AMPA receptor GluR1 subunit. Neuron *16*, 1179-1188.

Samuels, B.A., Hsueh, Y.P., Shu, T., Liang, H., Tseng, H.C., Hong, C.J., Su, S.C., Volker, J., Neve, R.L., Yue, D.T., *et al.* (2007). Cdk5 promotes synaptogenesis by regulating the subcellular distribution of the MAGUK family member CASK. Neuron *56*, 823-837.

Seeburg, D.P., Feliu-Mojer, M., Gaiottino, J., Pak, D.T., and Sheng, M. (2008). Critical role of CDK5 and Polo-like kinase 2 in homeostatic synaptic plasticity during elevated activity. Neuron *58*, 571-583.

Silva, A.J., Kogan, J.H., Frankland, P.W., and Kida, S. (1998). CREB and memory. Annu Rev Neurosci *21*, 127-148.

Squire, L.R. (1987). Memory and Brain. New York ; Oxford : Oxford University Press.

Srinivas, S., Watanabe, T., Lin, C.S., William, C.M., Tanabe, Y., Jessell, T.M., and Costantini, F. (2001). Cre reporter strains produced by targeted insertion of EYFP and ECFP into the ROSA26 locus. BMC Dev Biol *1*, 4.

Tanaka, T., Serneo, F.F., Tseng, H.C., Kulkarni, A.B., Tsai, L.H., and Gleeson, J.G. (2004). Cdk5 phosphorylation of doublecortin ser297 regulates its effect on neuronal migration. Neuron *41*, 215-227.

Tsien, J.Z. (1998). Behavioral genetics: subregion- and cell type-restricted gene knockout in mouse brain. Pathol Biol (Paris) *46*, 699-700.

Tsien, J.Z., Chen, D.F., Gerber, D., Tom, C., Mercer, E.H., Anderson, D.J., Mayford, M., Kandel, E.R., and Tonegawa, S. (1996a). Subregion- and cell type-restricted gene knockout in mouse brain. Cell *87*, 1317-1326.

Tsien, J.Z., Huerta, P.T., and Tonegawa, S. (1996b). The essential role of hippocampal CA1 NMDA receptor-dependent synaptic plasticity in spatial memory. Cell *87*, 1327-1338.

Vitolo, O.V., Sant'Angelo, A., Costanzo, V., Battaglia, F., Arancio, O., and Shelanski, M. (2002). Amyloid beta -peptide inhibition of the PKA/CREB pathway and long-term potentiation: reversibility by drugs that enhance cAMP signaling. Proc Natl Acad Sci U S A *99*, 13217-13221.

Wachtel, H. (1983). Potential antidepressant activity of rolipram and other selective cyclic adenosine 3',5'-monophosphate phosphodiesterase inhibitors. Neuropharmacology *22*, 267-272.

Weber, P., Metzger, D., and Chambon, P. (2001). Temporally controlled targeted somatic mutagenesis in the mouse brain. Eur J Neurosci *14*, 1777-1783.

Wong, S.T., Athos, J., Figueroa, X.A., Pineda, V.V., Schaefer, M.L., Chavkin, C.C., Muglia, L.J., and Storm, D.R. (1999). Calcium-stimulated adenylyl cyclase activity is critical for hippocampus-dependent long-term memory and late phase LTP. Neuron *23*, 787-798.

Zeng, H., Chattarji, S., Barbarosie, M., Rondi-Reig, L., Philpot, B.D., Miyakawa, T., Bear, M.F., and Tonegawa, S. (2001). Forebrain-specific calcineurin knockout selectively impairs bidirectional synaptic plasticity and working/episodic-like memory. Cell *107*, 617-629.

Zhang, S., Edelmann, L., Liu, J., Crandall, J.E., and Morabito, M.A. (2008). Cdk5 regulates the phosphorylation of tyrosine 1472 NR2B and the surface expression of NMDA receptors. J Neurosci *28*, 415-424.

Zukerberg, L.R., Patrick, G.N., Nikolic, M., Humbert, S., Wu, C.L., Lanier, L.M., Gertler, F.B., Vidal, M., Van Etten, R.A., and Tsai, L.H. (2000). Cables links Cdk5 and c-Abl and facilitates Cdk5 tyrosine phosphorylation, kinase upregulation, and neurite outgrowth. Neuron *26*, 633-646.

Chapter 3

Regulation of N-type voltage-gated calcium channels and presynaptic function by cyclin-dependent kinase 5[3]

Summary

N-type voltage-gated calcium channels ($Ca_V2.2$) localize to presynaptic nerve terminals and mediate key events including synaptogenesis and neurotransmission. While several kinases have been implicated in the modulation of calcium channels, their impact on presynaptic functions remains unclear. Here we report that the N-type calcium channel is a substrate for cyclin-dependent kinase 5 (Cdk5). The pore-forming α_1 subunit of the N-type calcium channel is phosphorylated in the C-terminal domain, and phosphorylation results in enhanced calcium influx due to increased channel open probability. Phosphorylation of the N-type calcium channel by Cdk5 facilitates neurotransmitter release and alters presynaptic plasticity by increasing the number of docked vesicles at the synaptic cleft. These effects are mediated by an altered interaction between N-type calcium channels and RIM1, which tethers presynaptic calcium channels to the active zone. Collectively, our results highlight a molecular mechanism by which N-type calcium channels are regulated by Cdk5 to affect presynaptic functions.

---

[3] The findings presented in this chapter were previously published as: Su SC, Seo J, Pan JQ, Samuels BA, Rudenko A, Ericsson M, Neve RL, Yue DT, Tsai LH. 2012. Regulation of N-type voltage-gated calcium channels and presynaptic function by cyclin-dependent kinase 5. Neuron 75(4):675-87.

I conducted the kinase assays, generated and purified and characterized the phospho-specific antibody, cloned the full-length 8X $Ca_V2.2$ phosphorylation mutant, cloned the constructs into viral vectors, maintained stable cell lines, cultured primary neurons, conducted the electrophysiology recordings in heterologous cells and primary neurons and analyzed the data, prepared samples for electron microscopy processing and acquired images for analysis, conducted surface biotinylation and protein binding biochemical experiments and analysis, and performed the stereotaxic injections.

Introduction

Calcium channels in the Ca_V2 voltage-gated calcium channel family are enriched in neurons and are composed of multiple subunits. The α_{1B} subunit encodes the pore-forming subunit of N-type calcium channels ($Ca_V2.2$) (Westenbroek et al., 1992). In addition to their well-established roles in spinal nociception and neuropathic pain signaling mediated by Gβγ G-protein subunits (Snutch, 2005), N-type calcium channels contribute to synaptic transmission in the hippocampus (Catterall and Few, 2008). Together with the P/Q-type calcium channels, these two major classes of presynaptic calcium channels are sufficient to account for synaptic transmission at the hippocampal CA3-CA1 synapse (Luebke et al., 1993; Wheeler et al., 1994).

N-type calcium channels play a prominent role in neurotransmitter release and directly bind several key synaptic transmission proteins. The intracellular domain between the II-III loops of the $Ca_V2.2$ pore-forming α_1 subunit is known as the synaptic protein interaction (synprint) region (Sheng et al., 1994). The synprint region binds syntaxin and synaptotagmin, two important components of the SNARE complex (Sheng et al., 1998). Synaptic transmission at the presynaptic terminal involves calcium influx, which triggers vesicle fusion and exocytosis by the 'zippering' of SNARE proteins with the plasma membrane (Jahn et al., 2003). The synprint region of $Ca_V2.2$ is also a binding site for the active zone protein RIM1 (Coppola et al., 2001). RIM1 can interact with the β auxiliary subunit of P/Q-type calcium channels to suppress inactivation, allow calcium influx, and facilitate synaptic vesicle docking to the active zone (Kiyonaka et al., 2007). Furthermore, RIM1 directly binds the C-terminal regions of the α_1 subunit of both N- and P/Q-type calcium channels, and it tethers these channels to presynaptic terminals in order to facilitate synchronous transmitter release (Han et al., 2011; Kaeser et al., 2011). The interaction between N-type calcium channels and SNARE complex proteins is significant because kinases, such as protein kinase C (PKC) and calcium calmodulin-dependent kinase II (CaMKII), phosphorylate the II-III loop of the calcium channel, which affects the N-type calcium channel interaction with various components of the SNARE complex and impacts neurotransmitter release (Yokoyama et al., 1997). However, it remains unknown whether other kinases play a role in modulating N-type calcium channel function. Recently, the scaffolding molecule CASK, which contains a binding domain for N-type calcium channels, was identified as a cyclin-dependent kinase 5 (Cdk5) substrate (Samuels et al., 2007). Upon phosphorylation by Cdk5, CASK increases its interaction with N-type calcium channels to regulate synaptogenesis.

Cdk5 is a proline-directed serine/threonine kinase that is highly expressed in postmitotic cells of the central nervous system and requires its binding partner, p35, for activity (Chae et al., 1997; Tsai et al., 1994). Cdk5-mediated phosphorylations of a wide variety of substrates highlights its diverse roles in neuronal functions, including migration (Ohshima et al., 1996), cytoskeletal dynamics (Fu et al., 2007), synaptic vesicle cycle (Tan et al., 2003), and synaptic plasticity (Guan et al., 2011). Under excitotoxic conditions, calcium influx through the NMDA receptors activates the calcium-dependent protease calpain to cleave p35 to p25, which in turn hyperactivates Cdk5 (Lee et al., 2000; Patrick et al., 1999). The Cdk5/p25 complex has been implicated in neurodegenerative diseases, including Alzheimer's disease (Su and Tsai, 2011).

Recent evidence suggests that Cdk5 plays a critical role in regulating synapse formation (Cheung et al., 2007) and in synaptic scaling (Seeburg et al., 2008). Additionally, Cdk5 is proposed to be a major regulator of neurotransmitter release by regulating the size of the synaptic vesicle pool (Kim and Ryan, 2010), and has also been implicated in the modification of synaptic connectivity and strength of hippocampal CA3 recurrent synapses (Mitra et al., 2011). However, the Cdk5 substrates directly responsible for neurotransmitter release are still poorly understood. Cdk5 was previously demonstrated to phosphorylate an intracellular domain of presynaptic P/Q-type calcium channels (Tomizawa et al., 2002). As a consequence of this phosphorylation event, neurotransmitter release is decreased due to the dissociation of P/Q-type calcium channels from the SNAP-25 and synaptotagmin complex.

Although several kinases have been implicated in phosphorylating and thereby affecting the binding of voltage-gated calcium channels to various synaptic proteins, no specific mechanisms have been elucidated by which a particular kinase regulates calcium channels to ultimately impact neurotransmitter release and presynaptic plasticity. Here we demonstrate that the N-type voltage-gated calcium channel ($Ca_V2.2$), a major presynaptic calcium channel, is a Cdk5 substrate. Phosphorylation of the $Ca_V2.2$ pore-forming α_1 subunit by Cdk5 increases calcium influx by enhancing channel open probability and also facilitates neurotransmitter release. These events are mediated by an interaction between $Ca_V2.2$ and RIM1, which impacts vesicle docking at the active zone. Our results outline a mechanism by which Cdk5 regulates N-type calcium channels and affects presynaptic functions.

Methods

In vitro kinase assay

GST vector alone or various GST-$Ca_V2.2$ intracellular fusion protein fragments were purified and incubated with purified p25/Cdk5 kinase (Cell Signaling Technology) in kinase buffer (30 mM HEPES [pH 7.2], 10 mM $MgCl_2$, 5 mM $MnCl_2$, 100 mM ATP, 5 mCi [32P] γATP (Perkin-Elmer, MA, USA), 1 mM DTT), for 30 min at room temperature. The reaction was stopped with the addition of 2X sample buffer (100 mM Tris [pH 6.8], 4% SDS (w/v), 0.2% Bromophenol blue (w/v), 20% glycerol (v/v), 200 mM DTT), separated by 10% SDS-PAGE polyacrylamide gels (Bio-Rad), stained with Coomassie blue (SimplyBlue Safestain, Invitrogen) and then dried prior to analysis by autoradiography.

Antibodies

To generate the phospho-specific antibody to S2013 in rat $Ca_V2.2$, a 13-amino acid phosphorylated and non-phosphorylated peptide NH2-QPAPNASPMKRSC-COOH was synthesized and purified using high performance liquid chromatography (Tufts Core Facility, Physiology Dept). The peptides were conjugated to KLH for polyclonal rabbit antibody production (Covance Research Products). Antisera were affinity purified and collected after passing through non-phospho peptide columns using a SulfoLink immobilization kit for peptides (Thermo Scientific). The following antibodies were used for immunoblotting: β-actin (Sigma); anti-GST (Santa Cruz Biotechnology); anti-$Ca_V2.2$ (Millipore and Alomone Labs); anti-Munc18-1, anti-RIM1, anti-SNAP-25, anti-Syntaxin1A, anti-Synaptotagmin I (all from Synaptic Systems). Cdk5 (DC17) monoclonal and p35 polyclonal antibodies have previously been described (Tsai et al., 1994).

Expression plasmids and constructs

The vector pGEX-4T0-2 (GE Healthcare) was used for cloning the rat isoform of $Ca_V2.2$ into various GST-$Ca_V2.2$ fragments (Accession number AF055477). Mutagenesis of the GST-$Ca_V2.2$ fragments or full-length human isoform of $Ca_V2.2$ (Accession number NM_000718) was carried out as described using the outlined protocol (QuickChange, Stratagene) and sequence verified (MIT Biopolymer Facility, Cambridge).

To generate GST fusion proteins, BL21 competent cells were transformed with the desired construct. Protein expression was induced by adding 0.2 mM IPTG to the medium, and cells were harvested by centrifugation. Cells were resuspended in TNT buffer (100 mM Tris-HCl [pH 8], 150 mM NaCl, 5 mM EDTA, 0.05% Tween-20), sonicated, and bound to Glutathione Sepharose 4B beads (Amersham Biosciences). The bound protein was loaded onto a poly-prep chromatography column (Bio-Rad), washed with TNT buffer, and eluted in glutathione buffer (200 mM Tris [pH 8], 0.1% Triton-X 100, 15 mM glutathione). The eluate was de-salted and concentrated using high-speed centrifugation cellulose filter units (Centricon, Millipore), and the final protein concentration was assayed using the Bradford Protein Assay (Bio-Rad). Reagents were purchased from Sigma.

Primary neurons

Plates were coated with poly-d-lysine (BD Biosciences) and laminin (Invitrogen) at 37°C overnight. Pre-coated coverslips were used for lower density cultures (BD Biosciences). The neocortex or hippocampus was dissected from E15-17 timed-pregnant Swiss Webster mice (Taconic) on ice using 1X Hank's Balanced Salt Solution (Invitrogen) supplemented with 20 mM HEPES (pH 7.3) and treated with trypsin and DNase (0.1%, Sigma) for 10 min in a 37°C water bath. After dissociation and trituration, cells were diluted in Neurobasal media supplemented with 10% horse serum and 0.5 mM L-glutamine (all from Invitrogen). Cells were plated at a density of 50,000 cells/cm^2. Two to four hours after plating, the media was replaced with Neurobasal medium supplemented with B27 (Gibco), 0.5 mM L-glutamine and penicillin/streptomycin.

Electrophysiology

Confluent tSA-201 cells were transfected using Lipofectamine 2000 at a 1:2:1 ratio of the α_{1B}, β3, and $\alpha 2_b\delta$ subunits with either GFP or Cdk5/p35-GFP according to the protocol (Invitrogen). For whole-cell patch clamp recordings, electrodes were pulled to a resistance of 3-6 MΩ (Sutter Instruments) and fire-polished (Narishige Instruments). The external solution consisted of (in mM) 150 TEA-Cl, 5 $BaCl_2$, 1 $MgCl_2$, 10 glucose, 10 HEPES, pH 7.3 (TEAOH), osmolality 320±5. The internal solution contained (in mM) 135 CsCl, 4 $MgCl_2$, 4 Mg-ATP, 10 HEPES, 10 EGTA, and 1 EDTA, adjusted to pH 7.2 with TEAOH, osmolality 300±10. For

whole-cell patch clamp recordings obtained from cultured hippocampal neurons at DIV12-15, cells were transduced with HSV for 1-2 days prior to recordings (Neve et al., 2005). The external media was the same as above except for TEA-Cl (140 mM) and $BaCl_2$ (10 mM) and was supplemented with 1 μM tetrodotoxin (TTX), 10 μM Nifedipine (Tocris), 200 nM ω-agatoxin-TK (Peptides International) to isolate $Ca_V2.2$ currents or 2μM ω-conotoxin GVIA to isolate $Ca_V2.1$ currents.

For miniature recordings, the external solution consisted of (in mM) 140 NaCl, 4 KCl, 2 $CaCl_2$, 2 $MgCl_2$, 10 HEPES, 10 glucose, pH 7.3 with NaOH, 315 mOsm. The internal solution contained (in mM) 145 CsCl, 5 NaCl, 10 HEPES, 10 EGTA, 4 Mg-ATP, 0.3 Na_2-GTP, pH 7.3 with CsOH, 305 mOsm. The external solution also contained 1 μM TTX, 50 μM picrotoxin (PTX) and 50 μM D-APV for mEPSCs, or 1 μM TTX, 10 μM CNQX or 50 μM D-APV for mIPSCs. Series resistance was compensated by 70-90% with a 10-μs lag and online leak correction was performed with a P/–4 protocol. Recordings were obtained at room temperatures using an inverted fluorescent microscope (Zeiss). Data was acquired using the Axopatch 200B amplifier and analyzed with the pClamp10 and Origin8 software (Molecular Devices).

For field excitatory postsynaptic potential (fEPSP) recordings, slices were prepared from mice transduced with GFP, WT $Ca_V2.2$ or 8X $Ca_V2.2$ HSV by rapidly removing the brain and transferring to ice-cold, oxygenated (95% O_2 and 5% CO_2) cutting solution containing (mM) 211 sucrose, 3.3 KCl, 1.3 NaH_2PO_4, 0.5 $CaCl_2$, 10 $MgCl_2$, 26 $NaHCO_3$ and 11 glucose. Hippocampal slices were cut with a VT1000S vibratome (Leica) and transferred for recovery to a holding chamber containing oxygenated artificial cerebrospinal fluid (ACSF) consisting of (mM) 124 NaCl, 3.3 KCl, 1.3 NaH_2PO_4, 2.5 $CaCl_2$, 1.5 $MgCl_2$, 26 $NaHCO_3$ and 11 glucose at 28-30°C for at least 1 hr prior to Schaffer collateral stimulation recording. CA1 field potentials in the stratum radiatum were measured after stimulation of the Schaffer collateral fibers using a concentric bipolar electrode. After recording stable responses for at least 20 min of baseline, LTP was induced by high frequency stimulation (HFS) at 100 Hz for 1 s. Recordings were performed using a MultiClamp 700B amplifier and a Digidata 1440A A-D converter (Axon Instruments). All data were digitized and analyzed with pClamp10 software (Axon Instruments). Experiments were performed blind to the group of subjects. Sample traces represent fEPSPs at 1 min before (gray trace) and 30 min after (black trace) HFS. Bar graphs represent average slopes of fEPSP during the first 5 min after HFS or the last 5 min of recording (percentage of baseline response).

Surface biotinylation assay

Surface biotinylation assay was conducted as essentially described according to the protocol (Thermo Scientific). Transfected tSA201 cells were washed with ice-cold PBS, followed by Sulfo-NHS-SS-Biotin labeing. After 30 min on ice, the reaction was quenched and the cells were harvested. After rinsing with TBS, cells were lysed in RIPA buffer, sonicated, and centrifuged at 10,000 × *g* for 2 minutes at 4°C for clarified supernatant. The NeutrAvidin Agarose slurry to isolate surface proteins. After washing three times, protein was eluted using SDS-PAGE sample buffer and analyzed by immunoblotting.

Biochemistry

Cdk5 control or Cdk5 cKO mice were generated as previously described (Guan et al., 2011). Brain lysates or primary neurons were homogenized in radioimmunoprecipitation (RIPA) buffer (50 mM Tris [pH 8], 150 mM NaCl, 1% NP-40, 0.5% sodium deoxycholate, 0.1% SDS with protease and phosphatase inhibitor tablets (Roche), incubated on ice for 30 min, cleared with a 13,000 rpm spin at 4°C, and protein content quantified using the BCA protein assay (Bio-Rad). For immunoprecipitations, lysates were incubated overnight with primary antibody, immunoprecipitated with Protein A sepharose beads (GE Healthcare) for 1 hr at 4°C, and washed four times at 4°C with 3,000 rpm spin. Protein samples were diluted with 2X sample buffer (100 mM Tris pH 6.8, 4% SDS (w/v), 0.2% bromophenol blue (w/v), 20% glycerol (v/v), 200 mM DTT), heated at 75°C for 5 minutes and resolved on a SDS-polyacrylamide gel with 8% stacking gels using Laemmli buffer. Proteins were transferred by electrophoresis using Tris-Glycine buffer onto PVDF membranes (Millipore). Blocking buffer (5% BSA/0.1% Tween-20/PBS, or PBS for infrared detection) was applied for 1 hr, and membranes were probed with various primary antibodies overnight at 4°C. Membranes were washed four times using PBST (PBS with 0.1% Tween-20) for 10 min each, incubated with secondary antibodies (enhanced chemiluminescence mouse or rabbit IgG, HRP-Linked F(ab')2 fragment from sheep, GE Healthcare, 1:10,000) for 1 hr at room temperature, washed again and developed using Western Lightning ECL substrate (Perkin Elmer) or infrared secondaries (Li-Cor). All antibodies were diluted in blocking buffer. Membrane stripping was performed with stripping buffer (Pierce) prior to reprobing. Immunoblots were quantified using ImageJ (NIH) or with Odyssey Image (Li-Cor). Statistical analysis was performed using Prism software (GraphPad).

Electron microscopy

For conventional layer electron microscopy, DIV14-17 primary neurons transduced with HSV containing either GFP, WT $Ca_V2.2$, or 8X $Ca_V2.2$ and fixed for 1 hr at room temperature using 2.5% glutaraldehyde, 1.25% paraformaldehyde, and 0.03% picric acid in 0.1 M sodium cacodylate buffer, pH 7.4 (Electron Microscopy Sciences). After washing in 0.1 M sodium cacodylate buffer, cells were postfixed for 30 min in 1% osmium tetroxide (OsO4)/1.5% potassiumferrocyanide (KFeCN6), washed in water 3x and incubated in 1% aqueous uranyl acetate for 30 min followed by 2 washes in water and subsequent dehydration in grades of alcohol (5 min each; 50%, 70%, 95%, 2x 100%). Cells were removed from the dish in propyleneoxide, pelleted at 3000 rpm for 3 min and infiltrated for 2 hr in a 1:1 mixture of propyleneoxide and TAAB Epon (Marivac Canada Inc). Samples were subsequently embedded in TAAB Epon and polymerized at 60°C for 48 hr. Ultrathin sections (60 nm) were cut on a Reichert Ultracut-S microtome, picked up on to copper grids stained with lead citrate and examined in a JEOL 1200EX Transmission electron microscope or a TecnaiG² Spirit BioTWIN and images were recorded with an AMT 2k CCD camera. Vesicles were quantified according to distance: docked vesicles were touching the synaptic face, readily releasable pool of vesicles were within 150 nm of the presynaptic terminal, and the rest were counted in the resting pool.

For immunogold labeling, neurons were fixed with 4% paraformaldehyde/0.1 M sodium phosphate buffer (pH 7.4), permeabilized in PBS/0.1% Triton X-100 for 2 min, blocked with PBS/1% BSA for 30 min, and incubated in primary antibody overnight in blocking solution at 4°C. The next day, cells were washed with PBS 3x in 30 min each, incubated with protein A-gold (5 nm) for 1 hr, and washed again with PBS 5x in 1 hr. Samples were then fixed in 2.5% glutaraldehyde/0.1M cacodylate buffer (pH 7.4) and ultrathin sections were prepared as above.

Immunocytochemistry

Primary hippocampal neurons at DIV13-15 were fixed with 4% paraformaldehyde (PFA) for 10 min at RT. Fixation was stopped by substituting PFA with 10 mM glycine/PBS quench buffer. The quenching procedure was repeated 2 times. Neurons were rinsed with cold PBS, permeabilized/blocked in 0.1% Triton X-100/10% normal donkey serum/3% BSA/PBS for 1 hr and incubated overnight at 4°C in blocking solution with anti-N-type calcium channel ($Ca_V2.2$) rabbit polyclonal antibodies (Santa Cruz Biotechnology) and anti-Synaptophysin mouse

monoclonal antibody (Abcam). Neurons were then incubated in blocking buffer with Cy3 anti-rabbit and Cy5 anti-mouse secondary antibodies (Jackson Labs) for 1 hr at RT. Cells were washed for 5 min with PBS, followed by 2 min incubation with Hoechst dye (Invitrogen) and 2 additional washes with PBS. Samples were prepared for imaging using ProLong Gold anti-fade reagent (Invitrogen). Images were acquired using high-resolution multi-channel scanning confocal microscopy (Zeiss LSM 510). The whole-field views were obtained using 10X air objective (NA0.45). Individual neurons were imaged using 63X oil objective (NA1.4) with 3X zoom. Single optical sections were acquired with identical settings applied to all samples. Between 5 and 7 HSV-transduced neurons per culture in three independent experiments were used to quantify the relative synaptic localization of $Ca_V2.2$ by assessing its co-localization with presynaptic Synaptophysin. Quantitative immunolocalization analysis was conducted using ImageJ software (NIH). All the counts were performed blind to the treatment conditions. Synaptic levels of $Ca_V2.2$ under different conditions were compared by one-way ANOVA.

Surgery and viruses

Animals were group housed in the small animal facility at the Department of Brain and Cognitive Sciences of Massachusetts Institute of Technology (Cambridge) and handled according to the protocols in accordance with the National Institute of Health Guide for the Care and Use of Laboratory Animals. Eight-week old C57Bl/6J male mice were used for bilateral stereotaxic injections into hippocampal area CA3 (Jackson Labs). Ketamine/xylazine (100/10 mg/kg) was injected intraperitoneally prior to surgery, and sterilized instruments were applied using aseptic technique. Herpes-simplex virus (HSV) containing the cDNA of interest were generated as previously described (Neve et al., 2005; Samuels et al., 2007) and delivered into hippocampal area CA3 using a microinjector (Stoelting Company) according to the Bregma coordinates (Paxinos and Franklin, 2001): AP –2, ML ± 2.6, DV –2.3 (1.5μl, $1.5x10^8$ infectious units/mL, at a rate of 0.15μl/min). The needle was left in the injection site for 3-5 min after injection to allow for diffusion. Animals were monitored during post-operative care with subcutaneous administration of buprenorphine (100 mg/kg). Experiments were conducted at days 2–3 post-surgery, when HSV expression is highest (Han et al., 2007; Lobo et al., 2010).

Results

The N-type calcium channel is a Cdk5 substrate

To investigate if the N-type ($Ca_V2.2$) calcium channel is a Cdk5 substrate, we cloned the intracellular domains of the $Ca_V2.2$ α_1 subunit into GST fusion protein constructs for *in vitro* kinase assays (**Figure 1A**). Each purified GST-$Ca_V2.2$ protein fragment was incubated with an activated Cdk5/p25 protein complex along with radioactive [γ32-P]ATP to assay the level of Cdk5 kinase activity (**Figure 1B**). Two GST-$Ca_V2.2$ fusion protein fragments, the C-terminal 3 (CT 3, amino acids 1981-2120) and C-terminal 4 fragments (CT 4, amino acids 2121-2240) were consistently phosphorylated by Cdk5 (**Figure 1C**). Mutagenesis of serine 2013 (S2013), a consensus Cdk5 site on the CT 3 fragment, to alanine abolished Cdk5 phosphorylation. However, several combinations of point mutations on the CT 4 fragment were insufficient to reduce Cdk5/p25 phosphorylation (**Figure 2**). Only mutagenesis of all seven putative Cdk5 phosphorylation sites on the CT 4 fragment resulted in undetectable phosphorylation levels (**Figure 1D**). These kinase assays identify the N-type calcium channel as a Cdk5 substrate.

The N-type calcium channel is phosphorylated by Cdk5 *in vivo*

To confirm phosphorylation of the N-type calcium channel, we generated and purified a phosphorylation state-specific antibody to S2013, a well-conserved residue (**Figure 3A**). The phospho-$Ca_V2.2$ antibody ($pCa_V2.2$) signal was robust when the CT 3 fragment, but not the CT 3 (S2013A) fragment, was co-incubated with Cdk5/p25, indicating that the antibody was specific to S2013-phosphorylated $Ca_V2.2$ *in vitro* (**Figure 4**). Furthermore, the $pCa_V2.2$ antibody signal was observed only in the presence of Cdk5/p35 in a cell line stably expressing the rat isoform of $Ca_V2.2$ (Lin et al., 2004), and alkaline phosphatase (CIP) treatment abolished the signal (**Figure 3B**). Since S2013 is also conserved in P/Q-type calcium channels, we tested the specificity of the Cdk5-dependent S2013 phosphorylation by immunoprecipitation of brain lysates with an anti-$Ca_V2.2$ antibody, followed by immunoblotting for $pCa_V2.2$ in lysates of control and Cdk5 conditional knockout (cKO) mice (Guan et al., 2011). We noted that $pCa_V2.2$ levels were significantly reduced in forebrain lysates of adult Cdk5 cKO mice, providing *in vivo* evidence that the N-type calcium channel is a Cdk5 substrate (**Figure 3C**).

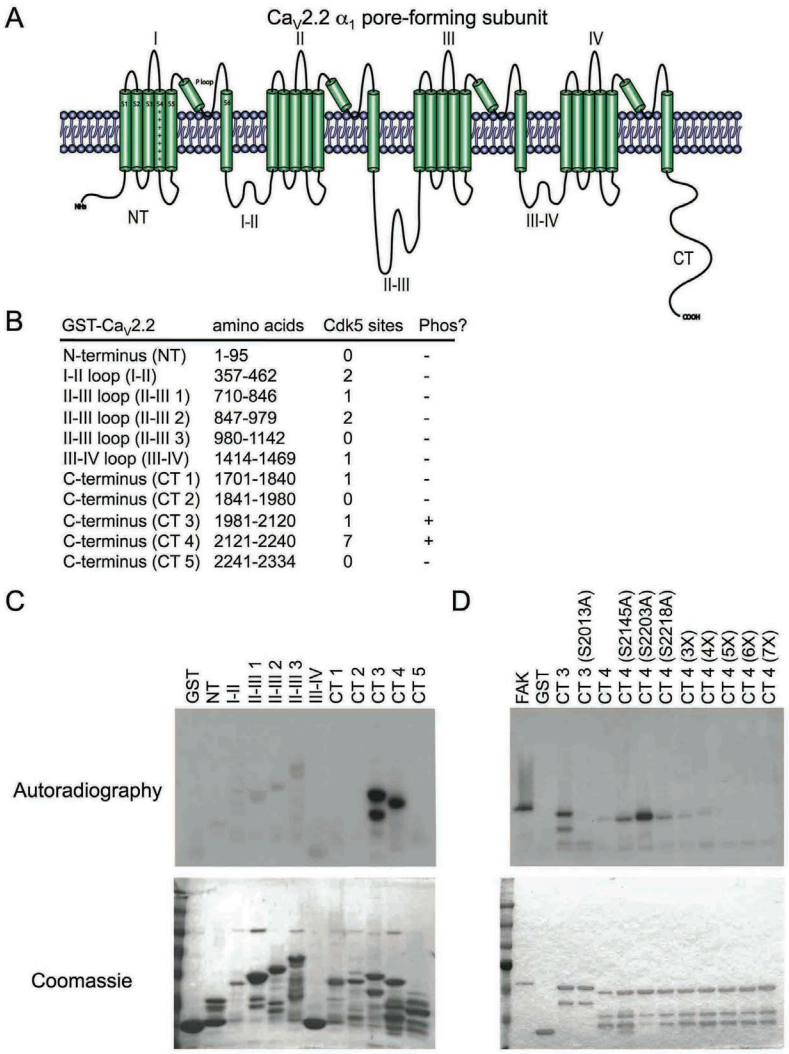

GST-$Ca_V2.2$	amino acids	Cdk5 sites	Phos?
N-terminus (NT)	1-95	0	-
I-II loop (I-II)	357-462	2	-
II-III loop (II-III 1)	710-846	1	-
II-III loop (II-III 2)	847-979	2	-
II-III loop (II-III 3)	980-1142	0	-
III-IV loop (III-IV)	1414-1469	1	-
C-terminus (CT 1)	1701-1840	1	-
C-terminus (CT 2)	1841-1980	0	-
C-terminus (CT 3)	1981-2120	1	+
C-terminus (CT 4)	2121-2240	7	+
C-terminus (CT 5)	2241-2334	0	-

Figure 1. Phosphorylation mapping of the N-type calcium channel *in vitro*.
(A) Schematic of the N-type voltage-gated calcium channel α_1 pore-forming subunit. The α_1 subunit is the functional core of the voltage-gated calcium channel containing the gating mechanisms, toxin-binding domains and the ion conducting pore. Voltage-gated calcium channels form heteromeric subunit complexes consisting of the pore-forming α_1 subunit and auxiliary β, $\alpha 2\delta$, and γ subunits.
(B) Diagram of the various GST fusion protein constructs. The intracellular domains spanning the entire $Ca_V2.2$ α_1 subunit were cloned into GST fusion protein constructs (GST-$Ca_V2.2$).
(C) GST-$Ca_V2.2$ fragments were subjected to an *in vitro* kinase assay with purified Cdk5/p25. The C-terminal fragments 3 and 4 (CT 3 and CT 4) were phosphorylated by autoradiography (top). GST-$Ca_V2.2$ proteins expression as revealed by Coomassie staining (bottom).
(D) Mutagenesis of the single Cdk5 consensus site on the CT 3 fragment (S2013A) abolished Cdk5 phosphorylation. A combination of serine/threonine to alanine point mutations at Cdk5 phosphorylation sites dramatically decreased Cdk5/p25 phosphorylation of the CT 4 fragment. Sequential mutations were generated from the C-terminus end (7X represents all the combination of 7 phosphorylation mutations spanning CT 4). GST: negative control, FAK: positive control.

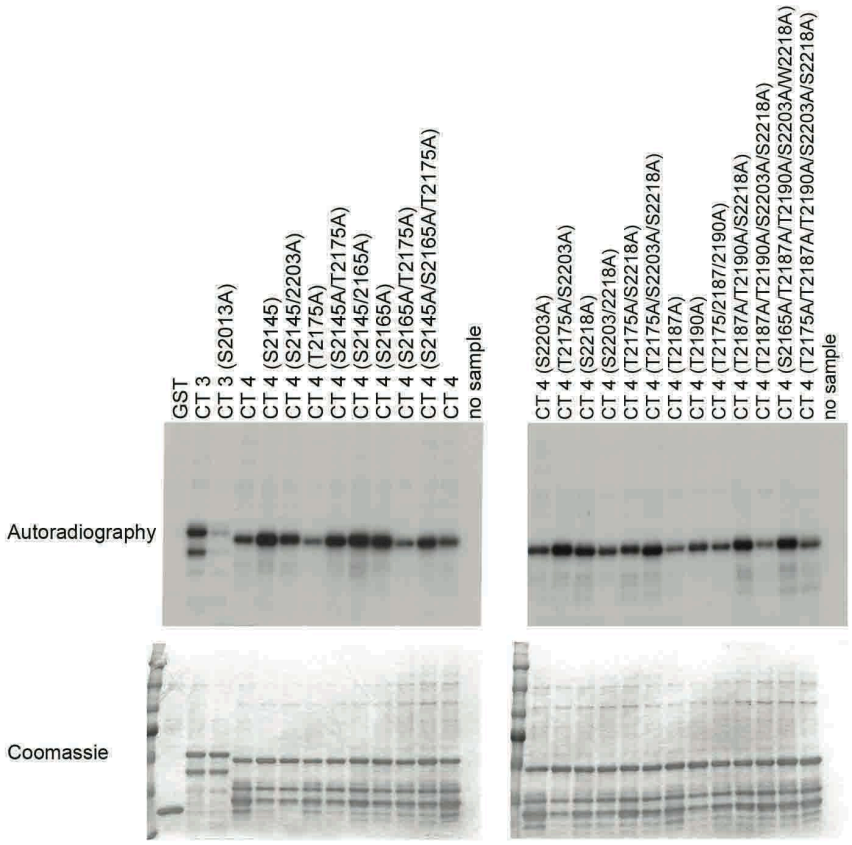

Figure 2. Mapping $Ca_V2.2$ phosphorylation sites by Cdk5.
Whereas mutagenesis of the single site on C-terminal 3 fragment (S2013A) consistently abolished Cdk5/p25 phosphorylation, various combinations of single, double, or triple point mutations in the C-terminal 4 fragments failed to reduce Cdk5/p25 phosphorylation.

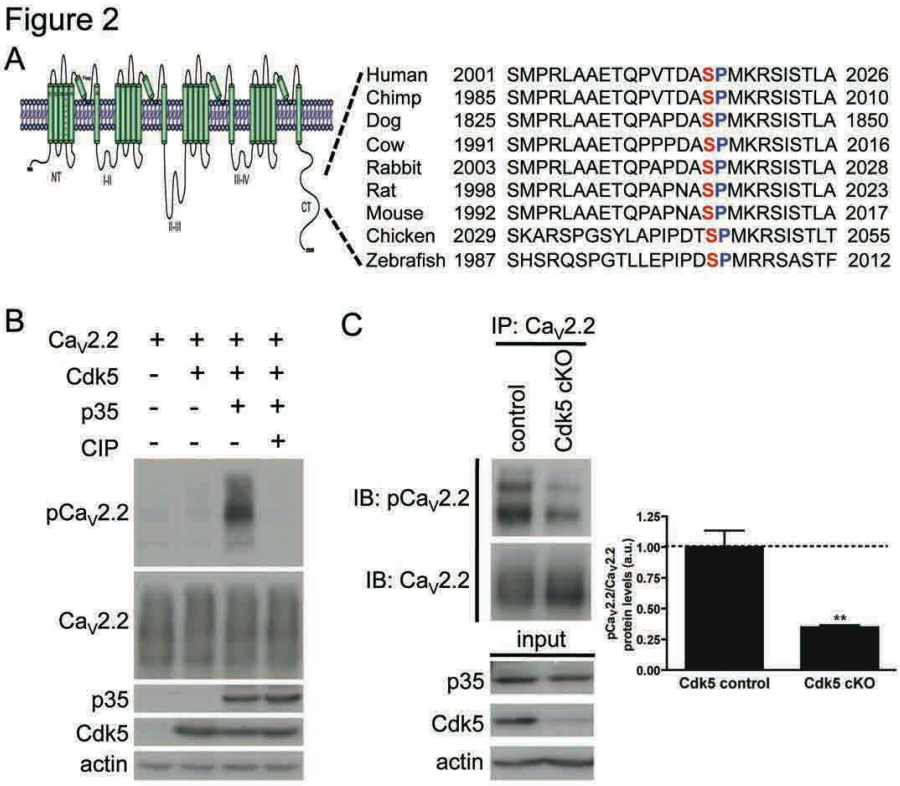

Figure 3. Phosphorylation of the N-type calcium channel *in vivo* at Serine 2013.
(A) Serine 2013 (S2013) is a highly conserved residue on the C-terminal domain of the N-type calcium channel α_1 subunit.
(B) Verification of the specificity of the phospho-specific antibody pCa$_V$2.2 in a stable cell line in the presence of Cdk5/p35. Upon phosphatase treatment, the pCa$_V$2.2 signal was abolished.
(C) After immunoprecipitation with anti-Ca$_V$2.2 antibody, the pCa$_V$2.2 antibody was used to probe for phosphorylated N-type calcium channel signal. In the Cdk5 cKO brain lysates, phosphorylation was significantly decreased, indicating that the S2013 site of Ca$_V$2.2 is indeed an *in vivo* Cdk5 substrate. Right: Quantification of phosphorylation levels in Cdk5 cKO brain lysates. Normalized protein levels are shown, with n=3 per condition. Control, 1.00 ± 0.14; Cdk5 cKO, 0.35 ± 0.02; **p<0.01. Data shown are means ± SEM. Statistical significance was calculated using Student's t-test (*p < 0.05; **p < 0.01; ***p < 0.001).

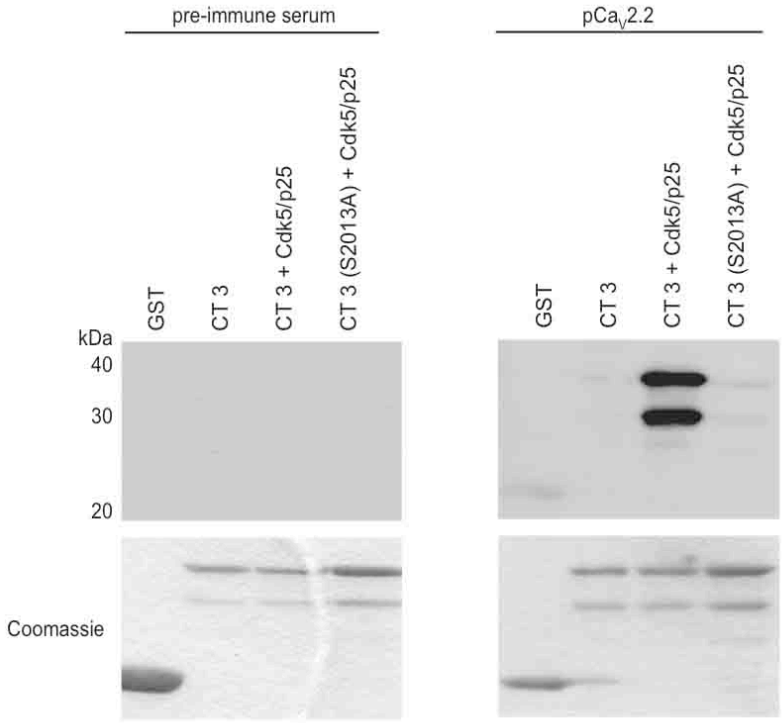

Figure 4. Phospho-specific antibody generation for $Ca_V2.2$.
The purified $pCa_V2.2$ antibody recognized the phosphorylated form of $Ca_V2.2$ at S2013 using *in vitro* kinase assays, as the $pCa_V2.2$ signal is robustly observed only in the presence of activated Cdk5/p25 kinase and GST-$Ca_V2.2$ C-terminal 3 (CT 3) protein fragment but is abolished in the CT 3 protein fragment harboring the point mutation S2013A.

Increased N-type calcium current density as a consequence of Cdk5-mediated phosphorylation

To examine the functional significance of Cdk5-mediated phosphorylation of $Ca_V2.2$ on the biophysical properties of the channel, we conducted whole-cell recordings in heterologous tSA-201 cells transfected with either the full-length wild-type human $Ca_V2.2$ α_1 subunit (WT $Ca_V2.2$) or the phosphorylation mutant $Ca_V2.2$ α_1 subunit, in which all eight Cdk5 phosphorylation sites in the C-terminal region were abolished (8X $Ca_V2.2$), in addition to the obligatory β3 and α2δ auxiliary subunit cDNAs. Using 5 mM barium as the charge carrier, we found that the expression of WT $Ca_V2.2$ elicited canonical voltage-gated N-type currents. The phosphorylation mutant 8X $Ca_V2.2$ expressed a current-density profile similar to that of WT $Ca_V2.2$. Remarkably, following coexpression with Cdk5/p35, the WT $Ca_V2.2$ peak current amplitude and current density were significantly increased compared to those of WT $Ca_V2.2$ alone (**Figure 5A, 5B, Table 1**). In contrast to WT $Ca_V2.2$ however, cells transfected with 8X $Ca_V2.2$ in the presence of Cdk5/p35 did not display an increase in N-type current density (**Figure 5A, 5B**). In a cell line stably expressing the rat isoform of $Ca_V2.2$ (Lin et al., 2004), phosphorylation of $Ca_V2.2$ by Cdk5/p35 also dramatically increased N-type current density, providing independent support that the increase in N-type current density is mediated by Cdk5 phosphorylation (**Figure 6A, 6B, Table 2**). There were no differences in activation kinetics or voltage dependence of activation between the WT $Ca_V2.2$ and 8X $Ca_V2.2$ channels in the presence or absence of Cdk5/p35 (**Figure 5C, 5D, Figure 6C, 6D**). In examining inactivation kinetics, co-transfection with Cdk5/p35 increased the WT $Ca_V2.2$ inactivation time constant at the first test potential; however, the presence of Cdk5/p35 did not affect the inactivation kinetics of the 8X $Ca_V2.2$ channel at three different test potentials (**Figure 5E, Figure 6E**). In steady-state inactivation (SSI) profiles, WT $Ca_V2.2$ demonstrated a greater availability of channels for opening in the presence of Cdk5/p35, as denoted by the rightward shift of the SSI curve (**Figure 5F, Figure 6F**). Taken together, these data indicate that phosphorylation of $Ca_V2.2$ by Cdk5 increases the availability of calcium channels. Notably, there were no differences in SSIs at the holding potential at which N-type current density was measured (−100 mV), suggesting that differences in channel availability cannot account for the increased N-type current density mediated by Cdk5 phosphorylation.

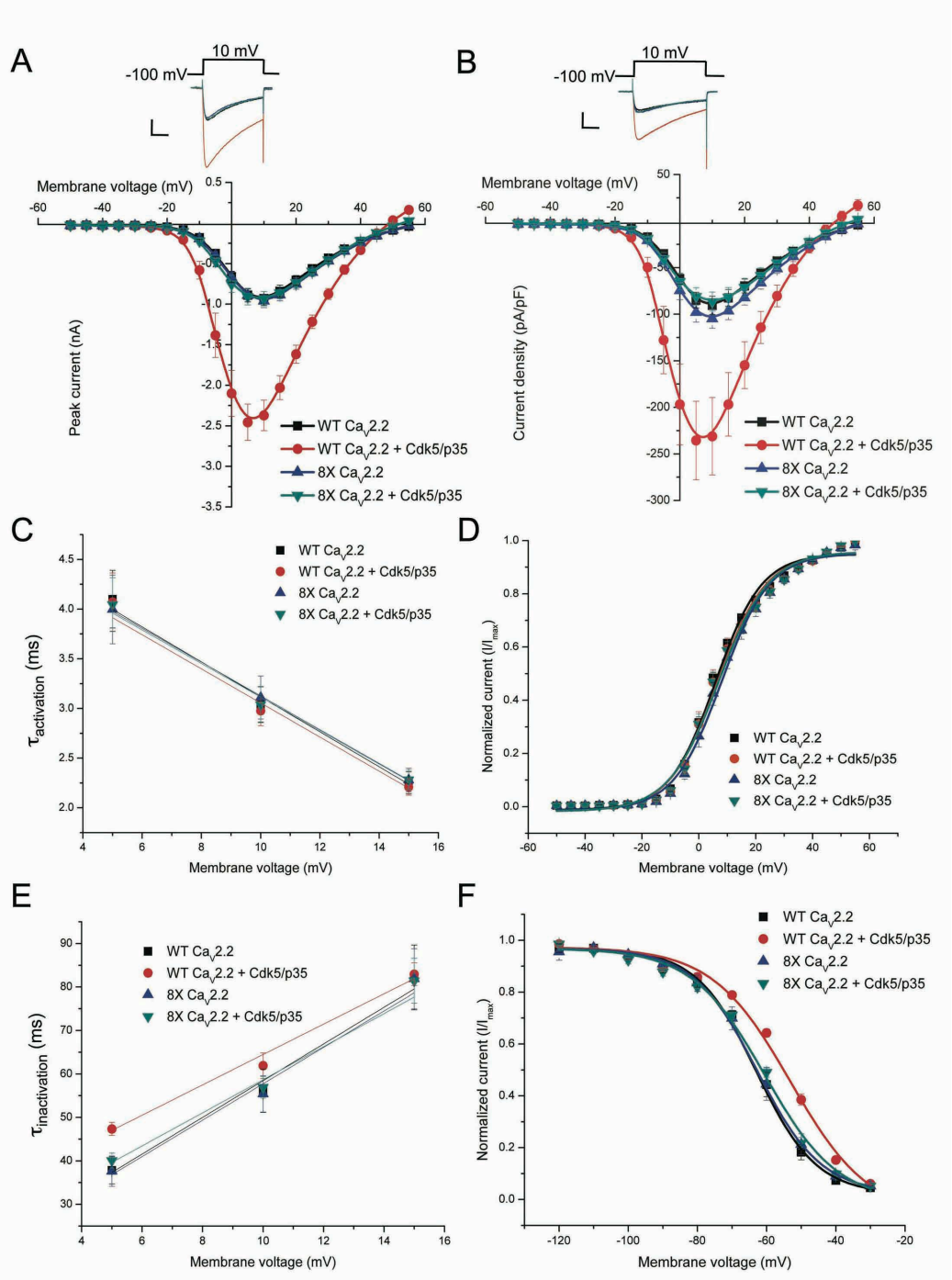

Figure 5. Modulation of biophysical properties of N-type calcium channels by Cdk5/p35.
(A) Cdk5 dramatically increased N-type current amplitude in cells expressing WT $Ca_V2.2$. Inward currents were evoked by 100 ms step depolarizations applied to test potentials between –55 mV to +55 mV from a holding potential of –100 mV. Peak current amplitudes were plotted on a current-voltage (I/V) curve. While cells expressing 8X $Ca_V2.2$ passed inward current at similar levels to WT $Ca_V2.2$, the presence of Cdk5/p35 failed to increase N-type current in cells expressing 8X $Ca_V2.2$. Scale bars, 50 nA, 20 ms. **(B)** Current density measurements were obtained by normalizing peak $Ca_V2.2$ current amplitude to cell capacitance. The current density of cells expressing WT $Ca_V2.2$ was significantly enhanced with

co-expression of Cdk5/p35. Scale bars, 50 nA, 20 ms. **(C)** A voltage-step protocol was applied and fitted an exponential curve to the timepoint spanning the maximal inward calcium current to obtain time constants for channel activation. Lines were plotted from best fit linear regression. Cdk5/p35 phosphorylation of WT $Ca_V2.2$ did not affect activation kinetics at any of the membrane potentials tested (5 mV, 10 mV, 15 mV). **(D)** Cdk5-mediated phosphorylation of $Ca_V2.2$ did not alter voltage dependence of activation. Cells were held at −100 mV, and tail currents from the test pulse were normalized to the largest tail current from each series. The normalized curves were fit by a single Boltzmann distribution $I/I_{max} = A2+(A1-A2)/(1+\exp((V_m-V_{1/2})/d_x))$, with $V_{1/2}$ as the midpoint for half-maximal activation, A1 and A2 being the normalized amplitudes and d_x as the slope. **(E)** A long voltage-step protocol was applied and fitted to an exponential curve to the timepoint at the peak inward current towards the end of the protocol to obtain inactivation time constants. Co-expression of Cdk5/p35 increased inactivation kinetics of WT $Ca_V2.2$ at the test potential of 5 mV. **(F)** Cdk5-mediated phosphorylation of WT $Ca_V2.2$ affected the voltage-dependence of steady state inactivation (SSI), a measure of the number of available channels at a given potential. Cells were held at −100 mV, and SSI values from the test pulse were normalized to the largest tail current. SSI curves were fitted by a single Boltzmann equation to calculate the membrane potential in which half of the channels are inactivated ($V_{1/2,inact}$). The rightward-shift of the SSI curve indicated that co-expression of Cdk5/p35 augmented the number of WT $Ca_V2.2$ channels available for opening. Data shown are the values (mean ± SEM) in **Table 1**. Statistical significance was calculated by one-way ANOVA (Bonferroni multiple comparison test) (*$p < 0.05$; **$p < 0.01$; ***$p < 0.001$).

Table 1. Values of electrophysiology experiments found in Figure 5

Measure	Condition	Value (mean± SEM)	n (cells/ cultures)	p-value	Statistics test	Fig
Peak current amplitude (pA)	WT $Ca_V2.2$ WT $Ca_V2.2$+Cdk5/p35 8X $Ca_V2.2$ 8X $Ca_V2.2$+Cdk5/p35	0.93±0.09 2.46±0.22 0.96±0.08 0.93±0.09	32/10 28/12 23/11 25/14	<0.001 (1 vs. 2) >0.05 (1 vs. 3) >0.05 (1 vs. 4) <0.001 (2 vs. 3) <0.001 (2 vs. 4) >0.05 (3 vs. 4)	One-way ANOVA	Fig. 5A
Current density (pA/pF)	WT $Ca_V2.2$ WT $Ca_V2.2$+Cdk5/p35 8X $Ca_V2.2$ 8X $Ca_V2.2$+Cdk5/p35	90.51±9.85 235.57±42.17 104.88±10.25 86.52±10.26	32/10 28/12 23/11 25/14	<0.001 (1 vs. 2) >0.05 (1 vs. 3) >0.05 (1 vs. 4) <0.001 (2 vs. 3) <0.001 (2 vs. 4) >0.05 (3 vs. 4)	One-way ANOVA	Fig. 5B
Activation kinetics τ (ms) (5 mV)	WT $Ca_V2.2$ WT $Ca_V2.2$+Cdk5/p35 8X $Ca_V2.2$ 8X $Ca_V2.2$+Cdk5/p35	4.10±0.29 4.07±0.29 4.00±0.35 4.04±0.27	18/9 14/8 9/6 7/5	>0.05 (1 vs. 2) >0.05 (1 vs. 3) >0.05 (1 vs. 4) >0.05 (2 vs. 3) >0.05 (2 vs. 4) >0.05 (3 vs. 4)	One-way ANOVA	Fig. 5C
Activation kinetics τ (ms) (10 mV)	WT $Ca_V2.2$ WT $Ca_V2.2$+Cdk5/p35 8X $Ca_V2.2$ 8X $Ca_V2.2$+Cdk5/p35	3.04±0.18 2.97±0.15 3.11±0.22 3.04±0.18	18/9 14/8 9/6 7/5	>0.05 (1 vs. 2) >0.05 (1 vs. 3) >0.05 (1 vs. 4) >0.05 (2 vs. 3) >0.05 (2 vs. 4) >0.05 (3 vs. 4)	One-way ANOVA	Fig. 5C
Activation kinetics τ (ms) (15 mV)	WT $Ca_V2.2$ WT $Ca_V2.2$+Cdk5/p35 8X $Ca_V2.2$ 8X $Ca_V2.2$+Cdk5/p35	2.25±0.11 2.21±0.08 2.28±0.12 2.28±0.10	18/9 14/8 9/6 7/5	>0.05 (1 vs. 2) >0.05 (1 vs. 3) >0.05 (1 vs. 4) >0.05 (2 vs. 3) >0.05 (2 vs. 4) >0.05 (3 vs. 4)	One-way ANOVA	Fig. 5C
Activation kinetics (intercept)	WT $Ca_V2.2$ WT $Ca_V2.2$+Cdk5/p35 8X $Ca_V2.2$ 8X $Ca_V2.2$+Cdk5/p35	4.88±0.21 4.77±.026 4.83±0.04 4.80±0.18	18/9 14/8 9/6 7/5	>0.05 (1 vs. 2) >0.05 (1 vs. 3) >0.05 (1 vs. 4) >0.05 (2 vs. 3) >0.05 (2 vs. 4) >0.05 (3 vs. 4)	One-way ANOVA	Fig. 5C
Activation kinetics (slope)	WT $Ca_V2.2$ WT $Ca_V2.2$+Cdk5/p35 8X $Ca_V2.2$ 8X $Ca_V2.2$+Cdk5/p35	-0.18±0.02 -0.17±0.02 -0.17±0.00 -0.17±0.01	18/9 14/8 9/6 7/5	>0.05 (1 vs. 2) >0.05 (1 vs. 3) >0.05 (1 vs. 4) >0.05 (2 vs. 3) >0.05 (2 vs. 4) >0.05 (3 vs. 4)	One-way ANOVA	Fig. 5C
Tail current ($V_{1/2}$)	WT $Ca_V2.2$ WT $Ca_V2.2$+Cdk5/p35 8X $Ca_V2.2$ 8X $Ca_V2.2$+Cdk5/p35	5.86±0.62 6.61±0.70 6.91±0.61 6.95±0.74	13/8 17/8 10/6 13/8	>0.05 (1 vs. 2) >0.05 (1 vs. 3) >0.05 (1 vs. 4) >0.05 (2 vs. 3) >0.05 (2 vs. 4) >0.05 (3 vs. 4)	One-way ANOVA	Fig. 5D

Tail current (A1)	WT $Ca_V2.2$ WT $Ca_V2.2$+Cdk5/p35 8X $Ca_V2.2$ 8X $Ca_V2.2$+Cdk5/p35	-0.013±0.01 -0.017±0.01 -0.014±0.01 -0.017±0.01	13/8 17/8 10/6 13/8	>0.05 (1 vs. 2) >0.05 (1 vs. 3) >0.05 (1 vs. 4) >0.05 (2 vs. 3) >0.05 (2 vs. 4) >0.05 (3 vs. 4)	One-way ANOVA	Fig. 5D
Tail current (A2)	WT $Ca_V2.2$ WT $Ca_V2.2$+Cdk5/p35 8X $Ca_V2.2$ 8X $Ca_V2.2$+Cdk5/p35	0.95±0.014 0.95±0.016 0.95±0.014 0.96±0.017	13/8 17/8 10/6 13/8	>0.05 (1 vs. 2) >0.05 (1 vs. 3) >0.05 (1 vs. 4) >0.05 (2 vs. 3) >0.05 (2 vs. 4) >0.05 (3 vs. 4)	One-way ANOVA	Fig. 5D
Tail current (d_x)	WT $Ca_V2.2$ WT $Ca_V2.2$+Cdk5/p35 8X $Ca_V2.2$ 8X $Ca_V2.2$+Cdk5/p35	8.13±0.56 8.60±0.64 8.19±0.55 8.84±0.67	13/8 17/8 10/6 13/8	>0.05 (1 vs. 2) >0.05 (1 vs. 3) >0.05 (1 vs. 4) >0.05 (2 vs. 3) >0.05 (2 vs. 4) >0.05 (3 vs. 4)	One-way ANOVA	Fig. 5D
Inactivation kinetics τ (ms) (5 mV)	WT $Ca_V2.2$ WT $Ca_V2.2$+Cdk5/p35 8X $Ca_V2.2$ 8X $Ca_V2.2$+Cdk5/p35	37.80±3.13 47.34±1.50 37.63±3.50 40.05±1.72	9/3 9/3 6/2 9/3	<0.05 (1 vs. 2) >0.05 (1 vs. 3) >0.05 (1 vs. 4) <0.05 (2 vs. 3) <0.05 (2 vs. 4) >0.05 (3 vs. 4)	One-way ANOVA	Fig. 5E
Inactivation kinetics τ (ms) (10 mV)	WT $Ca_V2.2$ WT $Ca_V2.2$+Cdk5/p35 8X $Ca_V2.2$ 8X $Ca_V2.2$+Cdk5/p35	56.10±4.97 61.90±2.94 55.40±4.16 56.92±2.49	9/3 9/3 6/2 9/3	>0.05 (1 vs. 2) >0.05 (1 vs. 3) >0.05 (1 vs. 4) >0.05 (2 vs. 3) >0.05 (2 vs. 4) >0.05 (3 vs. 4)	One-way ANOVA	Fig. 5E
Inactivation kinetics τ (ms) (15 mV)	WT $Ca_V2.2$ WT $Ca_V2.2$+Cdk5/p35 8X $Ca_V2.2$ 8X $Ca_V2.2$+Cdk5/p35	82.19±7.45 82.93±2.59 81.89±6.92 81.43±5.16	9/3 9/3 6/2 9/3	>0.05 (1 vs. 2) >0.05 (1 vs. 3) >0.05 (1 vs. 4) >0.05 (2 vs. 3) >0.05 (2 vs. 4) >0.05 (3 vs. 4)	One-way ANOVA	Fig. 5E
Inactivation kinetics (intercept)	WT $Ca_V2.2$ WT $Ca_V2.2$+Cdk5/p35 8X $Ca_V2.2$ 8X $Ca_V2.2$+Cdk5/p35	16.22±3.59 29.54±2.54 15.88±4.81 20.61±3.58	9/3 9/3 6/2 9/3	>0.05 (1 vs. 2) >0.05 (1 vs. 3) >0.05 (1 vs. 4) >0.05 (2 vs. 3) >0.05 (2 vs. 4) >0.05 (3 vs. 4)	One-way ANOVA	Fig. 3E
Inactivation (slope)	WT $Ca_V2.2$ WT $Ca_V2.2$+Cdk5/p35 8X $Ca_V2.2$ 8X $Ca_V2.2$+Cdk5/p35	4.22±0.44 3.49±0.29 4.19±0.54 3.80±0.46	9/3 9/3 6/2 9/3	>0.05 (1 vs. 2) >0.05 (1 vs. 3) >0.05 (1 vs. 4) >0.05 (2 vs. 3) >0.05 (2 vs. 4) >0.05 (3 vs. 4)	One-way ANOVA	Fig. 5E
Steady-state inactivation ($V_{1/2}$)	WT $Ca_V2.2$ WT $Ca_V2.2$+Cdk5/p35 8X $Ca_V2.2$ 8X $Ca_V2.2$+Cdk5/p35	-62.95±1.08 -53.12±2.07 -62.72±0.76 -60.53±1.44	17/9 19/11 11/8 21/13	<0.05 (1 vs. 2) >0.05 (1 vs. 3) >0.05 (1 vs. 4) <0.05 (2 vs. 3) <0.05 (2 vs. 4)	One-way ANOVA	Fig. 5F

				>0.05 (3 vs. 4)		
Steady-state inactivation (A1)	WT $Ca_V2.2$ WT $Ca_V2.2$+Cdk5/p35 8X $Ca_V2.2$ 8X $Ca_V2.2$+Cdk5/p35	0.97±0.01 0.97±0.01 0.97±0.01 0.97±0.01	17/9 19/11 11/8 21/13	>0.05 (1 vs. 2) >0.05 (1 vs. 3) >0.05 (1 vs. 4) >0.05 (2 vs. 3) >0.05 (2 vs. 4) >0.05 (3 vs. 4)	One-way ANOVA	Fig. 5F
Steady-state inactivation (A2)	WT $Ca_V2.2$ WT $Ca_V2.2$+Cdk5/p35 8X $Ca_V2.2$ 8X $Ca_V2.2$+Cdk5/p35	0.02±0.01 -0.06±0.06 0.02±0.01 -0.01±0.04	17/9 19/11 11/8 21/13	>0.05 (1 vs. 2) >0.05 (1 vs. 3) >0.05 (1 vs. 4) >0.05 (2 vs. 3) >0.05 (2 vs. 4) >0.05 (3 vs. 4)	One-way ANOVA	Fig. 5F
Steady-state inactivation (d_x)	WT $Ca_V2.2$ WT $Ca_V2.2$+Cdk5/p35 8X $Ca_V2.2$ 8X $Ca_V2.2$+Cdk5/p35	8.66±0.78 11.30±1.50 9.25±0.55 10.54±1.27	17/9 19/11 11/8 21/13	<0.05 (1 vs. 2) >0.05 (1 vs. 3) >0.05 (1 vs. 4) <0.05 (2 vs. 3) <0.05 (2 vs. 4) >0.05 (3 vs. 4)	One-way ANOVA	Fig. 5F

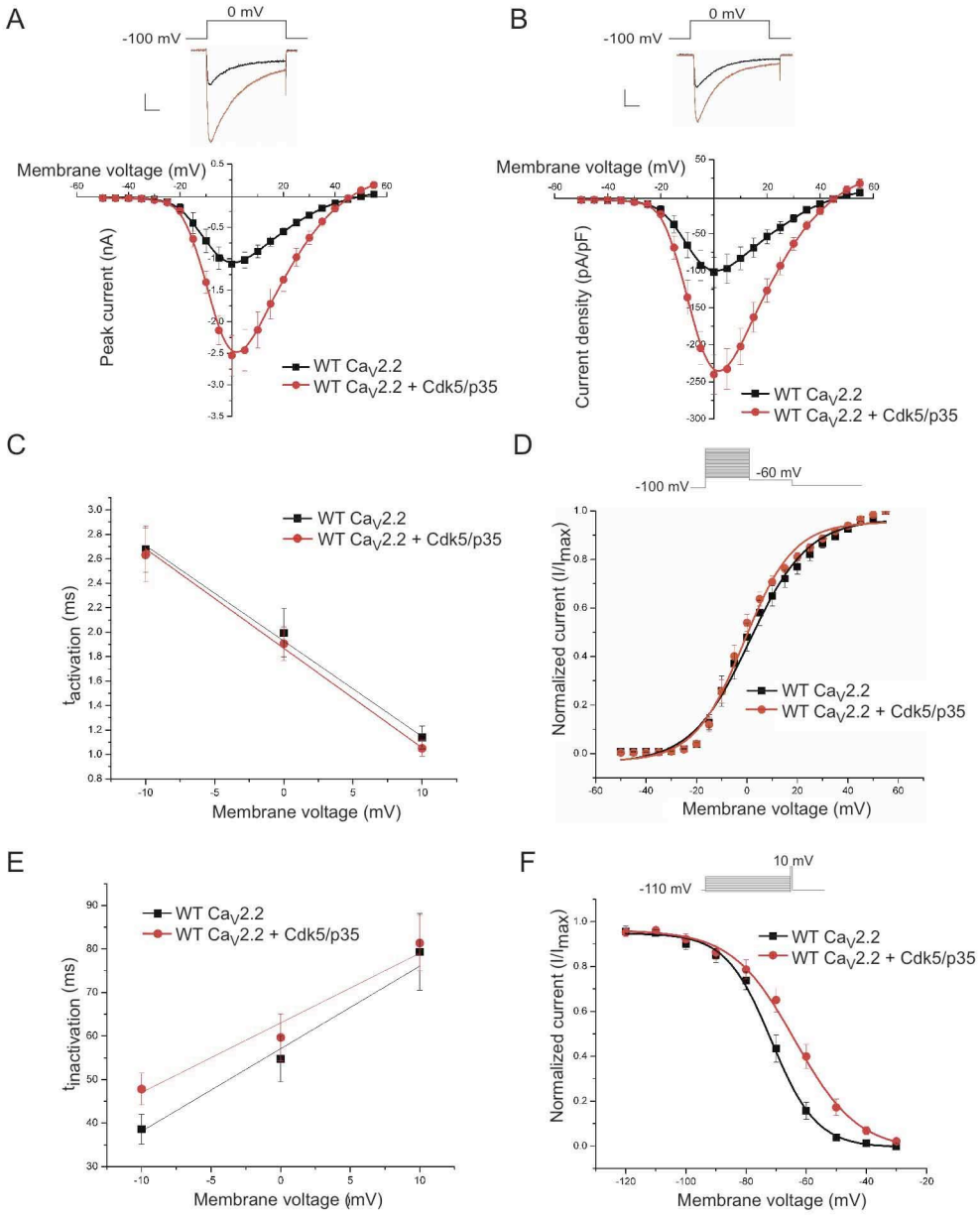

Figure 6. Modulation of biophysical properties of $Ca_V2.2$ by Cdk5/p35 in heterologous cells.
(A) In a cell line stably expressing the rat isoform of $Ca_V2.2$, co-expression of Cdk5/p35 resulted in a significant increase of peak N-type current. Scale bars, 100 nA, 20 ms. **(B)** The current density calculation showed a dramatic effect when Cdk5/p35 was co-expressed with $Ca_V2.2$ in the heterologous system. Scale bars, 100 nA, 20 ms. **(C)** Cdk5-mediated phosphorylation of the rat isoform of $Ca_V2.2$ in a stable cell line did not alter activation kinetics. **(D) T**he voltage dependence of activation, as measured by tail currents, was unaffected by co-expression of Cdk5/p35. **(E)** The inactivation kinetics of $Ca_V2.2$ were increased following Cdk5/p35 co-expression only at the test potential of −10 mV. **(F)** Cdk5/p35-mediated phosphorylation of $Ca_V2.2$ caused a rightward shift in the voltage-dependence of steady state inactivation, resulting in greater channel availability. Data shown are means ± s.e.m. in **Table 2**. Statistical significance was calculated using Student's t-test (*p < 0.05; **p < 0.01; ***p < 0.001).

Table 2. Values of electrophysiology experiments found in Supplementary Figure 6

Measure	Condition	Value (mean±SEM)	n (cells/ cultures)	p-value	Statistical test	Figure
Peak current amplitude (pA)	$Ca_V2.2$ $Ca_V2.2$ + Cdk5/p35	1.09±0.16 2.53±0.32	16/5 21/4	<0.001	Student's t-test	Fig. 6A
Current density (pA/pF)	$Ca_V2.2$ $Ca_V2.2$ + Cdk5/p35	102.13±20.63 240.00±26.72	16/5 21/4	<0.001	Student's t-test	Fig. 6B
Activation τ (ms) (-10 mV)	$Ca_V2.2$ $Ca_V2.2$ + Cdk5/p35	2.48±0.19 2.69±0.20	12/4 13/3	>0.05	Student's t-test	Fig. 6C
Activation τ (ms) (0 mV)	$Ca_V2.2$ $Ca_V2.2$ + Cdk5/p35	2.05±0.20 2.02±0.14	12/4 13/3	>0.05	Student's t-test	Fig. 6C
Activation τ (ms) (10 mV)	$Ca_V2.2$ $Ca_V2.2$ + Cdk5/p35	1.15±0.10 1.08±0.07	12/4 13/3	>0.05	Student's t-test	Fig. 6C
Activation (intercept)	$Ca_V2.2$ $Ca_V2.2$ + Cdk5/p35	1.93±0.04 -0.08±0.00	12/5 11/6	>0.05	Student's t-test	Fig. 6C
Activation (slope)	$Ca_V2.2$ $Ca_V2.2$ + Cdk5/p35	1.87±0.03 -0.08±0.00	12/5 11/6	>0.05	Student's t-test	Fig. 6C
Tail current (V_h)	$Ca_V2.2$ $Ca_V2.2$ + Cdk5/p35	1.00±0.96 -0.77±0.89	12/5 11/6	>0.05	Student's t-test	Fig. 6D
Tail current (A1)	$Ca_V2.2$ $Ca_V2.2$ + Cdk5/p35	-0.04±0.02 -0.03±0.02	12/5 11/6	>0.05	Student's t-test	Fig. 6D
Tail current (A2)	$Ca_V2.2$ $Ca_V2.2$ + Cdk5/p35	0.97±0.02 0.96±0.02	12/5 11/6	>0.05	Student's t-test	Fig. 6D
Tail current (d_x)	$Ca_V2.2$ $Ca_V2.2$ + Cdk5/p35	11.56±0.95 10.17±0.84	12/5 11/6	>0.05	Student's t-test	Fig. 6D
Inactivation τ (ms) (-10 mV)	$Ca_V2.2$ $Ca_V2.2$ + Cdk5/p35	35.59±1.75 47.81±3.66	12/6 13/6	<0.01	Student's t-test	Fig. 6E
Inactivation τ (ms) (0 mV)	$Ca_V2.2$ $Ca_V2.2$ + Cdk5/p35	54.79±5.25 59.68±5.41	12/6 13/6	>0.05	Student's t-test	Fig. 6E
Inactivation τ (ms) (10 mV)	$Ca_V2.2$ $Ca_V2.2$ + Cdk5/p35	79.33±8.83 81.37±6.39	12/6 13/6	>0.05	Student's t-test	Fig. 6E
Inactivation (intercept)	$Ca_V2.2$ $Ca_V2.2$ + Cdk5/p35	57.10±2.08 63.04±2.28	12/5 11/6	>0.05	Student's t-test	Fig. 6E
Inactivation (slope)	$Ca_V2.2$ $Ca_V2.2$ + Cdk5/p35	1.90±0.24 1.60±0.26	12/5 11/6	>0.05	Student's t-test	Fig. 6E
Steady-state inactivation ($V_{1/2}$)	$Ca_V2.2$ $Ca_V2.2$ + Cdk5/p35	-71.64±0.76 -63.79±0.95	13/7 13/7	<0.05	Student's t-test	Fig. 6F
Steady-state	$Ca_V2.2$	0.95±0.01	13/7	>0.05	Student's	Fig.

inactivation (A1)	$Ca_V2.2$ + Cdk5/p35	0.96±0.01	13/7		t-test	6F
Steady-state inactivation (A2)	$Ca_V2.2$ $Ca_V2.2$ + Cdk5/p35	-0.01±0.01 -0.02±0.02	13/7 13/7	>0.05	Student's t-test	Fig. 6F
Steady-state inactivation (slope)	$Ca_V2.2$ $Ca_V2.2$ + Cdk5/p35	7.54±0.51 10.42±0.76	13/7 13/7	<0.05	Student's t-test	Fig. 6F

Cdk5 plays a critical role in regulating channel open probability of $Ca_V2.2$

In addition to effects on steady-state inactivation, we reasoned that a distinct mechanism must underlie the dramatic increase in $Ca_V2.2$ current density following Cdk5/p35-mediated phosphorylation. Previous reports have indicated a role for scaffolding proteins in the modulation of calcium channels and enhanced calcium influx due to increased channel surface expression (Brittain et al., 2009; Lai et al., 2005; Leenders et al., 2008). Accordingly, we conducted cell surface biotinylation assays to examine whether Cdk5/p35 increases $Ca_V2.2$ surface expression in our heterologous system. However, $Ca_V2.2$ surface expression was not upregulated by Cdk5/p35 in stable cell lines or after co-expression with WT $Ca_V2.2$ or 8X $Ca_V2.2$, indicating that altered channel surface expression was not responsible for the enhancement of the $Ca_V2.2$ current density by Cdk5/p35-mediated phosphorylation (**Figure 7A, 7B, Table 3**). We next assessed channel open probability (P_o) of $Ca_V2.2$ in the presence of Cdk5/p35 as previously described (Agler et al., 2005). To obtain maximal channel open probability, P_o, for each cell, the maximal ionic current conductance G_{max} (**Figure 7C**) was plotted as a function of the integral of the channel gating current at the reversal potential Q_{max} (**Figure 7D**). Interestingly, Cdk5/p35-mediated phosphorylation of $Ca_V2.2$ increased the channel open probability P_o (**Figure 7E, 7F**). Importantly, the Cdk5/p35-mediated increase in the WT $Ca_V2.2$ channel open probability was not observed in 8X $Ca_V2.2$.

To further determine whether the dramatic increase in $Ca_V2.2$ current density impacts $Ca_V2.2$ surface expression in primary neurons, we cloned the full-length WT $Ca_V2.2$ α_1 subunit or the 8X $Ca_V2.2$ α_1 subunit cDNA into a bi-cistronic HSV (herpes simplex virus) backbone that co-expresses GFP (Neve et al., 2005). In primary neurons, transduction with HSV yields about 90% GFP-positive cells after 24 hours (**Figure 8A**). Upon transduction of primary neurons with WT $Ca_V2.2$ or 8X $Ca_V2.2$ HSV, however, there were no alterations in $Ca_V2.2$ surface levels compared to neurons transduced with control GFP HSV (**Figure 8B**). Collectively, these data suggest that in addition to increased channel availability, Cdk5-mediated phosphorylation of $Ca_V2.2$ results in increased calcium influx due to enhanced channel open probability.

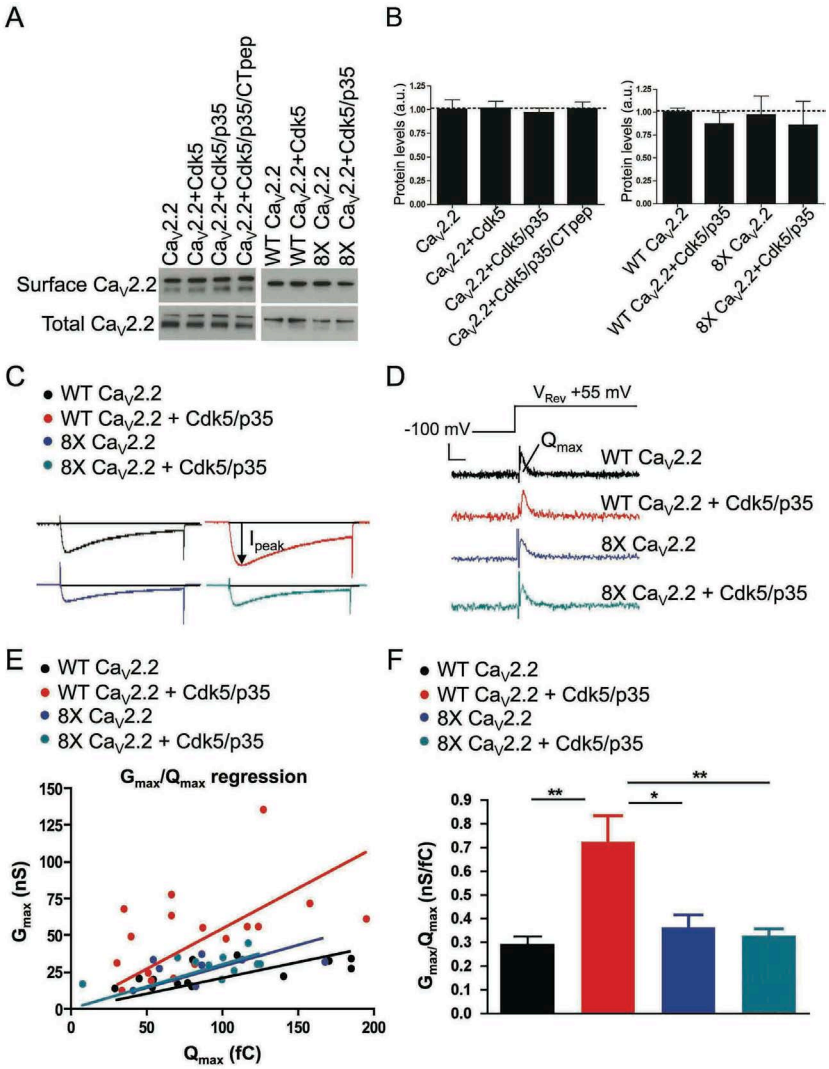

Figure 7. Analysis of surface expression levels and channel open probability after Cdk5-mediated phosphorylation of $Ca_V2.2$.

(A) $Ca_V2.2$ surface expression levels were not altered by Cdk5-mediated phosphorylation. Left: In the stable cell line expressing $Ca_V2.2$, $Ca_V2.2$ was co-expressed with Cdk5 alone, Cdk5/p35, or Cdk5/p35 and a competing C-terminal peptide. Right: Compared to expression of WT $Ca_V2.2$ alone, surface levels of $Ca_V2.2$ protein were unaltered after WT $Ca_V2.2$ coexpression with Cdk5/p35, 8X $Ca_V2.2$ expression, or 8X $Ca_V2.2$ coexpression with Cdk5/p35. **(B)** Quantification was performed across independent experiments. Normalized protein levels are shown, with n=3 experiments per condition. **(C)** Representative traces shown for peak current as a function of test-pulse potential. The I_{peak} was calculated by dividing the peak current by the cell capacitance to obtain maximal current. **(D)** Transient currents occur when the cell is brought from its resting potential to the reversal potential (approximately +55 mV). The area under the transient current was calculated as Q_{max}. Scale bars, 0.1 nA, 2 ms. **(E)** G_{max} (slope of the maximal current) was plotted against Q_{max}, with the ratio established as a measurement of the channel open probability. **(F)** Quantification of G_{max}/Q_{max}. Cdk5-mediated phosphorylation of WT $Ca_V2.2$ increased channel open probability (P_o). Data shown are the values (mean ± SEM) in **Table 3**. Statistical significance was calculated using one-way ANOVA (Tukey's multiple comparison test) (*$p < 0.05$; **$p < 0.01$; ***$p < 0.001$).

Table 3. Values of electrophysiology experiments and protein quantitation found in Figure 7

Measure	Condition	Value (mean± SEM)	n (cultures)	p-value	Statistical test	Figure
Surface $Ca_V2.2$	$Ca_V2.2$ $Ca_V2.2$+Cdk5 $Ca_V2.2$+Cdk5/p35 $Ca_V2.2$+Cdk5/p35/ CTpep	1.00±0.10 1.01±0.07 0.97±0.05 1.01±0.07	4 (1) 4 (2) 4 (3) 4 (4)	>0.05 (1 vs. 2) >0.05 (1 vs. 3) >0.05 (1 vs. 4) >0.05 (2 vs. 3) >0.05 (2 vs. 4) >0.05 (3 vs. 4)	One-way ANOVA	Fig. 7B
Surface $Ca_V2.2$	WT $Ca_V2.2$ WT $Ca_V2.2$+Cdk5 8X $Ca_V2.2$ 8X $Ca_V2.2$+Cdk5/p35	1.00±0.04 0.87±0.13 0.97±0.21 0.86±0.26	4 (1) 4 (2) 4 (3) 4 (4)	>0.05 (1 vs. 2) >0.05 (1 vs. 3) >0.05 (1 vs. 4) >0.05 (2 vs. 3) >0.05 (2 vs. 4) >0.05 (3 vs. 4)	One-way ANOVA	Fig. 7B
Slope of G_{max}/Q_{max}	WT $Ca_V2.2$ WT $Ca_V2.2$+Cdk5 8X $Ca_V2.2$ 8X $Ca_V2.2$+Cdk5/p35	0.29±0.03 0.72±0.11 0.36±0.05 0.32±0.03	13 (1) 17 (2) 8 (3) 10 (4)	<0.01 (1 vs. 2) >0.05 (1 vs. 3) >0.05 (1 vs. 4) <0.05 (2 vs. 3) <0.01 (2 vs. 4) >0.05 (3 vs. 4)	One-way ANOVA	Fig. 7F

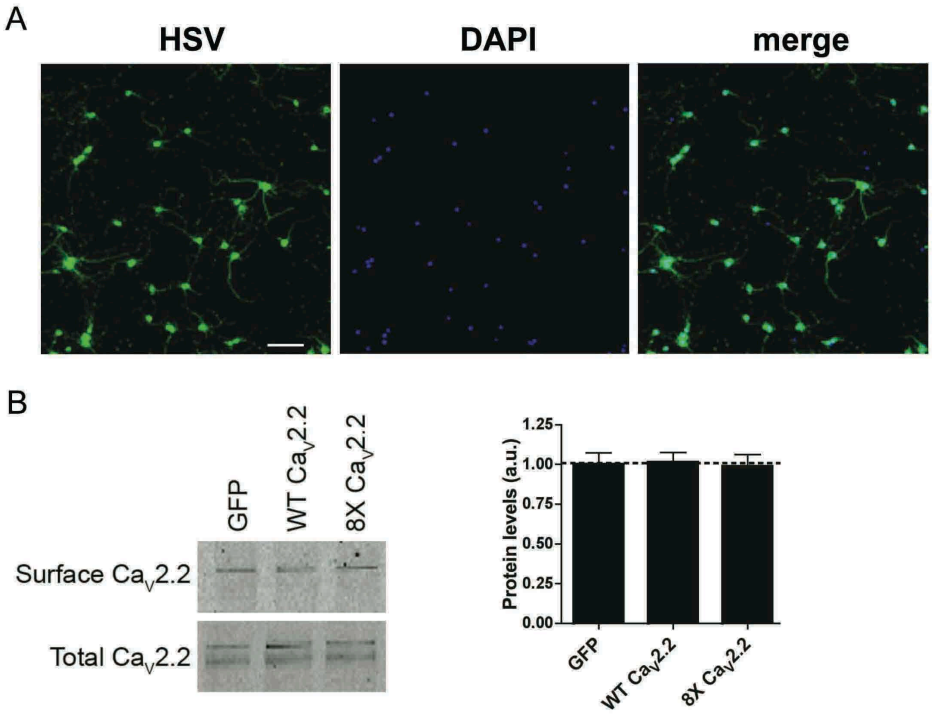

Figure 8. HSV-mediated transduction of primary neurons and $Ca_V2.2$ surface expression.
(A) A representative image highlighting the transduction efficiency of HSV in primary hippocampal cultures. Almost all neurons (90%) were successfully transduced with the GFP HSV. Scale bar, 100 μm. **(B)** Surface biotinylation assays of primary neurons transduced with GFP, WT $Ca_V2.2$, or 8X $Ca_V2.2$ HSV. Expression of WT $Ca_V2.2$ or 8X $Ca_V2.2$ HSV had no significant effects on $Ca_V2.2$ surface levels when compared to neurons expressing control GFP HSV. Normalized protein levels are shown, with n=4 experiments per condition. GFP, 1.00±0.07; WT $Ca_V2.2$, 1.01±0.06; 8X $Ca_V2.2$, 0.99±0.08; $p>0.05$. Data shown are means ± s.e.m. Statistical significance was calculated using one-way ANOVA (Tukey's multiple comparison test) (*$p < 0.05$; **$p < 0.01$; ***$p < 0.001$).

Altered synaptic properties in neurons expressing $Ca_V2.2$

We predicted that Cdk5-mediated phosphorylation of $Ca_V2.2$ might play an important physiological role in $Ca_V2.2$-mediated neurotransmission. To test this hypothesis, whole-cell $Ca_V2.2$ currents were isolated in neurons transduced with HSV expressing control GFP, WT $Ca_V2.2$, or 8X $Ca_V2.2$. Consistent with our heterologous cell data, Cdk5-mediated phosphorylation of WT $Ca_V2.2$, but not 8X $Ca_V2.2$, increased neuronal $Ca_V2.2$ current density when compared to neurons expressing control GFP HSV (**Figure 9A, Table 4**). Furthermore, inhibition of Cdk5 activity using a dominant-negative Cdk5 (DNK5) HSV further reduced $Ca_V2.2$ current density (**Figure 9A)**, suggesting that Cdk5 is the major kinase responsible for $Ca_V2.2$ phosphorylation and increased $Ca_V2.2$ current density. We also examined if the P/Q-type calcium channel ($Ca_V2.1$), the other major presynaptic calcium channel in neurons, was affected by expression of WT $Ca_V2.2$ or 8X $Ca_V2.2$ HSV but found no differences in $Ca_V2.1$ current densities compared to neurons expressing GFP HSV (**Figure 10, Table 5**). $Ca_V2.1$ current density was also unaffected by the expression of DNK5 HSV (**Figure 10)**.

We next measured miniature postsynaptic currents to determine whether Cdk5-mediated phosphorylation of $Ca_V2.2$ impacts neurotransmitter release. To obtain miniature excitatory and inhibitory postsynaptic currents (mEPSCs and mIPSCs), primary neurons at DIV13-15 were transduced with GFP, WT $Ca_V2.2$, or 8X $Ca_V2.2$ HSV, and recordings were conducted 24-48 hrs later. In neurons expressing WT $Ca_V2.2$ HSV, compared to those expressing GFP HSV, we observed increased frequencies of both mEPSCs and mIPSCs, with no changes in current amplitude (**Figure 9B, 9C**). However, neither the miniature frequency nor the amplitude of neurons expressing 8X $Ca_V2.2$ HSV differed significantly from those of neurons expressing GFP HSV (**Figure 9B, 9C**). The increased frequency of the miniature currents strongly suggests that Cdk5-mediated phosphorylation of WT $Ca_V2.2$ modulates presynaptic function by enhancing vesicle release.

To explore the effects of expressing $Ca_V2.2$ in presynaptic terminals at a higher resolution, cultured neurons were transduced with HSV expressing GFP, WT $Ca_V2.2$ or 8X $Ca_V2.2$ and fixed for monolayer electron microscopy. Consistent with the notion that increased release probability is related to the size of the readily releasable vesicle pool (Dobrunz and Stevens, 1997; Murthy et al., 1997), we found that the number of docked vesicles in the readily releasable pool was greater in the presynaptic terminals of neurons transduced with WT $Ca_V2.2$,

but not 8X $Ca_V2.2$, HSV when compared to neurons transduced with GFP HSV (**Figure 9D**). These observations indicate that expression of WT $Ca_V2.2$ HSV in primary neurons facilitates neurotransmitter release due to an increased number of docked vesicles at the synaptic terminal.

In order to examine whether $Ca_V2.2$ localization itself might be affected by HSV expression, we performed immunocytochemistry and immunogold electron microscopy studies. Similar to previous reports (Maximov and Bezprozvanny, 2002), and consistent with the increased frequency of mEPSCs and mIPSCs, expression of WT $Ca_V2.2$ HSV facilitated the synaptic localization of $Ca_V2.2$ (**Figure 9E**).While immunogold-labeled $Ca_V2.2$ was associated with the presynaptic terminal in neurons expressing GFP HSV, neurons transduced with WT $Ca_V2.2$ HSV displayed higher co-localization of $Ca_V2.2$ to the presynaptic area (**Figure 9F**). The localization effects were not observed in neurons transduced with 8X $Ca_V2.2$ HSV, which displayed a similar profile to neurons expressing GFP HSV. Therefore, Cdk5-mediated phosphorylation of WT $Ca_V2.2$ HSV facilitates neurotransmitter release by affecting the number of docked vesicles and also by increasing $Ca_V2.2$ localization at the synapse.

Interactions between $Ca_V2.2$ and active zone proteins are affected by Cdk5

To gain additional insight into the molecular mechanisms underlying the effects of Cdk5-mediated N-type calcium channel phosphorylation on neurotransmitter release, we transduced primary hippocampal neurons at DIV13-15 with GFP, WT $Ca_V2.2$, or 8X $Ca_V2.2$ HSV. The associations between $Ca_V2.2$ and various presynaptic proteins involved in synaptic vesicle scaffolding or fusion were then examined using co-immunoprecipitation and immunoblotting after 24-48 hrs in vitro. While the overall protein levels of multiple presynaptic components were unaltered, the binding of $Ca_V2.2$ to the active zone protein RIM1 was significantly increased in neurons transduced with WT $Ca_V2.2$ HSV when compared to neurons transduced with GFP HSV (**Figure 11A, Table 6**). Since RIM1 directly binds and tethers both $Ca_V2.1$ (P/Q-type) and $Ca_V2.2$ (N-type) channels to the synaptic cleft to facilitate synchronous neurotransmitter release (Kaeser et al., 2011), these results indicate that Cdk5-mediated phosphorylation of $Ca_V2.2$ may play a role in modulating $Ca_V2.2$ and RIM1 binding, thereby affecting vesicle docking and neurotransmitter release. We found that acute inhibition of Cdk5 by DNK5 HSV in primary neurons reduced the association between $Ca_V2.2$ and RIM1, providing further support that Cdk5-mediated phosphorylation of $Ca_V2.2$ regulates its association with RIM1 (**Figure 12A, Table 7)**.

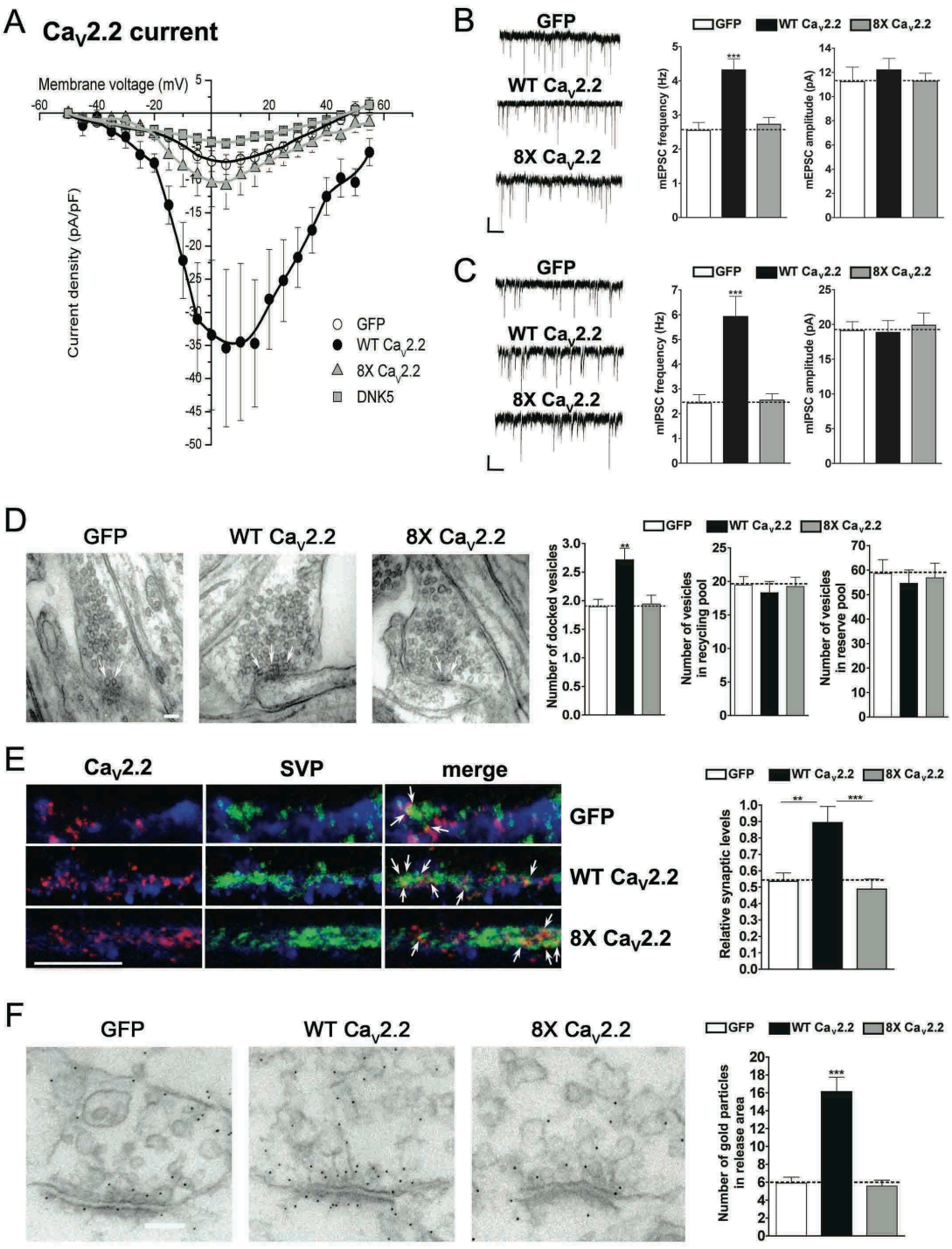

Figure 9. Neurotransmitter release impacted by Cdk5-mediated phosphorylation of Ca$_V$2.2.
(A) Current-voltage relationship of neurons expressing GFP, WT Ca$_V$2.2, 8X Ca$_V$2.2 or DNK5 HSV. Compared to Ca$_V$2.2-mediated current density in neurons expressing GFP, Cdk5-mediated phosphorylation of WT Ca$_V$2.2, but not 8X Ca$_V$2.2, enhanced Ca$_V$2.2 current density. However, expression of DNK5 HSV further reduced Ca$_V$2.2 current. **(B)** Sample traces (left) and quantification (right) of the frequency and amplitude of the miniature excitatory postsynaptic currents (mEPSCs). Compared to neurons expressing GFP HSV, the frequency of mEPSCs was increased in hippocampal

neurons expressing WT $Ca_V2.2$ HSV. There were no significant differences in mEPSC amplitudes. Scale bars, 10 pA, 2 s. **(C)** Sample traces (left) and quantification (right) of the frequency and amplitude of the miniature inhibitory postsynaptic currents (mIPSCs). Compared to neurons expressing GFP HSV, the frequency of mIPSCs was increased in hippocampal neurons expressing WT $Ca_V2.2$ HSV. There were no significant differences in mIPSC amplitudes. Scale bars, 10 pA, 2 s. **(D)** Electron microscopy images from neurons transduced with GFP, WT $Ca_V2.2$ or 8X $Ca_V2.2$ HSV. Scale bar, 100 nm. Compared to neurons expressing GFP HSV, there was an increase in the number of docked vesicles in the presynaptic terminal of neurons expressing WT $Ca_V2.2$ HSV. There were no significant differences in vesicle properties of neurons expressing 8X $Ca_v2.2$ HSV when compared to neurons expressing GFP HSV. **(E)** Approximately 5–7 HSV-transduced neurons (GFP-positive cells from HSV transduction; blue) per culture in three independent experiments were used to quantify the relative synaptic localization of $Ca_V2.2$ (red) by assessing its co-localization with presynaptic marker Synaptophysin (green). Compared to neurons expressing GFP HSV, expression of WT $Ca_V2.2$ HSV increased the synaptic co-localization of $Ca_V2.2$ and Synaptophysin. Right: quantification of synaptic levels. Scale bar, 5 μm. **(F)** Immunogold labeling for primary hippocampal neurons at DIV16 transduced with GFP, WT $Ca_V2.2$, or 8X $Ca_V2.2$ HSV. There was increased $Ca_V2.2$ localization to the presynaptic terminal in neurons expressing WT $Ca_V2.2$ HSV when compared to neurons expressing GFP HSV. Scale bar, 100 nm. Right: quantification of the immunogold labeling. Data shown are the values (mean ± SEM) in **Table 4**. Statistical significance was calculated using one-way ANOVA (Tukey's multiple comparison test). (*$p < 0.05$; **$p < 0.01$; ***$p < 0.001$).

Table 4. Values of electrophysiology experiments and electron microscopy found in Figure 9

Measure	Condition	Value (mean± SEM)	n (cells/ cultures)	p-value	Statistical test	Figure
$Ca_V2.2$ peak current density (pA/pF)	GFP WT $Ca_V2.2$ 8X $Ca_V2.2$ DNK5	7.70±1.49 35.41±11.87 10.91±3.52 4.55±0.47	12/4 (1) 10/3 (2) 8/3 (3) 13/4 (4)	<0.01 (1 vs. 2) >0.05 (1 vs. 3) >0.05 (1 vs. 4) <0.05 (2 vs. 3) <0.01 (2 vs. 4) >0.05 (3 vs. 4)	One-way ANOVA	Fig. 9A
mEPSC frequency (Hz)	GFP WT $Ca_V2.2$ 8X $Ca_V2.2$	2.55±0.23 4.32±0.33 2.73±0.20	13/4 (1) 12/4 (2) 13/4 (3)	<0.001 (1 vs. 2) >0.05 (1 vs. 3) <0.001 (2 vs. 3)	One-way ANOVA	Fig. 9B
mEPSC amplitude (pA)	GFP WT $Ca_V2.2$ 8X $Ca_V2.2$	11.23±1.20 12.21±0.95 11.26±0.67	13/4 (1) 12/4 (2) 13/4 (3)	>0.05(1 vs. 2) >0.05 (1 vs. 3) >0.05 (2 vs. 3)	One-way ANOVA	Fig. 9B
mIPSC frequency (Hz)	GFP WT $Ca_V2.2$ 8X $Ca_V2.2$	2.43±0.34 5.92±082 2.55±0.26	12/3 (1) 14/3 (2) 13/3 (3)	<0.001 (1 vs. 2) >0.05 (1 vs. 3) <0.001 (2 vs. 3)	One-way ANOVA	Fig. 9C
mIPSC amplitude (pA)	GFP WT $Ca_V2.2$ 8X $Ca_V2.2$	19.10±1.31 18.85±1.72 19.88±1.77	12/3 (1) 14/3 (2) 13/3 (3)	>0.05(1 vs. 2) >0.05 (1 vs. 3) >0.05 (2 vs. 3)	One-way ANOVA	Fig. 9C
EM docked vesicles	GFP WT $Ca_V2.2$ 8X $Ca_V2.2$	1.90±0.13 2.72±0.20 1.94±0.15	38 (1) 32 (2) 37 (3)	<0.01(1 vs. 2) >0.05 (1 vs. 3) <0.01 (2 vs. 3)	One-way ANOVA	Fig. 9D
EM recycling pool	GFP WT $Ca_V2.2$ 8X $Ca_V2.2$	19.50±1.25 18.34±1.67 19.26±1.39	38 (1) 32 (2) 37 (3)	>0.05(1 vs. 2) >0.05 (1 vs. 3) >0.05 (2 vs. 3)	One-way ANOVA	Fig. 9D
EM reserve pool	GFP WT $Ca_V2.2$ 8X $Ca_V2.2$	58.63±5.67 54.69±5.48 56.91±5.94	38 (1) 32 (2) 37 (3)	>0.05(1 vs. 2) >0.05 (1 vs. 3) >0.05 (2 vs. 3)	One-way ANOVA	Fig. 9D
Relative synaptic co-localization	GFP WT $Ca_V2.2$ 8X $Ca_V2.2$	0.54±0.05 0.89±0.10 0.49±0.06	17/3 (1) 15/3 (2) 17/3 (3)	<0.01 (1 vs. 2) >0.05 (1 vs. 3) <0.001 (2 vs. 3)	One-way ANOVA	Fig. 9E
Gold particles (immunogold EM)	GFP WT $Ca_V2.2$ 8X $Ca_V2.2$	5.91±0.67 16.12±1.63 5.58±0.67	23 (1) 42 (2) 24 (3)	<0.001 (1 vs. 2) >0.05 (1 vs. 3) <0.001 (2 vs. 3)	One-way ANOVA	Fig. 9F

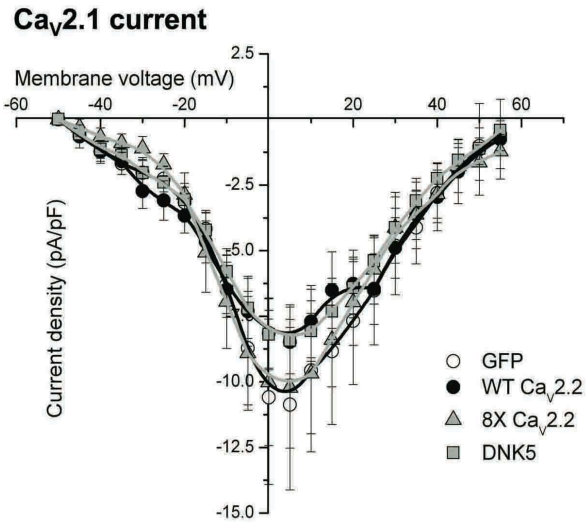

Figure 10. Measurement of $Ca_V2.1$ current density after $Ca_V2.2$ expression in primary neurons. Measurement of $Ca_V2.1$ (P/Q-type calcium channel) current density in primary neurons transduced with GFP, WT $Ca_V2.2$, 8X $Ca_V2.2$ or DNK5 HSV. There were no significant differences in P/Q-type calcium current density. Data shown are means ± s.e.m. in **Table 5**. Statistical significance was calculated using one-way ANOVA (Tukey's multiple comparison test) (*$p < 0.05$; **$p < 0.01$; ***$p < 0.001$).

Table 5. Values of electrophysiology experiments found in Figure 10

Measure	Condition	Value (mean±SEM)	n (cells/ cultures)	p-value	Statistical test	Figure
$Ca_V2.1$ peak current density (pA/pF)	GFP WT $Ca_V2.2$ 8X $Ca_V2.2$ DNK5	10.87±3.25 8.48±1.42 10.23±2.30 8.42±1.27	15/5 (1) 13/4 (2) 12/3 (3) 19/5 (4)	>0.05 (1 vs. 2) >0.05 (1 vs. 3) >0.05 (1 vs. 4) >0.05 (2 vs. 3) >0.05 (2 vs. 4) >0.05 (3 vs. 4)	One-way ANOVA	Fig. 10

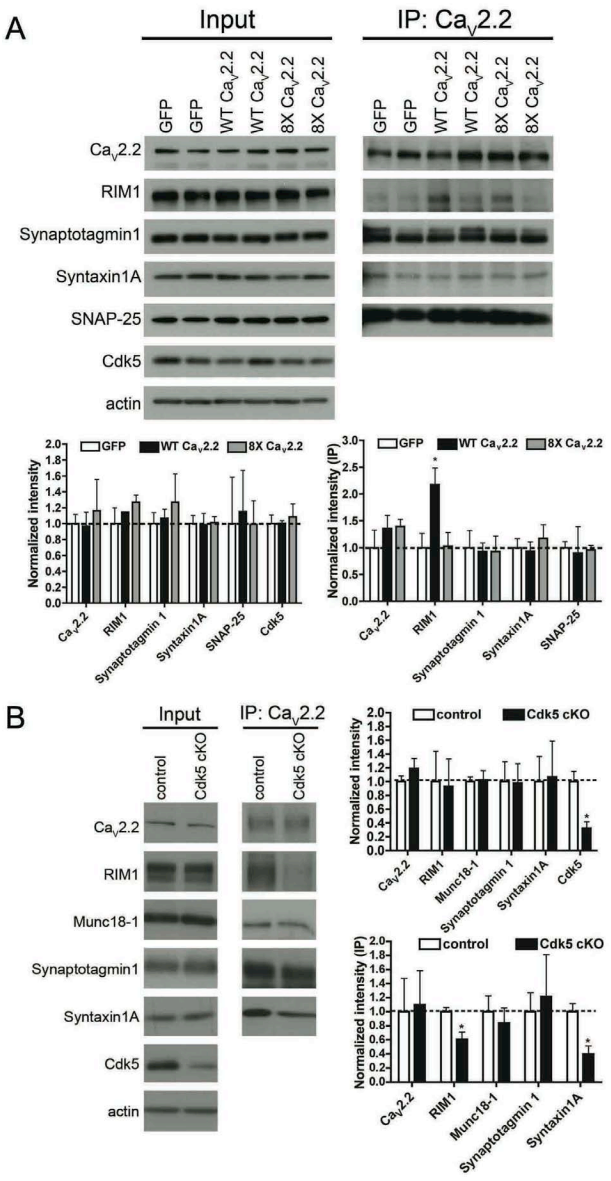

Figure 11. Interactions between $Ca_V2.2$ and active zone proteins are affected by Cdk5.
(A) Presynaptic proteins were probed in neurons transduced with GFP, WT $Ca_V2.2$ or 8X $Ca_V2.2$ HSV. Immunoprecipitation with $Ca_V2.2$ revealed an increase in the association between $Ca_V2.2$ and RIM1 in neurons expressing WT $Ca_V2.2$ HSV relative to neurons expressing GFP HSV. **(B)** Chronic Cdk5 depletion reduced the association between $Ca_V2.2$ and RIM1. The interaction between $Ca_V2.2$ and Syntaxin1A was also reduced. Normalized protein levels are shown, with n=3 mice per condition. Data shown are the values (mean ± SEM) in **Table 6**. Statistical significance was calculated using one-way ANOVA (Tukey's multiple comparison test, Bonferroni multiple comparison test) or Student's t-test (*$p < 0.05$; **$p < 0.01$; ***$p < 0.001$).

Table 6. Values of protein quantitation found in Figure 11

Measure	Condition	Value (mean± SEM	n (mice)	p-value	Statistical test	Figure
RIM1 (input)	GFP WT $Ca_V2.2$ 8X $Ca_V2.2$	1.00±0.20 1.15±0.01 1.27±0.09	3 (1) 3 (2) 3 (3)	>0.05 (1 vs. 2) >0.05 (1 vs. 3) >0.05 (2 vs. 3)	One-way ANOVA	Fig. 11A
$Ca_V2.2$ (input)	GFP WT $Ca_V2.2$ 8X $Ca_V2.2$	1.00±0.12 0.97±0.18 1.16±0.40	3 (1) 3 (2) 3 (3)	>0.05 (1 vs. 2) >0.05 (1 vs. 3) >0.05 (2 vs. 3)	One-way ANOVA	Fig. 11A
Synapto-tagmin1 (input)	GFP WT $Ca_V2.2$ 8X $Ca_V2.2$	1.00±0.14 1.07±0.12 1.27±0.36	3 (1) 3 (2) 3 (3)	>0.05 (1 vs. 2) >0.05 (1 vs. 3) >0.05 (2 vs. 3)	One-way ANOVA	Fig. 11A
Syntaxin1A (input)	GFP WT $Ca_V2.2$ 8X $Ca_V2.2$	1.00±0.10 0.99±0.14 1.01±0.08	3 (1) 3 (2) 3 (3)	>0.05 (1 vs. 2) >0.05 (1 vs. 3) >0.05 (2 vs. 3)	One-way ANOVA	Fig. 11A
SNAP25 (input)	GFP WT $Ca_V2.2$ 8X $Ca_V2.2$	1.00±0.58 1.15±0.52 0.99±0.30	3 (1) 3 (2) 3 (3)	>0.05 (1 vs. 2) >0.05 (1 vs. 3) >0.05 (2 vs. 3)	One-way ANOVA	Fig. 11A
Cdk5 (input)	GFP WT $Ca_V2.2$ 8X $Ca_V2.2$	1.00±0.11 1.00±0.03 1.08±0.16	3 (1) 3 (2) 3 (3)	>0.05 (1 vs. 2) >0.05 (1 vs. 3) >0.05 (2 vs. 3)	One-way ANOVA	Fig. 11A
RIM1 (IP)	GFP WT $Ca_V2.2$ 8X $Ca_V2.2$	1.00±0.27 2.17±0.31 1.03±0.26	3 (1) 3 (2) 3 (3)	<0.05 (1 vs. 2) >0.05 (1 vs. 3) <0.05 (2 vs. 3)	One-way ANOVA	Fig. 11A
$Ca_V2.2$ (IP)	GFP WT $Ca_V2.2$ 8X $Ca_V2.2$	1.00±0.33 1.36±0.54 1.39±0.14	3 (1) 3 (2) 3 (3)	>0.05 (1 vs. 2) >0.05 (1 vs. 3) >0.05 (2 vs. 3)	One-way ANOVA	Fig. 11A
Synapto-tagmin1 (IP)	GFP WT $Ca_V2.2$ 8X $Ca_V2.2$	1.00±0.32 0.93±0.16 0.93±0.29	3 (1) 3 (2) 3 (3)	>0.05 (1 vs. 2) >0.05 (1 vs. 3) >0.05 (2 vs. 3)	One-way ANOVA	Fig. 11A
Syntaxin1A (IP)	GFP WT $Ca_V2.2$ 8X $Ca_V2.2$	1.00±0.17 0.94±0.18 1.17±0.26	3 (1) 3 (2) 3 (3)	>0.05 (1 vs. 2) >0.05 (1 vs. 3) >0.05 (2 vs. 3)	One-way ANOVA	Fig. 11A
SNAP25 (IP)	GFP WT $Ca_V2.2$ 8X $Ca_V2.2$	1.00±0.17 0.90±0.45 0.96±0.09	3 (1) 3 (2) 3 (3)	>0.05 (1 vs. 2) >0.05 (1 vs. 3) >0.05 (2 vs. 3)	One-way ANOVA	Fig. 11A
RIM1 input	Control Cdk5 cKO	1.00±0.44 0.93±0.40	3 3	>0.05	Student's t-test	Fig. 11B
$Ca_V2.2$ (input)	Control Cdk5 cKO	1.00±0.08 1.19±0.15	3 3	>0.05	Student's t-test	Fig. 11B
Munc-18 (input)	Control Cdk5 cKO	1.00±0.07 1.03±0.14	3 3	>0.05	Student's t-test	Fig. 11B
Synapto-tagmin1 (input)	Control Cdk5 cKO	1.00±0.29 0.98±0.28	3 3	>0.05	Student's t-test	Fig. 11B
Syntaxin1A (input)	Control Cdk5 cKO	1.00±0.37 1.07±0.53	3 3	>0.05	Student's t-test	Fig. 11B
Cdk5	Control	1.00±0.15	3	<0.05	One-way	Fig. 11B

(input)	Cdk5 cKO	0.33±0.09	3		ANOVA	
$Ca_V2.2$ (IP)	Control Cdk5 cKO	1.00±0.48 1.10±0.49	3 3	>0.05	Student's t-test	Fig. 11B
RIM1 (IP)	Control Cdk5 cKO	1.00±0.06 0.47±0.10	3 3	<0.05	Student's t-test	Fig. 11B
Munc18 (IP)	Control Cdk5 cKO	1.00±0.23 0.84±0.22	3 3	>0.05	Student's t-test	Fig. 11B
Synapto-tagmin 1 (IP)	Control Cdk5 cKO	1.00±0.27 1.21±0.60	3 3	>0.05	Student's t-test	Fig. 11B
Syntaxin1A (IP)	Control Cdk5 cKO	1.00±0.12 0.40±0.12	3 3	<0.05	Student's t-test	Fig. 11B

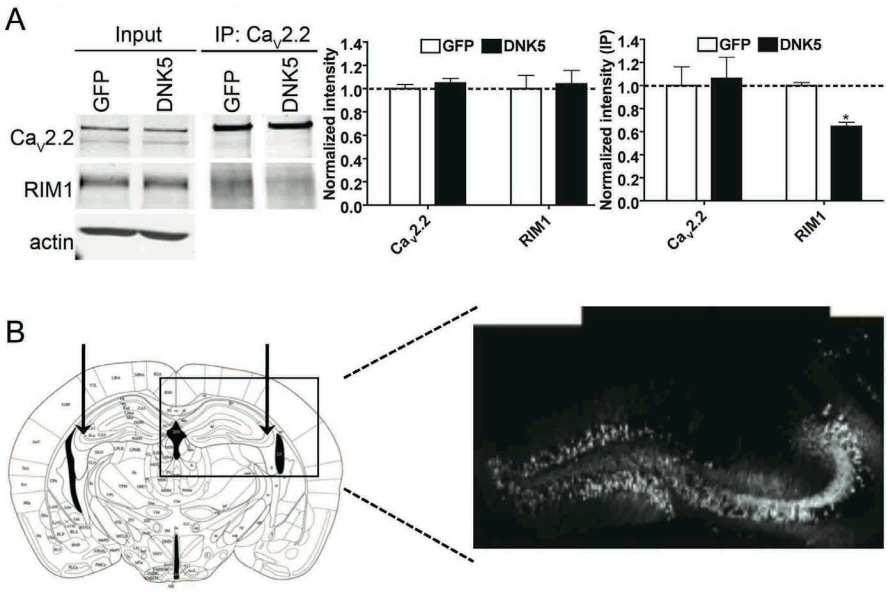

Figure 12. $Ca_V2.2$ association with RIM1 affected by Cdk5-mediated phosphorylation.
(A) Compared to neurons transduced with GFP, acute inhibition of Cdk5 using DNK5 HSV in primary neurons decreased the association between $Ca_V2.2$ and RIM1. Right: quantification of the biochemistry experiments. **(B)** Diagram highlighting HSV delivery into hippocampal area CA3. Mice were injected bilaterally with GFP, WT $Ca_V2.2$, or 8X $Ca_V2.2$ HSV (or co-injected with WT $Ca_V2.2$ and DNK5 HSV or 8X $Ca_V2.2$ and DNK5 HSV) and allowed to recover for 2–3 days. Right: magnification of the injection site demonstrating successful transduction of HSV into hippocampal area CA3. Data shown are means ± s.e.m. in **Table 7**. Statistical significance was calculated using Student's t-test (*$p < 0.05$; **$p < 0.01$; ***$p < 0.001$).

Table 7. Values of protein quantitation found in Figure 12

Measure	Condition	Value (mean± SEM)	n (cultures)	p-value	Statistical test	Figure
$Ca_V2.2$ (input)	GFP DNK5	1.00±0.04 1.05±0.04	3 3	>0.05	Student's t-test	Fig. 12A
RIM1 (input)	GFP DNK5	1.00±0.12 1.05±0.12	3 3	>0.05	Student's t-test	Fig. 12A
$Ca_V2.2$ (IP)	GFP DNK5	1.00±0.16 1.06±0.19	3 3	>0.05	Student's t-test	Fig. 12A
RIM1 (IP)	GFP DNK5	1.00±0.03 0.65±0.04	3 3	<0.05	Student's t-test	Fig. 12A

Furthermore, in brain lysates from control and Cdk5 cKO mice, chronic Cdk5 depletion reduced the binding of $Ca_V2.2$ to RIM1, indicating that Cdk5 is necessary for maintaining the association between $Ca_V2.2$ and RIM1 (**Figure 11B**). We observed that $Ca_V2.2$ binding to Syntaxin1A in Cdk5 cKO lysates was also reduced. These data demonstrate that Cdk5-mediated phosphorylation of $Ca_V2.2$ is required for its interaction with RIM1 and other SNARE proteins.

$Ca_V2.2$ phosphorylation by Cdk5 affects basal synaptic transmission and alters paired-pulse facilitation

Because Cdk5-mediated phosphorylation of $Ca_V2.2$ enhances miniature excitatory and inhibitory postsynaptic currents by modulating presynaptic release probability, we reasoned that synaptic plasticity is also affected. To address this hypothesis, we performed stereotaxic delivery of GFP, WT $Ca_V2.2$, or 8X $Ca_V2.2$ HSV into hippocampal area CA3 (**Figure 12B**). In an separate set of experiments, WT $Ca_V2.2$ or 8X $Ca_V2.2$ HSV was coinjected with DNK5 HSV, and the results were compared to those from injection of WT $Ca_V2.2$ or 8X $Ca_V2.2$ HSV alone. Acute transverse hippocampal slices were prepared to assess various forms of synaptic plasticity. We stimulated the Schaffer collateral/commissural pathway fibers, and field recordings were obtained from the dendritic region of hippocampal area CA1.

In contrast to slices expressing control GFP HSV, we discovered a significant enhancement of basal synaptic transmission in slices transduced with WT $Ca_V2.2$ HSV. This enhancement of basal synaptic transmission was not present in slices expressing 8X $Ca_V2.2$ HSV (**Figure 13A, Table 8**). Furthermore, the enhanced basal synaptic transmission observed in slices expressing WT $Ca_V2.2$ HSV alone was abolished in the presence of DNK5 HSV (**Figure 14A, Table 9**). We next examined paired-pulse facilitation (PPF), a form of short-term synaptic plasticity that predicts release probability (Zucker and Regehr, 2002). Strikingly, the PPF ratios calculated at multiple intervals were significantly lower in slices expressing WT $Ca_V2.2$ HSV than in those expressing GFP HSV. The PPF ratios were not significantly different between slices expressing GFP HSV and 8X $Ca_V2.2$ HSV (**Figure 13B**). However, the reduction in PPF ratio observed in slices expressing WT $Ca_V2.2$ HSV alone was absent in slices co-expressing WT $Ca_V2.2$ and DNK5 HSV (**Figure 14B**). The results are consistent with the hypothesis that neurons transduced with WT $Ca_V2.2$ HSV have a higher release probability and indicate that the enhancement of synaptic transmission relies on the activity of Cdk5.

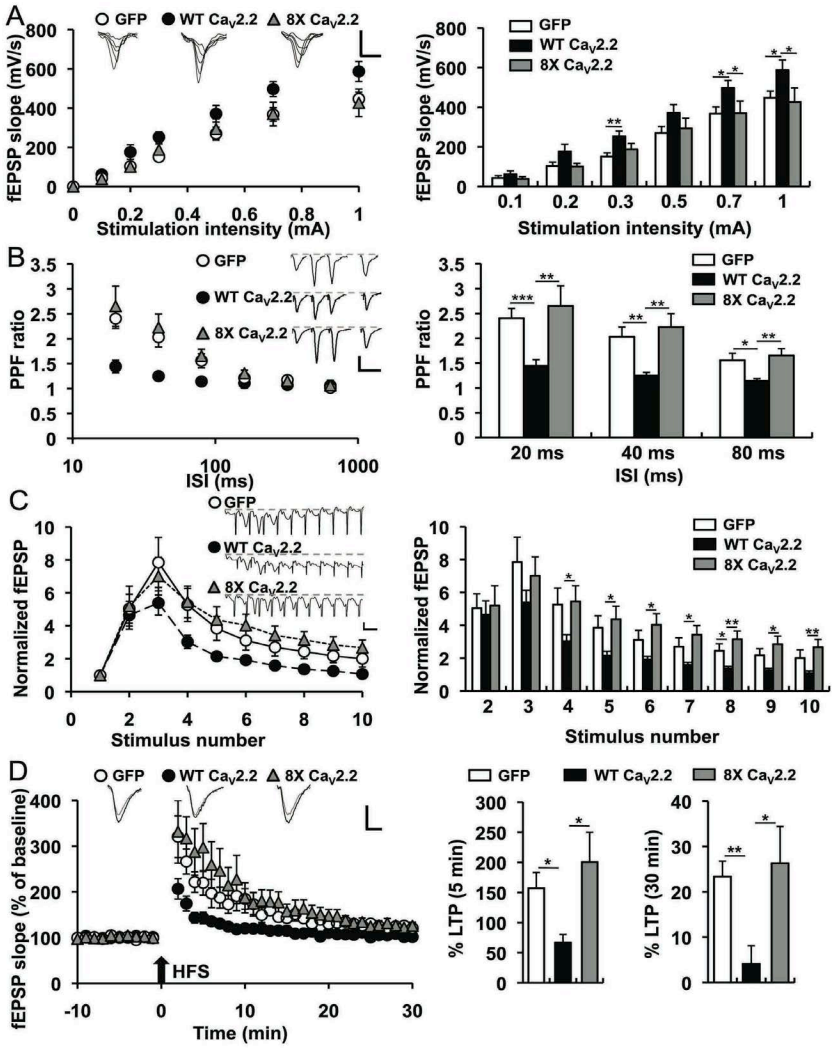

Figure 13. Synaptic plasticity measurements after expression of $Ca_v2.2$ HSV in hippocampus.
(A) Representative traces and quantification of the input/output curve in acute hippocampal slices transduced in area CA3 with GFP, WT $Ca_v2.2$, or 8X $Ca_v2.2$ HSV. Compared to slices expressing control GFP HSV, slices expressing WT $Ca_v2.2$ HSV exhibited enhanced basal synaptic transmission in the Schaffer collateral pathway. Scale bars, 0.5 mV, 10 ms. Right: quantification of the input/output curve. **(B)** Representative traces and quantification of the paired-pulse facilitation (PPF) response in acute hippocampal slices transduced in area CA3 with GFP, WT $Ca_v2.2$, or 8X $Ca_v2.2$ HSV. Scale bars, 0.5 mV, 25 ms. Compared to slices expressing GFP HSV, slices expressing WT $Ca_V2.2$ exhibited significantly lower paired-pulse facilitation (PPF) ratios. Scale bars, 0.5 mV, 25 ms. Right: quantification of the PPF ratio at various stimuli. **(C)** Representative traces and quantification of short-term facilitation during the 100 Hz stimulus at 0.5 mM $[Ca^{2+}]_o$. Slices expressing WT $Ca_V2.2$ HSV exhibited an overall reduction in synaptic facilitation during the 100 Hz stimulus train when compared to slices expressing GFP HSV. Scale bars, 0.5 mV, 10 ms. Right: quantification of the short-term plasticity at various stimuli. **(D)** Representative traces and quantification before and after HFS induction. Compared to hippocampal slices expressing GFP HSV, the fEPSP slope was markedly decreased in slices expressing WT $Ca_V2.2$ HSV. In all plasticity measurements, there were no significant differences in synaptic properties between slices expressing GFP HSV alone and 8X $Ca_v2.2$ HSV. Scale bars, 0.5 mV, 10 ms. Right: quantification of the fEPSP slope immediately after HFS (5 min) and at the end of the 30 min period. Data shown are the values (mean ± SEM) in **Table 8**. Statistical significance was calculated using one-way ANOVA (t-test) (*$p < 0.05$; **$p < 0.01$; ***$p < 0.001$).

Table 8. Values of electrophysiology experiments found in Figure 13

Measure	Condition	Value (mean± SEM)	n (slices/ mice)	p-value	Statistical test	Figure
Input/output (0.1 mA)	GFP WT $Ca_V2.2$ 8X $Ca_V2.2$	42.93±11.71 61.56±17.47 37.96±11.38	11/6 (1) 11/6 (2) 11/5 (3)	>0.05 (1 vs. 2) >0.05 (1 vs. 3) >0.05 (2 vs. 3)	One-way ANOVA	Fig. 13A
Input/output (0.2 mA)	GFP WT $Ca_V2.2$ 8X $Ca_V2.2$	103.39±19.59 175.82±37.18 100.49±16.30	11/6 (1) 11/6 (2) 11/5 (3)	>0.05 (1 vs. 2) >0.05 (1 vs. 3) >0.05 (2 vs. 3)	One-way ANOVA	Fig. 13A
Input/output (0.3 mA)	GFP WT $Ca_V2.2$ 8X $Ca_V2.2$	150.61±19.18 252.59±27.04 187.61±29.79	11/6 (1) 11/6 (2) 11/5 (3)	<0.01 (1 vs. 2) >0.05 (1 vs. 3) >0.05 (2 vs. 3)	One-way ANOVA	Fig. 13A
Input/output (0.5 mA)	GFP WT $Ca_V2.2$ 8X $Ca_V2.2$	270.11±32.86 371.41±42.29 293.26±51.52	11/6 (1) 11/6 (2) 11/5 (3)	>0.05 (1 vs. 2) >0.05 (1 vs. 3) >0.05 (2 vs. 3)	One-way ANOVA	Fig. 13A
Input/output (0.7 mA)	GFP WT $Ca_V2.2$ 8X $Ca_V2.2$	367.67±34.38 497.00±37.93 370.02±60.47	11/6 (1) 11/6 (2) 11/5 (3)	<0.05 (1 vs. 2) >0.05 (1 vs. 3) <0.05 (2 vs. 3)	One-way ANOVA	Fig. 13A
Input/output (1 mA)	GFP WT $Ca_V2.2$ 8X $Ca_V2.2$	447.33±33.88 586.82±51.40 424.77±70.20	11/6 (1) 11/6 (2) 11/5 (3)	<0.05 (1 vs. 2) >0.05 (1 vs. 3) <0.05 (2 vs. 3)	One-way ANOVA	Fig. 13A
PPF ratio (20 ms)	GFP WT $Ca_V2.2$ 8X $Ca_V2.2$	2.40±0.20 1.44±0.13 2.65±0.40	11/6 (1) 11/6 (2) 11/5 (3)	<0.001 (1 vs. 2) >0.05 (1 vs. 3) <0.01 (2 vs. 3)	One-way ANOVA	Fig. 13B
PPF ratio (40 ms)	GFP WT $Ca_V2.2$ 8X $Ca_V2.2$	2.03±0.20 1.25±0.07 2.22±0.27	11/6 (1) 11/6 (2) 11/5 (3)	<0.01 (1 vs. 2) >0.05 (1 vs. 3) <0.01 (2 vs. 3)	One-way ANOVA	Fig. 13B
PPF ratio (80 ms)	GFP WT $Ca_V2.2$ 8X $Ca_V2.2$	1.56±0.14 1.14±0.04 1.65±0.14	11/6 (1) 11/6 (2) 11/5 (3)	<0.05 (1 vs. 2) >0.05 (1 vs. 3) <0.01 (2 vs. 3)	One-way ANOVA	Fig. 13B
STP 100 Hz Stim. 2	GFP WT $Ca_V2.2$ 8X $Ca_V2.2$	5.04±0.88 4.64±0.84 5.19±1.21	9/5 (1) 13/5 (2) 9/5 (3)	>0.05 (1 vs. 2) >0.05 (1 vs. 3) >0.05 (2 vs. 3)	One-way ANOVA	Fig. 13C
STP 100 Hz Stim. 3	GFP WT $Ca_V2.2$ 8X $Ca_V2.2$	7.85±1.52 5.37±0.74 7.01±1.15	9/5 (1) 13/5 (2) 9/5 (3)	>0.05 (1 vs. 2) >0.05 (1 vs. 3) >0.05 (2 vs. 3)	One-way ANOVA	Fig. 13C
STP 100 Hz Stim. 4	GFP WT $Ca_V2.2$ 8X $Ca_V2.2$	5.26±1.00 3.03±0.40 5.45±0.96	9/5 (1) 13/5 (2) 9/5 (3)	>0.05 (1 vs. 2) >0.05 (1 vs. 3) <0.05 (2 vs. 3)	One-way ANOVA	Fig. 13C
STP 100 Hz Stim. 5	GFP WT $Ca_V2.2$ 8X $Ca_V2.2$	3.85±0.73 2.15±0.27 4.37±0.79	9/5 (1) 13/5 (2) 9/5 (3)	>0.05 (1 vs. 2) >0.05 (1 vs. 3) <0.05 (2 vs. 3)	One-way ANOVA	Fig. 13C
STP 100 Hz Stim. 6	GFP WT $Ca_V2.2$ 8X $Ca_V2.2$	3.11±0.58 1.92±0.19 4.03±0.68	9/5 (1) 13/5 (2) 9/5 (3)	>0.05 (1 vs. 2) >0.05 (1 vs. 3) <0.05 (2 vs. 3)	One-way ANOVA	Fig. 13C
STP 100 Hz	GFP WT $Ca_V2.2$	2.70±0.54 1.59±0.15	9/5 (1) 13/5 (2)	>0.05 (1 vs. 2) >0.05 (1 vs. 3)	One-way ANOVA	Fig. 13C

Stim. 7	8X $Ca_V2.2$	3.43±0.56	9/5 (3)	<0.05 (2 vs. 3)		
STP 100 Hz Stim. 8	GFP WT $Ca_V2.2$ 8X $Ca_V2.2$	2.44±0.44 1.37±0.13 3.15±0.50	9/5 (1) 13/5 (2) 9/5 (3)	<0.05 (1 vs. 2) >0.05 (1 vs. 3) <0.01 (2 vs. 3)	One-way ANOVA	Fig. 13C
STP 100 Hz Stim. 9	GFP WT $Ca_V2.2$ 8X $Ca_V2.2$	2.17±0.40 1.26±0.12 2.85±0.49	9/5 (1) 13/5 (2) 9/5 (3)	>0.05 (1 vs. 2) >0.05 (1 vs. 3) <0.05 (2 vs. 3)	One-way ANOVA	Fig. 13C
STP 100 Hz Stim. 10	GFP WT $Ca_V2.2$ 8X $Ca_V2.2$	2.01±0.50 1.08±0.14 2.67±0.47	9/5 (1) 13/5 (2) 9/5 (3)	>0.05 (1 vs. 2) >0.05 (1 vs. 3) <0.01 (2 vs. 3)	One-way ANOVA	Fig. 13C
fEPSP slope (first 5 min)	GFP WT $Ca_V2.2$ 8X $Ca_V2.2$	256.98±26.13 166.80±13.42 300.52±49.54	8/5 (1) 10/5 (2) 9/4 (3)	<0.05 (1 vs. 2) >0.05 (1 vs. 3) <0.05 (2 vs. 3)	One-way ANOVA	Fig. 13D
fEPSP slope (last 5 min)	GFP WT $Ca_V2.2$ 8X $Ca_V2.2$	123.38±3.39 104.10±4.03 126.31±8.11	8/5 (1) 10/5 (2) 9/4 (3)	<0.01 (1 vs. 2) >0.05 (1 vs. 3) <0.05 (2 vs. 3)	One-way ANOVA	Fig. 13D

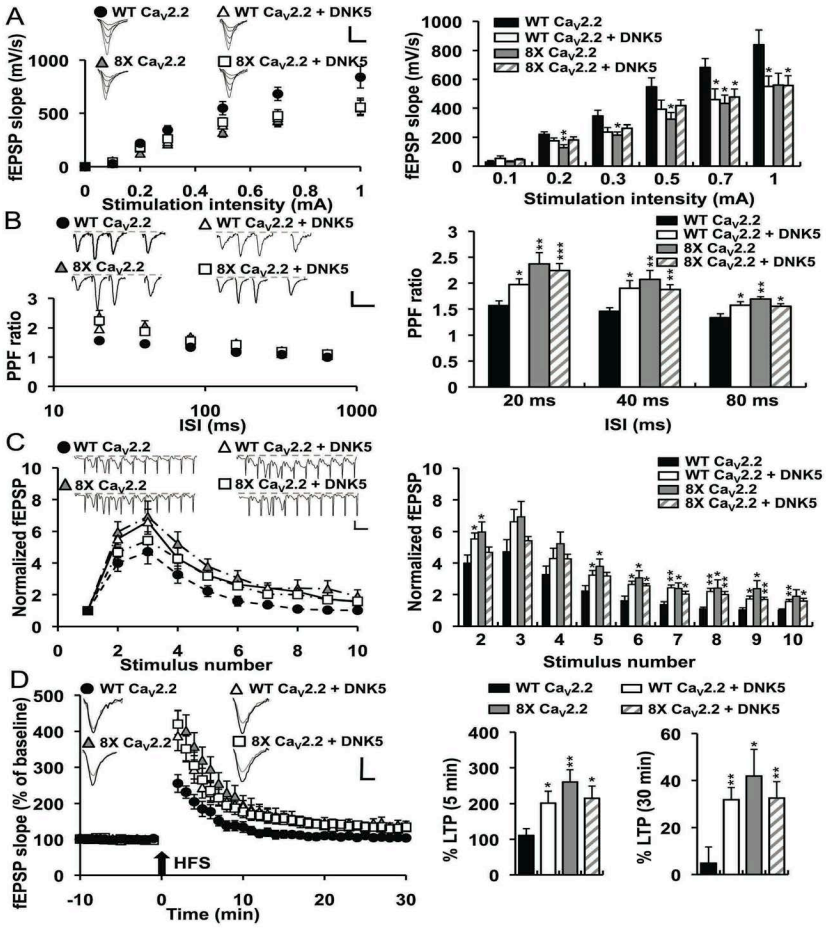

Figure 14. Synaptic plasticity measurements after co-expression of $Ca_v2.2$ and DNK5 HSV in hippocampus.

(A) Representative traces of the input/output curves in hippocampal slices transduced with WT $Ca_v2.2$, WT $Ca_v2.2$ and DNK5, 8X $Ca_v2.2$, or 8X $Ca_v2.2$ and DNK5 HSV. The enhanced basal synaptic transmission in slices expressing WT $Ca_v2.2$ HSV alone is abolished in the presence of DNK5 HSV. Scale bars, 0.5 mV, 10 ms. Right: quantification of the input/output curve. **(B)** Representative traces of the paired-pulse facilitation (PPF) response in hippocampal slices expressing WT $Ca_v2.2$, WT $Ca_v2.2$ and DNK5, 8X $Ca_v2.2$ or 8X $Ca_v2.2$ and DNK5 HSV. The decreased paired-pulse facilitation (PPF) ratio observed with the expression of WT $Ca_v2.2$ HSV alone is absent in slices co-expressing WT $Ca_v2.2$ and DNK5 HSV. Scale bars, 0.5 mV, 25 ms. Right: quantification of the PPF ratios at various stimulus intensities. **(C)** Representative traces and quantification of short-term facilitation during the 100 Hz stimulus at 0.5 mM $[Ca^{2+}]_o$. While hippocampal slices transduced with WT $Ca_V2.2$ HSV alone exhibited a significant reduction in synaptic facilitation during the 100 Hz stimulus train, the reduction in synaptic facilitation was not present in slices co-expressing WT $Ca_V2.2$ and DNK5 HSV. Scale bars, 0.5 mV, 10 ms. Right: quantification of the short-term plasticity at various stimuli. **(D)** Representative traces and quantification before and after HFS induction. In contrast to the markedly decreased fEPSP slope after expression of WT $Ca_V2.2$ HSV alone in hippocampal area CA3, there were no alterations in synaptic plasticity after co-injection of WT $Ca_V2.2$ and DNK5 HSV into hippocampal area CA3. In all experiments, there were no significant differences in plasticity measurements between slices expressing 8X $Ca_V2.2$ HSV alone and slices co-expressing 8X $Ca_V2.2$ and DNK5 HSV. Scale bars, 0.5 mV, 5 ms. Right: quantification of the fEPSP slope immediately following HFS (5 min) and at the end of the 30 min period. Data shown are means ± s.e.m. in **Table 9**. Statistical significance was calculated using one-way ANOVA (t-test) (*$p < 0.05$; **$p < 0.01$; ***$p < 0.001$).

Table 9. Values of electrophysiology experiments found in Figure 14

Measure	Condition	Value (mean± SEM)	n (slices/ mice)	p-value	Statistical test	Figure
Input/ output (0.1 mA)	WT $Ca_V2.2$ WT $Ca_V2.2$+DNK5 8X $Ca_V2.2$ 8X $Ca_V2.2$+DNK5	27.93±10.32 53.72±17.12 30.87±6.04 44.88±7.00	7/4 (1) 7/4 (2) 6/3 (3) 9/4 (4)	>0.05 (1 vs. 2) >0.05 (1 vs. 3) >0.05 (1 vs. 4) >0.05 (2 vs. 3) >0.05 (2 vs. 4) >0.05 (3 vs. 4)	One-way ANOVA	Fig. 14A
Input/ output (0.2 mA)	WT $Ca_V2.2$ WT $Ca_V2.2$+DNK5 8X $Ca_V2.2$ 8X $Ca_V2.2$+DNK5	219.89±18.03 175.70±19.80 127.80±21.09 181.76±21.35	7/4 (1) 7/4 (2) 6/3 (3) 9/4 (4)	>0.05 (1 vs. 2) <0.01 (1 vs. 3) >0.05 (1 vs. 4) >0.05 (2 vs. 3) >0.05 (2 vs. 4) >0.05 (3 vs. 4)	One-way ANOVA	Fig. 14A
Input/ output (0.3 mA)	WT $Ca_V2.2$ WT $Ca_V2.2$+DNK5 8X $Ca_V2.2$ 8X $Ca_V2.2$+DNK5	345.47±39.68 236.37±31.47 214.69±22.51 262.56±23.63	7/4 (1) 7/4 (2) 6/3 (3) 9/4 (4)	>0.05 (1 vs. 2) <0.05 (1 vs. 3) >0.05 (1 vs. 4) >0.05 (2 vs. 3) >0.05 (2 vs. 4) >0.05 (3 vs. 4)	One-way ANOVA	Fig. 14A
Input/ output (0.5 mA)	WT $Ca_V2.2$ WT $Ca_V2.2$+DNK5 8X $Ca_V2.2$ 8X $Ca_V2.2$+DNK5	547.59±62.87 392.30±63.23 323.20±46.24 417.45±39.84	7/4 (1) 7/4 (2) 6/3 (3) 9/4 (4)	>0.05 (1 vs. 2) <0.05 (1 vs. 3) >0.05 (1 vs. 4) >0.05 (2 vs. 3) >0.05 (2 vs. 4) >0.05 (3 vs. 4)	One-way ANOVA	Fig. 14A
Input/ output (0.7 mA)	WT $Ca_V2.2$ WT $Ca_V2.2$+DNK5 8X $Ca_V2.2$ 8X $Ca_V2.2$+DNK5	681.72±62.38 459.37±74.44 432.72±57.82 477.11±55.85	7/4 (1) 7/4 (2) 6/3 (3) 9/4 (4)	<0.05 (1 vs. 2) <0.05 (1 vs. 3) <0.05 (1 vs. 4) >0.05 (2 vs. 3) >0.05 (2 vs. 4) >0.05 (3 vs. 4)	One-way ANOVA	Fig. 14A
Input/ output (1 mA)	WT $Ca_V2.2$ WT $Ca_V2.2$+DNK5 8X $Ca_V2.2$ 8X $Ca_V2.2$+DNK5	839.40±102.20 550.57±71.87 559.80±82.26 556.93±67.74	7/4 (1) 7/4 (2) 6/3 (3) 9/4 (4)	<0.05 (1 vs. 2) >0.05 (1 vs. 3) <0.05 (1 vs. 4) >0.05 (2 vs. 3) >0.05 (2 vs. 4) >0.05 (3 vs. 4)	One-way ANOVA	Fig. 14A
PPF ratio (20 ms)	WT $Ca_V2.2$ WT $Ca_V2.2$+DNK5 8X $Ca_V2.2$ 8X $Ca_V2.2$+DNK5	1.57±0.09 1.97±0.11 2.37±0.22 2.24±0.14	7/4 (1) 7/4 (2) 8/4 (3) 10/4 (4)	<0.05 (1 vs. 2) <0.01 (1 vs. 3) <0.001 (1 vs. 4) >0.05 (2 vs. 3) >0.05 (2 vs. 4) >0.05 (3 vs. 4)	One-way ANOVA	Fig. 14B
PPF ratio	WT $Ca_V2.2$	1.46±0.07	7/4 (1)	<0.05 (1 vs. 2)	One-way	Fig.

(40 ms)	WT $Ca_V2.2$+DNK5 8X $Ca_V2.2$ 8X $Ca_V2.2$+DNK5	1.90±0.15 2.07±0.17 1.88±0.09	7/4 (2) 8/4 (3) 10/4 (4)	<0.01 (1 vs. 3) <0.01 (1 vs. 4) >0.05 (2 vs. 3) >0.05 (2 vs. 4) >0.05 (3 vs. 4)	ANOVA	14B
PPF ratio (80 ms)	WT $Ca_V2.2$ WT $Ca_V2.2$+DNK5 8X $Ca_V2.2$ 8X $Ca_V2.2$+DNK5	1.34±0.07 1.57±0.07 1.69±0.05 1.55±0.05	7/4 (1) 7/4 (2) 8/4 (3) 10/4 (4)	<0.05 (1 vs. 2) <0.01 (1 vs. 3) <0.05 (1 vs. 4) >0.05 (2 vs. 3) >0.05 (2 vs. 4) >0.05 (3 vs. 4)	One-way ANOVA	Fig. 14B
STP 100 Hz Stim. 2	WT $Ca_V2.2$ WT $Ca_V2.2$+DNK5 8X $Ca_V2.2$ 8X $Ca_V2.2$+DNK5	3.99±0.52 5.53±0.38 5.97±0.64 4.68±0.34	7/4 (1) 5/3 (2) 8/4 (3) 9/4 (4)	>0.05 (1 vs. 2) <0.05 (1 vs. 3) <0.05 (1 vs. 4) >0.05 (2 vs. 3) >0.05 (2 vs. 4) >0.05 (3 vs. 4)	One-way ANOVA	Fig. 14C
STP 100 Hz Stim. 3	WT $Ca_V2.2$ WT $Ca_V2.2$+DNK5 8X $Ca_V2.2$ 8X $Ca_V2.2$+DNK5	4.72±0.77 6.62±0.79 6.94±0.96 5.42±0.26	7/4 (1) 5/3 (2) 8/4 (3) 9/4 (4)	>0.05 (1 vs. 2) >0.05 (1 vs. 3) >0.05 (1 vs. 4) >0.05 (2 vs. 3) >0.05 (2 vs. 4) >0.05 (3 vs. 4)	One-way ANOVA	Fig. 14C
STP 100 Hz Stim. 4	WT $Ca_V2.2$ WT $Ca_V2.2$+DNK5 8X $Ca_V2.2$ 8X $Ca_V2.2$+DNK5	3.26±0.54 4.29±0.65 5.23±0.74 4.27±0.29	7/4 (1) 5/3 (2) 8/4 (3) 9/4 (4)	>0.05 (1 vs. 2) >0.05 (1 vs. 3) >0.05 (1 vs. 4) >0.05 (2 vs. 3) >0.05 (2 vs. 4) >0.05 (3 vs. 4)	One-way ANOVA	Fig. 14C
STP 100 Hz Stim. 5	WT $Ca_V2.2$ WT $Ca_V2.2$+DNK5 8X $Ca_V2.2$ 8X $Ca_V2.2$+DNK5	2.22±0.34 3.23±0.30 3.79±0.47 3.17±0.23	7/4 (1) 5/3 (2) 8/4 (3) 9/4 (4)	<0.05 (1 vs. 2) <0.05 (1 vs. 3) >0.05 (1 vs. 4) >0.05 (2 vs. 3) >0.05 (2 vs. 4) >0.05 (3 vs. 4)	One-way ANOVA	Fig. 14C
STP 100 Hz Stim. 6	WT $Ca_V2.2$ WT $Ca_V2.2$+DNK5 8X $Ca_V2.2$ 8X $Ca_V2.2$+DNK5	1.60±0.30 2.64±0.21 3.06±0.46 2.55±.013	7/4 (1) 5/3 (2) 8/4 (3) 9/4 (4)	<0.05 (1 vs. 2) <0.05 (1 vs. 3) <0.05 (1 vs. 4) >0.05 (2 vs. 3) >0.05 (2 vs. 4) >0.05 (3 vs. 4)	One-way ANOVA	Fig. 14C
STP 100 Hz Stim. 7	WT $Ca_V2.2$ WT $Ca_V2.2$+DNK5 8X $Ca_V2.2$ 8X $Ca_V2.2$+DNK5	1.37±0.18 2.42±0.18 2.38±0.36 2.02±0.18	7/4 (1) 5/3 (2) 8/4 (3) 9/4 (4)	<0.01 (1 vs. 2) <0.05 (1 vs. 3) <0.05 (1 vs. 4) >0.05 (2 vs. 3) >0.05 (2 vs. 4) >0.05 (3 vs. 4)	One-way ANOVA	Fig. 14C
STP 100 Hz Stim. 8	WT $Ca_V2.2$ WT $Ca_V2.2$+DNK5 8X $Ca_V2.2$	1.11±0.11 2.19±0.20 2.40±0.53	7/4 (1) 5/3 (2) 8/4 (3)	<0.01 (1 vs. 2) <0.05 (1 vs. 3) <0.01 (1 vs. 4)	One-way ANOVA	Fig. 14C

	8X $Ca_V2.2$+DNK5	2.00±0.19	9/4 (4)	>0.05 (2 vs. 3) >0.05 (2 vs. 4) >0.05 (3 vs. 4)		
STP 100 Hz Stim. 9	WT $Ca_V2.2$ WT $Ca_V2.2$+DNK5 8X $Ca_V2.2$ 8X $Ca_V2.2$+DNK5	1.04±0.14 1.71±0.19 2.37±0.51 1.69±0.14	7/4 (1) 5/3 (2) 8/4 (3) 9/4 (4)	<0.05 (1 vs. 2) <0.05 (1 vs. 3) <0.01 (1 vs. 4) >0.05 (2 vs. 3) >0.05 (2 vs. 4) >0.05 (3 vs. 4)	One-way ANOVA	Fig. 14C
STP 100 Hz Stim. 10	WT $Ca_V2.2$ WT $Ca_V2.2$+DNK5 8X $Ca_V2.2$ 8X $Ca_V2.2$+DNK5	1.02±0.08 1.57±0.12 1.88±0.42 1.59±0.17	7/4 (1) 5/3 (2) 8/4 (3) 9/4 (4)	<0.01 (1 vs. 2) >0.05 (1 vs. 3) <0.05 (1 vs. 4) >0.05 (2 vs. 3) >0.05 (2 vs. 4) >0.05 (3 vs. 4)	One-way ANOVA	Fig. 14C
fEPSP slope (first 5 min)	WT $Ca_V2.2$ WT $Ca_V2.2$+DNK5 8X $Ca_V2.2$ 8X $Ca_V2.2$+DNK5	210.60±19.40 301.66±32.89 360.04±34.49 315.30±33.27	10/5 (1) 8/5 (2) 10/5 (3) 12/5 (4)	<0.05 (1 vs. 2) <0.01 (1 vs. 3) <0.05 (1 vs. 4) >0.05 (2 vs. 3) >0.05 (2 vs. 4) >0.05 (3 vs. 4)	One-way ANOVA	Fig. 14D
fEPSP slope (last 5 min)	WT $Ca_V2.2$ WT $Ca_V2.2$+DNK5 8X $Ca_V2.2$ 8X $Ca_V2.2$+DNK5	104.80±6.93 131.91±5.07 141.85±11.38 132.62±6.87	10/5 (1) 8/5 (2) 10/5 (3) 12/5 (4)	<0.01 (1 vs. 2) <0.05 (1 vs. 3) <0.01 (1 vs. 4) >0.05 (2 vs. 3) >0.05 (2 vs. 4) >0.05 (3 vs. 4)	One-way ANOVA	Fig. 14D

Cdk5-mediated phosphorylation of N-type calcium channels impacts presynaptic plasticity

To explore whether Cdk5-mediated phosphorylation of $Ca_V2.2$ affects synaptic facilitation, another form of presynaptic plasticity, we applied different stimulus trains to the Schaffer collateral pathway. Synaptic facilitation did not differ between slices expressing GFP and 8X $Ca_V2.2$ HSV. As predicted for neurons with lower PPF, and therefore a higher release probability, slices expressing WT $Ca_V2.2$ HSV exhibited a reduction in transient facilitation elicited during the stimulation (100 Hz at 0.5 mM $[Ca^{2+}]_o$) (**Figure 13C**). Moreover, the facilitation in slices expressing WT $Ca_V2.2$ HSV alone was absent when DNK5 HSV was co-expressed with WT $Ca_V2.2$ HSV, demonstrating the requirement of Cdk5 activity for $Ca_V2.2$-mediated synaptic facilitation (**Figure 14C**).

We next examined short-term synaptic plasticity elicited by high-frequency stimuli (HFS). Compared to slices transduced with GFP HSV, there was a strong reduction in the initial fEPSP slope following HFS in slices transduced with WT $Ca_V2.2$ HSV (**Figure 13D**). There were no differences in initial fEPSP slope between slices expressing GFP and 8X $Ca_V2.2$ HSV. Early-phase long-term potentiation (LTP), measured at 30 min post-stimulation, was also considerably reduced in slices expressing WT $Ca_V2.2$ HSV when compared to slices expressing GFP HSV (**Figure 13D**). However, the altered plasticity in slices expressing WT $Ca_V2.2$ HSV alone was not observed with co-expression of DNK5 HSV (**Figure 14D**). In all experiments, there were no significant differences in plasticity measurements between slices expressing 8X $Ca_V2.2$ HSV alone and slices co-expressing 8X $Ca_V2.2$ and DNK5 HSV (**Figure 14A-D**). Collectively, these results demonstrate that Cdk5-mediated phosphorylation of WT $Ca_V2.2$ increases basal synaptic transmission and enhances presynaptic release probability, which in turn decreases synaptic facilitation and early-phase LTP.

Discussion

Here we demonstrated that the N-type calcium channel ($Ca_V2.2$) is a Cdk5 substrate. Phosphorylation of $Ca_V2.2$ by Cdk5 significantly increased calcium current density and channel open probability. We further showed that the interaction between $Ca_V2.2$ and RIM1 was modulated by Cdk5, which provided a molecular mechanism for the increased number of docked vesicles at the presynaptic terminal in neurons expressing $Ca_V2.2$. We also found presynaptic alterations in plasticity associated with Cdk5-mediated phosphorylation of $Ca_V2.2$ that included enhanced basal synaptic transmission, enhanced presynaptic release probability, and an overall reduction in short-term facilitation. Importantly, these effects were not observed with the Cdk5 phosphorylation mutant 8X $Ca_V2.2$, either alone or in the presence of Cdk5. Taken together, these studies demonstrate a pivotal role for Cdk5-mediated post-translational modifications of the N-type calcium channel in regulating presynaptic function, and highlight the close interaction between kinases and calcium channels in neurons.

Protein kinases that impact calcium channel function

While this study is the first to show that $Ca_V2.2$ is a Cdk5 substrate, previous work has implicated several kinases in the modulation of voltage-gated calcium channels (Bannister et al., 2005). The calcium-calmodulin kinase II (CaMKII) interacts with the P/Q-type calcium channel to facilitate transmitter release (Jiang et al., 2008), and the glycogen synthase kinase (GSK3β) phosphorylates the P/Q-type calcium channel in the intracellular II-III loop (Zhu et al., 2010) to inhibit vesicle exocytosis by disrupting SNARE complex formation. Other kinases that target $Ca_V2.2$ include protein kinases A and C (PKA and PKC), and both PKA- and PKC-mediated phosphorylation of $Ca_V2.2$ inhibit $Ca_V2.2$ interaction with SNARE complexes (Yokoyama et al., 1997). PKC-mediated phosphorylation of $Ca_V2.2$ also enhances N-type calcium current by reducing the G-protein inhibition of $Ca_V2.2$ (Swartz et al., 1993). Furthermore, PKC phosphorylation of $Ca_V2.2$ in the I-II linker region reduces the inhibitory effect of the Gβγ subunits on $Ca_V2.2$ (Zamponi et al., 1997). Notably, the $Ca_V2.2$ N-terminus, together with the I-II region, plays a fundamental role in modulating Gβγ inhibition (Agler et al., 2005). Altogether, these results provide a complex representation of signaling pathways involving kinases, second messengers such as Gβγ subunits, and synaptic release machinery such as SNARE proteins leading up to neurotransmitter release.

Pharmacological inhibition of Cdk5 using roscovitine was previously used to examine calcium channel function (Tomizawa et al., 2002). However, in addition to inhibiting Cdk5, roscovitine is an inhibitor of cyclin-dependent kinases 1, 2, 5, and 7 (Bach et al., 2005) and also acts directly on calcium channels by binding to the extracellular domain of L-type calcium channels (Yarotskyy and Elmslie, 2007). Furthermore, extracellular roscovitine application potentiates (P/Q-type) $Ca_V2.1$-mediated neurotransmitter release to slow deactivation kinetics (Yan et al., 2002) and increase the inactivation of $Ca_V2.2$ (Buraei et al., 2005). This may account for the differences observed between our study and a previous study demonstrating fEPSP enhancement following roscovitine application on hippocampal slices, which preferentially affected P/Q-type calcium channels (Tomizawa et al., 2002). Therefore, in our efforts to understand how $Ca_V2.2$ is regulated at the presynaptic terminal, we examined the regulation of $Ca_V2.2$ in the context of endogenous Cdk5 activity in neurons and inhibited Cdk5 with a dominant-negative Cdk5 virus rather than using roscovitine.

Regulation of protein-protein interactions and presynaptic plasticity by Cdk5

Our findings also revealed a role for Cdk5-mediated phosphorylation of $Ca_V2.2$ in modulating the interactions of $Ca_V2.2$ with various active zone proteins, including RIM1, to regulate neurotransmission and presynaptic plasticity. It was previously reported that RIM1 binds the auxiliary β subunit of both N-type and P/Q-type calcium channels to facilitate calcium influx and tether vesicles to the presynaptic terminal (Kiyonaka et al., 2007). Intriguingly, RIM1 also further reduces the G-protein-mediated inhibition of $Ca_V2.2$, which subsequently contributes to a prolonged increase in calcium influx (Weiss et al., 2011). As RIM1 is required for calcium channel density and vesicle docking at the active zone of calyx of Held synapses and central synapses (Han et al., 2011; Kaeser et al., 2011), our results are consistent with the notion that the $Ca_V2.2$ interaction with RIM1 allows for coordinated transmitter release, and we propose that this interaction is regulated in part by Cdk5-mediated phosphorylation of $Ca_V2.2$.

$Ca_V2.2$ and RIM1 are both closely associated with other active zone proteins and SNARE complexes. In this study, we examined the binding of $Ca_V2.2$ to a number of presynaptic proteins, and showed that RIM binding increased in neurons expressing WT $Ca_V2.2$ HSV. Several groups previously reported a direct interaction between RIM1, or the RIM1 binding protein (RIMBP), and $Ca_V2.2$ (Coppola et al., 2001; Hibino et al., 2002; Kaeser et al., 2011).

However, our results differ from other reports that RIM1 does not bind $Ca_V2.2$, even though both localize to the presynaptic terminal (Khanna et al., 2006; Khanna et al., 2007b). A possible explanation might be the previous use of an antibody targeting the synprint region of chicken $Ca_V2.2$ (Li et al., 2004), even though one study was conducted on rat brain preparations (Khanna et al., 2007a). The chicken synprint region shares only about 59% homology to the mouse and rat synprint regions, which share 88% homology with each other. Therefore, the different antibodies that were used might explain the discrepancies between our findings and those published previously.

Although we did not observe a decrease in $Ca_V2.2$ binding to Syntaxin1A in primary neurons, in contrast to our Cdk5 cKO samples, we hypothesize that acute manipulations differ from chronic Cdk5 knockdown *in vivo*, which may in turn directly or indirectly affect the interaction of $Ca_V2.2$ with various SNARE proteins to alter neurotransmission. We also cannot exclude the possibility that other kinases, such as PKA, may phosphorylate $Ca_V2.2$ at similar residues and promote similar functions. It is also possible that the β or the α2δ auxiliary subunits, which also modulate calcium channel function and have previously been shown to be regulated by phosphorylation (Viard et al., 2004), are additional Cdk5 substrates that can modify $Ca_V2.2$ and SNARE protein interactions.

We demonstrated that Cdk5 impacts $Ca_V2.2$ channel availability and channel open probability. It will be intriguing to further elucidate how Cdk5-mediated phosphorylation of $Ca_V2.2$ may result in conformational alterations between the α_1 subunit and other channel subunits, or potentially with the pore-forming domain, to influence channel gating properties. In line with previous reports, overexpression of $Ca_V2.2$ did not affect the $Ca_V2.1$ (P/Q-type calcium channel) current (Cao and Tsien, 2010). However, in our study, acute slices expressing WT $Ca_V2.2$ HSV exhibited decreased PPF, which is in agreement with some previous findings (Ahmed and Siegelbaum, 2009), but in contrast to others where no alterations in PPF were observed (Cao and Tsien, 2010). This may be due to differences in Schaffer collateral field recordings versus single-cell recordings of dissociated hippocampal neurons. Thus, in future studies it will be important to further probe how Cdk5-mediated phosphorylation of $Ca_V2.2$ affects its contribution to excitatory postsynaptic currents. As Cdk5 and $Ca_V2.2$ are present in GABAergic interneurons (Poncer et al., 1997; Rakic et al., 2009), it would also be interesting to determine whether Cdk5 differentially affects excitatory and inhibitory neurotransmission.

The role of Cdk5 in homeostatic mechanisms

Combined with previous studies, our data suggest that both $Ca_V2.2$ and Cdk5 mediate presynaptic plasticity by regulating neurotransmitter release. Recent literature suggests that Cdk5 is a central regulator of synaptic homeostasis. Cdk5 activity is required for the downregulation of heightened synaptic activity via phosphorylation of the postsynaptic protein SPAR. This priming effect allows polo-like kinase 2 to promote the degradation of SPAR during homeostatic scaling (Seeburg et al., 2008). Cdk5 also serves as a control point for neurotransmission, as inhibition of Cdk5 activity by roscovitine results in access to the resting synaptic vesicle pool (Kim and Ryan, 2010). Furthermore, Cdk5 activity is critical for the presynaptic adaptation of hippocampal CA3 recurrent circuitry under chronic inactivity, as it mediates reduced connectivity after silencing synapses but enhances synaptic strength of the remaining connections (Mitra et al., 2011). Precisely how Cdk5 levels, and Cdk5/p35 activity, are regulated under physiological or excitotoxic conditions to impart its action on $Ca_V2.2$ in specific cell populations remains an exciting topic for future work, which may also reveal additional $Ca_V2.2$ binding partners as well as Cdk5 substrates that play a vital role in synaptic homeostasis.

In summary, our data demonstrate a previously uncharacterized interaction between $Ca_V2.2$ and Cdk5 that results in a Cdk5-mediated increase in $Ca_V2.2$ current density, channel open probability, and altered $Ca_V2.2$ interaction with the active zone protein RIM1 to ultimately affect neurotransmission and plasticity by promoting vesicle docking and release. These findings provide a framework to examine how $Ca_V2.2$ is regulated in the context of endogenous Cdk5 activity. Given the significant implications of Cdk5 in synaptic homeostasis, a compelling question is how post-translational modifications of $Ca_V2.2$ impact its interactions with other key presynaptic proteins involved in vesicle docking, neurotransmission, and plasticity.

References

Agler, H.L., Evans, J., Tay, L.H., Anderson, M.J., Colecraft, H.M., and Yue, D.T. (2005). G protein-gated inhibitory module of N-type (ca(v)2.2) ca2+ channels. Neuron *46*, 891-904.

Ahmed, M.S., and Siegelbaum, S.A. (2009). Recruitment of N-Type Ca(2+) channels during LTP enhances low release efficacy of hippocampal CA1 perforant path synapses. Neuron *63*, 372-385.

Bach, S., Knockaert, M., Reinhardt, J., Lozach, O., Schmitt, S., Baratte, B., Koken, M., Coburn, S.P., Tang, L., Jiang, T.*, et al.* (2005). Roscovitine targets, protein kinases and pyridoxal kinase. J Biol Chem *280*, 31208-31219.

Bannister, R.A., Mezu, U., and Adams, S. (2005). Phosphorylation-dependent voltage-gated Ca2+ channels, Gerald Zamponi, ed. (Kluwer Academic / Plenum Publishers), pp. 168-182.

Brittain, J.M., Piekarz, A.D., Wang, Y., Kondo, T., Cummins, T.R., and Khanna, R. (2009). An atypical role for collapsin response mediator protein 2 (CRMP-2) in neurotransmitter release via interaction with presynaptic voltage-gated calcium channels. J Biol Chem *284*, 31375-31390.

Buraei, Z., Anghelescu, M., and Elmslie, K.S. (2005). Slowed N-type calcium channel (CaV2.2) deactivation by the cyclin-dependent kinase inhibitor roscovitine. Biophys J *89*, 1681-1691.

Cao, Y.Q., and Tsien, R.W. (2010). Different relationship of N- and P/Q-type Ca2+ channels to channel-interacting slots in controlling neurotransmission at cultured hippocampal synapses. J Neurosci *30*, 4536-4546.

Catterall, W.A., and Few, A.P. (2008). Calcium channel regulation and presynaptic plasticity. Neuron *59*, 882-901.

Chae, T., Kwon, Y.T., Bronson, R., Dikkes, P., Li, E., and Tsai, L.H. (1997). Mice lacking p35, a neuronal specific activator of Cdk5, display cortical lamination defects, seizures, and adult lethality. Neuron *18*, 29-42.

Cheung, Z.H., Chin, W.H., Chen, Y., Ng, Y.P., and Ip, N.Y. (2007). Cdk5 is involved in BDNF-stimulated dendritic growth in hippocampal neurons. PLoS Biol *5*, e63.

Coppola, T., Magnin-Luthi, S., Perret-Menoud, V., Gattesco, S., Schiavo, G., and Regazzi, R. (2001). Direct interaction of the Rab3 effector RIM with Ca2+ channels, SNAP-25, and synaptotagmin. J Biol Chem *276*, 32756-32762.

Dobrunz, L.E., and Stevens, C.F. (1997). Heterogeneity of release probability, facilitation, and depletion at central synapses. Neuron *18*, 995-1008.

Fu, W.Y., Chen, Y., Sahin, M., Zhao, X.S., Shi, L., Bikoff, J.B., Lai, K.O., Yung, W.H., Fu, A.K., Greenberg, M.E.*, et al.* (2007). Cdk5 regulates EphA4-mediated dendritic spine retraction through an ephexin1-dependent mechanism. Nat Neurosci *10*, 67-76.

Guan, J.S., Su, S.C., Gao, J., Joseph, N., Xie, Z., Zhou, Y., Durak, O., Zhang, L., Zhu, J.J., Clauser, K.R.*, et al.* (2011). Cdk5 Is Required for Memory Function and Hippocampal Plasticity via the cAMP Signaling Pathway. PLoS One *6*, e25735.

Han, J.H., Kushner, S.A., Yiu, A.P., Cole, C.J., Matynia, A., Brown, R.A., Neve, R.L., Guzowski, J.F., Silva, A.J., and Josselyn, S.A. (2007). Neuronal competition and selection during memory formation. Science *316*, 457-460.

Han, Y., Kaeser, P.S., Sudhof, T.C., and Schneggenburger, R. (2011). RIM determines Ca(2)+ channel density and vesicle docking at the presynaptic active zone. Neuron *69*, 304-316.

Hibino, H., Pironkova, R., Onwumere, O., Vologodskaia, M., Hudspeth, A.J., and Lesage, F. (2002). RIM binding proteins (RBPs) couple Rab3-interacting molecules (RIMs) to voltage-gated Ca(2+) channels. Neuron *34*, 411-423.

Jahn, R., Lang, T., and Sudhof, T.C. (2003). Membrane fusion. Cell *112*, 519-533.

Jiang, X., Lautermilch, N.J., Watari, H., Westenbroek, R.E., Scheuer, T., and Catterall, W.A. (2008). Modulation of CaV2.1 channels by Ca2+/calmodulin-dependent protein kinase II bound to the C-terminal domain. Proc Natl Acad Sci U S A *105*, 341-346.

Kaeser, P.S., Deng, L., Wang, Y., Dulubova, I., Liu, X., Rizo, J., and Sudhof, T.C. (2011). RIM proteins tether Ca2+ channels to presynaptic active zones via a direct PDZ-domain interaction. Cell *144*, 282-295.

Khanna, R., Li, Q., Bewersdorf, J., and Stanley, E.F. (2007a). The presynaptic CaV2.2 channel-transmitter release site core complex. Eur J Neurosci *26*, 547-559.

Khanna, R., Li, Q., Sun, L., Collins, T.J., and Stanley, E.F. (2006). N type Ca2+ channels and RIM scaffold protein covary at the presynaptic transmitter release face but are components of independent protein complexes. Neuroscience *140*, 1201-1208.

Khanna, R., Zougman, A., and Stanley, E.F. (2007b). A proteomic screen for presynaptic terminal N-type calcium channel (CaV2.2) binding partners. J Biochem Mol Biol *40*, 302-314.

Kim, S.H., and Ryan, T.A. (2010). CDK5 serves as a major control point in neurotransmitter release. Neuron *67*, 797-809.

Kiyonaka, S., Wakamori, M., Miki, T., Uriu, Y., Nonaka, M., Bito, H., Beedle, A.M., Mori, E., Hara, Y., De Waard, M.*, et al.* (2007). RIM1 confers sustained activity and neurotransmitter vesicle anchoring to presynaptic Ca2+ channels. Nat Neurosci *10*, 691-701.

Lai, M., Wang, F., Rohan, J.G., Maeno-Hikichi, Y., Chen, Y., Zhou, Y., Gao, G., Sather, W.A., and Zhang, J.F. (2005). A tctex1-Ca2+ channel complex for selective surface expression of Ca2+ channels in neurons. Nat Neurosci *8*, 435-442.

Lee, M.S., Kwon, Y.T., Li, M., Peng, J., Friedlander, R.M., and Tsai, L.H. (2000). Neurotoxicity induces cleavage of p35 to p25 by calpain. Nature *405*, 360-364.

Leenders, A.G., Lin, L., Huang, L.D., Gerwin, C., Lu, P.H., and Sheng, Z.H. (2008). The role of MAP1A light chain 2 in synaptic surface retention of Cav2.2 channels in hippocampal neurons. J Neurosci *28*, 11333-11346.

Li, Q., Lau, A., Morris, T.J., Guo, L., Fordyce, C.B., and Stanley, E.F. (2004). A syntaxin 1, Galpha(o), and N-type calcium channel complex at a presynaptic nerve terminal: analysis by quantitative immunocolocalization. J Neurosci *24*, 4070-4081.

Lin, Y., McDonough, S.I., and Lipscombe, D. (2004). Alternative splicing in the voltage-sensing region of N-Type CaV2.2 channels modulates channel kinetics. J Neurophysiol *92*, 2820-2830.

Lobo, M.K., Covington, H.E., 3rd, Chaudhury, D., Friedman, A.K., Sun, H., Damez-Werno, D., Dietz, D.M., Zaman, S., Koo, J.W., Kennedy, P.J.*, et al.* (2010). Cell type-specific loss of BDNF signaling mimics optogenetic control of cocaine reward. Science *330*, 385-390.

Luebke, J.I., Dunlap, K., and Turner, T.J. (1993). Multiple calcium channel types control glutamatergic synaptic transmission in the hippocampus. Neuron *11*, 895-902.

Maximov, A., and Bezprozvanny, I. (2002). Synaptic targeting of N-type calcium channels in hippocampal neurons. J Neurosci *22*, 6939-6952.

Mitra, A., Mitra, S.S., and Tsien, R.W. (2011). Heterogeneous reallocation of presynaptic efficacy in recurrent excitatory circuits adapting to inactivity. Nat Neurosci.

Murthy, V.N., Sejnowski, T.J., and Stevens, C.F. (1997). Heterogeneous release properties of visualized individual hippocampal synapses. Neuron *18*, 599-612.

Neve, R.L., Neve, K.A., Nestler, E.J., and Carlezon, W.A., Jr. (2005). Use of herpes virus amplicon vectors to study brain disorders. Biotechniques *39*, 381-391.

Ohshima, T., Ward, J.M., Huh, C.G., Longenecker, G., Veeranna, Pant, H.C., Brady, R.O., Martin, L.J., and Kulkarni, A.B. (1996). Targeted disruption of the cyclin-dependent kinase 5 gene results in abnormal corticogenesis, neuronal pathology and perinatal death. Proc Natl Acad Sci U S A *93*, 11173-11178.

Patrick, G.N., Zukerberg, L., Nikolic, M., de la Monte, S., Dikkes, P., and Tsai, L.H. (1999). Conversion of p35 to p25 deregulates Cdk5 activity and promotes neurodegeneration. Nature *402*, 615-622.

Paxinos, G., and Franklin, K.B.J. (2001). The mouse brain in stereotaxic coordinates (San Diego: Academic Press), 2nd ed.

Poncer, J.C., McKinney, R.A., Gahwiler, B.H., and Thompson, S.M. (1997). Either N- or P-type calcium channels mediate GABA release at distinct hippocampal inhibitory synapses. Neuron *18*, 463-472.

Rakic, S., Yanagawa, Y., Obata, K., Faux, C., Parnavelas, J.G., and Nikolic, M. (2009). Cortical interneurons require p35/Cdk5 for their migration and laminar organization. Cereb Cortex *19*, 1857-1869.

Samuels, B.A., Hsueh, Y.P., Shu, T., Liang, H., Tseng, H.C., Hong, C.J., Su, S.C., Volker, J., Neve, R.L., Yue, D.T.*, et al.* (2007). Cdk5 promotes synaptogenesis by regulating the subcellular distribution of the MAGUK family member CASK. Neuron *56*, 823-837.

Seeburg, D.P., Feliu-Mojer, M., Gaiottino, J., Pak, D.T., and Sheng, M. (2008). Critical role of CDK5 and Polo-like kinase 2 in homeostatic synaptic plasticity during elevated activity. Neuron *58*, 571-583.

Sheng, Z.H., Rettig, J., Takahashi, M., and Catterall, W.A. (1994). Identification of a syntaxin-binding site on N-type calcium channels. Neuron *13*, 1303-1313.

Sheng, Z.H., Westenbroek, R.E., and Catterall, W.A. (1998). Physical link and functional coupling of presynaptic calcium channels and the synaptic vesicle docking/fusion machinery. J Bioenerg Biomembr *30*, 335-345.

Snutch, T.P. (2005). Targeting chronic and neuropathic pain: the N-type calcium channel comes of age. NeuroRx *2*, 662-670.

Su, S.C., and Tsai, L.H. (2011). Cyclin-dependent kinases in brain development and disease. Annu Rev Cell Dev Biol *27*, 465-491.

Swartz, K.J., Merritt, A., Bean, B.P., and Lovinger, D.M. (1993). Protein kinase C modulates glutamate receptor inhibition of Ca2+ channels and synaptic transmission. Nature *361*, 165-168.

Tan, T.C., Valova, V.A., Malladi, C.S., Graham, M.E., Berven, L.A., Jupp, O.J., Hansra, G., McClure, S.J., Sarcevic, B., Boadle, R.A.*, et al.* (2003). Cdk5 is essential for synaptic vesicle endocytosis. Nat Cell Biol *5*, 701-710.

Tomizawa, K., Ohta, J., Matsushita, M., Moriwaki, A., Li, S.T., Takei, K., and Matsui, H. (2002). Cdk5/p35 regulates neurotransmitter release through phosphorylation and downregulation of P/Q-type voltage-dependent calcium channel activity. J Neurosci *22*, 2590-2597.

Tsai, L.H., Delalle, I., Caviness, V.S., Jr., Chae, T., and Harlow, E. (1994). p35 is a neural-specific regulatory subunit of cyclin-dependent kinase 5. Nature *371*, 419-423.

Viard, P., Butcher, A.J., Halet, G., Davies, A., Nurnberg, B., Heblich, F., and Dolphin, A.C. (2004). PI3K promotes voltage-dependent calcium channel trafficking to the plasma membrane. Nat Neurosci *7*, 939-946.

Weiss, N., Sandoval, A., Kyonaka, S., Felix, R., Mori, Y., and De Waard, M. (2011). Rim1 modulates direct G-protein regulation of Ca(v)2.2 channels. Pflugers Arch *461*, 447-459.

Westenbroek, R.E., Hell, J.W., Warner, C., Dubel, S.J., Snutch, T.P., and Catterall, W.A. (1992). Biochemical properties and subcellular distribution of an N-type calcium channel alpha 1 subunit. Neuron *9*, 1099-1115.

Wheeler, D.B., Randall, A., and Tsien, R.W. (1994). Roles of N-type and Q-type Ca2+ channels in supporting hippocampal synaptic transmission. Science *264*, 107-111.

Yan, Z., Chi, P., Bibb, J.A., Ryan, T.A., and Greengard, P. (2002). Roscovitine: a novel regulator of P/Q-type calcium channels and transmitter release in central neurons. J Physiol *540*, 761-770.

Yarotskyy, V., and Elmslie, K.S. (2007). Roscovitine, a cyclin-dependent kinase inhibitor, affects several gating mechanisms to inhibit cardiac L-type (Ca(V)1.2) calcium channels. Br J Pharmacol *152*, 386-395.

Yokoyama, C.T., Sheng, Z.H., and Catterall, W.A. (1997). Phosphorylation of the synaptic protein interaction site on N-type calcium channels inhibits interactions with SNARE proteins. J Neurosci *17*, 6929-6938.

Zamponi, G.W., Bourinet, E., Nelson, D., Nargeot, J., and Snutch, T.P. (1997). Crosstalk between G proteins and protein kinase C mediated by the calcium channel alpha1 subunit. Nature *385*, 442-446.

Zhu, L.Q., Liu, D., Hu, J., Cheng, J., Wang, S.H., Wang, Q., Wang, F., Chen, J.G., and Wang, J.Z. (2010). GSK-3 beta inhibits presynaptic vesicle exocytosis by phosphorylating P/Q-type calcium channel and interrupting SNARE complex formation. J Neurosci *30*, 3624-3633.

Zucker, R.S., and Regehr, W.G. (2002). Short-term synaptic plasticity. Annu Rev Physiol *64*, 355-405.

Chapter 4

Cdk5-mediated phosphorylation of Shank3 impacts dendritic spine morphology and synaptic plasticity

Summary

The postsynaptic scaffolding protein Shank3 is involved in excitatory transmission and has been implicated in autism spectrum disorders. Shank3 is present in postsynaptic densities of dendritic spines, where it promotes synapse formation and anchors various glutamate receptors to the synaptic cleft. Although Shank3 mutations are associated with autism spectrum disorders, how Shank3 is regulated by post-translational modifications remains unclear. Here we demonstrate Shank3 is a cyclin-dependent kinase (Cdk5) substrate and identified the key phosphorylation site as Serine 985. Using a molecular replacement strategy in primary neurons, we examined dendritic spine formation and synaptic plasticity after knockdown of endogenous Shank3 levels while simultaneously overexpressing a Shank3 S985A phosphorylation mutant. Our results suggest that Cdk5-mediated phosphorylation of Shank3 is important for maintenance of mature dendritic spines and is integral to facilitating synaptic plasticity, and provide insight to the regulation of the Shank3 protein by Cdk5.

I prepared samples for the phosphoproteomic screen, cloned Shank3 fragments into GST constructs, conducted the kinase assays, generated full-length Shank3 phosphorylation mutants, screened the shRNAs in heterologous cells, cloned Shank3 shRNA-resistant constructs, cloned the Shank3 constructs into viral vectors, cultured primary neurons, analyzed data after transducing neurons with virus, conducted biochemical experiments, and performed the stereotaxic injections.

Introduction

Autism spectrum disorders are thought to arise from a combination of genetic and environmental factors, which in turn contribute to the proper development and maturation of synaptic connections in the developing brain (Geschwind and Levitt, 2007). Moreover, an imbalance between excitatory and inhibitory transmission has been implicated in social interaction deficits in animal models (Han et al., 2012). Excitatory synapses are identified by their presynaptic terminals opposite a prominent, postsynaptic dendritic spine. The postsynaptic density of the dendritic spine is comprised of an abundant set of proteins that form tight multimeric complexes to mediate synaptic transmission (Kim and Sheng, 2004). Scaffolding molecules such as PSD-95, GRIP, and Homer anchor NMDA, AMPA, and metabotropic glutamate receptors to the surface of the dendritic spine to mediate synapse maturation and transmission (Brakeman et al., 1997; Dong et al., 1997; Kim et al., 1995).

Shank3 is part of a family of large, multi-domain scaffolding proteins that include Shank1 and Shank2, and they are highly homologous to each other and similar in structure (Naisbitt et al., 1999; Tu et al., 1999). Enriched in the synapse, Shank3 is regulated by multiple pathways, including dimerization and ubiquitination (Bangash et al., 2011; Hayashi et al., 2009) and participates in dendritic spine formation (Roussignol et al., 2005). However, other forms of post-translational modifications on Shank3 are not well-studied. Recent studies have linked de novo mutations in the SHANK3 and SHANK2 genes to autism spectrum disorders (Berkel et al., 2010; Durand et al., 2007). Intriguingly, Shank3 has also been associated with other psychiatric disorders including childhood schizophrenia (Gauthier et al., 2010). Different Shank3 knockout mouse models display a range of alterations including a reduction in the synaptic glutamate receptors (Wang et al., 2011), deficits in hippocampal long-term potentiation (Bozdagi et al., 2010) or striatal transmission (Peca et al., 2011), alterations in ultrasonic vocalization (Bozdagi et al., 2010), anxiety phenotypes (Peca et al., 2011), cognitive deficits (Wang et al., 2011), and deficits in social interaction (Peca et al., 2011). Additionally, Shank2 knockout mice exhibit hyperactivity, reduced dendritic spines, and deficits in LTP and cognition (Schmeisser et al., 2012; Won et al., 2012). Interestingly, however, Shank1 knockout mice exhibit smaller dendritic spines and reduced postsynaptic protein composition, but have enhanced spatial memory (Hung et al., 2008). Despite the availability of multiple mouse models, the regulation of Shank3 by post-translational modifications such as phosphorylation has not yet been explored.

The proline-directed serine/threonine kinase cyclin-dependent kinase 5 (Cdk5) is a key mediator in various aspects of neuronal function including cortical layering, axon guidance, and neuropathic pain. Multiple studies have identified Cdk5 as a regulator of synapse formation (Li et al., 2001; Lin et al., 2005; Samuels et al., 2007), synaptic transmission (Guan et al., 2011; Li et al., 2001), and homeostatic plasticity (Mitra et al., 2012; Seeburg et al., 2008). At the presynaptic terminal, Cdk5 plays a role in vesicle endocytosis (Tomizawa et al., 2003) and vesicle recycling pool to modulate neurotransmitter release (Kim and Ryan, 2010). At the postsynaptic density, Cdk5 has previously been demonstrated to regulate PSD-95 and NMDA receptor surface levels (Morabito et al., 2004; Zhang et al., 2008). Cdk5 requires its regulatory subunit, p35, for function; upon dysregulation and neurotoxic insults, p35 is cleaved to p25 to promote Cdk5 hyperactivity and subsequently disrupt cellular function and impair cognition (Cruz et al., 2003; Lee et al., 2000; Patrick et al., 1999). The collective studies underscore how Cdk5 is tightly regulated in the nervous system through its association with p35 and p25 under physiological and neurotoxic conditions.

In this study, we provide evidence that Shank3, a major postsynaptic scaffolding protein, is a Cdk5 substrate. Phosphorylation of Shank3 was mapped to a key residue at S985. Overexpression of the Shank3 S985A phosphorylation mutant in primary neurons resulted in a striking phenotype resembling acute knockdown of Shank3 that was partially reversed by overexpression of wild-type full-length Shank3. Synaptic plasticity experiments revealed a reduction in LTP after Shank3 knockdown, whereas overexpression of wild-type – and, unexpectedly, the S985A phosphorylation mutant – were able to restore LTP to control levels. Our collective results suggest that Shank3 phosphorylation by Cdk5 plays an important component in the maintenance of mature dendritic spines to ultimately affect synaptic plasticity.

Methods

Constructs

The rat Shank3 cDNA corresponding to GenBank accession number NM_021676 was a kind gift from Dr. Morgan Sheng (Genentech, USA) and cloned into GST-Shank3 fusion constructs using the pGEX4T2 vector (Phusion, NEB). The GST fragments were subdivided into the ankyrin (aa 1-400), SH3 (aa 401-540), PDZ (aa 541-667), proline-rich region (five fragments: aa 660-860, 861-1000, 1001-1147, 1148-1300, 1301-1500, 1301-1680), and SAM (aa 1600-1741) domains. Mutagenesis was conducted using QuickChange Lightning Kit (Stratagene) and verified by sequencing.

To generate GST fusion proteins, constructs were transformed into BL21 competent cells. After adding 0.2 mM IPTG to the growth medium to induce protein expression, cells were harvested by centrifugation, resuspended in TNT buffer (100 mM Tris-HCl [pH 8], 150 mM NaCl, 5 mM EDTA, 0.05% Tween-20), sonicated, and bound to Glutathione Sepharose 4B beads (Amersham Biosciences). The protein complex was loaded onto a chromatography column (Bio-Rad), washed with TNT buffer, and eluted using glutathione buffer (200 mM Tris [pH 8], 0.1% Triton-X 100, 15 mM glutathione). Following de-salting and concentration of the eluate using high-speed centrifugation and cellulose filter units (Centricon, Millipore), the final protein concentration was assayed using the Bradford Protein Assay (Bio-Rad). Reagents were purchased from Sigma.

Viral vectors

Full-length mouse Shank3 cDNA corresponding to GenBank accession number NM_021423 was a generous gift from Dr. Shigeo Uchino (Tokyo, Japan). Vectors containing Shank3 shRNAs were obtained for screening (Open Biosystems). Both Shank3 shRNA and the full-length, shRNA-resistant Shank3 construct were cloned into the herpes simplex virus vector p1006+ (a gift from Dr. Rachael L. Neve). Simultaneous knockdown of Shank3 was achieved by the HSV vector co-expressing a Shank3 shRNA under the CMV promoter and a full-length shRNA-resistant wild-type Shank3 or phosphorylation mutant S985A Shank3 under the I/E 4/5 promoter. HSVs were packaged according to the standard protocol (Neve et al., 2005) and contained scrambled shRNA, Shank3 shRNA, Shank3 shRNA + wild-type shRNA-resistant Shank3 or Shank3 shRNA + S985A full-length shRNA-resistant phosphomutant Shank3.

In vitro kinase assay

Kinase assays were conducted by co-incubating Cdk5/p25 active kinase (Cell Signaling) with 10-20 μg of purified GST protein fused with various Shank3 fragments diluted in kinase buffer (30 mM HEPES [pH 7.2], 10 mM $MgCl_2$, 5 mM $MnCl_2$, 100 mM ATP, 5 mCi [32P] γATP (Perkin-Elmer, MA, USA), 1 mM DTT). The reaction was terminated by the addition of sample buffer (100 mM Tris [pH 6.8], 4% SDS (w/v), 0.2% Bromophenol blue (w/v), 20% glycerol (v/v), 200 mM DTT), separated by SDS-PAGE (Bio-Rad), stained with Coomassie blue (Invitrogen) and dried prior to autoradiography. GST alone was a negative control, and Histone H1, a Cdk5 substrate, was a positive control.

Surgeries

All surgeries were performed according to the guidelines in the National Institute of Health Guide for the Care and Use of Laboratory. Adult (8-10 week old) male mice (Jackson Laboratory) were group housed in the small animal facility at MIT (Cambridge, MA). For anesthesia, ketamine/xylazine were administered intraperitoneally at a dosage of 100 mg/kg (ketamine) and 10 mg/kg (xylazine) followed by buprenorphine administration at a dosage of 0.05 mg/kg. After exposing the skull, HSVs were delivered bilaterally using a computer-controlled micropump injector with a thin glass capillary at coordinates relative to Bregma: –2.0 mm posterior, +/– 1,6 medial/lateral, –1.2 ventral for hippocampal area CA1. The needle was left in place for 5 min after viral delivery for virus diffusion. Post-operative care consisted of buprenorphine administration every 12 hours and monitoring animals.

Electrophysiology

To record field excitatory postsynaptic potentials, transverse hippocampal slices were prepared from 8-week old mice 2-3 days post-surgery. In brief, the brain was rapidly removed and transferred to ice-cold, oxygenated (95 % O_2 and 5 % CO_2) cutting solution containing (mM) 211 sucrose, 3.3 KCl, 1.3 NaH_2PO_4, 0.5 $CaCl_2$, 10 $MgCl_2$, 26 $NaHCO_3$ and 11 glucose. Hippocampal slices were cut with a Leica VT1000S vibratome (Leica) and transferred for recovery to a holding chamber containing oxygenated artificial cerebrospinal fluid (ACSF) consisted of (mM) 124 NaCl, 3.3 KCl, 1.3 NaH_2PO_4, 2.5 $CaCl_2$, 1.5 $MgCl_2$, 26 $NaHCO_3$ and 11 glucose at 28-30 °C for at least 1 h before recording. CA1 field potentials evoked by Schaffer

collateral stimulation were measured. After recording of stable baseline (at least 20 min of stable responses), LTP was induced by theta-burst stimulation (4x TBS, 10 s intervals). Recordings were performed using AM-1800 Microelectrode amplifier (A-M systems) and a Digidata 1440A A-D converter and analyzed by pClamp 10 software (Axon Instruments). All experiments were performed blind to the group of subjects.

Results

Shank3 is a Cdk5 substrate

We previously conducted a proteomics screen on synaptosomal preparations from control and Cdk5 conditional knockout mice (Guan et al., 2011). In addition to alterations in synaptic protein composition, a separate phospho-proteomic study conducted using Cdk5 conditional knockout synaptosomal preparations suggested that Shank2 and Shank3 are potential Cdk5 substrates (**Table 1**). Known substrates of Cdk5 that were detected in the phosphoproteomics screen include Dlg4, also known as PSD-95. Other notable phosphopeptides detected that are potential Cdk5 substrates included synapsin, piccolo, bassoon, and CaMKII, and other intriguing Cdk5 candidate substrates include the presynaptic protein Rims1 and the postsynaptic, multistructural-domain proteins Dlg1 (SAP97), and Dlg2 (PSD-93).

To confirm that Shank3 is a Cdk5 substrate, we cloned Shank3 into various fragments spanning the ankyrin repeats, the SH3, PDZ domain, proline-rich and SAM domains (**Figure 1A**). In vitro kinase assays were then conducted using active Cdk5/p25 kinase co-incubated with purified Shank3 protein fragments (**Figure 1B**). We consistently observed that one of fragments containing the proline-rich region (aa 861-1000) was robustly phosphorylated by Cdk5. This purified protein fragment in the proline-rich region contains six potential Cdk5 phosphorylation sites (**Figure 1C**). Upon further examination using single and combinatorial point mutations, one key phosphorylation site was mapped to Serine 985 (**Figure 1D**).

Dendritic spine regulation by Cdk5-mediated phosphorylation of Shank3

Having established Shank3 as a Cdk5 substrate, we next investigated whether Cdk5-mediated phosphorylation of Shank3 is involved in dendritic spine formation and maintenance. To this end, we screened for a series of shRNA to mediate knockdown of Shank3 (**Figure 2A**) and generated a bi-cistronic herpes simplex virus (HSV)-based vector to simultaneously reduce endogenous levels of Shank3 while overexpressing either full-length wild-type (WT) or phosphorylation mutant (S985A) Shank3 (**Figure 2B**). Consistent with previous reports that Shank3 is required for dendritic spine formation, knockdown of endogenous Shank3 in DIV 17 primary neurons resulted in a significant increase in immature, thin, filopodia-like spines (**Figure 3A, 3B**). Strikingly, however, Shank3 knockdown while overexpressing S985A Shank3 revealed a dendritic spine phenotype that is reminiscent of Shank3 shRNA alone (**Figure 3A, 3B**).

Biological process	Protein name
Actin cytoskeleton	Grit Rac GTPase activating protein
Actin filament capping	Spectrin alpha chain Isoform1
ARF GTPase activity	GTPase-activing protein GIT1
ARF protein signal transduction	Psd3 Guanine nucleotide exchange factor for ADP ribosylation factor 6
Calmodulin binding	Alpha-adducin Isoform1
Cell adhesion	Claudin-11
Cellular process	Abl interactor1 Isoform1
Cytoskeleton organization & biogenesis	Paralemmin Isoform1
	Synaptopodin Isoform2
	Actin-binding LIM protein1 Isoform1
Dendritic development	Microtubule-associated protein 1A
GPCR signaling	Rgs7 protein
GTPase mediated signal trandsduction	SynGAP-1
Microtubule cytoskeleton organization	Neurofilament medium polypeptide
Microtubule depolymerization	Microtubule-associated protein 1A
mRNA transport	Ras GTPas-activating protein-binding protein2 IsoformA
Neurite development	G protein-regulated inducer of neurite outgrowth1
Neuronal synaptic plasticity	Grin2b glutamate [NMDA] receptor subunit epsilon-2 precursor
Neurotransmitter secretion	Synapsin-1 Isoform 1a
Protein amino acid dephosphorylation	Protein tyrosine phosphatase, receptor type Z, polypeptide1
	Calcium/calmodulin-depedent protein kinase type II gamma chain
	cAMP-dependent protein kinase, beta-catalytic subunit Isoform4
	Protein kinase C beta type
	MARK1 serine/threonine-protein kinase
Protein binding	Disks large homolog 1 Isoform2
	Disks large homolog 2 84 kDa protein
	Leucine rich repeat contining 7
	Plakophilin-4 Isoform1
Regulation of synaptic plasticity	Disks large homolog 4 Isoform 2
	Catenin delta-2 Isoform1
Rho protein signal transduction	Guanine nucleotide release/exchange factor Ras-GRF2
Signal transduction	GABAB receptor, subunit1 precursor, Isoform 1A
	Ank2 ankyrin2, Isoform3
Synapse-related functions	Cortactin
	Bassoon Isoform1
	Piccolo Isoform4
	Shank2 Isoform2 of SH3 and multiple ankyrin repeat domains protein2
	Syntaphilin
	Myosin-Va
	Shank3 SH3 and multiple ankyrin repeat domains protein 3

Table 1. Phospho-proteomics screen of synaptosomal proteins from Cdk5 conditional knockout mice suggest multiple Cdk5 substrates.

A proteomics screen revealed potential Cdk5 phosphorylation sites within synapse-specific proteins, including bassoon, piccolo, multiple actin and microtubule-associated proteins, and Shank2 and Shank3, proteins whose dysfunction has been implicated in autism spectrum disorders.

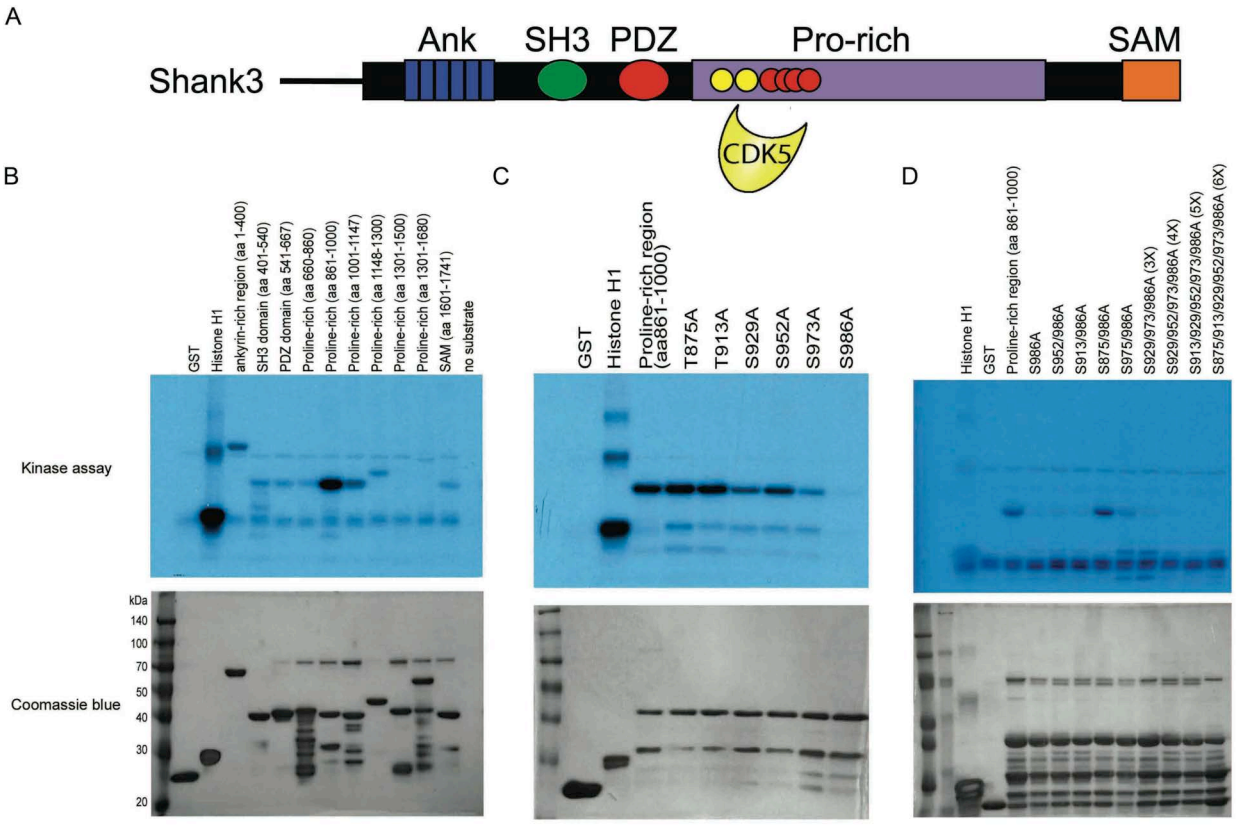

Figure 1. Shank3 is a Cdk5 substrate.

(A) Shank3 was cloned into GST expression vectors consisting of various regions: ankyrin, SH3, PDZ, the proline-rich, or the SAM domain. The purified protein fragments were incubated with active Cdk5/p25 kinase and subjected to in vitro kinase assays.

(B) The proline-rich region (aa 861-1000) was consistently and robustly phosphorylated by Cdk5/p25 in vitro. GST alone served as a negative control, while Histone H1 was used as a positive control.

(C) The potential Cdk5 phosphorylation sites were mapped to six residues using site-directed mutagenesis. Only the S986A phosphorylation mutant in rat Shank3 (S985A in mouse Shank3) completely eliminated Cdk5 phosphorylation.

(D) A combination of single, double, and multi-site phosphorylation mutants revealed S986 as the critical Cdk5 phosphorylation site. Whereas single point mutations in the other sites failed to abolish phosphorylation, double and multiple point mutations containing S986A reduced the phosphorylation signal. The only combination in which S985A failed to abolish phosphorylation was in conjunction with S975.

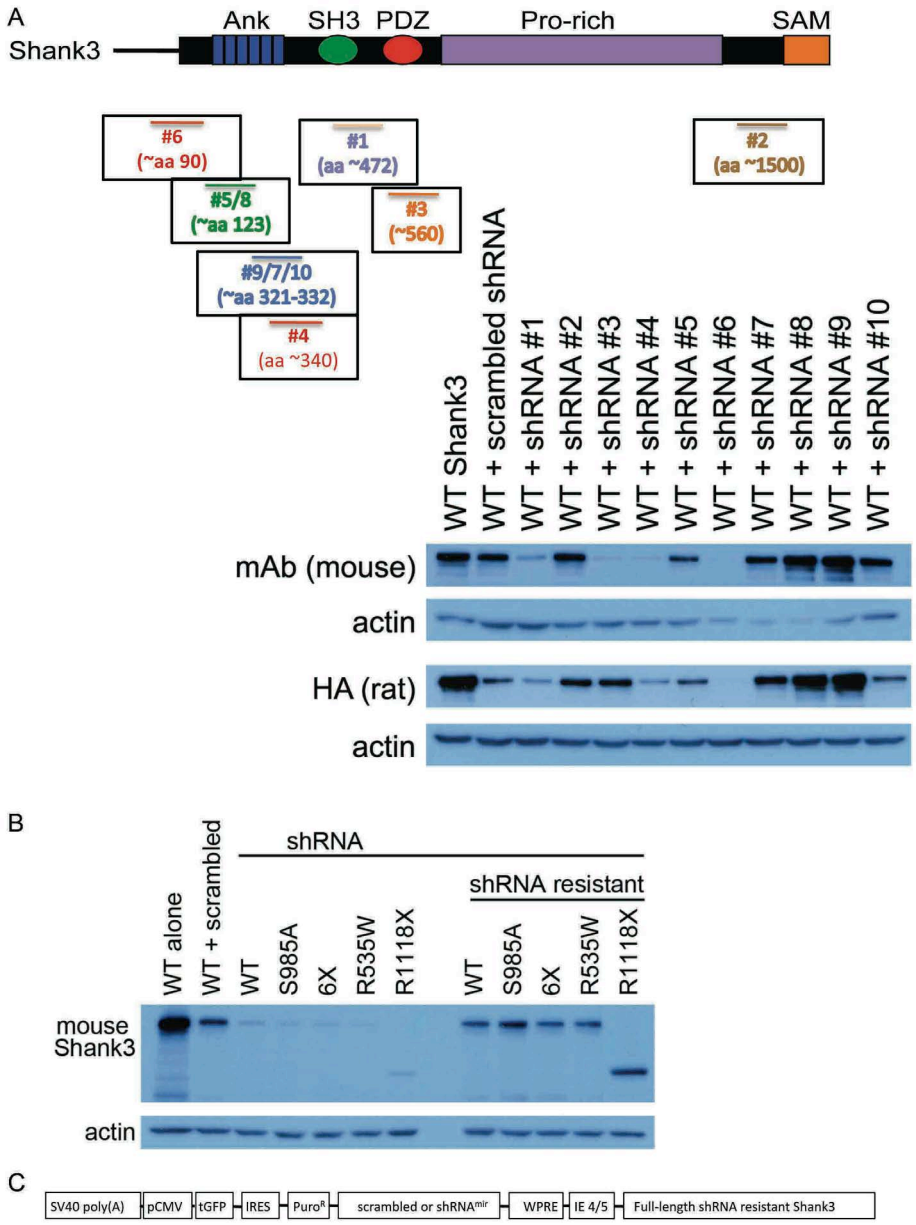

Figure 2. Screening Shank3 shRNA and generation of bi-cistronic viral vectors.
(A) Several shRNAs were screened against both mouse and rat Shank3 constructs. shRNA #4 and #6, targeted against the N-terminus ankyrin region of Shank3, reduced protein levels of both mouse and rat Shank3, and shRNA #6 was used for cloning into the viral vector for further studies.
(B) The Shank3 shRNA was successful in reducing Shank3 protein in heterologous H293 cells overexpressing full-length mouse Shank3 cDNA. Furthermore, shRNA-resistant full-length mouse Shank3 constructs were generated by site-directed mutagenesis and tested in conjuction with Shank3 shRNA. The R535W and R1118X mutants were generated due to its association with childhood schizophrenia but were not used for further experiments.
(C) Schematic of the HSV bi-cistronic construct. Simultaneous knockdown of Shank3 was achieved under the CMV promoter expressing a fluorescent, GFP-tagged micro-RNA-based hairpin, while full-length shRNA-resistant Shank3 was expressed under the IE 4/5 promoter. The S985A, 6X, R535W, and R1118X mutations were generated in the full-length mouse Shank3 construct, but only the WT and S985A Shank3 were used in this study.

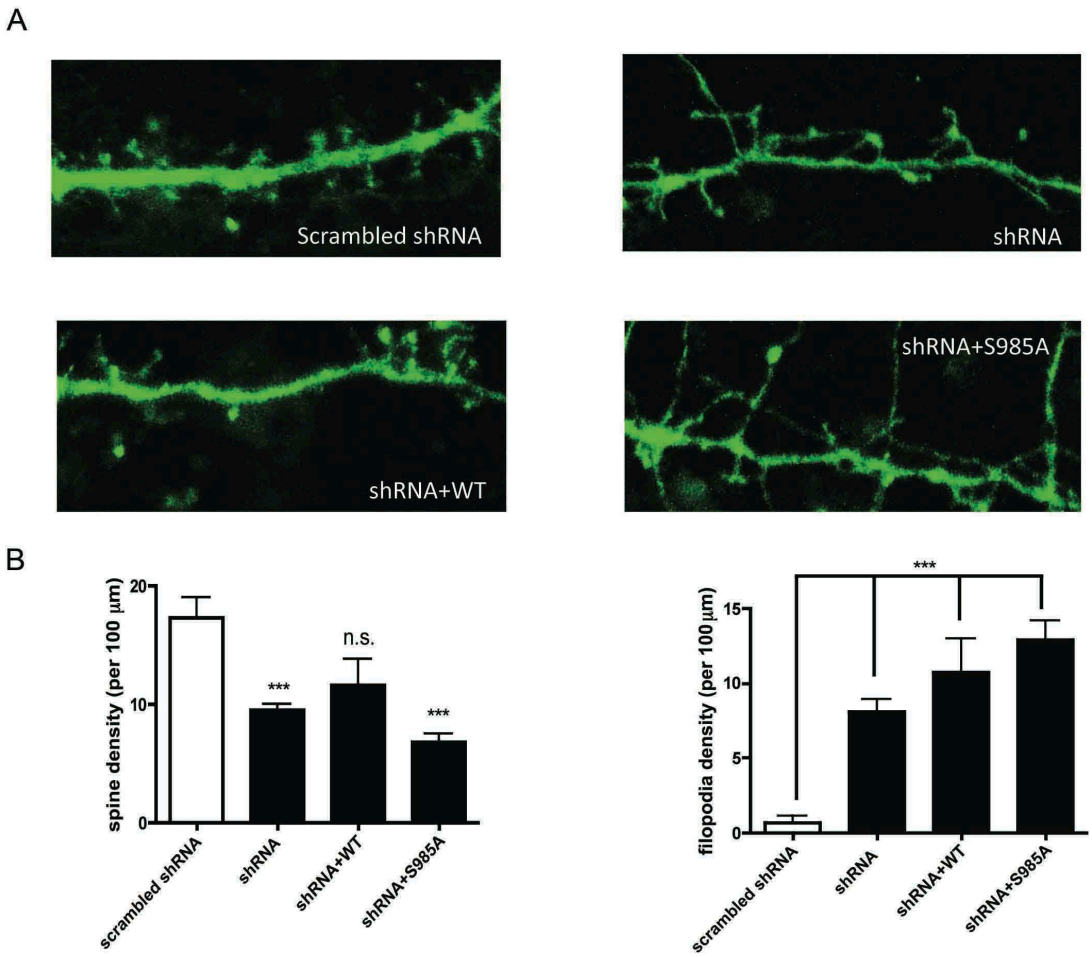

Figure 3. Cdk5-mediated phosphorylation of Shank3 alters dendritic spine morphology.
(A) Primary neurons were fixed at DIV19 following 48 hr transduction with HSV co-expressing Shank3 shRNA and shRNA-resistant WT Shank3 (shRNA+WT) or S985A phosphorylation mutant Shank3 (shRNA+S985A). Scrambled shRNA HSV served as a control.
(B) Quantification of dendritic spine and filopodium protrusion following shRNA-mediated Shank3 knockdown and replacement with the indicted WT or mutant Shank3. Whereas scrambled shRNA did not result in increased filopodia-like formation, both shRNA and shRNA+S985A induced greater filopodia-like formation while decreasing the number of mature, study spines. Spine density was unaltered in shRNA+WT compared to scrambled shRNA alone but the filopodia density was also increased.

Together, our data suggests that Cdk5-mediated phosphorylation of Shank3 is required for maintaining mature dendritic spine morphology. Although Shank3 association with other synaptic proteins such as Homer and Cortactin were unaltered by the S985A Shank3 in vitro (data not shown), it is possible that total levels of key postsynaptic proteins may be decreased in these filopodia-like spines. As it was previously shown that Shank3 knockout mice exhibit lower NMDA receptors, and Shank2 knockout mice display lower levels of NMDA and AMPA receptors, we also predict that synaptic NMDA or AMPA receptor levels might be downregulated. Downstream signaling cascades involving the actin remodeling complex are also likely to be disrupted.

Synaptic plasticity is affected by Cdk5-mediated phosphorylation of Shank3

Synaptic plasticity as measured by long-term potentiation is a form of persistent transmission across synapses, and it is correlated with dendritic spine size and maturity as well as learning and memory (Bourne and Harris, 2008; Toni et al., 1999). Because of the striking observations that dendritic spines appear elongated and more filopodia-like in primary neurons expressing Shank3 shRNA or shRNA+S985A Shank3, we predicted that these alterations would in turn impact synaptic transmission and synaptic plasticity. We first examined acute hippocampal slices prepared from wild-type mice transduced with HSVs expressing scrambled shRNA, Shank3 shRNA alone, shRNA+WT Shank3 or shRNA+S985A Shank3. Measurements of basal synaptic transmission did not reveal any alterations compared to slices expressing control, scrambled shRNA (**Figure 4A**). Compared to slices expressing scrambled shRNA, paired-pulse facilitation ratios, a form of presynaptic plasticity, were not significantly affected (**Figure 4B**). We next induced LTP using a theta-burst stimulation protocol on acute hippocampal slices prepared from wild-type mice transduced with HSVs expressing scrambled control shRNA, Shank3 shRNA alone, shRNA+WT Shank3 or shRNA+S985A Shank3. Consistent with previous reports that Shank3 knockout mice exhibit impaired LTP and synaptic transmission (Wang et al., 2011), acute knockdown of Shank3 also significantly reduced LTP compared to control shRNA (**Figure 4C, 4D)**. Slices expressing shRNA+WT Shank3 exhibited somewhat enhanced LTP but did not completely restore LTP to control levels. Unexpectedly, however, in slices expressing shRNA+S985A Shank3, LTP is dramatically enhanced relative to shRNA and is similar to the level of LTP in control, scrambled shRNA slices (**Figure 4C, 4D**).

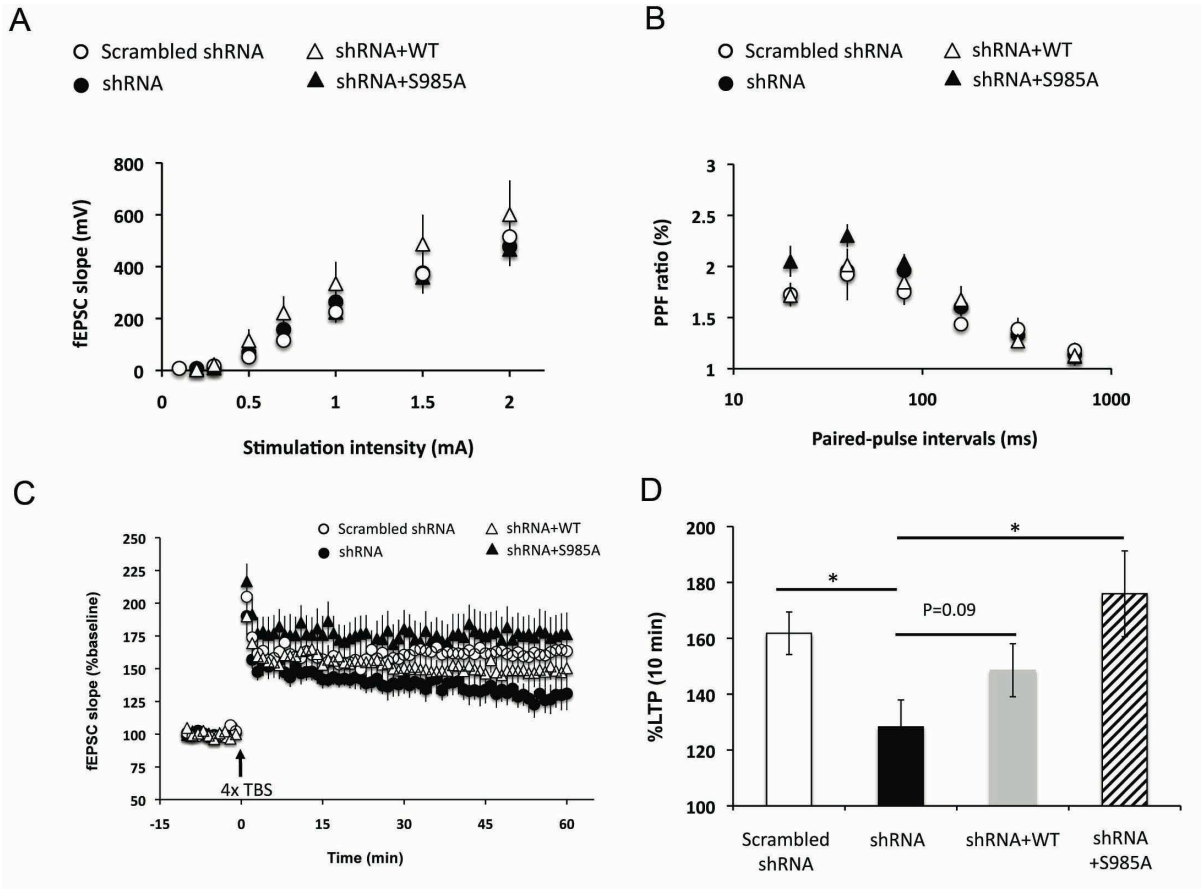

Figure 4. Synaptic plasticity is impacted by Cdk5-mediated phosphorylation of Shank3.
(A) Basal synaptic transmission and presynaptic plasticity are unaffected Cdk5-mediated phosphorylation of Shank3. HSVs expressing various Shank3 constructs were delivered to hippocampal area CA1, and acute hippocampal slices were prepared 2-3 days later. Basal synaptic transmission, as measured by the input-output curve where fEPSC slope is plotted against stimulation intensity, did not reveal any differences in synaptic transmission compared to slices expressing control, scrambled shRNA.
(B) Presynaptic plasticity was measured by paired-pulse facilitation ratios at different intervals, and compared to control, scrambled shRNA, there were no differences in PPF ratios.
(C) In slices expressing scrambled shRNA, LTP was reliably induced by three theta burst stimulations in the Schaffer collateral pathway. However, compared to scrambled shRNA, there was a deficit in LTP in slices expressing Shank3 shRNA. Slices expressing simultaneous knockdown and overexpression of wild-type Shank3 (shRNA+WT) exhibited LTP comparable to shRNA, whereas slices expressing simultaneous knockdown and overexpression of Cdk5-phosphorylation resistant Shank3 S985A (shRNA+S985A) showed elevated levels of LTP compared to shRNA.
(D) Quantification of the last 10 min of LTP. Data shown are means ± SEM. Statistical significance was calculated using one-way ANOVA followed by Tukey's multiple comparison test ($p < 0.05$; $^{**}p < 0.01$; $^{***}p < 0.001$). N=8 slices, 4-6 mice per group.

Discussion

In our study, we identified Shank3, a gene associated with autism spectrum disorder and intellectual disabilities, as a Cdk5 substrate and demonstrate a role for the phosphorylation on S985 in the maintenance of dendritic spines and in mediating synaptic plasticity. Our results highlight a novel aspect of post-translational regulation of Shank3 and suggest that actin-remodeling pathways may play a role in shaping dendritic spine formation and maturation.

Shank3 and dendritic spine remodeling

As Shank3 is known to associate with cortactin and homer to affect the actin cytoskeleton to remodel dendritic spines (Hering and Sheng, 2003), it will be essential to determine whether the S985A Shank3 phosphorylation mutant impacts the interaction of Shank3 with cortacin and homer to affect actin polymerization. Preliminary observations suggest that in heterologous cells, expression of S985A Shank3 phosphorylation mutant does not affect its binding with either cortacin and Homer, but the possibility that Shank1 or Shank2 proteins may be involved cannot be excluded. Shank3 is strongly associated with autism spectrum disorders due to the identification of de novo mutations in patients that, while not causative of autism, are implicated as risk factors for autism (Durand et al., 2007). Intriguingly, the human Shank3 mutations affect spine development in an actin-dependent manner and also affect synaptic plasticity (Durand et al., 2012). Other studies have identified de novo mutations in the Shank2 gene in autism spectrum disorder patients (Berkel et al., 2010), and expressing these mutations in mouse systems reduces dendritic spine volume and altered synaptic transmission mediated by AMPA receptors (Berkel et al., 2012).

Cdk5-mediated phosphorylation of Shank3 impacts synaptic plasticity

Notably, our results are somewhat unexpected due to the observation that slices expressing S985A Shank3 phosphorylation mutant demonstrate enhanced hippocampal LTP compared to slices expressing shRNA and do not differ from slices expressing control scrambled shRNA. However, previous studies have reported dendritic spine maturation with LTP induction (Engert and Bonhoeffer, 1999; Kopec et al., 2006; Maletic-Savatic et al., 1999). It is possible that LTP induction produced activity-dependent changes in the dendritic spines of synapses expressing S985A Shank3 phosphorylation mutant that enabled rapid spine maturation

throughout the LTP measurement period compared to the slices expressing Shank3 shRNA. It will be of great interest in future studies to determine how the S985A Shank3 phosphorylation mutant affects dendritic spine formation during LTP, and how it affects activity-dependent actin remodeling and surface expression of glutamate receptors. A potential future approaches includes generating transgenic mouse models. such as a knock-in mouse model, to gain better insight into how phosphorylation of Shank3 by Cdk5 may also impact synaptogenesis and synaptic plasticity.

Future directions of autism research

Recent advances in genome-wide association studies have revealed that copy number variations are associated with autism spectrum disorders and intellectual disabilities (Glessner et al., 2009; Sebat et al., 2007). Other studies using deep sequencing of affected and unaffected controls have identified de novo mutations in protein-coding exons of several key genes implicated in synaptic function to be strongly associated with autism spectrum disorders (Neale et al., 2012; O'Roak et al., 2012; Sanders et al., 2012). Shank3 is particularly interesting due to its association with Phelan-McDermid Syndrome, a disorder that affects deletion of Shank3 and other chromosomal regions on 22q13.3 (Phelan and Rogers, 1993). Patients diagnosed Phelan-McDermid Syndrome exhibit global developmental delays, speech delay, and hypotonia and in over half of the cases, the patients also show autism-like behavior. While the cause of the disorder is unknown, it is hypothesized that Shank3 haploinsufficiency may affect development of various organs as well as synaptic structures. Future studies on the biology underlying Phelan-McDermid Syndrome should also enhance our understanding of how Shank3 is involved in organization of synapses and proper development.

References

Bangash, M.A., Park, J.M., Melnikova, T., Wang, D., Jeon, S.K., Lee, D., Syeda, S., Kim, J., Kouser, M., Schwartz, J.*, et al.* (2011). Enhanced polyubiquitination of Shank3 and NMDA receptor in a mouse model of autism. Cell *145*, 758-772.

Berkel, S., Marshall, C.R., Weiss, B., Howe, J., Roeth, R., Moog, U., Endris, V., Roberts, W., Szatmari, P., Pinto, D.*, et al.* (2010). Mutations in the SHANK2 synaptic scaffolding gene in autism spectrum disorder and mental retardation. Nat Genet *42*, 489-491.

Berkel, S., Tang, W., Trevino, M., Vogt, M., Obenhaus, H.A., Gass, P., Scherer, S.W., Sprengel, R., Schratt, G., and Rappold, G.A. (2012). Inherited and de novo SHANK2 variants associated with autism spectrum disorder impair neuronal morphogenesis and physiology. Hum Mol Genet *21*, 344-357.

Bourne, J.N., and Harris, K.M. (2008). Balancing structure and function at hippocampal dendritic spines. Annu Rev Neurosci *31*, 47-67.

Bozdagi, O., Sakurai, T., Papapetrou, D., Wang, X., Dickstein, D.L., Takahashi, N., Kajiwara, Y., Yang, M., Katz, A.M., Scattoni, M.L.*, et al.* (2010). Haploinsufficiency of the autism-associated Shank3 gene leads to deficits in synaptic function, social interaction, and social communication. Mol Autism *1*, 15.

Brakeman, P.R., Lanahan, A.A., O'Brien, R., Roche, K., Barnes, C.A., Huganir, R.L., and Worley, P.F. (1997). Homer: a protein that selectively binds metabotropic glutamate receptors. Nature *386*, 284-288.

Cruz, J.C., Tseng, H.C., Goldman, J.A., Shih, H., and Tsai, L.H. (2003). Aberrant Cdk5 activation by p25 triggers pathological events leading to neurodegeneration and neurofibrillary tangles. Neuron *40*, 471-483.

Dong, H., O'Brien, R.J., Fung, E.T., Lanahan, A.A., Worley, P.F., and Huganir, R.L. (1997). GRIP: a synaptic PDZ domain-containing protein that interacts with AMPA receptors. Nature *386*, 279-284.

Durand, C.M., Betancur, C., Boeckers, T.M., Bockmann, J., Chaste, P., Fauchereau, F., Nygren, G., Rastam, M., Gillberg, I.C., Anckarsater, H.*, et al.* (2007). Mutations in the gene encoding the synaptic scaffolding protein SHANK3 are associated with autism spectrum disorders. Nat Genet *39*, 25-27.

Durand, C.M., Perroy, J., Loll, F., Perrais, D., Fagni, L., Bourgeron, T., Montcouquiol, M., and Sans, N. (2012). SHANK3 mutations identified in autism lead to modification of dendritic spine morphology via an actin-dependent mechanism. Mol Psychiatry *17*, 71-84.

Engert, F., and Bonhoeffer, T. (1999). Dendritic spine changes associated with hippocampal long-term synaptic plasticity. Nature *399*, 66-70.

Gauthier, J., Champagne, N., Lafreniere, R.G., Xiong, L., Spiegelman, D., Brustein, E., Lapointe, M., Peng, H., Cote, M., Noreau, A.*, et al.* (2010). De novo mutations in the gene encoding the synaptic scaffolding protein SHANK3 in patients ascertained for schizophrenia. Proc Natl Acad Sci U S A *107*, 7863-7868.

Geschwind, D.H., and Levitt, P. (2007). Autism spectrum disorders: developmental disconnection syndromes. Curr Opin Neurobiol *17*, 103-111.

Glessner, J.T., Wang, K., Cai, G., Korvatska, O., Kim, C.E., Wood, S., Zhang, H., Estes, A., Brune, C.W., Bradfield, J.P.*, et al.* (2009). Autism genome-wide copy number variation reveals ubiquitin and neuronal genes. Nature *459*, 569-573.

Guan, J.S., Su, S.C., Gao, J., Joseph, N., Xie, Z., Zhou, Y., Durak, O., Zhang, L., Zhu, J.J., Clauser, K.R.*, et al.* (2011). Cdk5 is required for memory function and hippocampal plasticity via the cAMP signaling pathway. PLoS One *6*, e25735.

Han, S., Tai, C., Westenbroek, R.E., Yu, F.H., Cheah, C.S., Potter, G.B., Rubenstein, J.L., Scheuer, T., de la Iglesia, H.O., and Catterall, W.A. (2012). Autistic-like behaviour in Scn1a(+/-) mice and rescue by enhanced GABA-mediated neurotransmission. Nature.

Hayashi, M.K., Tang, C., Verpelli, C., Narayanan, R., Stearns, M.H., Xu, R.M., Li, H., Sala, C., and Hayashi, Y. (2009). The postsynaptic density proteins Homer and Shank form a polymeric network structure. Cell *137*, 159-171.

Hering, H., and Sheng, M. (2003). Activity-dependent redistribution and essential role of cortactin in dendritic spine morphogenesis. J Neurosci *23*, 11759-11769.

Hung, A.Y., Futai, K., Sala, C., Valtschanoff, J.G., Ryu, J., Woodworth, M.A., Kidd, F.L., Sung, C.C., Miyakawa, T., Bear, M.F.*, et al.* (2008). Smaller dendritic spines, weaker synaptic transmission, but enhanced spatial learning in mice lacking Shank1. J Neurosci *28*, 1697-1708.

Kim, E., Niethammer, M., Rothschild, A., Jan, Y.N., and Sheng, M. (1995). Clustering of Shaker-type K+ channels by interaction with a family of membrane-associated guanylate kinases. Nature *378*, 85-88.

Kim, E., and Sheng, M. (2004). PDZ domain proteins of synapses. Nat Rev Neurosci *5*, 771-781.

Kim, S.H., and Ryan, T.A. (2010). CDK5 serves as a major control point in neurotransmitter release. Neuron *67*, 797-809.

Kopec, C.D., Li, B., Wei, W., Boehm, J., and Malinow, R. (2006). Glutamate receptor exocytosis and spine enlargement during chemically induced long-term potentiation. J Neurosci *26*, 2000-2009.

Lee, M.S., Kwon, Y.T., Li, M., Peng, J., Friedlander, R.M., and Tsai, L.H. (2000). Neurotoxicity induces cleavage of p35 to p25 by calpain. Nature *405*, 360-364.

Li, B.S., Sun, M.K., Zhang, L., Takahashi, S., Ma, W., Vinade, L., Kulkarni, A.B., Brady, R.O., and Pant, H.C. (2001). Regulation of NMDA receptors by cyclin-dependent kinase-5. Proc Natl Acad Sci U S A *98*, 12742-12747.

Lin, W., Dominguez, B., Yang, J., Aryal, P., Brandon, E.P., Gage, F.H., and Lee, K.F. (2005). Neurotransmitter acetylcholine negatively regulates neuromuscular synapse formation by a Cdk5-dependent mechanism. Neuron *46*, 569-579.

Maletic-Savatic, M., Malinow, R., and Svoboda, K. (1999). Rapid dendritic morphogenesis in CA1 hippocampal dendrites induced by synaptic activity. Science *283*, 1923-1927.

Mitra, A., Mitra, S.S., and Tsien, R.W. (2012). Heterogeneous reallocation of presynaptic efficacy in recurrent excitatory circuits adapting to inactivity. Nat Neurosci *15*, 250-257.

Morabito, M.A., Sheng, M., and Tsai, L.H. (2004). Cyclin-dependent kinase 5 phosphorylates the N-terminal domain of the postsynaptic density protein PSD-95 in neurons. J Neurosci *24*, 865-876.

Naisbitt, S., Kim, E., Tu, J.C., Xiao, B., Sala, C., Valtschanoff, J., Weinberg, R.J., Worley, P.F., and Sheng, M. (1999). Shank, a novel family of postsynaptic density proteins that binds to the NMDA receptor/PSD-95/GKAP complex and cortactin. Neuron *23*, 569-582.

Neale, B.M., Kou, Y., Liu, L., Ma'ayan, A., Samocha, K.E., Sabo, A., Lin, C.F., Stevens, C., Wang, L.S., Makarov, V.*, et al.* (2012). Patterns and rates of exonic de novo mutations in autism spectrum disorders. Nature *485*, 242-245.

Neve, R.L., Neve, K.A., Nestler, E.J., and Carlezon, W.A., Jr. (2005). Use of herpes virus amplicon vectors to study brain disorders. Biotechniques *39*, 381-391.

O'Roak, B.J., Vives, L., Girirajan, S., Karakoc, E., Krumm, N., Coe, B.P., Levy, R., Ko, A., Lee, C., Smith, J.D.*, et al.* (2012). Sporadic autism exomes reveal a highly interconnected protein network of de novo mutations. Nature *485*, 246-250.

Patrick, G.N., Zukerberg, L., Nikolic, M., de la Monte, S., Dikkes, P., and Tsai, L.H. (1999). Conversion of p35 to p25 deregulates Cdk5 activity and promotes neurodegeneration. Nature *402*, 615-622.

Peca, J., Feliciano, C., Ting, J.T., Wang, W., Wells, M.F., Venkatraman, T.N., Lascola, C.D., Fu, Z., and Feng, G. (2011). Shank3 mutant mice display autistic-like behaviours and striatal dysfunction. Nature *472*, 437-442.

Phelan, K., and Rogers, C. (1993). Phelan-McDermid Syndrome.

Roussignol, G., Ango, F., Romorini, S., Tu, J.C., Sala, C., Worley, P.F., Bockaert, J., and Fagni, L. (2005). Shank expression is sufficient to induce functional dendritic spine synapses in aspiny neurons. J Neurosci *25*, 3560-3570.

Samuels, B.A., Hsueh, Y.P., Shu, T., Liang, H., Tseng, H.C., Hong, C.J., Su, S.C., Volker, J., Neve, R.L., Yue, D.T.*, et al.* (2007). Cdk5 promotes synaptogenesis by regulating the subcellular distribution of the MAGUK family member CASK. Neuron *56*, 823-837.

Sanders, S.J., Murtha, M.T., Gupta, A.R., Murdoch, J.D., Raubeson, M.J., Willsey, A.J., Ercan-Sencicek, A.G., DiLullo, N.M., Parikshak, N.N., Stein, J.L.*, et al.* (2012). De novo mutations revealed by whole-exome sequencing are strongly associated with autism. Nature *485*, 237-241.

Schmeisser, M.J., Ey, E., Wegener, S., Bockmann, J., Stempel, A.V., Kuebler, A., Janssen, A.L., Udvardi, P.T., Shiban, E., Spilker, C.*, et al.* (2012). Autistic-like behaviours and hyperactivity in mice lacking ProSAP1/Shank2. Nature *486*, 256-260.

Sebat, J., Lakshmi, B., Malhotra, D., Troge, J., Lese-Martin, C., Walsh, T., Yamrom, B., Yoon, S., Krasnitz, A., Kendall, J.*, et al.* (2007). Strong association of de novo copy number mutations with autism. Science *316*, 445-449.

Seeburg, D.P., Feliu-Mojer, M., Gaiottino, J., Pak, D.T., and Sheng, M. (2008). Critical role of CDK5 and Polo-like kinase 2 in homeostatic synaptic plasticity during elevated activity. Neuron *58*, 571-583.

Tomizawa, K., Sunada, S., Lu, Y.F., Oda, Y., Kinuta, M., Ohshima, T., Saito, T., Wei, F.Y., Matsushita, M., Li, S.T.*, et al.* (2003). Cophosphorylation of amphiphysin I and dynamin I by Cdk5 regulates clathrin-mediated endocytosis of synaptic vesicles. J Cell Biol *163*, 813-824.

Toni, N., Buchs, P.A., Nikonenko, I., Bron, C.R., and Muller, D. (1999). LTP promotes formation of multiple spine synapses between a single axon terminal and a dendrite. Nature *402*, 421-425.

Tu, J.C., Xiao, B., Naisbitt, S., Yuan, J.P., Petralia, R.S., Brakeman, P., Doan, A., Aakalu, V.K., Lanahan, A.A., Sheng, M.*, et al.* (1999). Coupling of mGluR/Homer and PSD-95 complexes by the Shank family of postsynaptic density proteins. Neuron *23*, 583-592.

Wang, X., McCoy, P.A., Rodriguiz, R.M., Pan, Y., Je, H.S., Roberts, A.C., Kim, C.J., Berrios, J., Colvin, J.S., Bousquet-Moore, D.*, et al.* (2011). Synaptic dysfunction and abnormal behaviors in mice lacking major isoforms of Shank3. Hum Mol Genet *20*, 3093-3108.

Won, H., Lee, H.R., Gee, H.Y., Mah, W., Kim, J.I., Lee, J., Ha, S., Chung, C., Jung, E.S., Cho, Y.S., *et al.* (2012). Autistic-like social behaviour in Shank2-mutant mice improved by restoring NMDA receptor function. Nature *486*, 261-265.

Zhang, S., Edelmann, L., Liu, J., Crandall, J.E., and Morabito, M.A. (2008). Cdk5 regulates the phosphorylation of tyrosine 1472 NR2B and the surface expression of NMDA receptors. J Neurosci *28*, 415-424.

Chapter 5

Forebrain-specific deletion of Cdk5 in pyramidal neurons results in hyperactivity, synaptic plasticity deficits, and cognitive impairment

Summary

Cyclin-dependent kinase 5 (Cdk5) is associated with synaptic plasticity and cognitive function. Although previous reports have described Cdk5 conditional knockout mouse models exhibiting enhanced learning and memory, others have shown that Cdk5 is necessary for memory formation. Despite the literature on various mouse models of Cdk5 ablation, its role in exact cell types are still unclear. Here we have generated and characterized a forebrain-specific Cdk5 conditional knockout mouse model using the αCaMKII-Cre driver line. When Cdk5 is reduced in excitatory pyramidal neurons of the forebrain, the number of dendritic spines is decreased. Additionally, we observed strong behavioral alterations including hyperactivitiy and reduced behavioral despair. The Cdk5 conditional knockout mice also exhibit impaired spatial learning in the watermaze and cognitive impairment in fear conditioning memory, along with deficits in synaptic plasticity. The hyperactivity can be restored to control levels by the administration of lithium chloride, an inhibitor of GSK3β signaling. Our data suggests that Cdk5 ablation from forebrain excitatory neurons have a deleterious effect on synaptic plasticity, emotional and cognitive behavior, and may alter the GSK3β signaling pathway.

I prepared samples for electron microscopy processing and acquired the images for analysis, conducted light/dark test, open field, forced swim test, pre-pulse inhibition test, contextual and tone fear conditioning tests and analyzed the data, and conducted biochemical experiments and analyzed the data.

Introduction

The neuronal kinase cyclin-dependent kinase 5 (Cdk5) is a multi-faceted kinase that plays an important role in synaptic plasticity and learning and memory (Guan et al., 2011; Hawasli et al., 2007). In addition to targeting NMDA receptors and postsynaptic scaffolding proteins such as PSD-95 (Li et al., 2001; Morabito et al., 2004), Cdk5 activity is involved in the formation of long-term potentiation (LTP) at hippocampal synapses (Fischer et al., 2005; Li et al., 2001). Recent studies have examined how Cdk5 regulates activity and modifies synaptic transmission to fine-tune homeostatic plasticity (Kim and Ryan, 2010; Mitra et al., 2011; Seeburg et al., 2008). Despite the wealth of evidence regarding Cdk5 and its influence on synaptic plasticity, recent studies on behavioral outcomes of Cdk5 loss-of-function is still unclear. One study reports an increase in learning and memory in a Cdk5 conditional knockout mouse line (Hawasli et al., 2007). Other mouse models in which p35, the regulatory subunit of Cdk5, has been deleted show hyperactivity and alterations in the dopaminergic and cholinergic system (Drerup et al., 2010; Krapacher et al., 2010). Yet other studies have indicated that loss of Cdk5 or inhibiting Cdk5 activity is detrimental to memory acquisition and synaptic plasticity (Guan et al., 2011; Li et al., 2001).

In this study, we examine a conditional knockout mouse model in which Cdk5 is selectively ablated in forebrain excitatory neurons. Through a series of behavioral tasks, we assessed the outcome of Cdk5 reduction in motor activity, cognitive function, and synaptic plasticity. We show that Cdk5 loss-of-function in αCaMKII-positive excitatory neurons results in hyperactivity, impaired cognitive function and deficits in synaptic plasticity. Upon closer examination, treatment of the Cdk5 conditional knockout mice with lithium chloride restores their locomoter activity. Further evaluation of the molecular mechanisms underlying the behavioral phenotype in this line of Cdk5 conditional knockout mice will be useful to better understand how Cdk5 may regulate synaptic function.

Methods

Animals

Cdk5 conditional knockout mice were generated by crossing the αCaMKII-Cre (CW2) line (generous gift from Dr. Susumu Tonegawa) with the Cdk5 floxed/floxed (Cdk5f/f) line to generate αCaMKII-Cre;Cdk5fl/fl mice, also referred to as Cdk5 conditional knockout (Cdk5f/f/CW2) mice. Mice were generated and maintained in a C57Bl/6J background and group-housed in a 12 hr light-dark cycle, with food and water ad libitum. Mice were handled according to the National Institutes of Health Care and Use of Laboratory Animals. All behavior studies were conducted using adult, 3-5 month old male mice.

Behavior

Light dark test

Mice were placed into a light-dark chamber apparatus and allowed to explore the arenas for 10 min. A video recorded the latency to enter the light for the first time, duration spent in the light chamber and the number of crossings from the dark to the light chamber. Statistical significance was calculated for the control (Cdk5f/f) and Cdk5 conditional knockout (Cdk5f/f/CW2) groups using unpaired Student's t-test.

Open Field Test

Mice were placed into 40 cm x 40 cm arenas with orthogonal lasers to track position and locomotor activity for 60 min (VersaMax). Data was collected and analyzed (Graphpad). Each activity was calculated as the mean with standard error and compared across control (Cdk5f/f) and Cdk5f/f/CW2 groups with unpaired Student's t-test. For LiCl treatment, LiCl was injected intraperitoneally 40 min before beginning the task at a dosage of 85 mg/kg.

Forced swim test

Animals were placed in a 4000 ml Pyrex cylindrical container at 24C and various parameters such as velocity, mobile duration and time, immobile duration and time, were automatically recorded for 6 min (VersaMax). Immobility was measured during the last 4 min of the test.

Morris water maze task

Spatial memory was performed using a circular tank (1.2 m in diameter) filled with opaque water at 22C. The walls contained spatial reference cues, and inside the tank was a fixed platform (10 cm in diameter) in a target quadrant. During pre-training (Day 1), mice were placed in the water, guided to the platform, and allowed to stay in the platform for 15 s. In the following days, mice were placed into the maze randomly and allowed to search for the platform for 60 s. Two trials a day were conducted with a 2 min interval. Mouse behavior was recorded and analyzed, and escape latency was scored (TSE Systems). On day 9, the platform was removed and a probe trial was conducted to assess spatial learning.

In vivo recordings

Mice were placed under isofluorane and placed into a custom stereotaxic stage. A small craniotomy was made over the somatosensory cortex, and spontaneous local field potentials (LFPs) were recorded using a glass electrode from layers II-IV of the somatosensory cortex. Relative power was calculated by measuring the ratio of power within the band of interest to total power (1-100 Hz) in the power spectrum of the unfiltered LTP.

Fear conditioning

Both contextual and cued fear conditioning was conducted over the course of 3 days. On day 1, mice were placed in a fear conditioning apparatus chamber for 3 min and then presented with a 2 s foot shock delivery at 0.8 mA preceded by a 30 s, 75 dB tone (TSE Systems). After the animals were placed in their homecage for 24 hr, they were assessed for contextual learning by recording the freezing behavior for 3 min in the training context. On day 3, the animals were presented with a different context but levels of freezing were assessed after exposure to the same tone. Prior to each trial, each context was cleaned with 70% ethanol except for on day 3, where it was cleaned with acetic acid.

Electrophysiology

To record field excitatory postsynaptic potentials, transverse hippocampal slices were prepared from 8-12 week old adult mice. In brief, the brain was rapidly removed and transferred to ice-cold, oxygenated (95 % O_2 and 5 % CO_2) cutting solution containing (mM) 211 sucrose,

3.3 KCl, 1.3 NaH_2PO_4, 0.5 $CaCl_2$, 10 $MgCl_2$, 26 $NaHCO_3$ and 11 glucose. Hippocampal slices were cut with a Leica VT1000S vibratome (Leica) and transferred for recovery to a holding chamber containing oxygenated artificial cerebrospinal fluid (ACSF) consisted of (mM) 124 NaCl, 3.3 KCl, 1.3 NaH_2PO_4, 2.5 $CaCl_2$, 1.5 $MgCl_2$, 26 $NaHCO_3$ and 11 glucose at 28-30 °C for at least 1 h before recording. CA1 field potentials evoked by Schaffer collateral stimulation were measured. Recordings were performed using a MultiClamp 700B amplifier and a Digidata 1440A A-D converter and analyzed by pClamp 10 software (Axon Instruments). Experiments were performed blind to the genotype.

For miniature recordings, whole-cell recordings were performed in CA1 pyramidal neurons for mEPSC and mIPSC measurements. Cells were held at -70 mV and data were acquired using a MultiClamp 700B amplifier and a Digidata 1440A A-D converter (Axon Instruments). The internal solution contained (mM) 145 CsCl, 5 NaCl, 10 HEPES-CsOH, 10 EGTA, 4 MgATP and 0.3 Na_2GTP. TTX (1 μM), D-APV (50 μM) and either picrotoxin (50 μM) or CNQX (10 μM) were added to ACSF for mEPSC or mIPSC, respectively.

Results

Conditional knockout of Cdk5 results in decreased number of synapses

Cdk5 conditional knockout mice (Cdk5f/f/CW2) were generated as previously described in which Cdk5 is ablated specifically in excitatory pyramidal neurons of the forebrain by crossing floxed Cdk5 mice to CW-2 Cre line driven by the αCaMKII (Guan et al., 2011; Zeng et al., 2001). The Cdk5f/f/CW2 mice do not exhibit gross developmental abnormalities and survive until 5-6 months of age, when they begin to suffer seizures. Using electron microscopy studies to obtain a higher resolution of the synapse, we observed a small but significant reduction in postsynaptic density (PSD) thickness and density in hippocampal CA1 (**Figure 1A, 1B**).

Reduced anxiety and hyperactivity in Cdk5f/f/CW2 mice

We next utilized a set of behavioral assays to examine how loss of Cdk5 affects anxiety and cognition. A well-characterized behavioral assay for anxiety, the light-dark test, revealed significantly and consistently decreased anxiety in the Cdk5f/f/CW2 mice compared to control (Cdk5f/f) mice due to a faster entry to the light, more time spent in the light and increased number of crossings between the two chambers (**Figure 2A-C**). Interestingly, Cdk5f/f/CW2 mice were hyperactive in the open field test as measured by the total distance traveled (**Figure 3A)**. This hyperactivity corresponded to Cdk5f/f/CW2 spending increased time and distance in the center of the open field arena (**Figure 3B, 3C**) as well as increased distance, but not time, in the margin area (**Figure 3D, 3E**). Furthermore, compared to control Cdk5f/f mice, Cdk5f/f/CW2 exhibited a significant enhancement of rearing activity (**Figure 3F**), increased horizontal and vertical movements (**Figure 3G, 3H**) but no changes stereotypic movements (**Figure 3I**), consistent with reduced anxiety. The hyperactivity is specific and may have affected their behavior in the forced swim test for learned helplessness, in which Cdk5f/f/CW2 mice show reduced behavioral despair by their overall increased distance and velocity and decreased immobility compared to control Cdk5f/f mice (**Figure 4A-D**). In a well-characterized test for sensorimotor gating, Cdk5f/f/CW2 exhibited increased startle to the training tones compared to control Cdk5f/f mice (**Figure 5A**), but did not exhibit any alterations in pre-pulse inhibition (**Figure 5B**).

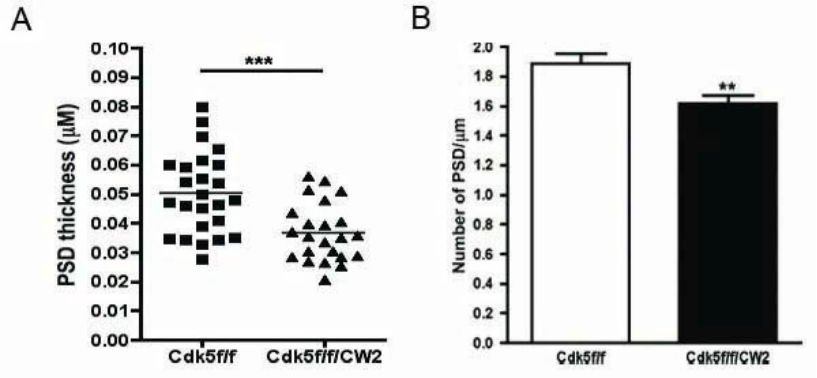

Figure 1. PSD thickness and overall density is reduced in Cdk5f/f/CW2 mice.
(A) Electron microscopy images acquired from hippocampal area CA1 synapses revealed a reduction in PSD thickness of Cdk5f/f/CW2 synapses compared to control Cdk5f/f synapses.
(B) The PSD density is also reduced in the Cdk5f/f/CW2 synapses compared to control Cdk5f/f synapses, consistent with a reduction in the total number of synapses. Data shown are means ± SEM. Statistical significance was calculated using Student's t-test (*p < 0.05; **p < 0.01; ***p < 0.001).

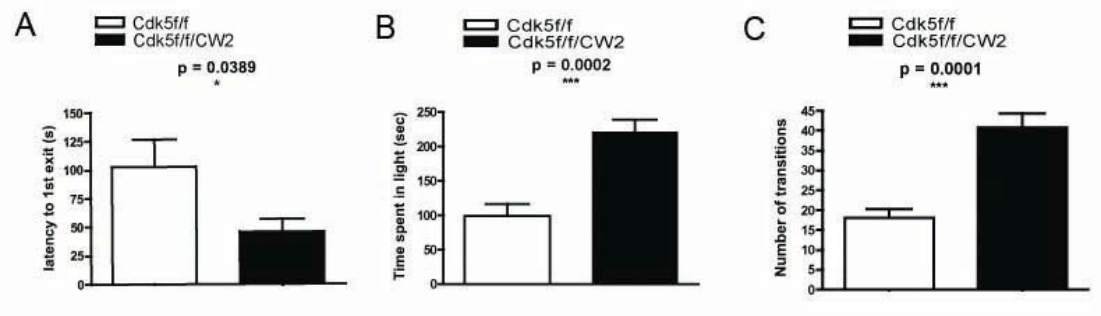

Figure 2. Cdk5f/f/CW2 exhibit reduced anxiety in the light/dark test.
(A) The light/dark test was used to assess anxiety in Cdk5f/f and Cdk5f/f/CW2 mice. While control Cdk5f/f animals were more anxious of the light region, Cdk5f/f/CW2 mice crossed over into the bright region faster than their control littermates.
(B) Compared to their control Cdk5f/f littermates, Cdk5f/f/CW2 mice spent more time overall in the light.
(C) Compared to their control Cdk5f/f littermates, Cdk5f/f/CW2 mice also crossed over into the light region with more frequency. N=8 for Cdk5f/f, N=9 for Cdk5f/f/CW2. Data shown are means ± SEM. Statistical significance was calculated using Student's t-test (*p < 0.05; **p < 0.01; ***p < 0.001).

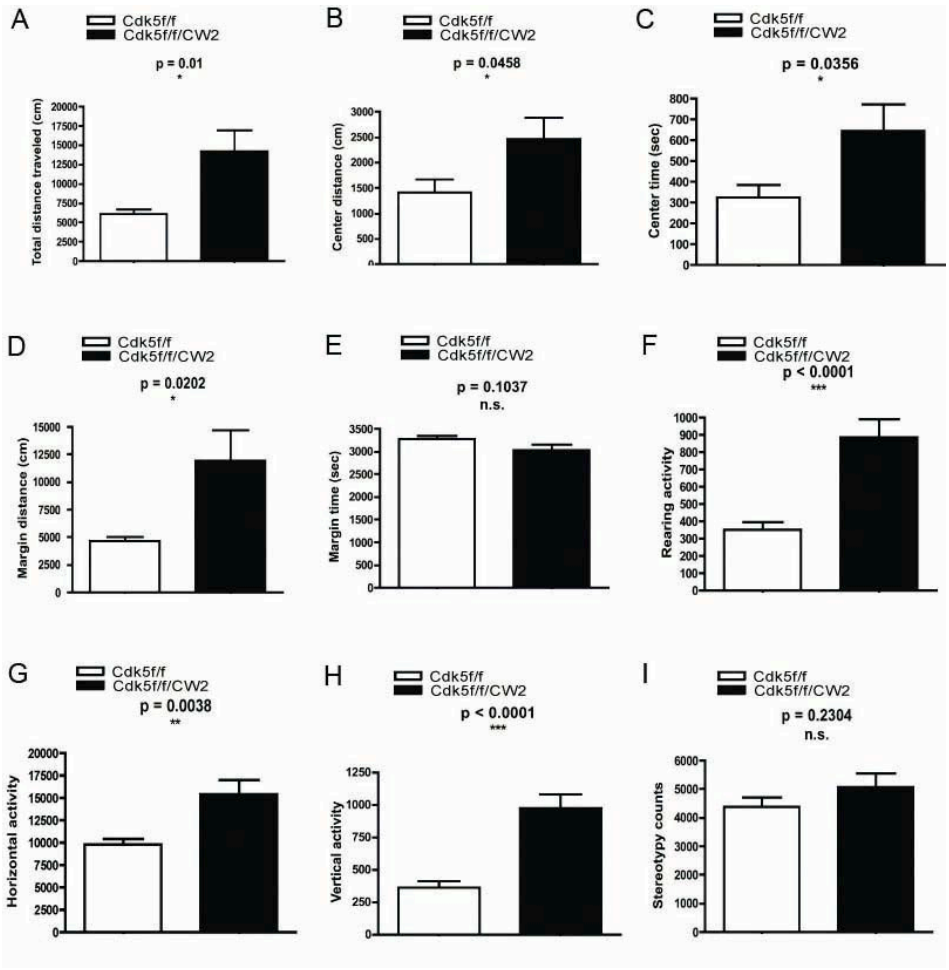

Figure 3. Cdk5f/f/CW2 are hyperactive as measured by the open field test.
(A) Compared to Cdk5f/f control littermates, Cdk5f/f/CW2 mice were consistently and significantly more active overall and traveled a greater distance in the open field arena over a period of 60 min.
(B) Cdk5f/f/CW2 traveled a greater distance in the center of the open field, indicating reduced anxiety.
(C) Upon further examination, Cdk5f/f/CW2 mice spent more time in the center of the open field arena, indicative of a reduction in anxiety that is consistent with observations from the light/dark test.
(D) Cdk5f/f/CW2 traveled a greater distance in the margin of the open field test, reflecting a generalized hyperactivity.
(E) There were no significant differences in time spent in the margin of the open field arena between control Cdk5f/f and Cdk5f/f/CW2 mice.
(F) Rearing activity, another way of measuring anxiety, indicated that Cdk5f/f/CW2 mice exhibited increased rearing and provided further evidence that Cdk5f/f/CW2 mice demonstrated a reduction in anxiety.
(G) Consistent with the observation that Cdk5f/f/CW2 display increased overall activity, their horizontal activity was also increased.
(H) Also consistent with the rearing activity, the number of infrared beam breaks detecting vertical movement was significantly higher in the Cdk5f/f/CW2 mice compared to Cdk5f/f control mice.
(I) Neither group of mice exhibited any alterations in stereotypy behaviors. N=9 animals for both Cdk5f/f and Cdk5f/f/CW2 genotypes. Data shown are means ± SEM. Statistical significance was calculated using Student's t-test (*$p < 0.05$; **$p < 0.01$; ***$p < 0.001$).

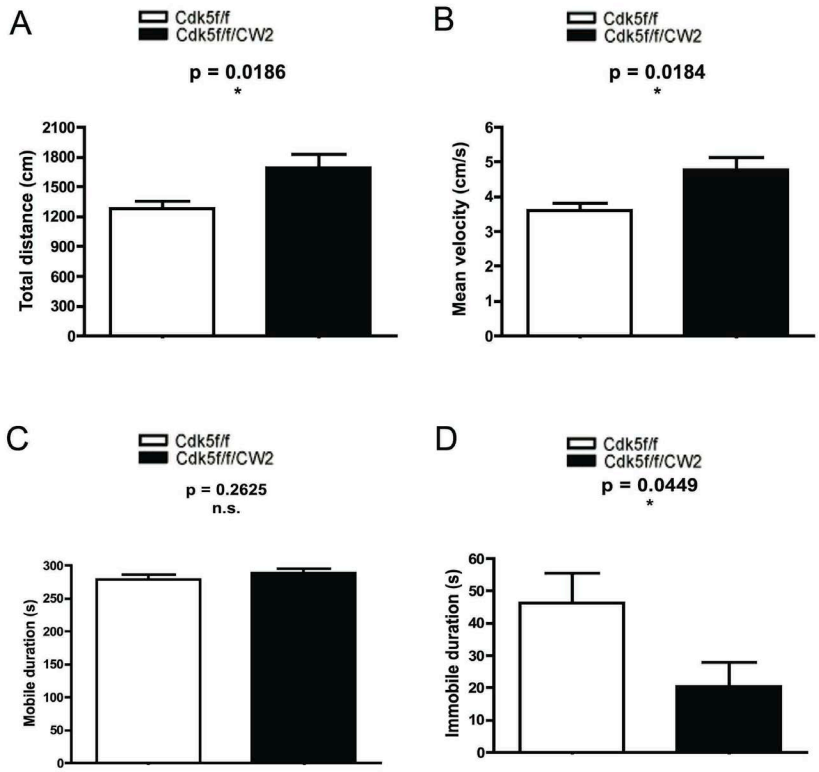

Figure 4. Forced swim test did not reveal any differences in learned helplessness behavior.
(A) Compared to Cdk5f/f control littermates, Cdk5f/f/CW2 mice were more active overall in the water during the forced swim test.
(B) Cdk5f/f/CW2 were more active in the forced swim test and also exhibited a greater velocity in their swimming movements.
(C) The mobile durations between Cdk5f/f and Cdk5f/f/CW2 mice were not significantly different.
(D) In the immobile duration, Cdk5f/f/CW2 mice spent less time immobile compared to control Cdk5f/f mice, indicating a reduction in behavior despair. N=8 animals for both Cdk5f/f and Cdk5f/f/CW2 genotypes. Data shown are means ± SEM. Statistical significance was calculated using Student's t-test (*$p < 0.05$; **$p < 0.01$; ***$p < 0.001$).

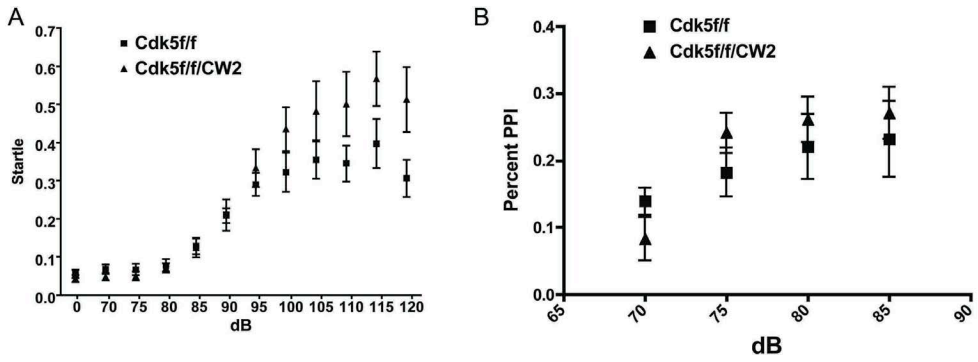

Figure 5. Cdk5f/f/CW2 mice did not reveal any deficits in pre-pulse inhibition.
(A) Compared to control Cdk5f/f mice, Cdk5f/f/CW2 mice exhibited greater startle in the pre-pulse inhibition test.
(B) The percent of pre-pulse inhibition, a measurement of sensorimotor gating, did not significantly differ between Cdk5f/f and Cdk5f/f/CW2 mice. N=9 animals for both Cdk5f/f and Cdk5f/f/CW2 genotypes. Data shown are means ± SEM. Statistical significance was calculated using Student's t-test (*$p < 0.05$; **$p < 0.01$; ***$p < 0.001$).

Cdk5f/f/CW2 mice are impaired in cognitive behavioral tasks

To further examine the cognitive abilities of the Cdk5f/f/CW2 animals, we performed the Morris water maze task to test for hippocampus-dependent spatial learning. Contrary to several reports (Hawasli et al., 2007), but consistent with others (Guan et al., 2011), Cdk5f/f/CW2 mice displayed a severe impairment in memory acquisition and retention during training (**Figure 6A**). Moreover, while control Cdk5f/f mice spent more time in the target quadrant during the probe test, Cdk5f/f/CW2 mice performed at chance, suggesting that Cdk5f/f/CW2 mice was unable to form a spatial memory (**Figure 6B**). In contextual fear conditioning, animals were placed in a conditioning chamber and presented with an unconditioned stimulus (footshock). Both Cdk5f/f and Cdk5f/f/CW2 mice displayed similar distance traveled, velocity, and response to footshock during the training period (**Figure 7A-C**). Upon testing for fear memory in the same chamber 1 hr and 24 hr later, however, Cdk5f/f/CW2 animals exhibited a dramatic reduction in freezing levels compared to control Cdk5f/f animals, indicating a severe impairment of cognitive function (**Figure 7D, 7E**). Tone-dependent fear conditioning, however, was not significantly impaired (**Figure 7F**).

Cdk5f/f/CW2 mice exhibit impairments in synaptic plasticity

Because Cdk5 loss-of-function in excitatory neurons may elicit a compensatory response in the inhibitory interneurons, we next examined if cortical oscillations, which have been implicated in cognition and are attributed to interneuron activity, were altered (Cardin et al., 2009). However, we did not detect any changes in cortical oscillations in the theta and gamma bands between control Cdk5f/f and Cdk5f/f/CW2 animals (**Figure 8A, 8B**). We next examined synaptic plasticity by preparing acute hippocampal slices from control Cdk5f/f and Cdk5f/f/CW2 animals and stimulating the Schaffer collateral pathway. Consistent with a reduction in the total number of synapses in hippocampal area CA1, basal synaptic transmission was severely reduced in slices prepared from Cdk5f/f/CW2 animals (**Figure 9A**). Paired-pulse facilitation ratios, a measurement of presynaptic transmitter release, did not significantly differ between control Cdk5f/f and Cdk5f/f/CW2 (**Figure 9B**). Moreover, the frequency (**Figure 9C**), but not amplitude (**Figure 9D**), of miniature excitatory postsynaptic current (mEPSCs) was reduced in the Cdk5f/f/CW2, supporting the notion of reduced synapse numbers.

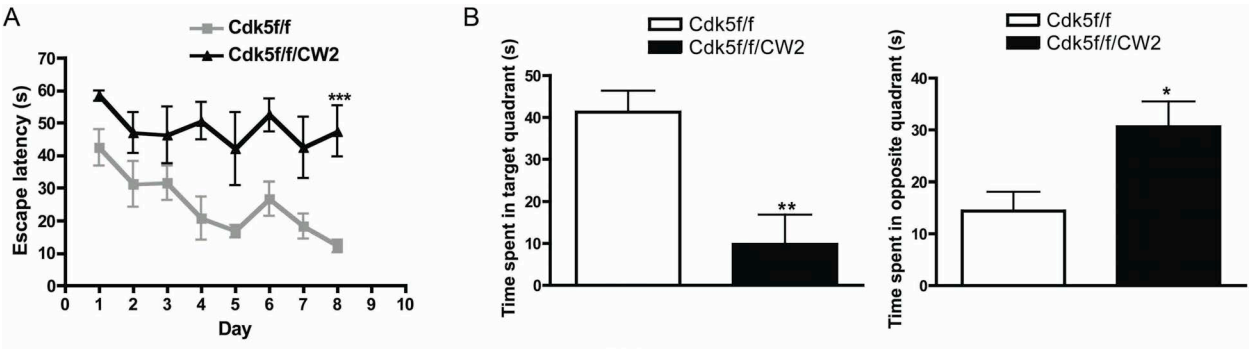

Figure 6. Cdk5f/f/CW2 exhibit spatial learning impairments in the Morris water maze.
(A) While control Cdk5f/f mice learned the spatial memory task during the 8 day training session, Cdk5f/f/CW2 mice were consistently impaired in acquisition of the spatial memory.
(B) During the probe trial on day 9, Cdk5f/f/CW2 mice spent significantly less time in the target quadrant ($p=0.0035$) and instead spent more time in the opposite quadrant ($p=0.0204$) compared to control Cdk5f/f littermates. N=8 for Cdk5f/f; N=5 for Cdk5f/f/CW2. Data shown are means ± SEM. Statistical significance was calculated using One-way ANOVA followed by Tukey's multiple comparison test (*$p < 0.05$; **$p < 0.01$; ***$p < 0.001$).

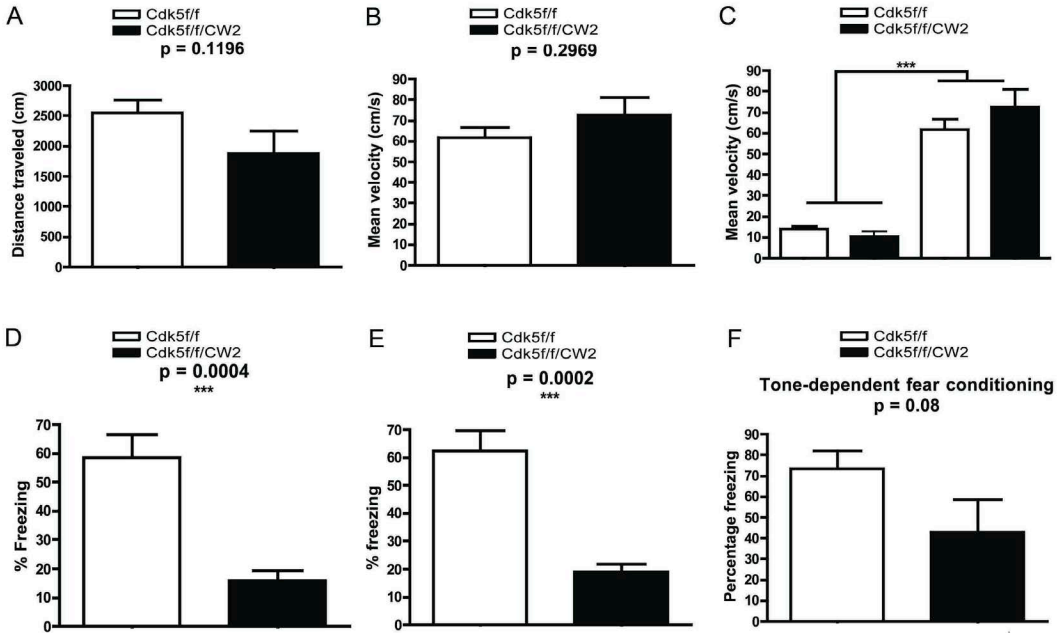

Figure 7. Cdk5f/f/CW2 are impired in contextual, but not tone, fear conditioning task.
(A) The distance traveled in the fear conditioning chamber did not significant differ between control Cdk5f/f and Cdk5f/f/CW2 mice in the 3 min exploration time before the footshock.
(B) The average velocity did not significantly differ between control Cdk5f/f and Cdk5f/f/CW2 mice in the 3 min exploration time before the footshock.
(C) Both Cdk5f/f and Cdk5f/f/CW2 groups responded to the footshock as shown by their increase in mean velocity before (left) and after (right) the shock.
(D) Whereas control Cdk5f/f mice displayed robust freezing levels upon testing 1 hr after the footshock, Cdk5f/f/CW2 were significantly impaired in fear memory.
(E) Whereas control Cdk5f/f mice displayed robust freezing levels upon testing 24 hr after the footshock, Cdk5f/f/CW2 were significantly impaired in fear memory.
(F) Tone-dependent fear conditioning is not significantly impacted in Cdk5f/f/CW2 mice compared to control Cdk5f/f mice. N=9 for Cdk5f/f; N=7 for Cdk5f/f/CW2. Data shown are means ± SEM. Statistical significance was calculated using Student's t-test (*$p < 0.05$; **$p < 0.01$; ***$p < 0.001$).

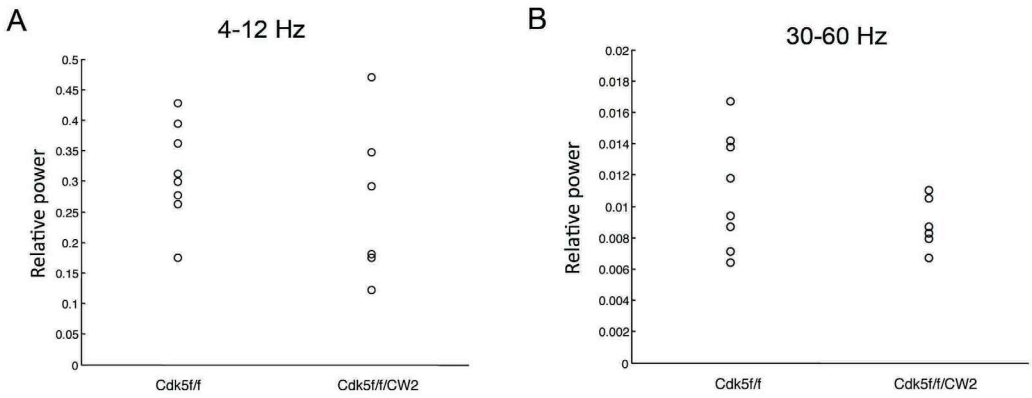

Figure 8. No alterations in cortical oscillations were observed in the Cdk5f/f/CW2 mice
(A) There were no differences in the relative power at the 4-12 Hz band of theta oscillations in the somatosensory cortex of anesthetized animals between control Cdk5f/f and Cdk5f/f/CW2 mice.
(B) There were no differences in the relative power at the 30-60 Hz band of gamma oscillations in the somatosensory cortex of anesthetized animals between control Cdk5f/f and Cdk5f/f/CW2 mice. N=3 animals for both Cdk5f/f and Cdk5f/f/CW2 genotypes.

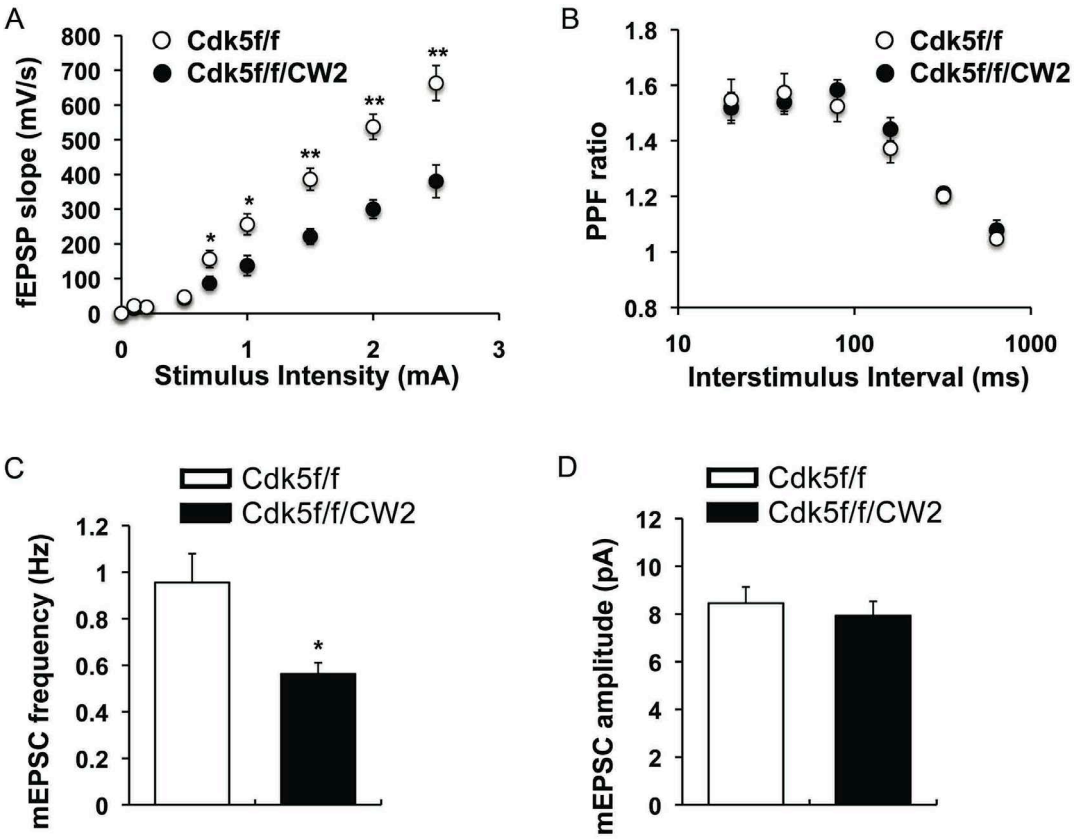

Figure 9. Basal synaptic transmission and spontaneous transmission is impaired in Cdk5f/f/CW2 mice.

(A) Basal synaptic transmission in the Schaffer collateral pathway is severely impaired in acute hippocampal slices prepared from Cdk5f/f/CW2 animals compared to control Cdk5f/f animals.

(B) Compared to control Cdk5f/f animals, the paired-pulse facilitation ratios at various interstimulus intervals are not significantly different from Cdk5f/f/CW2 animals.

(C) Compared to slices prepared from control Cdk5f/f animals, the frequency of spontaneous mEPSC is significantly decreased in slices prepared from Cdk5f/f/CW2.

(D) The mEPSC amplitude did not significantly differ between the control Cdk5f/f and Cdk5f/f/CW2 groups. N=3 animals, 9-14 slices, for both Cdk5f/f and Cdk5f/f/CW2 genotypes. Data shown are means ± SEM. Statistical significance was calculated using Student's t-test (*$p < 0.05$; **$p < 0.01$; ***$p < 0.001$).

Rescue of hyperactivity in Cdk5f/f/CW2 mice by lithium administration

Since our data suggests that Cdk5f/f/CW2 mice exhibit mania-like hyperactivity and reduced anxiety, we sought to address whether pharmacological administration may alleviate some of these symptoms. A previous mouse model exhibiting manic-like behavior including reduced anxiety, hyperactivity, and reduced depressive-like symptoms has been reported in a kainate receptor (GluR6) knockout, and successful amelioration of the symptoms was achieved by lithium administration (Shaltiel et al., 2008). Therefore, we asked whether lithium could improve some of the behavioral deficits that were observed in the open field test in the Cdk5f/f/CW2 animals. To test this possibility, lithium was administered to animals prior to the open field test. Remarkably, acute lithium administration was able to restore the hyperactivity of Cdk5f/f/CW2 to control levels as determined by overall activity, time spent in center versus margin, horizontal and vertical activity (**Figure 10A-F**). However, consistent with our observations that stereotypy was not initially affected in Cdk5f/f/CW2 mice, lithium treatment had no further effect (**Figure 10G**).

Cdk5f/f/CW2 display increased phosphorylation of GSK3αβ

As lithium is a well-known inhibitor of GSK3β, we examined protein levels of GSKβ as a potential molecular mechanism underlying the hyperactivity in Cdk5f/f/CW2 mice. Surprisingly, while total levels of GSK3β remained unchanged in the Cdk5f/f/CW2 mice, phospho-GSK3α/β (S21/9) levels were significantly increased in the Cdk5f/f/CW2 forebrain lysates. Other molecules in the GSK3β signaling pathway, including total levels of β-catenin, were unaltered (**Figure 11A-C**). Thus, Cdk5f/f/CW2 mice exhibit mania-like behavior that can be rescued by lithium treatment, and biochemical data hint at alterations in GSK3β activity as a potential mechanism underlying these behaviors.

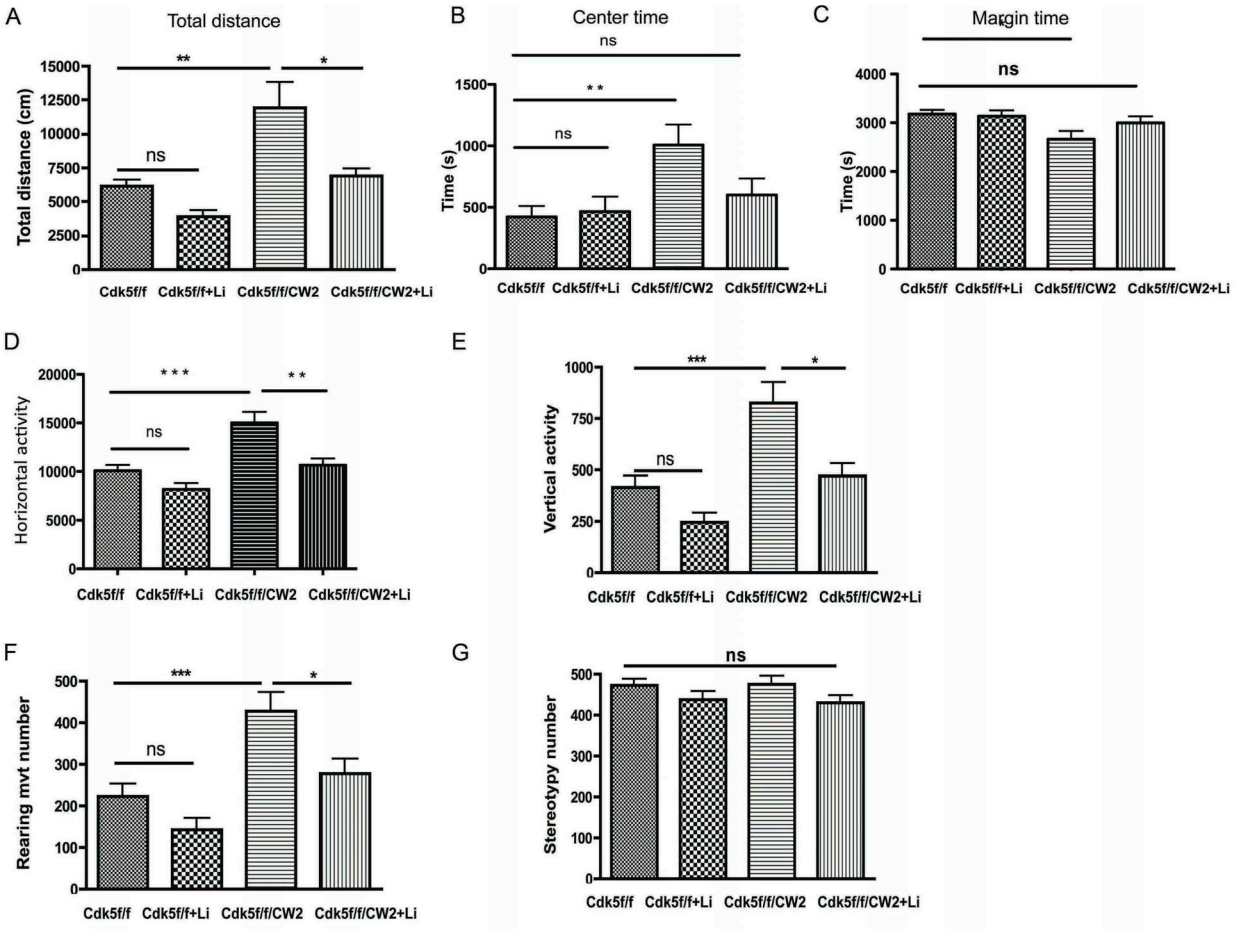

Figure 10. LiCl treatment rescues open field deficits.

(A) Lithium chloride administration prior to the open field test is able to restore the total distance traveled by the Cdk5f/f/CW2 to control Cdk5f/f levels, whereas lithium failed to further dampen the activity of Cdk5f/f mice.

(B) While the Cdk5f/f/CW2 mice spent more time in the center of the open field arena before treatment, lithium administration decreased the amount of time Cdk5f/f/CW2 spent in the center back to control Cdk5f/f levels.

(C) Conversely, while Cdk5f/f/CW2 mice initially sent less time in the margin of the open field arena before treatment, lithium administration ameliorated this effect and restored time spent in the margin to control Cdk5f/f levels.

(D) Horizontal activity was decreased to control Cdk5f/f levels after Cdk5f/f/CW2 were treated with lithium chloride.

(E) Similar to horizontal activity, vertical activity was decreased to control Cdk5f/f levels after Cdk5f/f/CW2 were treated with lithium chloride.

(F) Rearing movement number, a measurement of anxiety, was initially higher in Cdk5f/f/CW2 mice, consistent with earlier observations that these Cdk5f/f/CW2 mice have reduced anxiety. However, after treatment with lithium chloride, Cdk5f/f/CW2 mice exhibited similar rearing movements as control Cdk5f/f mice.

(G) As stereotypy was initially unaffected, lithium treatment on Cdk5f/f/CW2 mice had no further effect. Lithium had no significant effect on the Cdk5f/f control mice in all behavioral measurements. N=11 for Cdk5f/f; N=9 for Cdk5f/f/CW2. Data shown are means ± SEM. Statistical significance was calculated using One-way ANOVA (Tukey's multiple comparison test) (*$p < 0.05$; **$p < 0.01$; ***$p < 0.001$).

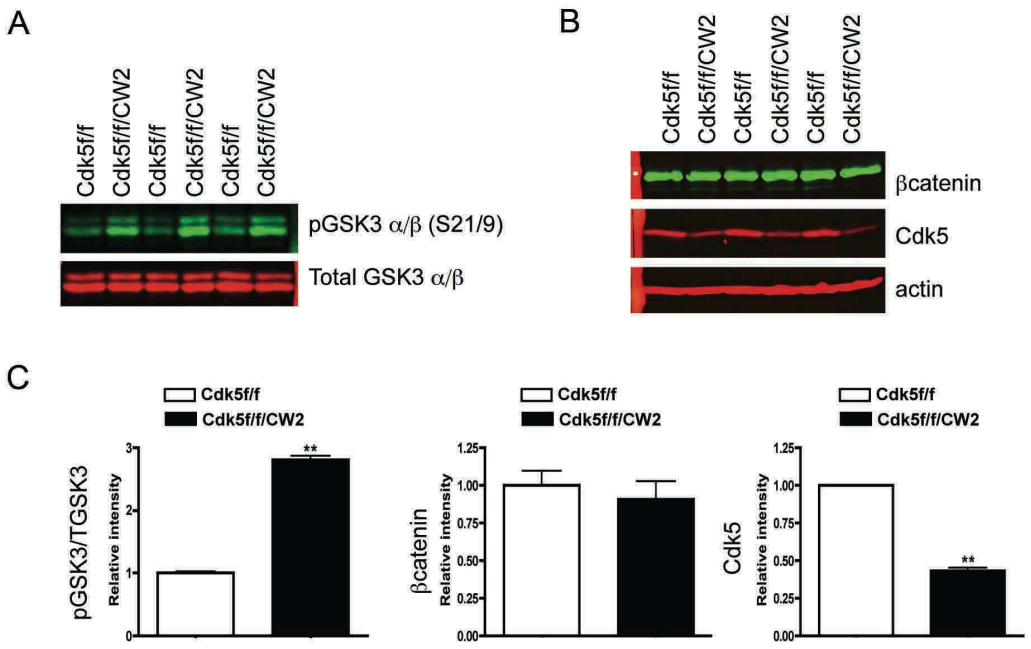

Figure 11. Increased GSK3α/β phosphorylation in Cdk5f/f/CW2 lysates.

(A) Levels of phospho-GSK3α/β (S21/9) are increased in Cdk5f/f/CW2 forebrain lysates compared to control Cdk5f/f lysates, where total GSK3α/β levels remain unaltered.

(B) Compared to control Cdk5f/f lysates, total levels of β-catenin were unchanged in the Cdk5f/f/CW2 lysates. Cdk5 levels are significantly reduced in the Cdk5f/f/CW2 mice.

(C) Quantification of the phospho-GSK3α/β (S21/9) protein levels, total β-catenin levels and Cdk5 levels. N=3 animals for Cdk5f/f and Cdk5f/f/CW2 genotypes. Data shown are means ± SEM. Statistical significance was calculated using Student's t-test (*$p < 0.05$; **$p < 0.01$; ***$p < 0.001$).

Discussion

Here we have described a mouse model in which Cdk5 deletion from αCaMKII-positive excitatory neurons of the forebrain results in a distinct hyperactivity phenotype, disrupted cognitive performance, and impaired synaptic plasticity as measured by basal synaptic transmission and spontaneous neurotransmitter release. Mechanistically, hints that the GSK3β signaling pathway may be impaired arise from the observation that treatment of the Cdk5f/f/CW2 mice with lithium can ameliorate the hyperactive movements. Intriguingly, we observed that phospho-GSK3β is increased in the forebrain lysates of Cdk5f/f/CW2. Taken together, our mouse model can serve as a useful tool to examine signaling cascades underlying mouse models exhibiting manic-like hyperactivity.

Cdk5 and homeostatic plasticity

Increasing number of studies have identified Cdk5 as a critical regulator of synaptic transmission and homeostatic plasticity by downregulating activity in response to heightened activity (Seeburg et al., 2008), affecting vesicle pool size during neurotransmitter release (Kim and Ryan, 2010), and silencing recurrent networks during prolonged inactivity (Mitra et al., 2011). While Cdk5 activity is important as a mediator of homeostatic plasticity, precisely how chronic Cdk5 loss-of-function impacts synaptic plasticity is still unclear. Earlier studies from p35 knockout mice and found that loss of one copy of p35 leads to pre-pulse inhibition deficits in female mice and impaired reverse learning in the water maze task (Engmann et al., 2011). However, the authors found that only male mice exhibited cognitive deficits in a spatial memory task, along with impaired social interaction. In these mice, treatment with a chromatin modifying enzyme inhibitor restored the behavioral deficits.

Our results differ from previous reports that Cdk5 conditional knockout mice exhibit enhanced learning and memory in the water maze task and fear conditioning, and increased NR2B surface expression levels due to a reduction in calpain-mediated cleavage and reduction of NR2B (Hawasli et al., 2007). One notable difference was the use of a prion promoter Cre mouse line, which provided temporal deletion of Cdk5 but targeted Cdk5 in a wider range of different cell types and brain regions including the retina, olfactory bulb, and cerebellum (Weber et al., 2001). In a separate study, the Cdk5 conditional knockout mice generated by the prion promoter Cre line exhibited enhanced hippocampal theta oscillations, which is in stark contrast to our mice

generated by the αCaMKII-Cre promoter (Hawasli et al., 2009). However, both Cdk5 mutant mouse models exhibit seizure phenotypes. Hawasli et al. proposed that an acute increase in p25 levels in their mouse model during seizure activity is a compensatory mechanism, and long-term loss of Cdk5 also results in a reduction in p25. While we have not yet examined the relationship of p35 to p25 levels in our Cdk5f/f/CW2 mice, we would predict normal expression of p35 and cleavage of p35 to p25 under neurotoxic conditions. Future experiments also include LTP and LTD studies, and based on the deficits in cognitive functions, we would also expect to observe a decrease in LTP in Cdk5f/f/CW2 mice. If we do observe a deficit in LTP, this would again contrast the findings from Hawasli et al. who determined that αCaMKII-restricted Cdk5 knockout results in an enhancement of LTP.

Our behavioral rescue of hyperactivity using lithium treatment prompted us to examine levels of GSK3β in Cdk5f/f/CW2 mice, as lithium is a well-known inhibitor of GSK3β. Surprisingly, our results differ from the prediction that because young p25 transgenic animals expressing hyperactive Cdk5 have increased GSK3αβ phosphorylation (S21/9), loss of Cdk5 would decrease levels of phospho-GSK3αβ (S21/9). (Plattner et al., 2006). Instead we found that loss of Cdk5 increased levels of phospho-GSK3αβ (S21/9). However, in older p25 transgenic animals, phospho-GSK3β (S21/9) levels do not differ from control animals and GSK3β activity is increased. Although seemingly contradictory, our mouse model could reflect a compensation mechanism in which loss of Cdk5 results in increased inhibition of GSK3β that is due to a reduction in phosphatase 2A (PP2A), which is known to interact with both Cdk5 and GSK3β. We also cannot exclude the possibility that other phosphatases targeting phospho-GSK3β (S21/9) are impaired in these Cdk5f/f/CW2 mice, in which steady loss of Cdk5 throughout the mouse lifespan may result in long-term compensatory changes. It will therefore be interesting to examine levels of GSK3β, PP2A, and p25 after lithium treatment in our Cdk5f/f/CW2 mice. Moreover, it will also be essential to examine the activation site of GSK3β on Tyr279/216, as we only evaluated the phosphorylation sites which result in GSK3β inhibition. Finally, it will be of great interest to measure how other components of the GSK3β signaling pathway, including Akt and ERK phosphorylation, are impacted by chronic loss of Cdk5 to address whether the GSK3β pathway is directly affected by lithium in our study.

References

Cardin, J.A., Carlen, M., Meletis, K., Knoblich, U., Zhang, F., Deisseroth, K., Tsai, L.H., and Moore, C.I. (2009). Driving fast-spiking cells induces gamma rhythm and controls sensory responses. Nature *459*, 663-667.

Drerup, J.M., Hayashi, K., Cui, H., Mettlach, G.L., Long, M.A., Marvin, M., Sun, X., Goldberg, M.S., Lutter, M., and Bibb, J.A. (2010). Attention-deficit/hyperactivity phenotype in mice lacking the cyclin-dependent kinase 5 cofactor p35. Biol Psychiatry *68*, 1163-1171.

Engmann, O., Hortobagyi, T., Pidsley, R., Troakes, C., Bernstein, H.G., Kreutz, M.R., Mill, J., Nikolic, M., and Giese, K.P. (2011). Schizophrenia is associated with dysregulation of a Cdk5 activator that regulates synaptic protein expression and cognition. Brain *134*, 2408-2421.

Fischer, A., Sananbenesi, F., Pang, P.T., Lu, B., and Tsai, L.H. (2005). Opposing roles of transient and prolonged expression of p25 in synaptic plasticity and hippocampus-dependent memory. Neuron *48*, 825-838.

Guan, J.S., Su, S.C., Gao, J., Joseph, N., Xie, Z., Zhou, Y., Durak, O., Zhang, L., Zhu, J.J., Clauser, K.R*., et al.* (2011). Cdk5 Is Required for Memory Function and Hippocampal Plasticity via the cAMP Signaling Pathway. PLoS One *6*, e25735.

Hawasli, A.H., Benavides, D.R., Nguyen, C., Kansy, J.W., Hayashi, K., Chambon, P., Greengard, P., Powell, C.M., Cooper, D.C., and Bibb, J.A. (2007). Cyclin-dependent kinase 5 governs learning and synaptic plasticity via control of NMDAR degradation. Nat Neurosci *10*, 880-886.

Hawasli, A.H., Koovakkattu, D., Hayashi, K., Anderson, A.E., Powell, C.M., Sinton, C.M., Bibb, J.A., and Cooper, D.C. (2009). Regulation of hippocampal and behavioral excitability by cyclin-dependent kinase 5. PLoS One *4*, e5808.

Kim, S.H., and Ryan, T.A. (2010). CDK5 serves as a major control point in neurotransmitter release. Neuron *67*, 797-809.

Krapacher, F.A., Mlewski, E.C., Ferreras, S., Pisano, V., Paolorossi, M., Hansen, C., and Paglini, G. (2010). Mice lacking p35 display hyperactivity and paradoxical response to psychostimulants. J Neurochem *114*, 203-214.

Li, B.S., Sun, M.K., Zhang, L., Takahashi, S., Ma, W., Vinade, L., Kulkarni, A.B., Brady, R.O., and Pant, H.C. (2001). Regulation of NMDA receptors by cyclin-dependent kinase-5. Proc Natl Acad Sci U S A *98*, 12742-12747.

Mitra, A., Mitra, S.S., and Tsien, R.W. (2011). Heterogeneous reallocation of presynaptic efficacy in recurrent excitatory circuits adapting to inactivity. Nat Neurosci.

Morabito, M.A., Sheng, M., and Tsai, L.H. (2004). Cyclin-dependent kinase 5 phosphorylates the N-terminal domain of the postsynaptic density protein PSD-95 in neurons. J Neurosci *24*, 865-876.

Plattner, F., Angelo, M., and Giese, K.P. (2006). The roles of cyclin-dependent kinase 5 and glycogen synthase kinase 3 in tau hyperphosphorylation. J Biol Chem *281*, 25457-25465.

Seeburg, D.P., Feliu-Mojer, M., Gaiottino, J., Pak, D.T., and Sheng, M. (2008). Critical role of CDK5 and Polo-like kinase 2 in homeostatic synaptic plasticity during elevated activity. Neuron *58*, 571-583.

Shaltiel, G., Maeng, S., Malkesman, O., Pearson, B., Schloesser, R.J., Tragon, T., Rogawski, M., Gasior, M., Luckenbaugh, D., Chen, G*., et al.* (2008). Evidence for the involvement of

the kainate receptor subunit GluR6 (GRIK2) in mediating behavioral displays related to behavioral symptoms of mania. Mol Psychiatry *13*, 858-872.

Weber, P., Metzger, D., and Chambon, P. (2001). Temporally controlled targeted somatic mutagenesis in the mouse brain. Eur J Neurosci *14*, 1777-1783.

Zeng, H., Chattarji, S., Barbarosie, M., Rondi-Reig, L., Philpot, B.D., Miyakawa, T., Bear, M.F., and Tonegawa, S. (2001). Forebrain-specific calcineurin knockout selectively impairs bidirectional synaptic plasticity and working/episodic-like memory. Cell *107*, 617-629.

Chapter 6

Conclusions

The central goal of the thesis was to further our understanding of how a prolific neuronal serine/threonine kinase such as Cdk5 contributes to various aspects of synaptic function, synaptic plasticity, and learning and memory. I began in Chapter 1 with an introduction to the diversity of Cdk5 substrates in the nervous system, followed by an overview of how dysregulation of Cdk5 is implicated in various neurodegenerative disorders. In Chapter 2, I described a specific signaling pathway that is affected in a hippocampus-specific knockout of Cdk5 that impairs learning and memory, which can be restored by phosphodiesterase inhibitors. In Chapter 3, I presented evidence for Cdk5-mediated phosphorylation of a presynaptic voltage-gated N-type calcium channel. The phosphorylation event enhances calcium influx and promotes vesicle docking and interaction with the active zone protein RIM1 to enhance synaptic transmission. I then provided data in Chapter 4 that Cdk5-mediated phosphorylation of a postsynaptic density protein, Shank3, is involved in dendritic spine maturation and synaptic plasticity. Finally, I extended our initial proteomic characterizations of our forebrain-specific Cdk5 deletion mouse model from Chapter 2 by investigating whether these mice display impairments in learning and memory. The animals were subjected to various behavior tasks, and the findings are summarized in Chapter 5.

These collective studies raise a more general question of how the activity of Cdk5 itself is regulated. To address this topic, recent studies examined upstream, post-translational modifications of Cdk5 itself and noted that S-nitrosylation of Cdk5 at Cysteine 83 plays an important role in dendrite outgrowth (Zhang et al., 2010) and amyloid beta-induced spine loss, although how S-nitrosylation impacts Cdk5 activity remains unclear and may differ under pathological conditions (Qu et al., 2011). Furthermore, phosphorylation of Cdk5 itself at Tyrosine 15 (Y15) in response to ephrinA-1 ligand heightens its activity (Fu et al., 2007). A different future approach might be to limit the generation of p25, the Cdk5 subunit implicated in neurodegeneration (Patrick et al., 1999). Under physiological conditions p35 is associated with Cdk5 to the cytoplasm with a half life of approximately 20-30 min (Patrick et al., 1998). Furthermore, p35 undergoes ubiquitin-mediated proteolysis as a mechanism for rapid regulation of Cdk5 kinase activity. However, when neurons are subjected to neurotoxic insults including

excitotoxicity, oxidative stress, or amyloid peptides, the calcium-dependent protease calpain cleaves p35 to liberate the p25 fragment (Kusakawa et al., 2000; Lee et al., 2000). This p25 fragment, when bound to Cdk5, displays a longer half-life of approximately 60 min and can shuttle to the nucleus where it mediates cell death (O'Hare et al., 2005). These results raise the possibility of using genetic mouse models or pharmacological tools during excitotoxicity to prevent the generation of p25 or shorten its half-life. Moreover, one could potentially reduce the activity of calpain or increase levels of calpastatin, a calpain inhibitor. To test whether calpain directly contributes to p25 generation, transgenic mouse models of calpastatin were previously generated. In a mouse model overexpressing calpastatin, p25 is not produced, and p35 was subjected to calcium-dependent proteosomal degradation (Sato et al., 2011). Conversely, calpastatin knockout mice produced greater p25 levels. Interestingly, in brain tissue of Alzheimer's disease patients, downregulation of calpastatin is observed, suggesting a dysregulation of calpain activity. Future research into calpain and calpastatin activity may reveal how Cdk5 is preferentially associated with p35 or p25 in disease states.

Recent literature suggests that Cdk5 is one of the few candidates known to be involved in the regulation of synaptic homeostasis (Kim and Ryan, 2010; Mitra et al., 2012; Seeburg et al., 2008). Additional experiments using imaging, biophysical, and biochemical techniques to more precisely determine how Cdk5 controls the dynamics of neurotransmitter release will be informative. In particular, because Cdk5 loss of function studies presented in Chapters 2 and 5 focused primarily on excitatory neurons, it will also be compelling to address the activity of Cdk5 in inhibitory neurons. Due to its ubiquitous presence in both the presynaptic and postsynaptic terminals, silencing Cdk5 activity in a subset of neurons as well as in distinct spatial compartments using either mouse models or a combination of genetic and pharmacological manipulations will allow us to further probe how Cdk5 gates neurotransmission. Whether Cdk5 is upstream or acts in concert with other well-known synaptic homeostatic scaling candidate proteins including Arc (Beique et al., 2011), PSD-93 and PSD-95 (Sun and Turrigiano, 2011), MeCP2 (Qiu et al., 2012) remains to be determined, but nonetheless the importance of Cdk5 in fine-tuning synaptic transmission is quickly becoming one of the research highlights in the field of synaptic transmission and synaptic plasticity.

Although we focused mainly on the synaptic functions of Cdk5, further investigation of how aberrant Cdk5 activity contributes to neurological disorders is of great interest, as it may play a direct role in the neuropathological mechanisms underlying major neurodegenerative disorders including Alzheimer's disease, Parkinson's disease, Huntington's disease, amyotrophic lateral sclerosis, and Niemann-Pick Type C. To date, there have been no mutations identified in Cdk5 itself shown to be directly associated with neurodegeneration or psychiatric disorders. However, Cdk5 is implicated in almost every neuronal signaling pathway examined thus far, and its activity is essential during cell death of an autosomal dominant disease model in fruit flies (Kang et al., 2012). Moreover, there are also important non-neuronal functions involving Cdk5 involving adipose tissue and diabetes signaling pathway in mice (Choi et al., 2010; Choi et al., 2011) as well as the cancer signaling pathway in human cell lines (Ajay et al., 2010). Therefore, we hypothesize that deregulation of Cdk5 activity mediated by p35 and p25 levels is a key factor in contributing to the disease state (Chang et al., 2012). This prediction encompasses a complex interplay of kinases and phosphatases, including calcineurin, a calmodulin-dependent serine/threonine protein phosphatase which opposes Cdk5 activity and is also essential for learning and memory (Miyakawa et al., 2003; Zeng et al., 2001). Indeed, the protein phosphatase 2A (PP2A) is the phosphatase opposing Cdk5 phosphorylation of the neurofilament heavy chain (Veeranna et al., 1995), and knockout mouse models of PP2A exhibit dysregulated Cdk5 activity and increased tau phosphorylation (Louis et al., 2011). Furthermore, protein phosphatase 1 (PP1) is directly associated with Cdk5/p25 (Agarwal-Mawal and Paudel, 2001; Bibb et al., 2001), suggesting that phosphatases are also tightly regulated by Cdk5 activity. Intriguingly, phosphorylation of phosphatase inhibitor-1 by Cdk5 does not inhibit phosphatases directly, but instead modulates the activity of cAMP signaling pathways in striatal tissue, adding yet another element of complexity (Bibb et al., 2001). Future studies using a well-characterized Cdk5 substrate, DARPP-32, which can function as either a kinase or phosphatase (Bibb et al., 1999), will be helpful in mapping out the consequences of imbalanced activity of either Cdk5 or the phosphatases.

We did not explore other forms of post-translational modifications in our studies; however, it is notable that Cdk5 has also been implicated in the epigenetic regulation of histone-modifying enzymes (Graff et al., 2011). Recent work highlights the function of Cdk5-mediated

phosphorylation and PP2A-dephosphorylation on a histone deacetylase enzyme, HDAC5, in shuttling in and out of the nucleus during cocaine reward (Taniguchi et al., 2012). Strong evidence of an association between Cdk5 and epigenetic modification components was further provided by a study examining the how Cdk5-mediated phosphorylation of mSds3, a component of the HDAC co-repressor complex, regulates transcriptional repression and neuronal survival through histone acetylation (Fu et al., 2012; Li et al., 2004). Yet another study highlights how Cdk5/p25 deregulates the activity of HDAC1 during DNA damage and cell death processes (Kim et al., 2008). As the field of neuroepigenetics expands to include the examination of various kinases in conjunction with other post-translational modifications of acetylation, methylation, nitrosylation, ubiquitination, it will be of great interest to investigate the role of Cdk5 in regulating the transcriptional landscape of the mammalian genome and examine how this landscape is altered during neurodegeneration.

Future directions from work presented here include the pursuit of targeting Cdk5 activity as a potential therapeutic strategy in synaptic dysfunctions and in neurodegeneration. Specifically limiting Cdk5 activity by targeting the generation of p25 or by inhibiting Cdk5/p25 activity may ameliorate cognitive decline and attenuate neurodegeneration. Several molecules have been implicated in Alzheimer's Disease including Cdk5/p25, β-secretase (BACE1), and γ-secretase which cleaves the amyloid precursor protein (APP) into the pathogenic amyloid beta (Su and Tsai, 2011). In an intriguing study, mice overexpressing Cdk5/p25 exhibited increased BACE1 levels and enhanced APP processing due to the activity of Cdk5-responsive site in STAT3, a transcriptional activator in the BACE1 promoter region (Wen et al., 2008). As Cdk5 inhibitors are non-specific with potential side-effects, an ideal approach would consist of systematically targeting Cdk5 activity in a spatial and temporal manner. One such study that inhibited Cdk5 using RNA-mediated knockdown resulted in decreased neurofibrillary tangles in mouse models of Alzheimer's disease (Piedrahita et al., 2010). We predict that restricting Cdk5/p25 activity during a critical time frame during the early initiating events preceding neurodegeneration would be most beneficial for therapeutic intervention. By studying a Cdk5 in the dynamic context of synaptic function, synaptic plasticity, and learning and memory, we ultimately seek to address how neurons maintain their proper synaptic connectivity and functions in the brain.

References

Agarwal-Mawal, A., and Paudel, H.K. (2001). Neuronal Cdc2-like protein kinase (Cdk5/p25) is associated with protein phosphatase 1 and phosphorylates inhibitor-2. J Biol Chem *276*, 23712-23718.

Ajay, A.K., Upadhyay, A.K., Singh, S., Vijayakumar, M.V., Kumari, R., Pandey, V., Boppana, R., and Bhat, M.K. (2010). Cdk5 phosphorylates non-genotoxically overexpressed p53 following inhibition of PP2A to induce cell cycle arrest/apoptosis and inhibits tumor progression. Mol Cancer *9*, 204.

Beique, J.C., Na, Y., Kuhl, D., Worley, P.F., and Huganir, R.L. (2011). Arc-dependent synapse-specific homeostatic plasticity. Proc Natl Acad Sci U S A *108*, 816-821.

Bibb, J.A., Nishi, A., O'Callaghan, J.P., Ule, J., Lan, M., Snyder, G.L., Horiuchi, A., Saito, T., Hisanaga, S., Czernik, A.J*., et al.* (2001). Phosphorylation of protein phosphatase inhibitor-1 by Cdk5. J Biol Chem *276*, 14490-14497.

Bibb, J.A., Snyder, G.L., Nishi, A., Yan, Z., Meijer, L., Fienberg, A.A., Tsai, L.H., Kwon, Y.T., Girault, J.A., Czernik, A.J*., et al.* (1999). Phosphorylation of DARPP-32 by Cdk5 modulates dopamine signalling in neurons. Nature *402*, 669-671.

Chang, K.H., Vincent, F., and Shah, K. (2012). Deregulated Cdk5 Triggers Aberrant Activation of Cell Cycle Kinases and Phosphatases Inducing Neuronal Death. J Cell Sci.

Choi, J.H., Banks, A.S., Estall, J.L., Kajimura, S., Bostrom, P., Laznik, D., Ruas, J.L., Chalmers, M.J., Kamenecka, T.M., Bluher, M*., et al.* (2010). Anti-diabetic drugs inhibit obesity-linked phosphorylation of PPARgamma by Cdk5. Nature *466*, 451-456.

Choi, J.H., Banks, A.S., Kamenecka, T.M., Busby, S.A., Chalmers, M.J., Kumar, N., Kuruvilla, D.S., Shin, Y., He, Y., Bruning, J.B*., et al.* (2011). Antidiabetic actions of a non-agonist PPARgamma ligand blocking Cdk5-mediated phosphorylation. Nature *477*, 477-481.

Fu, A.K., Hung, K.W., Wong, H.H., Fu, W.Y., and Ip, N.Y. (2012). Cdk5 Phosphorylates a Component of the HDAC Complex and Regulates Histone Acetylation during Neuronal Cell Death. Neurosignals.

Fu, W.Y., Chen, Y., Sahin, M., Zhao, X.S., Shi, L., Bikoff, J.B., Lai, K.O., Yung, W.H., Fu, A.K., Greenberg, M.E*., et al.* (2007). Cdk5 regulates EphA4-mediated dendritic spine retraction through an ephexin1-dependent mechanism. Nat Neurosci *10*, 67-76.

Graff, J., Kim, D., Dobbin, M.M., and Tsai, L.H. (2011). Epigenetic regulation of gene expression in physiological and pathological brain processes. Physiol Rev *91*, 603-649.

Kang, M.J., Chung, J., and Ryoo, H.D. (2012). CDK5 and MEKK1 mediate pro-apoptotic signalling following endoplasmic reticulum stress in an autosomal dominant retinitis pigmentosa model. Nat Cell Biol *14*, 409-415.

Kim, D., Frank, C.L., Dobbin, M.M., Tsunemoto, R.K., Tu, W., Peng, P.L., Guan, J.S., Lee, B.H., Moy, L.Y., Giusti, P*., et al.* (2008). Deregulation of HDAC1 by p25/Cdk5 in neurotoxicity. Neuron *60*, 803-817.

Kim, S.H., and Ryan, T.A. (2010). CDK5 serves as a major control point in neurotransmitter release. Neuron *67*, 797-809.

Kusakawa, G., Saito, T., Onuki, R., Ishiguro, K., Kishimoto, T., and Hisanaga, S. (2000). Calpain-dependent proteolytic cleavage of the p35 cyclin-dependent kinase 5 activator to p25. J Biol Chem *275*, 17166-17172.

Lee, M.S., Kwon, Y.T., Li, M., Peng, J., Friedlander, R.M., and Tsai, L.H. (2000). Neurotoxicity induces cleavage of p35 to p25 by calpain. Nature *405*, 360-364.

Li, Z., David, G., Hung, K.W., DePinho, R.A., Fu, A.K., and Ip, N.Y. (2004). Cdk5/p35 phosphorylates mSds3 and regulates mSds3-mediated repression of transcription. J Biol Chem *279*, 54438-54444.

Louis, J.V., Martens, E., Borghgraef, P., Lambrecht, C., Sents, W., Longin, S., Zwaenepoel, K., Pijnenborg, R., Landrieu, I., Lippens, G.*, et al.* (2011). Mice lacking phosphatase PP2A subunit PR61/B'delta (Ppp2r5d) develop spatially restricted tauopathy by deregulation of CDK5 and GSK3beta. Proc Natl Acad Sci U S A *108*, 6957-6962.

Mitra, A., Mitra, S.S., and Tsien, R.W. (2012). Heterogeneous reallocation of presynaptic efficacy in recurrent excitatory circuits adapting to inactivity. Nat Neurosci *15*, 250-257.

Miyakawa, T., Leiter, L.M., Gerber, D.J., Gainetdinov, R.R., Sotnikova, T.D., Zeng, H., Caron, M.G., and Tonegawa, S. (2003). Conditional calcineurin knockout mice exhibit multiple abnormal behaviors related to schizophrenia. Proc Natl Acad Sci U S A *100*, 8987-8992.

O'Hare, M.J., Kushwaha, N., Zhang, Y., Aleyasin, H., Callaghan, S.M., Slack, R.S., Albert, P.R., Vincent, I., and Park, D.S. (2005). Differential roles of nuclear and cytoplasmic cyclin-dependent kinase 5 in apoptotic and excitotoxic neuronal death. J Neurosci *25*, 8954-8966.

Patrick, G.N., Zhou, P., Kwon, Y.T., Howley, P.M., and Tsai, L.H. (1998). p35, the neuronal-specific activator of cyclin-dependent kinase 5 (Cdk5) is degraded by the ubiquitin-proteasome pathway. J Biol Chem *273*, 24057-24064.

Patrick, G.N., Zukerberg, L., Nikolic, M., de la Monte, S., Dikkes, P., and Tsai, L.H. (1999). Conversion of p35 to p25 deregulates Cdk5 activity and promotes neurodegeneration. Nature *402*, 615-622.

Piedrahita, D., Hernandez, I., Lopez-Tobon, A., Fedorov, D., Obara, B., Manjunath, B.S., Boudreau, R.L., Davidson, B., Laferla, F., Gallego-Gomez, J.C.*, et al.* (2010). Silencing of CDK5 reduces neurofibrillary tangles in transgenic alzheimer's mice. J Neurosci *30*, 13966-13976.

Qiu, Z., Sylwestrak, E.L., Lieberman, D.N., Zhang, Y., Liu, X.Y., and Ghosh, A. (2012). The Rett syndrome protein MeCP2 regulates synaptic scaling. J Neurosci *32*, 989-994.

Qu, J., Nakamura, T., Cao, G., Holland, E.A., McKercher, S.R., and Lipton, S.A. (2011). S-Nitrosylation activates Cdk5 and contributes to synaptic spine loss induced by beta-amyloid peptide. Proc Natl Acad Sci U S A *108*, 14330-14335.

Sato, K., Minegishi, S., Takano, J., Plattner, F., Saito, T., Asada, A., Kawahara, H., Iwata, N., Saido, T.C., and Hisanaga, S. (2011). Calpastatin, an endogenous calpain-inhibitor protein, regulates the cleavage of the Cdk5 activator p35 to p25. J Neurochem *117*, 504-515.

Seeburg, D.P., Feliu-Mojer, M., Gaiottino, J., Pak, D.T., and Sheng, M. (2008). Critical role of CDK5 and Polo-like kinase 2 in homeostatic synaptic plasticity during elevated activity. Neuron *58*, 571-583.

Su, S.C., and Tsai, L.H. (2011). Cyclin-dependent kinases in brain development and disease. Annu Rev Cell Dev Biol *27*, 465-491.

Sun, Q., and Turrigiano, G.G. (2011). PSD-95 and PSD-93 play critical but distinct roles in synaptic scaling up and down. J Neurosci *31*, 6800-6808.

Taniguchi, M., Carreira, M.B., Smith, L.N., Zirlin, B.C., Neve, R.L., and Cowan, C.W. (2012). Histone deacetylase 5 limits cocaine reward through cAMP-induced nuclear import. Neuron *73*, 108-120.

Veeranna, Shetty, K.T., Link, W.T., Jaffe, H., Wang, J., and Pant, H.C. (1995). Neuronal cyclin-dependent kinase-5 phosphorylation sites in neurofilament protein (NF-H) are dephosphorylated by protein phosphatase 2A. J Neurochem *64*, 2681-2690.

Wen, Y., Yu, W.H., Maloney, B., Bailey, J., Ma, J., Marie, I., Maurin, T., Wang, L., Figueroa, H., Herman, M.*, et al.* (2008). Transcriptional regulation of beta-secretase by p25/cdk5 leads to enhanced amyloidogenic processing. Neuron *57*, 680-690.

Zeng, H., Chattarji, S., Barbarosie, M., Rondi-Reig, L., Philpot, B.D., Miyakawa, T., Bear, M.F., and Tonegawa, S. (2001). Forebrain-specific calcineurin knockout selectively impairs bidirectional synaptic plasticity and working/episodic-like memory. Cell *107*, 617-629.

Zhang, P., Yu, P.C., Tsang, A.H., Chen, Y., Fu, A.K., Fu, W.Y., Chung, K.K., and Ip, N.Y. (2010). S-nitrosylation of cyclin-dependent kinase 5 (cdk5) regulates its kinase activity and dendrite growth during neuronal development. J Neurosci *30*, 14366-14370.